UNIVERSIDAD DE LEÓN

Escuela de Ingenierías Industrial e Informática

Departamento de Ingeniería Eléctrica y de Sistemas y Automática

REDUCCIÓN DE CONTAMINANTES ATMOSFÉRICOS E HÍDRICOS EN AGRICULTURA DE PRECISIÓN UTILIZANDO SISTEMAS ROBOTIZADOS

TESIS DOCTORAL

Mariano González de Soto

León, 2016

TESIS DOCTORAL

REDUCCIÓN DE CONTAMINANTES ATMOSFÉRICOS E HÍDRICOS EN AGRICULTURA DE PRECISIÓN UTILIZANDO SISTEMAS ROBOTIZADOS

REDUCING AIR AND WATER POLLUTANTS IN PRECISION AGRICULTURE USING ROBOTIC SYSTEMS

universidad de león

CSIC
CONSEJO SUPERIOR DE INVESTIGACIONES CIENTÍFICAS

POLITÉCNICA

Autor:

Mariano González de Soto [a, b]

Directores:

Dr. Pablo González de Santos [a]

Dr. Isaias García Rodríguez [b]

[a] *Grupo de Robótica de Exteriores y Servicios*
Centro de Automática y Robótica
UPM-CSIC

[b] *Departamento de Ingeniería Eléctrica y de Sistemas y Automática*
Escuela de Ingenierías Industrial e Informática
Universidad de León

León, 2016

Reducing fuel consumption in weed and pest control using robotic tractors
M. Gonzalez-de-Soto, L. Emmi, I. Garcia, and P. Gonzalez-de-Santos
Computers and Electronics in Agriculture, ISSN 0168-1699, vol. 114, pp. 96–113, Jun. 2015.
DOI: *http://dx.doi.org/10.1016/j.compag.2015.04.003*
Impact Factor (2014): 1.761
Category: Agriculture, Multidisciplinary: 6/56 (Q1)
Category: Computer Science, Interdisciplinary Applications: 32/102 (Q2)

Reducing air pollution with hybrid-powered robotic tractors for precision agriculture
M. Gonzalez-de-Soto, L. Emmi, C. Benavides, I. Garcia, and P. Gonzalez-de-Santos
Biosystems Engineering, ISSN 1537-5110, vol. 143C, pp. 79-94
DOI: *http://dx.doi.org/10.1016/j.biosystemseng.2016.01.008*
Impact Factor (2014): 1.619
Category: Agriculture, Multidisciplinary: 9/56 (Q1)
Category: Agricultural, Engineering: 4/12 (Q2)

Autonomous systems for precise spraying – Evaluation of a robotised patch sprayer
M. Gonzalez-de-Soto, L. Emmi, M. Perez-Ruiz, J. Aguera, and P. Gonzalez-de-Santos
Biosystems Engineering, ISSN 1537-5110
DOI: *http://dx.doi.org/10.1016/j.biosystemseng.2015.12.018*
Impact Factor (2014): 1.619
Category: Agriculture, Multidisciplinary: 9/56 (Q1)
Category: Agricultural, Engineering: 4/12 (Q2)

Integrating sensory/actuation systems in agricultural vehicles
L. Emmi, M. Gonzalez-de-Soto, G. Pajares, and P. Gonzalez-de-Santos
Sensors, ISSN 1424-8220, vol. 14, no. 3, pp. 4014–4049, 2014.
DOI: *http://dx.doi.org/10.3390/s140304014*
Impact Factor (2014): 2.245
Category: Instruments & Instrumentation: 10/56 (Q1)
Category: Chemistry, Analytical: 31/74 (Q2)
Category: Electrochemistry: 14/28 (Q2)

A la memoria de mi madre

A Leticia y al niñ@ que crece en su interior

A mi padre y a toda mi familia

Financiación

La investigación llevada a cabo para obtener los resultados de las publicaciones expuestas en esta memoria de tesis doctoral (presentada en modalidad de compendio de publicaciones) ha recibido financiación del Séptimo Programa Marco de la Unión Europea [FP7 / 2007-2013] en virtud de Acuerdo de Subvención nº 245986.

Agradecimientos

Llegado este momento, en el que espero concluir mi formación como doctorando, quiero dedicar unas líneas a mostrar mi agradecimiento a todas aquellas personas que me han apoyado y ayudado a finalizar el programa de doctorado.

En primer lugar quiero agradecer a los directores de la presente tesis doctoral, el Dr. Pablo González de Santos y el Dr. Isaías García Rodríguez por todo el apoyo, ayuda y orientación que me han ofrecido durante el desarrollo de los artículos científicos y en la redacción de esta memoria. Quiero dar las gracias a Pablo por ofrecerme la posibilidad de realizar este doctorado abordando una temática de gran interés para mí, también le agradezco todo el tiempo, paciencia y dedicación invertido en la excelente dirección de esta tesis, así como toda su ayuda y valiosas enseñanzas durante estos años las cuales me han permito desarrollar mis dotes en investigación, redacción y divulgación de documentación científica. A Isaías le agradezco su apoyo, colaboración y consejos aportados para lograr sacar adelante esta tesis doctoral así como todos sus acertados consejos para mejorar la redacción y divulgación del trabajo realizado.

Agradezco la posibilidad de trabajar en un excelente centro de investigación como lo es el Centro de Automática y Robótica (CSIC-UPM), rodeado de grandes investigadores y trabajadores de los que he aprendido mucho, quiero felicitar a dicho centro por la

importante labor de investigación llevada a cabo y agradecerle todos los recursos prestados para el desarrollo de la presente tesis doctoral así como a todo su personal por el apoyo proporcionado. A su director, el Dr. Manuel A. Armada, le agradezco en interés en la evolución del proyecto. Al Dr. Luis Emmi, autor principal de la cuarta publicación compendiada en esta memoria de tesis, le quiero mostrar mi especial agradecimiento por todo el apoyo, ayuda, aportaciones y colaboración que ha prestado para el desarrollo de los trabajos compendiados en esta tesis doctoral. También quiero agradecer las aportaciones, consejos y apoyo moral de todos mis compañeros del CAR, principalmente del Departamento de Robótica de Exteriores y Servicios y la ayuda del personal del taller. Entre ellos, quisiera mencionar al Dr. José de No, Javier Sarria, Daniel Sanz, el Dr. Hector Montes, la Dra. Roemi Emilia Fernandez y la Dra. Carlota Salinas por el interés, ánimo, sugerencias e ideas que me han trasmitido para seguir adelante con esta tesis.

Considerando la gran importancia de conservar, preservar y cuidar del medio ambiente, quiero agradecer y felicitar a la Universidad de León por implantar programas de formación que abordan esta necesidad y ayudan a investigar tanto los trastornos medioambientales como las soluciones para subsanarlos. Agradezco a dicha universidad la posibilidad de llevar a cabo este programa de doctorado en "Ciencia y Tecnología del Medio Ambiente y Procesos" y a la Escuela Superior y Técnica de Ingeniería Agraria de esta universidad le agradezco la formación doctoral recibida en el Máster Universitario en Energía Renovables. Quiero resaltar mi agradecimiento al Dr. Antonio Moran, coordinador de dicho master, por su ayuda, colaboración y consejos, representando la figura de tutor de esta tesis doctoral. Y, también, quiero agradecer las enseñanzas de todo el profesado e instituciones que han contribuido en mi formación académica y recordar a todos mis compañeros de estudios.

Agradezco la financiación del proyecto RHEA por parte del Séptimo Programa Marco de la Unión Europea [FP7 / 2007-2013] con la cual se han podido llevar a cabo las investigaciones expuestas en esta tesis doctoral. Dentro de este proyecto RHEA, también quiero mostrar mi agradecimiento a los compañeros de proyecto por su ayuda, consejo y colaboración. Quiero agradecer las sugerencias, consejos, apoyo e interés mostrado en el avance de la tesis tanto por parte de la Dra. Ángela Ribeiro y el Dr. Jesús Conesa, desde el otro grupo del CAR participante en el proyecto RHEA, como por parte del Dr. Gonzalo

Pajares, el Dr. Martin Montalvo, el Dr. José Miguel Guerrero y la Dra. María Guijarro, desde el grupo de la UCM. También agradezco la colaboración del Dr. Manuel Pérez Ruiz y el Dr. Juan Agüera, desde el grupo de AgroSAP, para lograr llevar a cabo la tercera publicación compendiada en esta tesis. Además, quiero agradecer la disponibilidad y cooperación de George Kaplanis, del grupo de Tropical, y de Benoit Debilde, de la multinacional Case New Holland Industrial (CNHi), para proporcionarme información y documentación sobre sus sistemas.

Quiero agradecer todo el apoyo incondicional por parte de toda mi familia. A mis padres Heliodoro y Mª Consolación (†2014) les agradezco el haberme guiado a lo largo de toda mi vida, sin ellos no habría llegado hasta aquí. Desgraciadamente mi madre no ha llegado a verme concluir el doctorado, pero, sin duda, su recuerdo me sigue guiando y ayudando a mejorar desde allá donde esté. Deseo mostrar mi especial agradecimiento por todo el tiempo y la paciencia que ha dedicado Leticia Moreno para escucharme, ayudarme y apoyarme durante todo el desarrollo de esta tesis doctoral. Además, agradezco el apoyo por parte de mis hermanos Juan Ángel y Mª del Pilar y de mis sobrinos. Y también, quiero recordar y agradecer los consejos y orientación que recibí por parte de mis abuelos Félix (†2005) y Bonifacia (†1998), de mi abuela Benita (†2005) y de mi bisabuelo Pablo (†1998) durante mis años de educación y formación previos al doctorado e incluir a mi abuelo Rosalino (†1962) a quien no tuve la dicha de conocer en persona.

Para finalizar estos agradecimientos, quiero agradecer todo apoyo de mis amigos (mencionar a Herminio Sanz por su interés y comentarios sobre la tesis y los artículos), familiares y demás personas que no he nombrado en esta breve reseña de agradecimientos (disculpadme por ello) y que me han mostrado su apoyo sincero durante este tiempo de estudio y dedicación, y recordar al pueblo de Pedro Rodríguez (Ávila) en el que crecí.

¡Muchas gracias a todos!

Sinceramente:

Mariano González de Soto

A lo largo de espacio hay energía. ... es una mera cuestión de tiempo hasta que los hombres tengan éxito en sus mecanismos vinculados al aprovechamiento de esa energía.

***Nikola Tesla** (1856 – 1943)*

Resumen

En las últimas décadas se ha producido un gran aumento en la contaminación del medioambiente. El incesante uso de combustible fósil genera una gran contaminación atmosférica con las consecuentes alteraciones climáticas, además de los problemas de salud provocados por estas emisiones contaminantes. Estos combustibles son la principal fuente de energía para vehículos móviles, como lo son los vehículos agrícolas. Otra problemática generada en la actual agricultura intensiva es el uso de productos químicos utilizados para combatir las plagas indeseadas que merman y dañan la producción. Gran parte de estos productos suele terminar en el subsuelo contaminando las aguas freáticas. Abordando estas problemáticas, esta memoria de tesis doctoral presenta una serie de publicaciones de investigación para reducir la contaminación generada en las tareas agrícolas llevadas a cabo por sistemas automatizados.

Concretamente, las 4 publicaciones expuestas en esta memoria de tesis doctoral por compendio de publicaciones se centran en la reducción contaminantes atmosféricos e hídricos utilizando sistemas robotizados para tratamientos de precisión aplicados en agricultura. Para las pruebas experimentales presentadas en estas publicaciones se han utilizado los vehículos robóticos e implementos desarrollados en el proyecto RHEA (European Union FP7-NMP 245986), las tareas agrícolas consideradas en estas publicaciones también han sido las desarrolladas dentro de este proyecto: (a) control de

malas hierbas en cultivos agrícolas utilizando herbicidas; (b) control de malas hierbas en cultivos con surcos amplios y gran resistencia a temperaturas elevadas durante pequeños periodos de tiempo (como maíz, cebollas, ajos, puerros, etc.) mediante la aplicación directa de llamas; y (c) control de plagas en árboles aplicando insecticidas. Además, es importante tener en cuenta que gran parte de los resultados obtenidos se pueden extender a otras tareas, tanto del sector agrícola como de otros sectores.

En primer lugar se presenta y analiza una metodología para reducir el combustible empleado en tareas agrícolas. Para ello se desarrolla un modelo de consumo de combustible del robot agrícola y una representación tridimensional del terreno para analizar y estudiar el consumo en cada instante y en cada zona del cultivo. Con estos datos se aplican una serie de algoritmos diseñados para buscar la mejor secuencia de actuación respecto al consumo de combustible por parte del robot agrícola para llevar a cabo la tarea correspondiente. Finalmente, se valida el método realizando una serie de pruebas experimentales en cultivos reales para las tres tareas agrícolas consideradas mediante el análisis de los resultados obtenidos. Los resultados demuestran que el uso de este tipo de métodos reduce significativamente el combustible empleado, y que considerar las alturas del terreno es especialmente interesante para tareas donde existen variaciones importantes en la masa del sistema. Cabe destacar que el método descrito también es válido para otras tareas, tanto agrícolas como de otro tipo.

La segunda publicación presenta la reducción de los gases de escape nocivos para el medio ambiente y para la salud utilizando un sistema hibrido de energía. Para ello se reduce carga al motor de combustión interna añadiendo un sistema de abastecimiento energético eléctrico basado en fuentes limpias, el cual está formado por una pila de combustible, baterías y un panel fotovoltaico. Un primer estudio analiza que parte de la demanda energética es factible abastecer con el sistema eléctrico y se determinan los cambios más convenientes a realizar en los vehículos e implementos para un buen aprovechamiento del sistema hibrido de potencia. A continuación se desarrolla un modelo energético para calcular la demanda energética de las diferentes tareas, los picos de potencia y su valor medio, así como los demás datos necesarios para diseñar y dimensionar el sistema de abastecimiento de energía eléctrica. Finalmente, se analizan los gases de escape emitidos al utilizar este sistema hibrido de potencia y se comparan estos valores con

los resultados obtenidos al utilizar el motor de combustión interna como única fuente de potencia. En esta comparación se obtiene que la reducción de gases contaminantes alcanza valores cercanos al 50%.

La tercera publicación analiza el control de malezas en cultivos agrícolas mediante la aplicación precisa de herbicidas utilizando un sistema de sulfatación robotizado. En esta publicación se describe detalladamente el sistema robotizado para llevar a cabo una fumigación con herbicida sobre los parches de malezas en cultivos agrícolas, donde el mapa de malas hierbas puede ser conocido a priori o generado mientras se está realizando la tarea. Se presenta una serie de experimentos que demuestran que el uso de este sistema logra tratar más del 99% de las hierbas detectadas desperdiciando una cantidad mínima de herbicida. El uso de este tipo de sistemas reduce significativamente los productos químicos vertidos sobre el suelo que pueden llegar al nivel freático con la consecuente contaminación de las aguas subterráneas.

Finalmente, la cuarta publicación expuesta en esta tesis doctoral describe y analiza un sistema para el tratamiento ecológico de malas hierbas en cultivos con gran resistencia al fuego y surcos amplios. Este sistema sustituye los productos químicos empleados (herbicidas) por energía calorífica, lo que hace que pueda ser utilizado tanto en la agricultura ecológica como en la sostenible. Esta energía puede ser proporcionada por fuentes limpias como los son los diferentes tipos de biogás. Además, este tratamiento térmico se centra en las zonas de las líneas de cultivo infestadas de hierba, aplicando un proceso de aricado entre dichas líneas. La publicación describe una serie de experimentos de campo que demuestran que este sistema es capaz de tratar el 91% de las malas hierbas germinadas junto a las líneas del cultivo (en estas pruebas todo el espacio entre líneas de cultivo es aricado).

Abstract

In the last decades there has been a large increase in environmental pollution. The incessant use of fossil fuels generates large air pollution with consequent climate change, in addition to the health problems caused by these pollutant emissions. These fuels are the main energy source for mobile vehicles, such as agricultural ones. Another problem generated in the current intensive agriculture is the use of chemicals to combat undesired pests that undermine and damage the production. Many of these products usually arrive to the water table polluting groundwater. Considering these issues, this doctoral dissertation presents a series of research publications to reduce pollution in agricultural tasks using automated systems.

Concretely, the 4 publications presented in this doctoral dissertation by compendium of publications are focused on reducing atmospheric and water pollutants using robotic systems for precision treatments in agriculture. For the experimental tests presented in these publications, we have used robotic vehicles and implements developed in the RHEA project (European Union FP7-NMP 245986), the agricultural tasks considered in these publications have also been those developed within this project: (a) weed control in agricultural crops using herbicides; (b) weed control in crops with wide row spaces that can withstand high temperatures over short periods of times (such as corn, onions, garlic, leeks, etc.) by direct application of flame; and (c) pest control in trees using insecticides.

Furthermore, it is important to take into account that many of the obtained results can be extended to other tasks, both for the agriculture and others sector.

First, we present and analyze a methodology to reduce the fuel used in agricultural tasks. For this, we developed a fuel consumption model of the agricultural robot and a three-dimensional representation of the crop field to analyze and study the fuel consumption in real-time for every area of cultivation. With these data, we apply a series of algorithms designed to search for the best sequence of actions respect to the fuel consumption of the agricultural robot to perform the corresponding task. Finally, the method is validated analyzing the results obtained when we performed a series of experimental tests over true agricultural crops for the three tasks considered. The results demonstrate that the fuel consumed can be reduced by using the presented methods and considering the terrain elevations, which is particularly interesting for tasks where the system mass varies significantly.

The second publication presents the reduction of exhaust gases which are dangerous for the environment and for the health using a hybrid power system. For this, the internal combustion engine load is reduced by adding an electric power system based on clean energy sources, which is formed by a fuel cell, a photovoltaic panel and some batteries. In a first study, we analyze what part of the energy demand is feasible to be supplied with the electrical power system and we determine the most convenient changes on the vehicles and the implements to take advantage of the hybrid power system. Then, we develop an energy model to calculate the energy demand of the different tasks, power peaks and average values, as well as other necessary data to design and size the electrical power supply system. Finally, we analyze the exhaust gas using this hybrid power system and these values are compared with the results obtained using the internal combustion engine as the only power source. In this comparison it is obtained that the reduction of greenhouse gases reaches values close to 50%.

The third publication analyzes the weed control in agricultural crops applying herbicides with precision techniques using a robotised patch sprayer. This publication describes in detail the robotic system used to perform herbicide spraying over the weed patches in agricultural crops, where the weed map can be previously known or generated while the task is performed. This publication presents a series of experiments

demonstrating that the use of this type of system is able to treat more than 99% of the detected weeds wasting a minimal herbicide amount. The use of this type of system significantly reduces the chemical products poured over the floor which can reach the water table with a consequent pollution of groundwater.

Finally, the fourth publication exposed in this doctoral dissertation describes and analyzes a system for the organic weeds control in crops with high resistance to fire and wide grooves. This system replaces the chemical products (herbicides) by heat energy which could be provided by clean sources, such as some form of biogas; therefore this treatment can be used in organic agriculture and in sustainable agriculture. Furthermore, this heat treatment is focused on the areas of crop rows infested with weeds, applying a process of light tillage between these lines. The publication describes a series of field experiments which demonstrates that this system is capable of treating approximately 91% of the weed germinated close to the crop rows (in these tests the entire space between crop lines is plowed).

ÍNDICE DE CONTENIDOS

Índice de figuras

Índice de tablas

Nomenclatura

ASABE	Sociedad Americana de Ingenieros Agrícolas y Biológicos (American Society of Agricultural and Biological Engineers)
CAR	Centro de Automática y Robótica
CNHi	Case New Holland industrial
CO	monóxido de carbono
CO_2	dióxido de carbono
CSIC	Consejo Superior de Investigaciones Científicas
GNSS	Sistema Global de Navegación por Satélite (Global Navigation Satellite System)
GPS	Sistema de Posicionamiento Global (Global Positioning System)
GWP	potencial de calentamiento global (global-warming potential)
HC	hidrocarburos

ICA	Instituto de Ciencias Agrarias
MCI	motor de combustión interna
MDT	modelo digital de terreno
NO_X	óxidos de nitrógeno
O_2	oxígeno
PEM	membrana de intercambio de protones (proton exchange membrane)
PLC	controlador lógico programable (programmable logic controller)
PM	partículas en suspensión (particulate matter)
PTO	power take-off
rpm	revoluciones por minuto
SEE	sistema de energía eléctrica
SHE	sistema hibrido de energía
TDF	toma de fuerza
UMT	unidad móvil terrestre
UPM	Universidad Politécnica de Madrid
WGS84	Sistema Geodésico Mundial 1984 (World Geodetic System of 1984)
ASABE	Sociedad Americana de Ingenieros Agrícolas y Biológicos
CNHi	Case New Holland industrial
CO	monóxido de carbono
CO_2	dióxido de carbono

GNSS	sistema global de navegación por satélite
GPS	sistema de posicionamiento global (global positioning system)
GWP	potencial de calentamiento global
HC	hidrocarburos
MCI	motor de combustión interna
MDT	modelo digital de terreno
NO_X	óxidos de nitrógeno
O_2	oxígeno
PEM	membrana de intercambio de protones
PLC	controlador lógico programable
PM	partículas en suspensión
PTO	power take-off
rpm	revoluciones por minuto
SEE	sistema de energía eléctrica
SHE	sistema hibrido de energía
TDF	toma de fuerza
UMT	unidad móvil terrestre
WGS84	world geodetic system of 1984

1 INTRODUCCIÓN A LA TEMÁTICA Y SU JUSTIFICACIÓN

En la actualidad existe un gran problema con la contaminación del medio ambiente, principalmente con la contaminación atmosférica sin olvidar la contaminación de las aguas. Gran parte de esta contaminación se genera por el uso de fuentes de energía de origen fósil y por la multitud de productos químicos utilizados para infinidad de aplicaciones cotidianas e industriales de las cuales la sociedad es más dependiente cada día. La contaminación atmosférica genera alteraciones climáticas (como el incremento del efecto invernadero), daños en la capa de ozono, lluvia ácida, etc. Esto da lugar a graves problemas en los ecosistemas, en el clima, en la salud e incluso en la arquitectura. La contaminación del agua subterránea merma el agua potable y daña la biosfera fluvial y marina, repercutiendo en la flora y fauna de los ecosistemas así como en la salud y calidad de vida de la sociedad. La industria y el transporte son los principales causantes de esta problemática con la contaminación, siendo la industria agrícola una fuente importante en la generación de contaminación atmosférica y quizá la principal responsable en la contaminación de las aguas subterráneas.

1.1 Contaminación generada en la agricultura

La agricultura es la industria que más superficie de la tierra ocupa y a la que se destinan dos terceras partes del agua utilizada por el hombre. Las tareas de producción agrícola tienen importantes efectos en el medio ambiente, siendo una de las principales fuentes de contaminación del agua por nitratos, fosfatos y pesticidas. En estas tareas también se genera gran cantidad de contaminantes atmosféricos como dióxido de carbono, metano y óxido nitroso, los cuales en su mayoría son emitidos por los sistemas empleados. Además, las prácticas actuales están contribuyendo a la degradación de la tierra, la salinización, el decremento de las aguas subterráneas y la reducción de la biodiversidad genética [1].

Esta tesis doctoral se centra en la contaminación generada por los vehículos agrícolas y por los tratamientos químicos aplicados en los cultivos; por lo que, a continuación, se analiza la contaminación generada por estos vehículos y tratamientos.

1.1.1 Contaminación atmosférica

La principal causa de la contaminación atmosférica es el uso de combustibles fósiles tales como el petróleo, el carbón y el gas natural. Los motores de combustión interna de los vehículos utilizan principalmente gasóleo y gasolina, combustibles derivados del petróleo, aunque actualmente incorporan una pequeña cantidad de biocombustibles. Dentro de este tipo de vehículos tenemos las tecnologías empleadas en la agricultura, ya que los vehículos agrícolas en su inmensa mayoría funcionan con motores de combustión interna (MCI) que utilizan estos combustibles fósiles, principalmente gasóleo, y emiten niveles considerables de contaminantes atmosféricos, tales como dióxido de carbono (CO_2), óxidos de nitrógeno (NO_X), monóxido de carbono (CO), hidrocarburos (HC) y partículas en suspensión (PM).

El dióxido de carbono (CO_2), también conocido como anhídrido carbónico, es el principal gas de efecto invernadero, cuya proporción atmosférica esta aumentado excesivamente en los últimos años dando lugar a graves alteraciones en las temperaturas del planeta. Se genera en casi todos los procesos de combustión, aunque cuando el combustible es biomasa las emisiones no se consideran contaminantes al tratarse de un ciclo cerrado en el que el ecosistema reutiliza este CO_2 para producir nueva biomasa. Al ser el principal gas de efecto invernadero, se suele utilizar como referencia para la medida

del efecto invernadero de otros gases, hablando de toneladas equivalentes de CO_2 o del índice GWP (potencial de calentamiento global) cuyo valor es 1 para el CO_2 [2].

Los óxidos de nitrógeno son el conjunto de gases formados por nitrógeno y oxígeno en diferentes proporciones (su fórmula química generalizada es NO_X). La concentración de estos gases en las emisiones contaminantes es mucho menor que la de CO_2, sin embargo generan un efecto invernadero mucho mayor, concretamente, el NO_2 tiene un GWP de 296. Se originan en los procesos de combustión a altas temperaturas a partir del oxígeno y el nitrógeno presentes en la atmósfera. Además, los NO_X pueden contribuir a la formación de esmog[1] el cual genera problemas para la salud que afectan principalmente al sistema respiratorio provocando bronquitis y neumonía, reduciendo la resistencia a las infecciones de las vías respiratorias. También pueden producir irritación de los ojos, la nariz, la garganta, los pulmones, y causar tos y una sensación de falta de aliento, cansancio y náuseas. De igual forma, pueden repercutir sobre la vegetación y el patrimonio cultural ya que en la atmósfera pueden dar lugar a la formación de ácidos nítricos provocando lluvia ácida siendo considerados importantes precursores de la contaminación por ozono troposférico como consecuencia de las reacciones fotoquímicas entre los NO_X y los hidrocarburos, [3], [2], [4].

El monóxido de carbono (CO) es un gas inflamable, incoloro, insípido, ligeramente menos denso que el aire y altamente tóxico. Se genera en procesos de combustión incompleta, como puede ser en los motores de combustión interna, principalmente cuando trabajan a baja temperatura. Puede ser muy peligroso ya que es difícil de detectar y reacciona con la hemoglobina de la sangre (su afinidad por la hemoglobina es unas 240 veces mayor que la del oxígeno), formando carboxihemoglobina, lo que disminuye la capacidad de transporte de oxígeno desde los pulmones a los órganos y tejidos del cuerpo. Los síntomas por la inhalación de CO pueden ser: dificultad de concentración, perdida de reflejos y mala coordinación, disminución de las funciones neuroconductuales, somnolencia, cansancio, cefaleas, problemas cardiovasculares, durante el embarazo pone

[1] Definición del DRAE: Niebla mezclada con humo y partículas en suspensión, propia de las ciudades industriales.

en peligro el crecimiento y desarrollo mental del feto, y en altas concentraciones puede llegar a provocar la muerte [3], [2], [4].

Los hidrocarburos (HC) son restos de combustible en los gases de escape generados por una mala combustión. Esta combustión incompleta se debe generalmente a una mala proporción de oxígeno y carburante, falta de oxígeno durante la combustión o a una baja velocidad de inflamación. Estos HC se manifiestan en diferentes combinaciones, principalmente formando xilenos, tolueno, benceno o etilbenceno. Estos gases son nocivos para la salud, pueden provocar dolor de cabeza, náuseas, mareos, alteraciones en el sistema nervioso, etc., además, el benceno es considerado un agente cancerígeno que incrementa las posibilidades de padecer leucemia o cáncer de colon [3], [2], [4].

Las partículas en suspensión son un amplio espectro de sustancias liquidas o sólidas, orgánicas o inorgánicas, dispersas en el aire, con un diámetro menor de 500 micrómetros (μm) y, en este caso, procedentes de la combustión en motores sin ser incluidas en los grupos descritos anteriormente. Debido a su pequeño tamaño presentan un elevado grado de penetración en los organismos y pueden permanecer mucho tiempo en los órganos del sistema respiratorio dando lugar a problemas respiratorios, irritaciones en las vías respiratorias, agravamiento de enfermedades como el asma o cardiovasculares, además de aumentar la probabilidad de cáncer de pulmón y muerte prematura [3], [2], [4].

1.1.2 Contaminación de las aguas

Los procesos agrícolas cada vez utilizan más productos químicos incrementado la contaminación difusa o dispersa de las aguas subterráneas (se habla de contaminación difusa cuando no están localizados los focos donde se genera esta contaminación, como en este caso que se extienden a toda la superficie del cultivo [5]). La agricultura intensiva necesita un aporte externo de nutrientes para lo que se suelen utilizar abonos químicos y/o fertilizantes orgánicos (residuos de animales). Además, es muy habitual el uso de pesticidas para combatir las plagas que dañan los cultivos y herbicidas para eliminar las plantas indeseadas que quitan agua y nutrientes al cultivo. Estos productos se esparcen por el campo de cultivo, haciendo un uso excesivo de ellos en numerosas ocasiones, por lo que gran parte no es absorbida por el cultivo siendo disuelta por el agua que se filtra a través del terreno. Aunque el subsuelo tiene una cierta capacidad para depurar las aguas, mediante procesos microbiológicos (en la zona de aireación) y procesos químicos

(hidrólisis, oxidación, reducción, etc.) cuando el flujo de contaminantes es elevado estos procesos no son suficientes y gran parte alcanza el nivel freático del terreno yendo a parar a las aguas subterráneas y contaminando las mismas [5]. La escorrentía de estas aguas puede llegar a ríos, embalses, acuíferos, etc. generando los consecuentes problemas ambientales y de salud.

En la agricultura se utilizan gran variedad de pesticidas para eliminar o controlar organismos no deseados en los cultivos, principalmente herbicidas e insecticidas para combatir malas hierbas e insectos respectivamente. Aunque también existen fungicidas para combatir hongos, nematicidas contra los parásitos y rodenticidas para combatir las plagas de roedores. Estos plaguicidas presentan un nivel de toxicidad y persistencia que ha de tenerse muy en cuenta a la hora de su uso, ya que gran parte de ellos suele terminar en las aguas fluviales, pudiendo llegar a incorporarse en organismos acuáticos. Por ello su concentración en agua potable y pescados suele estar regulada. En el "Estudio FAO Riego y Drenaje (1997)" [6] podemos encontrar un amplio inventario de los plaguicidas más utilizados en todo el mundo con su nivel máximo permitido en el agua potable y en los pescados y mariscos. Estos productos químicos pueden ser nocivos para la salud, no solo de las personas, sino de todos los seres vivos, dañando los ecosistemas y la biodiversidad. Pueden tener los siguientes efectos en los seres vivos: provocar muertes de organismos, incrementar las probabilidades de cáncer, dificultar la reproducción, dañar los sistemas inmunológicos, generar alteraciones hormonales y deformaciones. Además, pueden dar lugar a otros problemas en la salud de los organismos o efectos intergeneracionales que aparecerán en generaciones futuras de la especie [6].

1.2 Temática del compendio de publicaciones

Considerando los problemas, descritos anteriormente, que puede acarrear la contaminación generada por los vehículos y procesos agrícolas, la temática del compendio de publicaciones que forman esta memoria de tesis doctoral se centra en la investigación de técnicas para reducir esta contaminación. Para ello, las publicaciones expuestas en esta tesis doctoral describen una metodología que reduce el uso de recursos, tanto energéticos como materiales (productos químicos), empleados en tareas agrícolas utilizando tractores robotizados e implementos automatizados, con la consiguiente reducción en la contaminación generada. Además, se describen y analizan posibles alternativas no

contaminantes o, al menos, poco contaminantes para reemplazar parte del uso de los recursos responsables de las emisiones contaminantes. Se propone y se analiza un sistema hibrido de energía en el cual se incorporan diferentes sistemas energéticos basados en fuentes limpias y un sistema basado en la aplicación de llama directa para el control de malas hierbas en ciertos cultivos como una posible alternativa a los productos químicos. Este sistema además puede ser empleado dentro de la agricultura ecológica, la agricultura sostenible o la agricultura de conservación.

Los estudios y modelos llevados a cabo en estas publicaciones se realizan considerando las características de los tractores robotizados e implementos agrícolas del proyecto RHEA (FP7-NMP 245986), los cuales también son utilizados en las pruebas experimentales. Denominamos implemento agrícola al utensilio o herramienta utilizada para llevar a cabo una tarea agrícola [7], en este caso acoplada a un tractor robotizado al cual nos referiremos como UMT (Unidad Móvil Terrestre). Estos sistemas están diseñados para realizar tareas de control de plagas de malas hierbas e insectos en cultivos agrícolas de forma autónoma, en las cuales se centraran los análisis y pruebas desarrolladas en las publicaciones presentadas. Estas tareas agrícolas son las siguientes [8]:

- Tratamiento de malas hierbas en cultivos agrícolas mediante sulfatación de herbicidas.

- Tratamiento de malas hierbas en cultivos con surcos amplios y con gran resistencia a temperaturas elevadas, tales como maíz, cebollas, ajos, puerros, etc. El proceso consiste en el arado del espacio entre las líneas de cultivo y la aplicación de ráfagas de fuego a la hierba germinada junto al cultivo.

- Tratamientos de plagas de insectos en árboles mediante fumigación de insecticidas.

Las dos primeras publicaciones se centran en reducir las emisiones atmosféricas generadas por el MCI. La primera publicación del compendio, titulada "*Reducing fuel consumption in weed and pest control using robotic tractors*", presenta una metodología para reducir el combustible empleado en tareas agrícolas, centrándose en las tres tareas agrícolas enumeradas anteriormente (control de malas hierbas con herbicidas y con un tratamiento mecánico - térmico, así como control de plagas de insectos en árboles). En esta publicación se analiza el consumo de combustible fósil en cada una de las tres tareas para

así calcular el plan de trabajo que reduce el combustible fósil empleado, logrando reducir las emisiones contaminantes generadas, además de aumentar el consecuente beneficio económico. Para ello, se desarrolla un modelo de consumo de la UMT y una representación en tres dimensiones del terreno que para estimar el consumo de combustible fósil en los diferentes escenarios.

La segunda publicación de esta memoria de tesis doctoral se titula "Reducing air pollution with hybrid-powered robotic tractors for precision agriculture", en esta publicación se propone un sistema hibrido de abastecimiento energético para aplicaciones agrícolas y se analizan los beneficios medioambientales que conlleva el uso de estas tecnologías híbridas en tareas agrícolas. Para ello, se libera de carga (demanda energética) al MCI original del tractor añadiendo un sistema de energía eléctrica (SEE) basado en fuentes de energía limpias, tales como pilas de combustible, baterías y paneles solares. Posteriormente, se evalúa la reducción de emisiones contaminantes al llevar a cabo cada tarea utilizando el sistema hibrido de energía (SHE), comparando estas emisiones con las generadas al utilizar el MCI como única fuente de potencia.

Las otras dos publicaciones se centran en la reducción de productos químicos que contribuyen a la contaminación de los recursos hídricos del planeta. Concretamente, la tercera publicación, "*Autonomous systems for precise spraying – Evaluation of a robotised patch sprayer*" describe y evalúa un sistema robotizado para el control de malas hierbas en cultivos agrícolas capaz de enfocar el tratamiento únicamente sobre las zonas afectadas. Para ello requiere de un sistema de detección de malas hierbas que genere un mapa con la distribución de las zonas infestadas por el cultivo, este mapa puede ser generado previamente a la tarea o mientras se está realizando la tarea (en tiempo real). Este sistema hace un mejor uso del pesticida y obtener una significativa reducción de la cantidad total de producto aplicado sobre la superficie total de cultivo.

Para finalizar, la cuarta publicación de este compendio de publicaciones titulada "*Integrating sensory/actuation systems in agricultural vehicles*" analiza la integración de sensores y actuadores en un sistema autónomo para el control de malas hierbas considerando la ideología de la agricultura ecológica, la cual se basa en optimizar el uso de los recursos naturales, sin emplear productos químicos de síntesis, u organismos genéticamente modificados [9], [10]. En esta publicación, se presenta una alternativa a los

herbicidas basada en la aplicación de calor, el cual puede obtenerse a partir de fuentes renovables como algún tipo de biogás; y además analiza un sistema capaz de detectar las áreas infestadas en tiempo real para activar el tratamiento únicamente en las zonas afectadas. Esta publicación analiza la integración del sistema de control del vehículo y del implemento, así como el sistema de detección de malas hierbas y surcos en un único controlador. Para ello, se evalúa un sistema de tratamiento de malas hierbas en cultivos con cierta resistencia al fuego y con surcos amplios mediante un proceso de arado en el espacio entre líneas de cultivo y aplicación directa de llama en las líneas de cultivo con malezas.

1.3 Estructura de la tesis

El resto del presente documento está organizado del siguiente modo: En el capítulo 2 se establecen los objetivos concretos de este trabajo para reducir la contaminación de la atmosfera y de las aguas generada por los sistemas y técnicas agrícolas mediante el uso de sistemas robotizados dentro de la agricultura de precisión. Además, en este mismo capítulo, se presentan los recursos y materiales empleados, haciendo una breve descripción de los diferentes sistemas al igual que del entorno de pruebas utilizado para llevar a cabo los distintos experimentos. Seguidamente, el capítulo 3 recoge el estado del arte concerniente a las diferentes investigaciones planteadas y realizadas en los últimos años que han perseguido objetivos cercanos o similares a los definidos en el capítulo 2.

Los capítulos 4, 5, 6 y 7 recogen cada una de las publicaciones que forman esta tesis doctoral por compendio de publicaciones. Las publicaciones asociadas a cada capítulo son:

- Capítulo 4:

  M. Gonzalez-de-Soto, L. Emmi, I. Garcia, y P. Gonzalez-de-Santos, P. 2015. Reducing fuel consumption in weed and pest control using robotic tractors. *Computers and Electronics in Agriculture*, 114, pp. 96–113

- Capítulo 5:

  M. Gonzalez-de-Soto, L. Emmi, C. Benavides, I. Garcia, and P. Gonzalez-de-Santos, P. 2016. Reducing air pollution with hybrid-powered robotic tractors for precision agriculture. *Biosystems Engineering*, 143C, pp. 79-94

- Capítulo 6:
  M. Gonzalez-de-Soto, L. Emmi, M. Perez-Ruiz, J. Aguera, and P. Gonzalez-de-Santos, P. 2016. Autonomous systems for precise spraying - Evaluation of a robotised patch sprayer. *Biosystems Engineering.*
- Capítulo 7:
  Emmi, L., Gonzalez-de-Soto, M., Pajares, G., Gonzalez-de-Santos, P. 2014. Integrating sensory/actuation systems in agricultural vehicles. *Sensors, 14,* pp. 4014-4049.[2]

Posteriormente, se han recogido los resultados obtenidos en cada una de estas publicaciones y su correspondiente discusión en el capítulo 8, en el cual se da una visión unificada del trabajo realizado a lo largo del desarrollo de la tesis. El capítulo 9 presenta las conclusiones obtenidas a partir de los trabajos de investigación realizados y, a continuación, el capítulo 10 presenta estas mismas conclusiones en inglés. En cada publicación correspondiente se puede encontrar la información contextualizada referente tanto a los resultados como a las conclusiones enumeradas en estos 3 últimos capítulos. Para finalizar, se dedica el último capítulo de esta tesis doctoral, numerado como el 11, a proponer futuras líneas de investigación relacionadas con la temática tratada.

[2] La investigación llevada a cabo para esta publicación se engloba en un proyecto de ámbito más amplio, parte de cuyos resultados fueron reflejados en el texto de otra tesis doctoral con formato tradicional [11]. Dicha tesis refleja una parte de la investigación enfocada a contribuir en la configuración informática para el control y manejo de flotas de robots en agricultura de precisión, claramente separada del objetivo y los resultados de la investigación reflejados en el presente documento. En cualquier caso, dado que se compartió y se utilizó el mismo material y los experimentos en ambas investigaciones, se podrán encontrar aquí ciertas informaciones (en el texto, las tablas y los resultados) que aparecen también en la tesis doctoral mencionada.

2 OBJETIVOS DE LA TESIS, RECURSOS Y MATERIALES

El objetivo principal de esta tesis doctoral es reducir la contaminación de la atmosfera y de los recursos hídricos de nuestro planeta Tierra generada en procesos agrícolas. Para lo cual se estudian, diseñan y prueban técnicas para reducir tanto el uso de combustibles de origen fósil como el de los productos químicos empleados en producción agrícola, así como investigar y analizar posibles alternativas a estas fuentes de contaminación. Considerando este objetivo principal se han obtenido las publicaciones compendiadas en esta tesis doctoral cuyos objetivos se pueden encontrar enumerados en la sección 2.1.

En las pruebas y demostraciones realizadas para estas publicaciones se han empleado una serie de recursos y materiales descritos en la sección 2.2. Estos recursos y materiales fueron diseñados para unos procesos concretos de control de plagas de malas hierbas e insectos en los cuales se basan los experimentos presentados en las publicaciones. Sin embargo, se pretende elaborar una metodología general para cada objetivo correspondiente (de los enumerados a continuación) que pueda ser aplicada a otras tareas agrícolas diferentes, e incluso a otro ámbito de actividad.

2.1 Objetivos

Para lograr reducir los contaminantes atmosféricos e hídricos generados en tareas agrícolas se han perseguido cuatro objetivos principales, obteniendo una publicación a partir de cada uno de ellos, con sus correspondientes subobjetivos, los cuales se enumeran a continuación.

- Reducir las emisiones atmosféricas contaminantes mediante la reducción del combustible empleado por tractores agrícolas robotizados, para lo cual se ha buscado:
    - Implementar un modelo de consumo de combustible del vehículo para analizar el consumo en las diferentes situaciones de trabajo.
    - Desarrollar una metodología de trabajo para conseguir el mejor aprovechamiento de los recursos energéticos empleados.
    - Obtener una representación tridimensional del entorno de trabajo para estimar los requerimientos energéticos de las posibles opciones que existen para realizar la tarea.
    - Implementar una serie de algoritmos para calcular las trayectorias óptimas de los distintos tratamientos agrícolas.
    - Estimar cuantitativamente el ahorro de combustible que se puede conseguir utilizando este tipo de medidas.
- Buscar y analizar una serie de alternativas de energía limpia que libere carga de trabajo al MCI del tractor robotizado con la consiguiente reducción en el combustible empleado y, por tanto, en la contaminación atmosférica emitida, para lo cual ha sido necesario:
    - Analizar la demanda energética y el uso de sistemas de energía limpia como apoyo al MCI principal para abastecer parte de esta demanda energética.

  - Diseñar y dimensionar un sistema hibrido de abastecimiento energético basado en el MCI y fuentes de energía no contaminantes para abastecer la demanda energética calculada.

  - Obtener un modelo de emisiones contaminantes del MCI para estimar los contaminantes emitidos en las diferentes situaciones de trabajo, considerando la carga y la velocidad del motor.

  - Proponer una serie de cambios y medidas para lograr un uso energético eficiente del sistema hibrido de energía desarrollado.

  - Calcular una aproximación de la reducción lograda para cada uno los principales contaminantes atmosféricos emitidos por los MCI al incorporar un sistema paralelo de energía basado en fuentes limpias.

- Reducir el uso de productos químicos en las aplicaciones agrícolas utilizando tractores robotizados y sistemas automatizados para conseguir mantener la efectividad del tratamiento, para lo cual ha sido necesario:

  - Describir un sistema robotizado capaz de utilizar eficientemente los productos químicos empleados en tratamientos agrícolas.

  - Definir una metodología para hacer un buen uso de este sistema y lograr reducir los productos químicos empleados.

  - Calcular la precisión teórica del tratamiento según las características del sistema así como medir estos valores empíricamente para diferentes situaciones.

  - A partir de los datos obtenidos, hacer una estimación de la reducción de productos químicos, considerados contaminantes, que se puede lograr utilizando este tipo de sistemas.

- Buscar alternativas basadas en tecnología robótica y automatización para los tratamientos basados en la aplicación de productos químicos obteniendo un resultado similar. Con esta alternativa se pretende dar una idea de las posibilidades

que puede aportar el campo de la robótica a las técnicas agrícolas respetuosas con el entorno y el medio ambiente. Los subobjetivos buscados han sido:

- Describir y analizar alternativas a la aplicación de productos químicos para llevar a cabo un tratamiento similar. Estas alternativas han de ser más respetuosas con el medio ambiente cumpliendo la normativa de agricultura ecológica, sostenible y/o de conservación.

- Estudiar y analizar las posibilidades que ofrece la robótica y la automatización para la ejecución del nuevo tratamiento alternativo propuesto.

- Obtener una estimación de los beneficios medioambientales obtenidos al utilizar el tratamiento alternativo propuesto respecto al uso de productos químicos.

2.2 Recursos y materiales empleados

Los resultados experimentales expuestos en esta memoria de tesis doctoral se han obtenido utilizando la flota de tractores robotizados, los implementos automatizados y la estación de control base desarrollados dentro del proyecto europeo RHEA[3] (FP7-NMP 245986) financiado por el Séptimo Programa Marco de la Unión Europea.

La flota de tractores robotizados está compuesta por tres UMTs que se ilustran en la Figura 1. Estos robots están basados en el tractor comercial modelo Boomer 3050 CVT del fabricante de maquinaria agrícola Case New Holland (CNHi) [12] que han sido modificados y adaptados para obtener estas UMTs. Concretamente, se han añadido

[3]El consorcio de empresas que ha participado en este proyecto estaba formado por: Agencia Estatal Consejo Superior de Investigaciones Científicas (CSIC), CogVis GmbH, Forschungszentrum Telekommunikation Wien Ltd. (FTW), Cyberbotics Ltd, Università di Pisa, Universidad Complutense de Madrid (UCM), Tropical, Soluciones Agrícolas de Precisión S.L., Universidad Politécnica de Madrid (UPM), AirRobot GmbH & Co. KG, Università degli Studi di Firenze, IRSTEA, Case New Holland Industrial N.V., Bluebotics S.A., CM Srl.

Figura 1. Flota de tractores robotizados y estación base

controladores, sensores y demás sistemas necesarios para lograr un control totalmente automático de los mismos. Las características de las 3 UMTs son prácticamente las mismas, salvo que una de ellas presenta la tecnología "SuperSteer^{TM}" de CNHi, que le permite maniobrar con un radio de giro menor al de las otras dos unidades [13]. En cada publicación expuesta se detallan las características de estas unidades que necesitamos conocer para llevar a cabo los análisis, modelos y pruebas correspondientes.

Los implementos desarrollados en el proyecto RHEA, y utilizados en los experimentos de esta tesis doctoral, han sido tres:

- Un implemento sulfatador automatizado (Figura 2).
- Un implemento cultivador y con tratamiento térmico automatizado (Figura 3).
- Un implemento fumigador autónomo (Figura 4).

El implemento sulfatador automatizado es utilizado para el control de malas hierbas en cultivos agrícolas aplicando herbicidas. La Figura 2 muestra una UMT utilizando este implemento para llevar a cabo dicho tratamiento sobre un campo de trigo. En esta aplicación el mapa de malas hierbas del cultivo es ya conocido, lo proporciona un sistema de detección de malas hierbas externo a partir de fotos aéreas del cultivo que permiten un

Figura 2. Implemento sulfatador automatizado aplicando el tratamiento de control de malas hierbas sobre un campo de trigo

mejor análisis en este tipo de cultivos con surcos muy próximos. El implemento es capaz de activar cada una de sus 12 boquillas individualmente, así como de controlar el caudal y la concentración del producto aplicado. La publicación "*Autonomous systems for precise spraying - Evaluation of a robotised patch sprayer*" (pág. 67) presenta una descripción detallada de este implemento, así como un análisis profundo del tratamiento que es capaz de llevar a cabo. En las publicaciones "*Reducing fuel consumption in weed and pest control using robotic tractors*" (pág. 29) y "*Reducing air pollution with hybrid-powered robotic tractors for precision agriculture*" (pág. 49) también se hace una descripción básica de este implemento y se enumeran sus características importantes para la temática de la publicación correspondiente

El implemento cultivador con tratamiento térmico se utiliza para el control de malas hierbas en cultivos de surcos anchos y con gran resistencia a temperaturas elevadas. En la Figura 3 se muestra una UMT utilizando este implemento para controlar las malas hierbas en un campo de maíz. En este caso la UMT incorpora un sistema capaz de detectar las malas hierbas y los surcos en tiempo real. Este sistema permite corregir la trayectoria acorde a las líneas de cultivo así como activar los quemadores únicamente en las zonas infestadas con malas hierbas. El implemento consta de 8 quemadores, 2 por cada línea de cultivo tratada, los cuales pueden activarse separadamente. Además, cada quemador tiene

Figura 3. Implemento cultivador y con tratamiento térmico automatizado aplicando el tratamiento de control de malas hierbas sobre un campo de maíz

dos opciones de activación, baja y alta presión de gas, que permiten regular la llama según la densidad de mala hierba. La publicación "*Integrating sensory/actuation systems in agricultural vehicles*" (pág. 87) presenta un estudio exhaustivo de este implemento así como del tratamiento que es capaz de llevar a cabo. Además, este implemento se utiliza para las pruebas de las publicaciones "*Reducing fuel consumption in weed and pest control using robotic tractors*" (pág. 29) y "*Reducing air pollution with hybrid-powered robotic tractors for precision agriculture*" (pág.49) en las que se hace una descripción básica de los datos necesarios para los experimentos presentados en estas publicaciones.

El implemento fumigador autónomo se utiliza para fumigar pesticidas en árboles. En la Figura 4 se muestra este implemento trabajando en un campo de olivos. En esta aplicación el controlador principal de la UMT es prácticamente ajeno al tratamiento, tan solo indica cuando empieza y finaliza el tratamiento, una vez por cada línea de árboles; por tanto, este implemento es autónomo e incorpora su propio controlador capaz de detectar las copas de los árboles que ha de tratar utilizando sensores de ultrasonidos. Está pensado para tratar un lado de dos líneas de árboles (separadas 4 metros) simultáneamente en cada pasada. Posee ocho difusores, cuatro a cada lado, puede activar cada uno de estos difusores separadamente según el tamaño de la copa del árbol, y además puede regular el ángulo de los difusores superiores e inferiores, para adaptarse a la copa del árbol enfocando los

Figura 4. Implemento fumigador autónomo aplicando el tratamiento de control de plagas de insectos sobre un campo de olivos

difusores correctamente. Este implemento se utilizó en las publicaciones "*Reducing fuel consumption in weed and pest control using robotic tractors*" (pág. 29) y "*Reducing air pollution with hybrid-powered robotic tractors for precision agriculture*" (pág. 49) las cuales incluyen una descripción general del mismo con sus características más importantes para obtener los modelos y realizar los experimentos de la publicación correspondiente.

Los experimentos incluidos en todas las publicaciones fueron realizados en campos experimentales del Centro de Automática y Robótica (CAR) y del Instituto de Ciencias Agrarias (ICA), en Arganda del Rey (Madrid). El CAR es un centro de investigación con titularidad compartida entre la Agencia Estatal Consejo Superior de Investigaciones Científicas (CSIC) y la Universidad Politécnica de Madrid (UPM).

Para el análisis de resultados y las simulaciones llevadas a cabo se han empleado algoritmos que han sido desarrollados utilizando como herramientas software de cálculo y programación: *Matlab* (*MathWorks, Inc.*), *Labview* (*National Instruments*) y *Microsoft Visual Studio* (*Microsoft Corporation*). También se ha utilizado el programa de simulación robótica *Webots* (*Cyberbotics Ltd.*) para llevar a cabo algunas simulaciones virtuales previas a las pruebas experimentales.

3 ESTADO DEL ARTE

En los últimos años podemos encontrar multitud de trabajos de investigación científica motivados por la creciente preocupación respecto a la contaminación medioambiental, tanto de la atmosfera como de los recursos hídricos del planeta. Gran parte de estos trabajos se centran en la polución atmosférica generada por el uso de fuentes energéticas de origen fósil y otros muchos abordan la contaminación de las aguas producida por la multitud de productos químicos utilizados en la industria.

En este capítulo se presenta un análisis bibliográfico de los trabajos de investigación desarrollados para reducir la contaminación producida en las tareas agrícolas. Para ello, en las dos primeras secciones se presentan publicaciones enfocadas a la reducción de contaminantes atmosféricos emitidos por los vehículos agrícolas, ya sea mediante la reducción del combustible empleado (sección 3.1) o mediante el uso de fuentes energéticas respetuosas con el medio ambiente (sección 3.2). Posteriormente, las dos siguientes secciones revisan las publicaciones basadas en la contaminación de los recursos hídricos, la sección 3.3 presenta las publicaciones basadas en la reducción del uso de productos químicos y la sección 3.4 expone las publicaciones que presentan y analizan técnicas alternativas para llevar a cabo tratamientos agrícolas respetuosos con el entorno y el medio ambiente.

3.1 Reducción del combustible empleado en tareas agrícolas

La eficiencia energética es un concepto muy presente en todos los campos. Dentro de la agricultura podemos encontrar numerosas publicaciones científicas que han abordado este campo desde hace años. Respecto a la eficiencia en tareas de labranza, Grečenko (1968) presentó un proceso para optimizar la energía de arado considerando el comportamiento de las ruedas y otros factores del tractor, en combinación con el implemento respecto al rendimiento del sistema y desarrollando un método para predecir el rendimiento del tractor con implementos de labranza [14]. También podemos encontrar publicaciones más recientes, como la de Mileusnić et al. (2010) que analiza y compara el consumo de combustible en diversas variantes de procesos de arado obteniendo que los sistemas modernos presentaban mejor eficiencia energética [15].

Otros investigadores han centrado sus trabajos en optimizar el rendimiento del MCI. Podemos encontrar publicaciones como la de Grogan et al. (1987) en la que define un método al que denomina "*shift-up and throttle-back*" que se basa en aumentar la marcha y aflojar el acelerador del tractor manteniendo la velocidad del sistema, para lo cual se basaron principalmente en los resultados de Larsen (1981) respecto a la eficiencia en la utilización de tractores con tracción en las 4 ruedas. Sus resultados demuestran que esta práctica puede permitir importantes ahorros de combustible. Además, desarrollaron un microcontrolador capaz de calcular la marcha y la velocidad de giro del motor óptimas con respecto al combustible y al par de las ruedas necesario para llevar a cabo la tarea agrícola [16], [17]. Unos años más tarde, Harris (1992) presentó un modelo matemático para predecir el combustible consumido por un motor diésel respecto al par generado, calculando el régimen de trabajo óptimo para que el motor pueda desarrollar ese par con el mínimo consumo [18]. Más recientemente, Grisso et al. (2001) presentaron un análisis de como seleccionar una marcha rápida manteniendo la velocidad y productividad del sistema mientras se reduce la velocidad del motor (rpm, revoluciones por minuto) disminuye las pérdidas energéticas por fricción interna y los gases expulsados para así reducir el combustible consumido [19].

En los últimos años, los esfuerzos de los investigadores para reducir el combustible empleado en tareas agrícolas se han centrado en la optimización del plan de rutas para llevar a cabo la tarea. Algunos de estos trabajos buscan la optimización en el cambio entre

calles (llamamos calle a la zona tratada en cada una de las pasadas del sistema a través del cultivo), como por ejemplo, Bochtis & Vougioukas (2008) y Bochtis & Sørensen (2009) que presentaron algoritmos para calcular un plan de rutas que permite mejorar la eficiencia de las máquinas agrícolas reduciendo las distancias recorridas en estos cambios de calle [20], [21]. También cabe destacar el trabajo de Hameed et al. (2011), en el que se desarrolla un método para calcular el mejor ángulo de las calles para minimizar la distancia al cambiar de una a otra [22].

Otras publicaciones se centran en la optimización del plan de rutas completo, como por ejemplo la de Oksanen and Visala (2009) que presenta y compara dos algoritmos para generar el plan de rutas. Uno de ellos divide el campo de cultivo en formas simples, trapezoides, y determina la mejor dirección en las calles para cada forma simple así como la mejor opción en la división del campo. El otro algoritmo busca el mejor plan de rutas para el campo completo analizando cada una de las posibles opciones [23]. También podemos encontrar otras publicaciones que emplean la metodología de dividir el campo en subregiones, como la de Jin and Tang (2010) que describe un proceso para obtener el mejor ángulo de los surcos para cada subregión [24].

Las publicaciones más recientes que podemos encontrar respecto a esta optimización del plan de rutas consideran las elevaciones del terreno, para lo cual utilizan representaciones del campo en tres dimensiones. Por ejemplo, Jin and Tang (2011) presentaron un método que, al igual que los anteriores, se basa en dividir el campo en subregiones para obtener el mejor plan de rutas en cada región respecto al coste en el cambio de calle y la erosión del suelo considerando las elevaciones del terreno, a diferencia de los anteriores. Además, compararon los resultados con los obtenidos al no considerar esta tercera dimensión obteniendo que al utilizar las elevaciones del terreno se logra reducir la erosión del suelo, el coste en los cambios de calle y la superficie no trabajada [25]. Hameed et al. (2013) presentaron un algoritmo para minimizar los requerimientos energéticos en procesos de fertilización orgánica (con purines) calculando el ángulo óptimo de las calles del plan de rutas, para lo cual obtenían una representación tridimensional del terreno a partir de información disponible en internet.

También podemos encontrar otras publicaciones que describen una metodología para optimizar el plan de rutas con un enfoque diferente. Por ejemplo, Bochtis et al. (2012)

analizaron como influye la compactación del terreno en el incremento de los requerimientos energéticos en tareas agrícolas de labranza y presentaron un sistema para optimizar el plan de rutas respecto a esta compactación [26].

3.2 Uso de fuentes energéticas limpias en vehículos agrícolas

Actualmente el uso de fuentes de energía renovables y respetuosas con el medio ambiente es cada vez más necesario, por lo que está sufriendo un aumento progresivo. Cada día aparecen nuevos sistemas y avances respecto al uso de estas fuentes energéticas, tanto en agricultura como en otros sectores. Dentro de la agricultura, una fuente de energía limpia considerada y analizada es la basada en biocombustibles. Gasparatos et al. (2011) analizaron la influencia del uso de biocombustibles en la sociedad y en el medio ambiente y obtuvieron que pueden generar numerosos impactos tanto sociales como medioambientales que han de ser considerados [27].

El principal problema de estas fuentes de energía limpias es su almacenamiento, una posibilidad son las baterías, las cuales van evolucionando y logrando mayor densidad energética y menor coste. Considerando este aspecto, Delucchi and Lipman (2001) analizaron el ciclo de vida y los costes de los vehículos eléctricos basados en baterías, considerando la inversión inicial y los costes de operación y mantenimiento. A partir de este análisis, desarrollaron un modelo de los costes del ciclo de vida en este tipo vehículos. Además, presentaron una comparativa de este modelo respecto a los vehículos a gasolina a partir de la cual obtuvieron, que en aquella época los vehículos eléctricos de batería necesitaban reducir costes para ser competitivos respecto a los vehículos con MCI [28]. Recientemente, Mousazadeh et al. (2010) analizaron los distintos tipos de baterías disponibles para su uso en tractores eléctricos híbridos asistidos con energía solar para realizar tareas ligeras [29]. Y posteriormente Mousazadeh et al. (2011) evaluaron el ciclo de vida de los tractores eléctricos híbridos asistidos con energía solar, y compararon los resultados con los que ofrece un tractor con MCI, considerando los costes económicos y medioambientales. A partir de esta comparativa, determinaron que el coste del ciclo de vida de tractores eléctricos híbridos asistidos con energía solar es menor que el de los basados en MCI [30].

Otro importante sistema para el abastecimiento de energía eléctrica en vehículos son las pilas de combustible. Abordando esta posibilidad, Mulloney Jr. (1993) propuso el uso de pilas de combustible como un sistema de abastecimiento energético respetuoso con el medioambiente para evitar el uso de combustibles fósiles en la producción y distribución agrícola y presentó un análisis de cómo esta práctica puede disminuir la contaminación [31]. Posteriormente, Eaves and Eaves (2004) compararon los costes de fabricación y mantenimiento en vehículos de pila de combustible respecto a vehículos de batería utilizando unos modelos desarrollados para realizar tareas agrícolas ligeras. A partir de los resultados, determinaron que el uso de vehículos de batería era más favorable respecto a costes, eficiencia energética, masa y volumen [32]. Unos años más tarde, Ahlgren et al. (2009) desarrollaron un modelo de granja en el que los tractores utilizaban pilas de combustible el cual se obtiene a partir de gasificación termoquímica de paja y presentaron el balance energético obtenido a partir de este modelo para varios escenarios. [33]. Recientemente, Offer et al. (2010) compararon los vehículos eléctricos a batería, los vehículos eléctricos a pila de combustible y los vehículos híbridos con pila de combustible. Como resultado, obtuvieron que los vehículos eléctricos a batería y los vehículos híbridos con pila de combustible tenían unos costes de ciclo de vida razonablemente parecidos aunque estos costes eran mayores que los de vehículos con MCI. Además, predijeron que los costes de los vehículos eléctricos e híbridos bajarán para 2030, época en la que este tipo de vehículos ofrecerá importantes ventajas [34].

Combustibles como el hidrógeno, pueden ser utilizados tanto para pilas de combustible como para MCI, como lo son los de ciclo Otto o de ciclo Wankel. Abordando esta posibilidad, Lutz et al. (2002) compararon la eficiencia teórica de las pilas de combustible con los motores de ciclo de Carnot considerando el mismo combustible en ambos casos. A partir de esta comparativa, determinaron que la eficiencia teórica es similar en ambos casos. Sin embargo, en la práctica, las pilas de combustible presentan una eficiencia mayor ya que los MCI no pueden operar en condiciones de máxima eficiencia las cuales se dan para una temperatura excesivamente elevada que generaría problemas en los materiales que componen el motor [35].

El principal combustible utilizado por las pilas de combustible es el hidrógeno cuya densidad energética por unidad de volumen en condiciones normales es muy baja (3

kWh/Nm^3) por lo que su almacenamiento normalmente requiere de un significativo aporte energético para paliar esta desventaja. Actualmente existen numerosas técnicas para el almacenamiento de hidrógeno las cuales se pueden dividir en dos grupos principales: almacenamiento físico (comprimido o licuado) y almacenamiento químico (combinado con otros elementos para formar hidruros). Los investigadores están trabajando actualmente para mejorar estas técnicas, por lo que podemos encontrar numerosas publicaciones recientes que presentan nuevas técnicas y mejoras. Como por ejemplo Zheng et al. (2012), que analizaron las tecnologías para almacenar hidrógeno a alta presión, [36]; Kelly and Girdwood (2012), que analizaron la cinética y termodinámica de un prototipo de compresor de hidrógeno de hidruro metálico [37]; Lebon et al. (2015), que investigaron el almacenamiento de hidrógeno mediante la absorción molecular en nanotubos de grafeno [38].

3.3 Reducción de productos químicos en tareas agrícolas

Los productos químicos más utilizados en agricultura son los pesticidas y los fertilizantes. Dentro de los pesticidas, los más comunes son los herbicidas para el control de malas hierbas y los insecticidas para el control de insectos. Un primer paso para optimizar el uso de estos productos es la detección de las zonas más necesitadas de los mismos. En las últimas décadas podemos encontrar numerosas publicaciones centradas en la detección de malas hierbas en cultivos agrícolas, como la de Luscier et al (2006) que presenta un método para cuantificar el porcentaje de cobertura de las distintas plantas a partir de fotografías digitales de la vegetación [39]. Anteriormente, Onyango & Marchant (2003) presentaron un algoritmo para la detección y clasificación de plantas considerando el color y la morfología [40]. Posteriormente, Tellaeche et al. (2008) describieron un enfoque basado en la visión diferencial para la fumigación de herbicidas en agricultura de precisión [41]. Otro ejemplo es la publicación de Lee et al. (2010), que presenta una revisión de las tecnologías de detección de plagas agrícolas y analiza la forma en que se utilizan para la agricultura de precisión así como los desafíos y las consideraciones sobre el uso de estos sensores y tecnologías para la producción agrícola [42]. También cabe destacar la publicación de Guerrero et al. (2012) que define un sistema de detección de malas hierbas basado en máquinas de soporte vectorial [43]; además, podemos encontrar un sistema experto para la identificación de malas hierbas en campos de maíz presentado

por Montalvo et al. (2013) [44]. Dentro de este campo para la detección de plantas y malas hierbas en agricultura también cabe destacar otras publicaciones como: [45], [46], [47], [48], [49], [50].

Para llevar a cabo un tratamiento automatizado y de precisión, una vez que se ha obtenido la información sobre las zonas del cultivo más necesitadas del tratamiento químico, lo siguiente es disponer de la tecnología necesaria para poder realizar este tratamiento selectivo de forma automática. Los sistemas de navegación empleados para llevar a cabo estos tratamientos se basan principalmente en la combinación de Sistemas Globales de Navegación por Satélite (GNSS) con unidades de medida dinámicas. Hasta el momento podemos encontrar numerosas publicaciones que exponen y analizan métodos y sistemas para llevar a cabo este tipo de tratamientos de forma automática. Por ejemplo, Gerhards & Oebel (2006) presentaron y analizaron experimentalmente un sistema para el control de malas hierbas basado en tratamientos de imágenes en tiempo real [51]. Después, Nørremark et al. (2008) presentaron un sistema para el manejo de malezas dentro de la línea de cultivo con un sistema no tripulado que se compone de un vehículo autónomo y una azada cicloide. El vehículo y la herramienta se controlaron de forma independiente para seguir una tarea pre-planeada con su propio sistema GNSS [52]. En este mismo año, Khot et al. (2008) propusieron una combinación de sensores para mejorar los errores en el ángulo de pulverización de tratamientos agrícolas [53]. Posteriormente, Jeon & Tian (2009) presentaron un robot con un brazo articulado capaz de cortar el tallo de la hierba y aplicar el herbicida directamente sobre el tejido vascular para mejorar la eficiencia del tratamiento y reducir la cantidad de herbicida [54]. También cabe destacar la publicación de Berge et al. (2012) que presenta un robot autónomo guiado por GPS (sistema de posicionamiento global) para el control de malas hierbas en cereales basado en la visión de la máquina, capaz de realizar la supervisión de malezas y de pulverizar en la misma operación [55].

3.4 Alternativas a los tratamientos químicos en agricultura

Actualmente existe un gran auge en la producción ecológica de alimentos (también denominada “orgánica” en países de habla inglesa o “biológica” en leguas germánicas), la cual se basa en utilizar de forma óptima los recursos naturales disponibles en el entorno e implica la prohibición en el uso de todo tipo de productos químicos de síntesis u

organismos genéticamente modificados (ya sea para el control de plagas y enfermedades o para la fertilización del terreno) durante todo el proceso de producción al que se le añade un periodo anterior que puede incluir de 2 o 3 años, según el tipo de cultivo. Este sistema de producción permite reducir la contaminación de las aguas subterráneas, reduce riesgos de enfermedades y aporta importantes beneficios a la biodiversidad natural del suelo y al ecosistema [9], [10], [56], [57], [58]. Considerando esta normativa de producción, en los últimos años podemos encontrar numerosas publicaciones que analizan y proponen sistemas y procesos agrícolas para mejorar la productividad de la agricultura ecológica los cuales se basan principalmente en el uso de tratamientos alternativos a los productos químicos de síntesis. Por ejemplo, Sandhu et al. (2010) analizaron aspectos como el control biológico, la polinización, la formación del suelo o el ciclo de nutrientes en la agricultura y discutieron que considerando estos aspectos la agricultura ecológica puede reportar ciertos aportes medioambientales y económicos. Este trabajo concluyó que la agricultura ecológica tiene un gran potencial para el abastecimiento alimenticio mundial, ya que permite utilizar pocos recursos junto con la tecnología ecológica local para lograr productos saludables a partir de procedimientos respetuosos con el medio ambiente [59]. Gran parte de estas publicaciones proponen y analizan métodos ecológicos para el control de plagas, por ejemplo, Zhang et al. (2012) presentaron un sistema automático basado en la visión multiespectral para el control de malas hierbas en cultivos ecológicos, como tomates, mediante la aplicación selectiva de pequeñas dosis de aceite caliente [60]. Posteriormente, Colloff et al. (2013) presentaron un método ecológico basado en ácaros para el control de pequeños insectos en cítricos [61]. En este mismo año, Datta & Knezevic (2013) analizaron el fuego como alternativa para el control de malas hierbas tanto en agricultura convencional como ecológica [62]. También podemos encontrar el análisis de distintos métodos ecológicos para el control de insectos y ácaros en el té presentado por Ye et al. (2014) [63]. Y recientemente, Garfinkel & Johnson (2015) analizaron el control ecológico de plagas de insectos proporcionado por las aves [64].

Otro tipo de agricultura con principios cercanos a la anterior pero no tan restrictivos en cuanto al uso de productos químicos, ya que permite el uso de fertilizantes y fitosanitarios obtenidos a partir de productos de origen natural, es la denominada agricultura sostenible. Este tipo de agricultura pretende garantizar la seguridad alimentaria mundial a la vez que preserva el medio ambiente haciendo un uso sostenible de la tierra, el agua y los recursos

naturales para lograr una producción rentable [65], [66], [67], [68]. Podemos encontrar numerosas publicaciones que analizan el uso de productos químicos dentro de este tipo de agricultura, como la de Kurstjens (2007) que revisa varios métodos no químicos para prevenir y subsanar infestaciones de malas hierbas y presenta un sistema de arado de precisión para el control de esas malas hierbas [69]. En este mismo año, Kathiresan (2007) analizó cómo la integración de distintas técnicas (rotación de cultivos, uso de los residuos producidos por explotación agrícolas, etc.) puede permitir incrementar la rentabilidad de la agricultura sostenible [70]. También cabe destacar a Rains et al. (2011) que propusieron una reorientación tecnología orientada a mejorar los sistemas de producción basados en agricultura sostenible [71]. En este mismo año, Reeve et al. (2011) presentaron un estudio de una pequeña granja basada en sistemas sostenibles [72]. Y recientemente, Chauhan et al. (2015) analizaron diversas técnicas para el control de malas hierbas en cultivos sostenibles de arroz de secano, a partir de lo cual definieron un sistema de control de malas hierbas rentable para este tipo de cultivos [73].

Por último, dentro de las técnicas agrícolas que pretenden reducir los impactos medioambientales tenemos la agricultura de conservación, definida por la FAO como "*conjunto de procesos para la producción de cultivos agrícolas con los objetivos de reducir los recursos empleados y lograr unos beneficios aceptables, manteniendo unos niveles de producción altos y sostenidos a la vez que se preserva el medio ambiente*" [74]. Este tipo de agricultura busca sostenibilidad y rentabilidad con tres principios principales: perturbación mínima del suelo, cobertura permanente del suelo y rotación de cultivos [75]. Podemos encontrar numerosas publicaciones que analizan el uso de productos químicos dentro de este tipo de agricultura. Por ejemplo, Farooq et al. (2011) analizaron el rendimiento y el control de malas hierbas en cultivos de secano en agricultura de conservación y obtuvieron que utilizando las técnicas y metodología adecuadas la producción conservativa de cultivos de secano puede ser competitiva con la producción tradicional [76]. Posteriormente, Chauhan et al. (2012) analizaron las malas hierbas y los sistemas de control dentro de la agricultura ecológica y de la agricultura de conservación. Determinaron que la efectividad de los herbicidas es menor sin los procesos de labranza, por lo que es necesario hacer un uso adecuado de estos herbicidas a la vez que se evalúan posibles técnicas para eliminar la mala hierba de forma mecánica con procesos de agricultura de conservación [77]. Además, Bajwa (2014) analizó los sistemas ecológicos

para el control de malas hierbas en agricultura de conservación. Concluyó que los sistemas de control de malas hierbas se han de combinar manteniendo los aspectos ecológicos, geográficos, climáticos y agronómicos del sistema de cultivo, para lo cual es necesario investigar la integración y combinación de distintas técnicas [78]. Recientemente, Ramesh (2015) analizó diferentes opciones para el control de malas hierbas en agricultura de conservación así como los impactos ecológicos de cada una de estas opciones. Concluyó que la agricultura de conservación no es tan dependiente de los tratamientos químicos como lo estima la percepción general, ya que un manejo adecuado de los diferentes mecanismos para el control de malas hierbas puede permitir una importante reducción de herbicidas logrando reducir los impactos ecológicos [79].

4 PUBLICACIÓN I:

Reducing fuel consumption in weed and pest control using robotic tractors

M. Gonzalez-de-Soto, L. Emmi, I. Garcia, and P. Gonzalez-de-Santos

Computers and Electronics in Agriculture, ISSN 0168-1699, vol. 114, pp. 96–113, Jun. 2015.

DOI: *http://dx.doi.org/10.1016/j.compag.2015.04.003*

Impact Factor (2014): 1.761

Category: Agriculture, Multidisciplinary: 6/56 (Q1)

Category: Computer Science, Interdisciplinary Applications: 32/102 (Q2)

Computers and Electronics in Agriculture 114 (2015) 96–113

Contents lists available at ScienceDirect

Computers and Electronics in Agriculture

journal homepage: www.elsevier.com/locate/compag

Reducing fuel consumption in weed and pest control using robotic tractors

Mariano Gonzalez-de-Soto [a,b,1,2,*], Luis Emmi [a,1], Isaias Garcia [b,2], Pablo Gonzalez-de-Santos [a,1]

[a] Centre for Automation and Robotics (UPM-CSIC), Ctra CAMPO REAL km 0,2, 28500 Arganda del Rey, Madrid, Spain
[b] Escuela de Ingenierías Industrial e Informática, Universidad de León, Dept. de Ingeniería Eléctrica y de Sistemas y Automática, Campus de Vegazana s/n, 24071 León, Spain

ARTICLE INFO

Article history:
Received 17 September 2014
Received in revised form 31 March 2015
Accepted 3 April 2015

Keywords:
Reducing fuel consumption
Path planning
Energy efficiency
Atmospheric emissions
Digital elevation model (DEM)

ABSTRACT

A significant problem exists concerning contamination of the environment, especially air pollution, and the consequent climatic change. Considering that agricultural vehicles that use fossil fuels emit significant amounts of atmospheric pollutants, the main objective of this paper is to include techniques to reduce the fuel consumption in the controls system of robotic tractors used in agriculture tasks and thereby reduce the atmospheric emissions from these automated applications. To achieve this goal, the first step is to analyze fuel consumption in real time for each of the applications to be improved and to implement the consumption model of a robotic tractor for each task, considering the mechanical energy variations, the performance losses, the energy used to overcome friction and the energy required by the given task. For calculating the mechanical energy, the model considers the potential energy of the system, which is a function of the mass, elevation and gravity. The terrain elevations are estimated from GeoTIFF images of DEM data, which have a pixel size equal to 1 arc second (approximately 30 m at the Equator), and an accuracy of integer meters. Regarding the system mass, the possible loss of mass from applying the treatment is considered. For estimating the frictional forces, the rolling resistance coefficient of the terrain surface conditions is used.

The consumption model has been validated experimentally using real agricultural vehicles and implements within the RHEA project (FP7-NMP 245986), in which the instantaneous fuel consumption was measured.

This fuel reduction method is applied to three different treatments: weed control on herbaceous crops through the spraying of herbicides, weed control on fire-resistant crops with wide furrows through plowing and flame treatment, and pest control on trees through fumigation using insecticides.

Finally, a fuel reduction procedure is applied to each task using the system model implemented to predict the energy requirements. This enables one to find the optimum path plan with respect to fuel consumption. These theoretical results are compared with the experimental results. In addition, the goal is to demonstrate the fuel reduction technique by performing field experiments to show that the use of this method of fuel reduction leads to an reduced fuel consumption and thus reduces atmospheric emissions from agricultural tasks. The results obtained revealed that this fuel reduction method significantly reduces the energy requirements, with the consequent reduction in fuel consumption and atmospheric pollutant emissions.

1. Introduction

It is widely accepted that contamination of the environment, especially air pollution, is an important concern with drastic climatic consequences. Agricultural combustion engine vehicles using fossil fuels emit significant amounts of atmospheric pollutants, primarily carbon dioxide (CO_2) and nitrogen oxide (NO_X), contributing to the increase in the greenhouse effect. Using the concept that the least-polluting energy is the energy that is not used, the objective of this paper is to develop and implement techniques in the control system of robotic tractors to reduce fuel consumption in agricultural tasks; in addition, we can obtain some economic benefits. Fuel consumption is directly related to the energy requirements of agricultural tasks and may be reduced by developing a control system capable of minimizing all energy

* Corresponding author at: Centre for Automation and Robotics (UPM-CSIC), Ctra CAMPO REAL km 0,2, 28500 Arganda del Rey, Madrid, Spain. Tel.: +34 650015576.
E-mail addresses: marianogds@outlook.com (M. Gonzalez-de-Soto), luisemmi@gmail.com (L. Emmi), isaias.garcia@unileon.es (I. Garcia), pablo.gonzalez@car.upm-csic.es (P. Gonzalez-de-Santos).
[1] Tel./fax: +34 650015576, +34 689876367, +34 918711900x221.
[2] Tel./fax: +34 650015576, +34 987291000x5289.

http://dx.doi.org/10.1016/j.compag.2015.04.003
0168-1699/

List of symbols and acronyms

Symbols

A	machine specific parameter function of the soil strength
a	no-load power requirement (kw)
B	machine specific parameter, coefficient of the speed
b	unloaded tire section width (m)
b	PTO power requirement per nozzle (kw/nozzle)
B_n	dimensionless ratio of the *MR*
C	machine specific parameter related to the soil bulk density
c	power per unit of material feed rate (kw h/t)
C_f	fluid flow (L/s).
C_I	cone index for the soil
D	implement draft force (kN)
d	unloaded overall tire diameter (m)
E	electric potential (V)
E_m	mechanical efficiency of the power transmission from the net flywheel to the PTO power
E_t	traction efficiency
F_i	dimensionless soil texture adjustment parameter
g	gravitational acceleration (9.8 m/s^2),
h	tire section height (m)
I	electric current (A)
m	mass (t)
MFR	material feed rate (t/h)
MR	motion resistance
NT	net traction
p	fluid pressure (kPa)
P_{el}	electric energy (kw)
P_{hyd}	hydraulic power (kw)
P_{PTO}	power requirement from the PTO shaft (kw)
P_{PTOeq}	equivalent PTO power (kw)
$P_{PTOrated}$	rated PTO power (kw)
P_{T_PTOeq}	total equivalent PTO demanded power (kw)
PTM	partial throttle multiplier
T	tillage depth (cm)
TFC	total fuel consumption
v	speed (m/s)
W	number of rows or tools
X	fraction of equivalent PTO power
α	terrain slope (radians)
δ	tire deflection (m),
ρ	*MR* ratio

Acronyms

ASTER	advanced spaceborne thermal emission
DEM	digital elevation model
EGM96	earth gravitational model 1996
GDEM	global digital elevation model
GeoTIFF	georeferenced tagged image file format
GMU	ground mobile unit
NASA	National Aeronautics and Space Administration
PTO	power take-off
RHEA	robotic for highly effective agriculture
RTK	real time kinematic
SFC_v	specific fuel consumption volume
TPH	three-point hitch
UTM	universal transverse mercator
WGS84	world geodetic system of 1984

requirements. In particular, the control system is tasked with choosing the best path to reduce the amount of mechanical and plowing energy used and to reduce friction losses. Additionally, to minimize the amount of energy used, it is also necessary to reduce and improve the usage of the following:

1. the PTO by deactivating it when not used,
2. the hydraulic actuators and
3. the electric actuators.

Finally, the engine operating conditions have to be adapted to achieve the maximum performance.

Currently, energy efficiency is a common concern in all fields; however, in researching this topic for agriculture machinery, we find that the scientific community has dedicated substantial amounts of effort to the topic of energy efficiency in many fields related to agriculture for many years. Grečenko (1968) optimized the plowing energy and analyzed the effect of tractor designs and its combination with implements on field performance and some other operational features. He also developed a method for predicting the performance of tractors in combination with implements. Recently, Mileusnić et al. (2010) presented an analysis and comparison of tillage systems based on fuel consumption. By leveraging the new technical solutions in tillage mechanization systems and the new technological variants in the tillage process, the systems consume significantly less energy compared to the older systems.

Other research efforts focused their activities on the improvement of engine performance. For example, Grogan et al. (1987) based mainly on the results of Larsen (1981) concerning the utilization efficiency of four-wheel-drive tractors, determined that practicing shift-up and throttle-back methods improves engine efficiency and developed a microcomputer algorithm that calculated the optimal gear and engine speeds with respect to fuel consumption and the wheel torque for carrying out a task. Harris (1992) developed a mathematical model to predict the relation between the torque generated by a diesel engine and the fuel that it consumes at any speed. Furthermore, he calculated the optimum operating point of engines. More recently Grisso et al. (2001) discussed how to select a faster gear to maintain travel speed and productivity while reducing the engine revolutions per minute (rpm), which avoids the increase of the engine friction and gases expelled, to reduce fuel consumption.

Recently, optimization has focused more on using path planning to reduce the rolling resistance forces. Bochtis and Vougioukas (2008) and Bochtis and Sørensen (2009) developed an algorithm for path planning that improves the field efficiency of machines by minimizing the total non-working distance traveled, which is the distance traveled when changing tracks (path followed by the vehicle through the treated crop). Oksanen and Visala (2009) presented and analyzed advantages and disadvantages of two algorithms. The first uses a trapezoidal decomposition algorithm based on a top-down approach to split complex-shaped fields into simple ones, and a search for the best driving direction and the selection of subfields was developed. The second algorithm uses a bottom-up approach to cover the field, searching for the best path plan for the whole field using prediction and brute-force methods. Jin and Tang (2010) also presented an algorithm capable of finding the optimal solution for decomposing a field into sub-regions and determining the coverage direction within each sub-region. Other examples of non-working-distance minimization is the algorithm by Hameed et al. (2011), who developed a

method to obtain the optimum track angle (track direction angle respect to UTM coordinates) to minimize the non-working distance in addition to a method of minimizing the overlapped area. Moreover, one can find studies that considered terrain elevations for path planning optimization, such as the method by Jin and Tang (2011), who developed an algorithm to determine an optimal path using 3D terrain maps of field representations that divide a field into sub-regions with similar field attributes and compared the results with those obtained without considering terrain elevation. Hameed et al. (2013) presented an algorithm to minimize the energy required by a task. The algorithm uses three-dimensional representations of the field characteristics to obtain the optimum tracks angle to minimize energy consumption.

Another example of path planning optimization using a different approach is found in Bochtis et al. (2012), who developed a decision support system to perform the route planning for agricultural vehicles carrying time-dependent loads to reduce the risk of soil compaction. In addition, they analyzed how the soil compaction leads to increased energy requirements, increased CO_2 emissions, and reduced yields.

Thus, the objective of this paper is to develop and implement a system to minimize fuel consumption for reducing pollutant emissions. To achieve this goal, we divide the main objective into the following sub-objectives:

- Analyze the features of the used systems (Section 2.1).
- Implement a fuel consumption model to predict the fuel requirements (Section 2.2).
- Obtain the field data, in three dimensions, to determine the distances and slopes of the paths followed by the vehicle (Section 2.3).
- Develop and implement an algorithm to reduce all of the energy requirements, for each application, using the implemented fuel consumption model and the field crop representation (Section 2.4).
- Conduct a series of field experiments to validate the fuel consumption model and discuss the results of the fuel reduction (Section 3).

2. Materials and methodology

2.1. System

2.1.1. Ground mobile unit

The GMU used in this work inherits features from the original tractor that it was based on: the New Holland Boomer 3050 CVT compact tractor. It has been mechanically, electrically and hydraulically modified and programmed using a special software package. These modifications enable the autonomous control of the main vehicle functions, supply part of the required electrical power to the added components and integrate all control systems. Safety has to also be ensured for the vehicle, the environment and, most importantly, the people involved. Another requirement was to modify the original cabin; Fig. 1a and b shows the original tractor and the modified one before of add the new electronic devices. In addition to the original equipment, the GMU has been equipped with control, location, safety, alternative energy and vision systems. Fig. 1c shows the final GMU after the different subsystems have been attached, which will be used for the analysis and tests of this article (RHEA, 2014).

After these modifications, some features of the GMU have become different than those of the original tractor. The weight and some dimensions have been modified due to the modifications of the cabin and due to the addition of new components, such as the alternative energy system, having a substantial mass of approximately 0.19 *t* and giving a final GMU weight of approximately 2.085 *t*. Furthermore, the maximum ground speed has been limited to 7 km/h for safety reasons; therefore, some gears are disabled. Table 1 shows the main features of the GMU.

Fig. 2 represents the engine performance curves provide by the manufacturer. In this figure, we can observe the power curve, the SFC_v and the torque. These curves will be considered when reducing the fuel consumption (Section 2.4).

2.1.2. Implements

In this work, three different tasks are analyzed: weed control using herbicide, weed control using plowing and flaming and pest control using insecticides. Each task requires a specific implement.

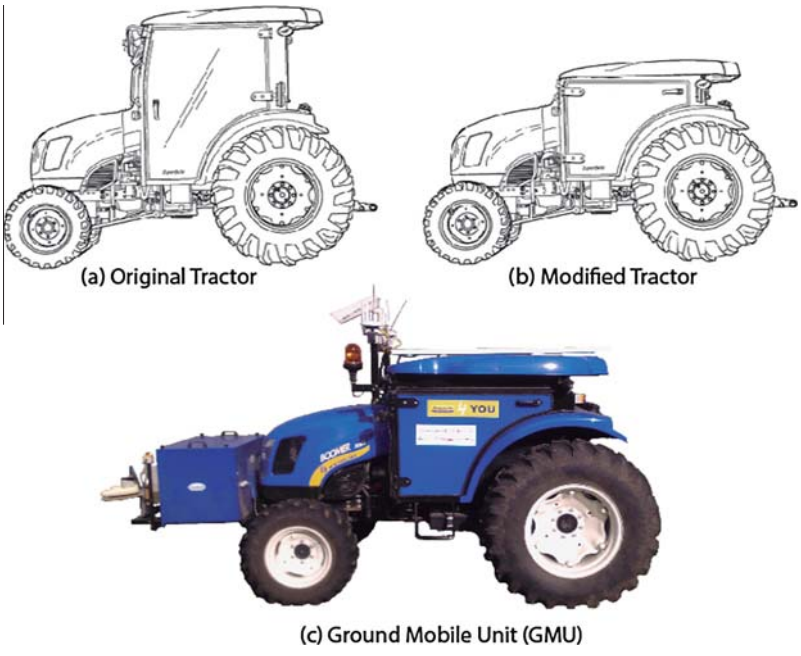

Fig. 1. Original and modified tractor and final GMU.

Table 1
Main characteristics of the GMU. *Source*: (CNH America LLC, 2009).

Feature	Value
Engine gross power	33.6 kW
Rated engine speed	2800 rpm
Low idle engine speed	1050 rpm
Maximum no-load engine speed	3050 rpm
PTO speed (engine speed)	540 rpm (2409 rpm)
PTO power observed	28.7 kW
Fuel tank	49.2 L
Total weight	2085 kg

2.1.2.1. Sprayer implement. A sprayer implement (see Fig. 3a) is used for spraying herbicides in weed-control treatments for herbaceous crops, such as wheat or barley, with small row spaces (approximately 10–17 cm).

This implement is controlled from the GMU, which has two different tanks for water and herbicide. It is able to regulate the water/herbicide ratio and the main water flow and is able to open or close each nozzle separately. Table 2 presents the main features of this implement (Carballido et al., 2012).

2.1.2.2. Flaming and row crop cultivator implement. A flaming and row crop cultivator implement (see Fig. 3b) is used for the physical treatment of weeds in crops with wide row spaces (approximately 75 cm) that can withstand high temperatures over short periods of times, such as maize, onion, garlic, and leek. The tractor performs a mechanical inter-row treatment, as performed by a row crop cultivator, and a thermal in-row treatment for the weed control. This implement is controlled from the GMU, which uses butane gas as fuel for the burners. The GMU is able to regulate the gas pressure of each burner separately in three states: zero, low and high. Table 3 shows the main features of this implement (Frasconi et al., 2014).

2.1.2.3. Canopy sprayer implement. A canopy sprayer implement (see Fig. 3c) is used for the fumigation using insecticides in pest control treatments in trees seeding in rows spaced at approximately 4 m, as in, for example, olives groves.

This implement has a tank for the water and insecticide mixture, a water pump to spray the mixture and an air fan to fumigate this mixture to the canopy tree. It is autonomous (the GMU only turns the implement on and off), is able to detect the tree canopy using ultrasonic sensors, and activates each nozzle and air valve separately. In addition, the upper and lower nozzles in each column can rotate from 0° to 30° to adapt the spray direction to the canopy size. Table 4 shows the main features of this implement (Sarri et al., 2014).

2.1.3. GMU hardware architecture

The GMU is equipped with a control system monitored by an operator at a base station, where he can monitor several GMUs (the RHEA project consists of three GMUs). The scheme of the hardware architecture is shown in Fig. 4 and is formed by the following subsystems (RHEA, 2014):

- A High-level Decision-making System is the main control system and is in charge of controlling the information flow between almost all other subsystems. It calculates the simple paths required to realize the task and decides when to set the trajectory, activate and deactivate the PTO, move the TPH, start or stop the implement, etc.
- A communication device links the mobile units to the base station and to the user-portable devices. This system enables the supervising, monitoring and controlling of the GMU by a remote device using a wireless network.
- A vehicle controller in charge of controlling the GMU systems inherited from the original tractor (the steering, hydraulic valves, lights, PTO, TPH, etc.), obtaining the GMU status (PTO speed, engine rpm, TPH positions, oil temperature, etc.), and controlling the implements using another subsystem, which is called the Low-level Actuation System.
- A Weed Detection System based on computer vision used to detect weed patches.

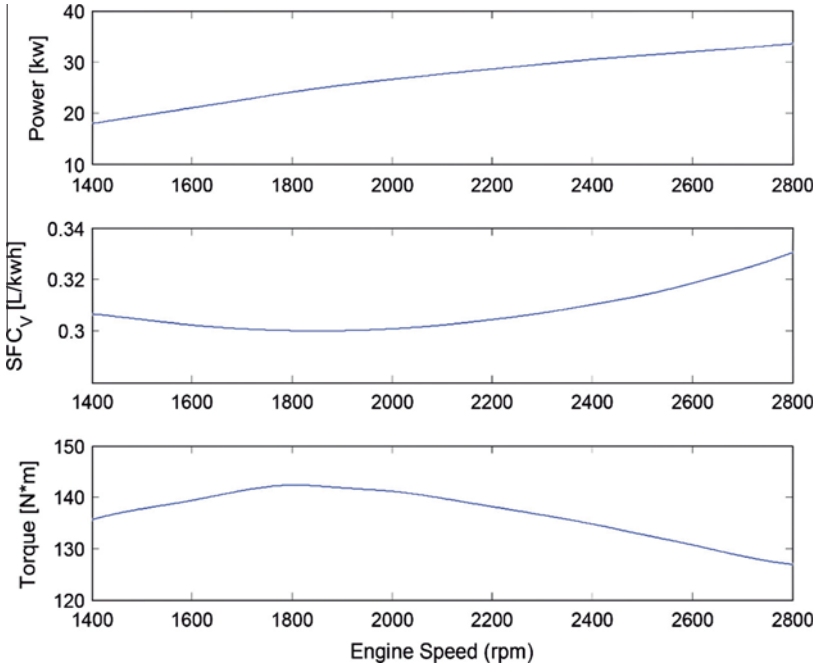

Fig. 2. GMU engine performance curves. *Source*: (CNH America LLC, 2009).

Fig. 3. Implement (a) sprayer, (b) flaming and row cultivator, and (c) canopy sprayer.

Table 2
Main characteristics of the sprayer implement. *Source*: (RHEA, 2014).

Feature	Value
Number of valves and nozzles	12
Nozzle nominal flow	0.757 L/min
Nozzle nominal pressure	276 kPa
Valves spacing	0.5 m
Pump power (from PTO)	2.4 kW
Electrical power supply	Maximum 0.516 kw
Total capacity of tanks	215 L
Total equipment weight (empty tank)	400 kg

Table 3
Main characteristics of the physical weed control implement. *Source*: (RHEA, 2014).

Feature	Value
Mechanical–thermal tools	4
Furrow	0.75 m
Electrical power supply	24 V DC 50 A/12 V DC 4 A
Total weight	940 kg

Table 4
Main characteristics of the canopy sprayer implement. *Source*: (RHEA, 2014).

Feature	Value
Tank capacity	300 L
Number of valves and nozzles	8
Nozzle nominal flow	1.25 L/min
Nozzle nominal pressure	650 kPa
Valve spacing	0.5 m
Maximal fan power (from PTO)	15 kW
Electrical power supply	~1.8 kW (24 and 12 V_{DC})
Total equipment weight (empty tank)	400 kg

- A Row Detection System based on computer vision used to detect crop rows to help to steer the vehicle.
- A Positioning System consisting of one GPS receiver and two antennas. This system uses RTK signal correction provided by a Base Station situated next to the field; it has an accuracy of approximately ±2.5 cm. The second antenna lets an operator know the GMU heading even when it is stopped.
- A safety system consisting of the following subsystems: Obstacle Detection System based on computer vision used to detect objects and people in the GMU path; A Laser Scanner used to detect any type of obstacle in the GMU path. This system can stop the GMU without using the High-level Decision-making System; A remote controller, which is independent of the High-level Decision-making System. It is a simple remote controller used by an operator that ensures the proximity of one person who can quickly take control over the remaining systems from the GMU.

2.1.4. Fuel consumption measurement

Fig. 5 shows the scheme of fuel flow in the GMU, whereby two flow sensors are used to measure the fuel flow. The instantaneous fuel consumption is the difference between the data from flow meter 1 and the data from flow meter 2. To protect the flow sensor, it must be placed after a fuel filter; therefore, the return line flow meter must be installed in the pipe between the injectors and the union with the fuel filter return line. The other flow meter can be installed between the fuel filter and the lift pump or between the latter and the injection pump. The best position is after the lift flow because the low pressure may increase the number of problems generated by small air bubbles in the sensor circuit. In addition, we had to add a cooling device in the return line just before the flow meter because we observed a substantial amount of noise in this measurement as a result of the high temperature of the fuel returned by the GMU engine.

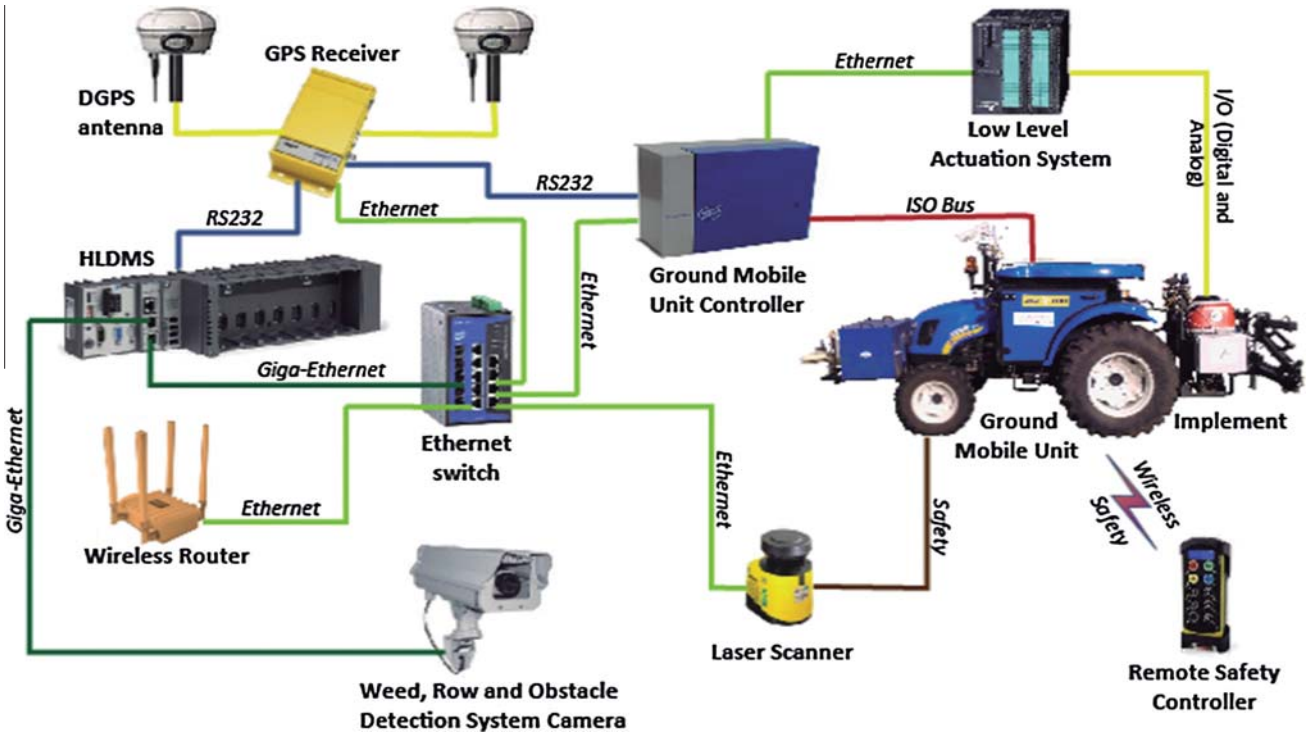

Fig. 4. General scheme of the hardware architecture.

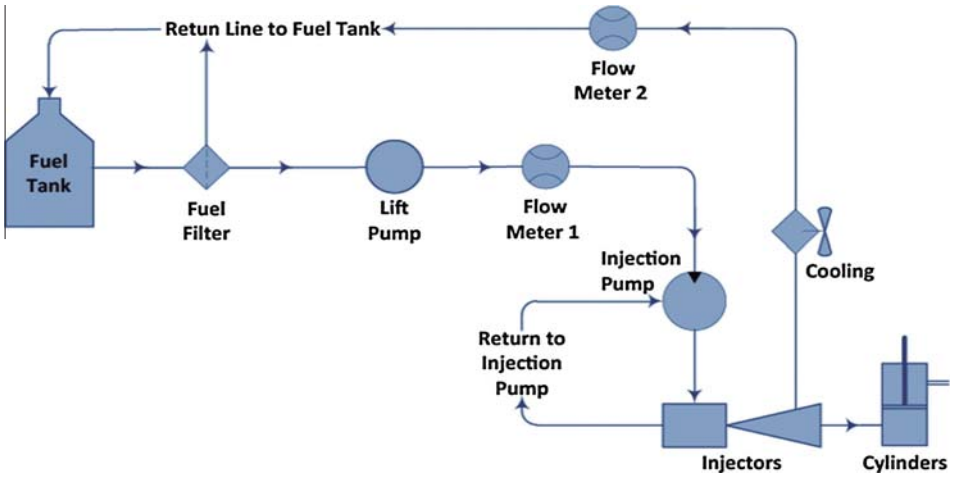

Fig. 5. Scheme of the fuel flow measurement system.

The selection of the flow meter is important for obtaining a good measurement of the fuel flow. This device must support the GMU fuel circuit conditions, and it must be suitable for measuring the liquid (Diesel fuel). According to the data of Table 5, we can observe that the flow meters do not need to support high pressures; the nominal flow must be approximately 12.54 l per hour, with a maximum flow of approximately 30 l per hour, which is adequate for oil with a low kinematic viscosity. Moreover, it must provide an independent measure of the temperature of the fluid, and the return line flow sensor must be sensitive to a low flow.

An effective flow meter for these applications is a small positive-displacement oval gear flow meter. The oval gear design ensures that the pressure loss across the sensor is very low (less than 150 mBar at full flow) and that the performance remains almost constant over the entire temperature and viscosity ranges.

Table 5
Main characteristics of the fuel and fuel system. *Sources*: (CNH America LLC, 2009), (España, 2006), and (International Energy Agency, 2013).

Feature	Value
Lift pump rated flow	12.54 L/h
Lift pump working pressure	0.2 bar ± 0.05
Maximum flow	≈30 L/h
Density at 15 °C	820–845 kg/m^3
Gross calorific value	10.40–10.72 kW h/L
Net calorific value	9.881–10.182 kW h/L
CO_2 emissions	2.616–2.696 kg CO_2/L fuel

For this application, the model PD400 from Titan Enterprises Ltd. is chosen (see Fig. 6) for both flow lines. Table 6 presents the main features of the PD400 flow meter, which has a small, oval,

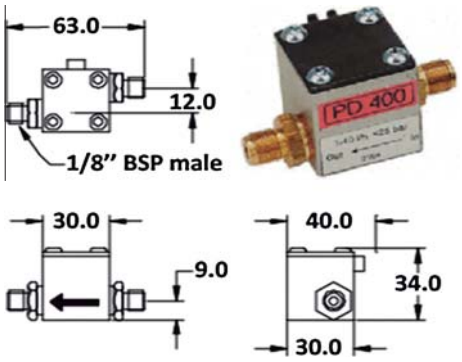

Fig. 6. PD400 flow meter.

Table 6
Main characteristics of the PD400 flow meter. *Source*: (Titan flow meter PD400, 2014).

Feature	Value
Flow rate	1–60 L/h
Maximum working pressure	25 bar
K factor	1830 pulses per liter
Temperature range	0–60 °C
Accuracy	±2.5% (at density 830 kg/m^3)

tooth-wheeled counter in addition to an easily replaceable filter that protects the sensor from any floating particles. Considering the flow meter accuracy and the rated flow of the fuel line we obtained an accuracy about of 0.3 L/h.

2.2. Consumption model

A number of mathematical consumption models for tractor engines have been proposed in recent years as part of the continuous interest in optimizing agriculture tasks, reducing fuel consumption and modeling farming operations. In this case, a fuel consumption model is estimated using in-cropping and machinery budgets based on the average annual fuel consumption from Agricultural Machinery Management engineering practices and ASAE Standards. The fuel consumption was assumed to be a function of the soil surfaces and slope, engine speed, throttle and load conditions, chassis type, total tested weight, drawbar, PTO, and hydraulic and electric power (Harris and Pearce, 1990; Grisso et al., 2004; Rahimi-Ajdadi and Abbaspour-Gilandeh, 2011).

To estimate the spent energy, it is necessary to know the total demanded energy and its relation to fuel consumption; we will use SFC_v, which is typically given in L/kw h. This value relates the energy, or power, demanded to the amount of fuel consumed. It is a function of the engine's throttle speed, whose value varies with time. The total demanded energy can be calculated by applying the time integral of the instantaneous power function. The TFC is thus

$$TFC = \int_t SFC_v(t) P_{T\_PTOeq}(t) \tag{1}$$

The value of SFC_v is given by ASAE (2011).

$$SFC_v = \left(0.22 + \frac{0.096}{X}\right) PTM \tag{2}$$

PTM values are defined by ASAE (2011).

$$X = \frac{P_{PTOeq}}{P_{PTOrated}} \tag{3}$$

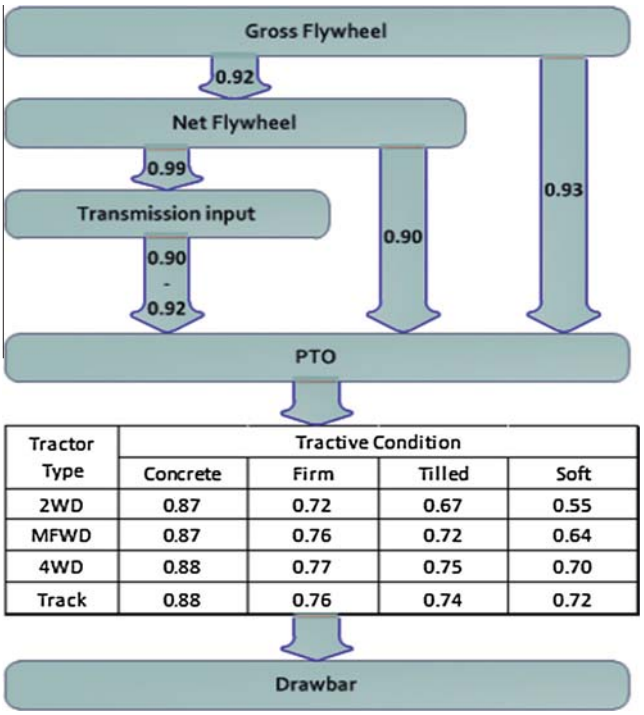

Tractor Type	Tractive Condition			
	Concrete	Firm	Tilled	Soft
2WD	0.87	0.72	0.67	0.55
MFWD	0.87	0.76	0.72	0.64
4WD	0.88	0.77	0.75	0.70
Track	0.88	0.76	0.74	0.72

Fig. 7. Power relations for agricultural tractors.

$$PTM = 1 - \left(\frac{n_{PT}}{n_{FT}} - 1\right)(0.45X - 0.877) \tag{4}$$

P_{T_PTOeq} can be obtained as the sum of different power contributions, where each power component is converted to the equivalent PTO power using the power relations from Fig. 7:

$$P_{T\_PTOeq} = \frac{Dv}{E_T} + \frac{MRv}{E_m} + P_{PTO} + P_{hyd} + P_{el} \tag{5}$$

The draft force (D) is required to pull many seeding implements and minor tillage tools that are operated at shallow depths, and it is primarily a function of the width of the implement and the speed at which it is pulled. For tillage tools operated at deeper depths, the draft also depends on the soil texture, depth, and the geometry of the tool. In this case, this force only appears in the plowing and fire treatment with the flaming and row crop cultivator implement; it is a C-shank row crop cultivator. Typical draft requirements are given by ASAE (2011):

$$D = F_i\left[A + B(3.6v) + C(3.6v)^2\right]\frac{WT}{1000} \tag{6}$$

The *MR* is the difference between the gross traction and the net traction. The gross traction is the input torque divided by the rolling radius, and the net traction is the force in the direction of travel generated by the traction device and transferred to the vehicle. *MR* depends on the wheel dimensions, tire pressure, soil type, and soil moisture. Moreover, it is assumed that the soil moisture is less than the field capacity for implement operations (ANSI/ASAE, 1995). *MR* is given by

$$MR = gm[\rho\cos\alpha + \sin\alpha] \tag{7}$$

The *MR* ratio (ρ) depends on the soil surfaces, slip, mass and tires, and it is given by

$$\rho = \frac{1}{B_n} + 0.04 + \frac{0.05s}{\sqrt{B_n}} \tag{8}$$

B_n depends on the soil surfaces, mass and tires, and it is defined by ASAE D497.4 (2003).

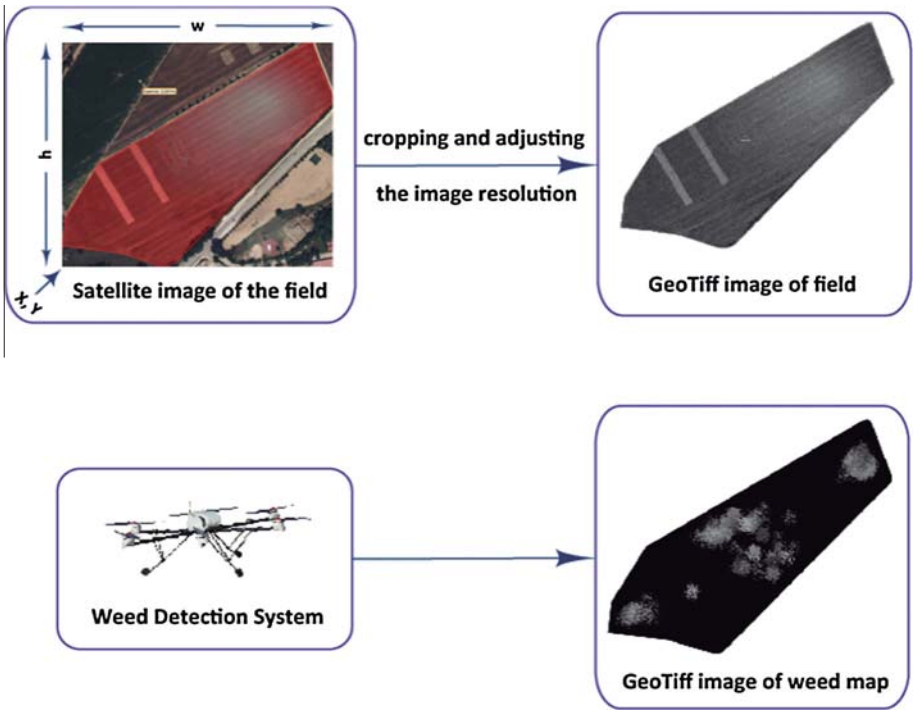

Fig. 8. Example of obtaining GeoTIFF images of terrain data.

$$B_n = \frac{CIbd}{mg}\left(\frac{1+5\frac{\delta}{h}}{1+3\frac{b}{d}}\right) \tag{9}$$

CI is the cone index for the soil, which is the force required to press the 30-deg circular cone through the soil and which is expressed in kilopascals. This index is an index of soil strength, whereby the values for typical soil surfaces are 1800, 1200, 900 and 450 for hard, firm, tilled and soft or sandy surfaces, respectively (in kPa) (ASAE S313.3, 2004).

The travel reduction (s) depends on the specified zero condition. It is the percentage of distance not advanced with respect to the distance it had advanced on the specified zero condition. This value is estimated from the function obtained using the following (Eq. (10)): (ASAE D497.4, 2003).

$$\begin{aligned} NT &= mg\left(0.88\left(1-e^{-0.1B_n}\right)\left(1-e^{-7.5s}\right)-\frac{1}{B_n}-\frac{0.05s}{\sqrt{B_n}}\right) \\ &= mg\sin(\alpha)+D \end{aligned} \tag{10}$$

For these applications, the aerodynamic resistance can be considered insignificant because the speed is very low, comparable to a simple breeze. The same approximation applies to the inertial force that appears as a result of the variations in kinetic energy.

The power requirement from the PTO is important for estimating the power consumption by the rotary tools. We need this power for the sprayer and the canopy sprayer implements, and it is given by ASAE D497.4, (2003).

$$P_{\mathrm{PTO}} = a + bw + c\mathrm{MFR} \tag{11}$$

a has a value of 2.4 kW for our sprayer implement and 13 kW for our canopy sprayer implement, b has a value of 0.004 and 0.348 kW/nozzle for our sprayer implement and our canopy sprayer implement, respectively), c and MFR are null for our implement.

P_{hyd} is the fluid power required by the implement from the hydraulic system of the tractor or from engine implements, which can be computed as

$$P_{hyd} = \frac{pC_f}{1000} \tag{12}$$

P_{el} is used by all the electrical systems: sensors, actuators, controllers, etc. Its value can be computed as

$$P_{el} = \frac{IE}{1000} \tag{13}$$

2.3. Field representation

The field data are represented using three GeoTIFF images, crop limits, a weed map and the digital elevation model for the zone where the field is located.

2.3.1. Limits and weed map

The crop limits and weed map (grayscale images in Fig. 8) use eight bits per color channel, have a pixel size of 0.5 m, and are georeferenced by the position of the lower-left pixel with geodesic coordinates that are translated to the UTM. The standard Earth reference ellipsoid used is the WGS 84.

Fig. 8 shows an example of the crop limit representation. If the pixel is not part of the crop, then it is white; otherwise, the pixel is

Table 7
ASTER GDEM characteristics. *Source*: (EOSDIS, 2014).

Feature	Value
Tile size	3601 × 3601 (1 × 1)
Pixel size	1 arc second
Geographic coordinate system	Geographic latitude and longitude

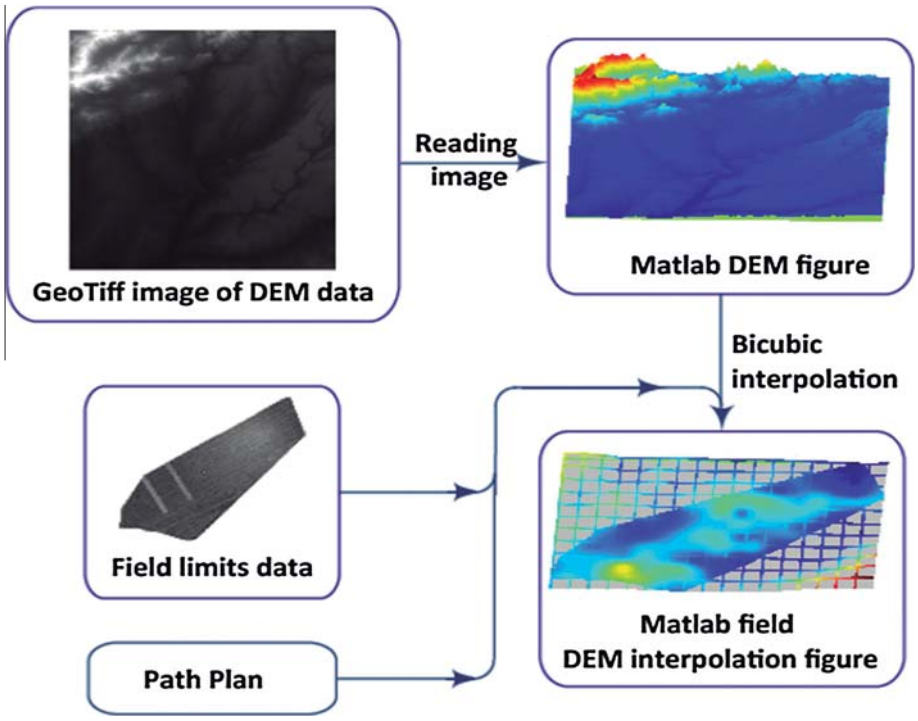

Fig. 9. Obtaining a 3D representation of the path planning and field using interpolation.

gray or black. This type of representation facilitates obtaining data from satellite images and can be found on different web sites. The representation can also define areas inside of the fields that do not contain crops, such as pools, wells, and light poles, which must be considered in the path planning process.

If the weed data are available before calculating the path planning, a weed map image (see Fig. 8), whereby each pixel value is the weed proportion in a given area, should be created. A white pixel indicates an area with maximum weeds proportion; a black pixel indicates no weeds. The values outside of the crop are not considered.

2.3.2. Terrain elevation data

To estimate the terrain elevation model, GeoTIFF ASTER GDEM images are used. These images have been obtained from the NASA website. The data are represented using a 1-arc-second (approximately 30 m at the Equator) grid and are referenced to the WGS84. Table 7 shows the main features of these GoeTIFF images (EOSDIS, 2014).

The terrain slope with the desired resolution is obtained by applying bicubic interpolation using Matlab. Fig. 9 shows this process with the geographic coordinates translated to UTM coordinates. This figure represents how this process can be applied both to path plan and the whole crop terrain. Bicubic interpolation is chosen because it provides a high degree of smoothness in places where the flats are connected and represents the plowing and tillage work generated on field surfaces. These data can be improved using the height data obtained from the GPS device during farm tasks.

2.4. Reducing fuel consumption

To minimize fuel consumption, it is necessary to minimize the SFC_v and the power values. For spraying herbicides, the draft force does not appear; therefore, the drawbar power cannot be reduced.

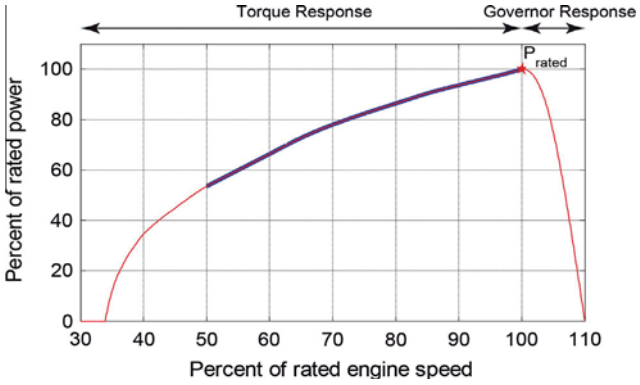

Fig. 10. Engine power and speed map.

2.4.1. Specific fuel consumption volume optimization

Fig. 10 represents a power map with the axes normalized to show how our GMU engine reacts to varying loads and engine speeds. This figure is constructed as follows:

- The *Y*-axis is the percentage of the rated power (the star indicates the rated power). The *X*-axis is the percentage of the rated engine speed.
- The solid line in the figure indicates the outside envelope, which is also known as the power curve.
- The portion of the curve where the engine speed exceeds 100% of the rated speed is called the "governor response".
- The portion of the curve where the engine speed is less than 100% of the rated speed is known as "the torque response".
- The thick portion of the curve (in blue[3]) is obtained from the data provided by the manufacturer (see Fig. 2).
- The thin portion of the curve (in red[3]) is estimated from common power maps for most engines (Grisso et al., 2006).

[3] For interpretation of color in Fig. 10, the reader is referred to the web version of this article.

Considering the engine power map shown in Fig. 10 and (Eq. (2)), it is possible to obtain the graph shown in Fig. 11a. The graph shows the relation between the engine speed and the SFC_v for different power values.

In this figure, it is possible to observe that there is an important difference between the data provided by the manufacturer, which is the thicker blue line, and the data obtained using (Eq. (2)). To determine this difference, we adjust the constants in (Eq. (2)) to obtain the data represented on Fig. 11b.

In Fig. 11b, we can observe that the minimum SFC_v does not correspond to the rated power and that for a similar demanded power, the fuel efficiency decreases as the engine speed increases. Therefore, if the engine is not performing at the rated power, we can adjust the throttle position to different values.

These graphs have been obtained blending the GMU data provides by the manufacturer and the typical tractor engine equations. Fig. 10 shows that the maximum tractor engine power is near its rated engine speed; however, in Fig. 11 we can observe that the minimum fuel efficiency is near 75% of this power. Considering that the field operations analyzed in this paper (light tillage and spraying) do not require full tractor power (although they require a specific speed), it is possible to reduce the fuel consumption by using a faster gear and by reducing the engine speed so that the specific treatment speed is maintained.

2.4.2. Improving the motion resistance

Motion resistance is the force that the tractor must overcome to move. The *MR* multiplied by the speed yields the required power. Note that although the power is proportional to the speed, the energy is not because as the speed decreases, the time required increases proportionally. To reduce the energy lost by modifying the *MR*, we can manipulate the following parameters:

- Weight: The *MR* is directly proportional to this value; hence, it must be minimized. To calculate this minimum value, it is necessary to consider the draft force, which can generate an important slippage increase. Fig. 12a shows how the slippage value decreases and how the motion reduction force increases as the system mass increases on tilled soil surfaces for a constant draft force equal to 5 kN.
- Wheels: The tire size influences the decrease in motion as well as the slippage. As shown in Fig. 12b, both the slippage and *MR* values decrease as the tire size increases on the tilled soil surfaces for a constant draft force. We analyze the rear tire width

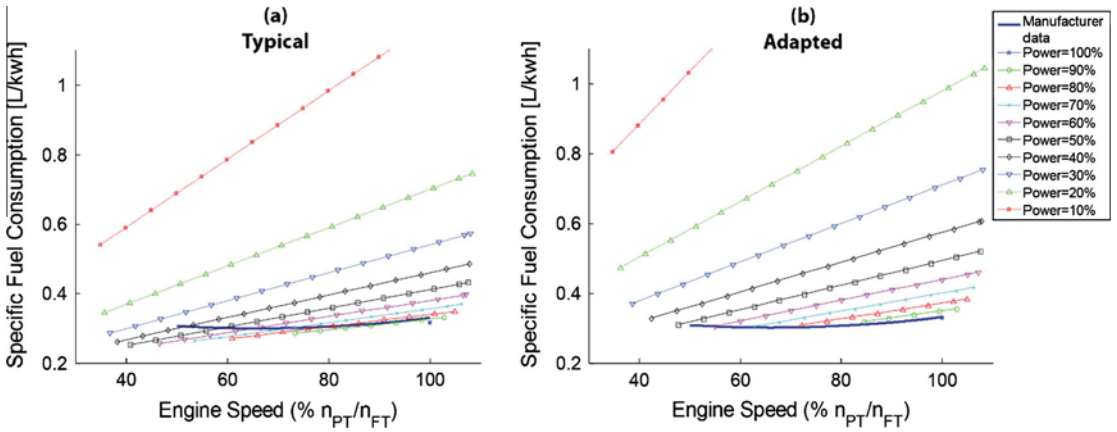

Fig. 11. Typical SFC_v respect to engine speed for different power values (% of rated power).

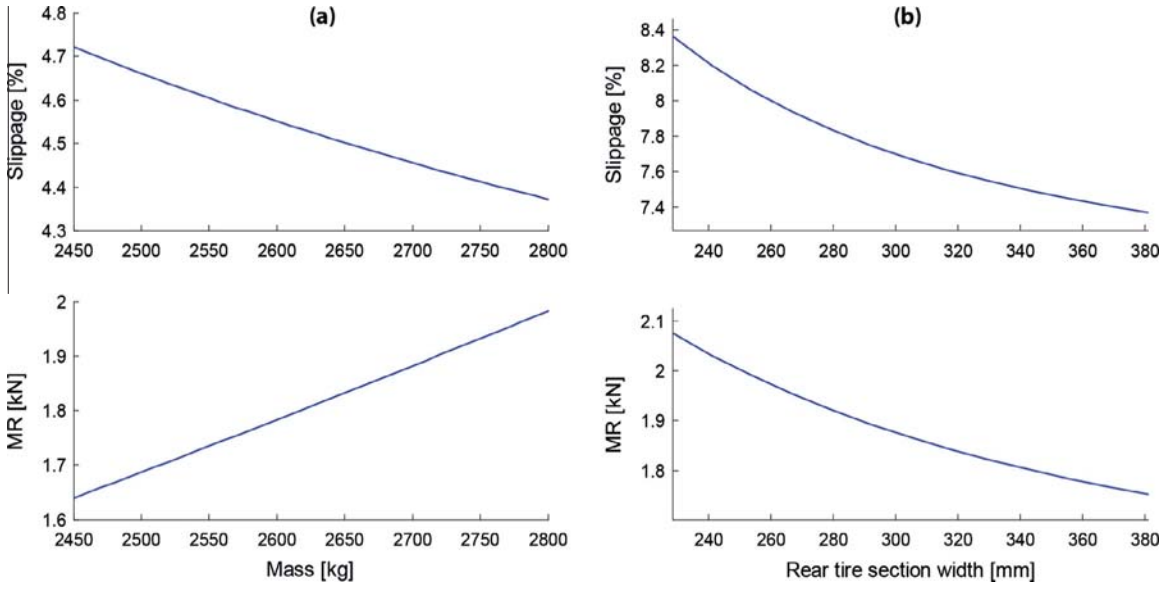

Fig. 12. Slippage and motion resistance with respect to the system weight (a) and with respect to the tire section (b).

influence because agriculture machines allow use different tire width, but these machines only allow very small changes on the wheel diameter. Therefore, the use of large tires, within normal limits, increases efficiency.

- Path planning: To reduce the energy employed in overcoming *MR*, it is necessary to minimize the total distance traveled. If the weed map is known, we can delete the tracks without weeds and minimize the non-working distance without skipping tracks that must be treated. To minimize the average *MR* value, it is necessary to simulate the possible path plan and to calculate the energy considering the field's DEM while considering that during the spraying task, the vehicle is losing mass. This process is addressed in depth in Section 3.3.

2.4.3. Drawbar energy reduction

The drawbar power is the product of the speed and the draft force used for the implement to perform the tillage tasks. This force is given by (Eq. (5)), where the speed also appears; thus, the power increases proportional to the square or cube of the speed. This case includes the flaming implement, which is light tillage and which is proportional to the speed squared. Thus, to reduce the draft energy, we must use the minimum speed and the tillage depth, which allows the treatment to be performed effectively.

To minimize the tillage depth, the treatment effectiveness is also improved, and each tillage tool is individually regulated. This is obtained using one wheel using a tool that performs the individual vertical movement of each of them (see Fig. 13).

2.4.4. PTO energy reduction

The power necessary for the sprayer and the canopy sprayer implements is calculated using (Eq. (11)) and decreases by closing the unused nozzles. The PTO energy can be reduced by stopping the PTO when it is not necessary, such as in non-working paths and when all nozzles are closed.

2.4.5. Hydraulic energy reduction

Hydraulic energy is used to move the implement up and down. This energy can be reduced by minimizing the upper position of the implement during the non-working distances (change of track) or by fixing the implement position for all tasks, whenever possible, such as in the herbicide spraying tasks.

2.4.6. Electric energy reduction

The control systems, sensors and electric actuators use electric energy. This energy can be reduced by disconnecting unused subsystems, such as the implement controller during the non-working distance, and by reducing the use of actuators, such as by keeping the sprayer boom unfolded during the duration of the task rather than folding/unfolding the implement bars.

Fig. 13. Tillage tool with the flaming and row crop cultivator implement.

3. Case studies

3.1. Calibration and validation of fuel consumption measure system

To compare the data obtained from the fuel consumption measure system, we use a different method, which consists of calculating the weight of the total amount of fuel consumed in each test. For this, in the beginning of the test, the fuel tank is completely filled, and when it is necessary to compare the measured total fuel consumption, it is completely refilled again using a portable fuel tank weighed before and after refilling. This method only allows the calculation of the fuel consumption for relatively long periods of time, but it has the advantage that the measurement accuracy is much better. When we finish each test, we have the weight of the total fuel consumed and the total number of pulses counted by our fuel flow measure system in addition to the exact fuel density (we have previously measured it); thus, we can calibrate the fuel consumption measuring system.

3.2. Headland turnings strategy

On the first run, we minimize the non-working distance to change to the next track. Because the tracks are parallel, the GMU always needs to increase its heading by 180°. Therefore, the minimum non-working distance ($L_{\min}$) for the change to the next track (in meters) is given by

$$L_{\min} = \pi r_{\min} \tag{14}$$

where $r_{\min}$ is the minimum turning radius.

For the case where the distance between the final point of a track and the initial point of the next track (d_{AB}) is equal to or greater than $2r_{\min}$, this distance (L) is given by

$$L = (\pi - 2)r_{\min} + d_{AB} \tag{15}$$

In the previous case, it is clear that the best option to minimize the non-working distance is always changing to the next track. Now, we analyze the case when d_{AB} is smaller than $2r_{\min}$. For this case, we have two main options:

- To change to the next track using a maximum of three curve segments, we have four options, which are represented on Fig. 14. In this figure, we can observe that options 'c' and 'd', which use reverse, are shorter than the options 'a' and 'b'. In addition to the length of the options that use reverse is the minimum length, which is given by (Eq. (14))
- To skip some track to minimize the non-working distance, in this case, the length of each track change is given by (Eq. (15)) and is equal to or greater than the minimum length.

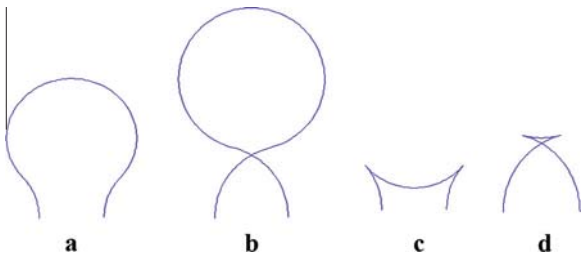

Fig. 14. Path of non-working distance for changing to the next track with $d_{AB} < 2r_{\min}$.

Therefore, we determined that the non-working distance is minimized when always changing to the next track and using reverse if we need it. According to our GMU consumption model, changing the direction of motion does not increase the fuel consumption because the kinematic energy is not considered. We can vary this by performing the test represented on Fig. 15 using the real GMU and the flaming implement for a track width of 3 m and a turning radius of 3 m.

Furthermore, in Fig. 15, we can observe the fuel data in the GMU for the three cases analyzed, where we can observe that the fuel flow is similar for the three cases and that the maximum total distance corresponds to the case when the motion is never reversed. For the other two cases, the total distance is the same. In addition, in these tests, we determined that the minimum total fuel consumed corresponds to the case with reverse and non-cross circles (case A). This amount of fuel consumed is only 1% smaller than that in case C because the change in direction requires a longer period of time (5%) despite the total distance being 3% shorter.

3.3. Path planning selection

To optimize the path plan, we need simulate a number of different possible paths, considering each possible track angle (integer degrees), and calculate the fuel consumed considering the field's DEM while also considering that during the spraying task, the vehicle is losing mass. Fig. 16 shows the block diagram of the procedure. The first step is to obtain the field data, field limits, DEM and weed map and to define the possible angles of the first track of the path plans to carry out the treatment. The proceeding step is to calculate the required energy of each path, considering that we can start the treatment from both sides of the crop and discarding the track with no weed. The last step is to select the best plan, which is the one with smallest fuel consumption.

We need to calculate the consumed fuel for both sides and for all possible track angles, from 0° to 360°, because for these types of treatments with mass losses, the *MR* at the same point can be different. Therefore, the instantaneous *MR* value at each point depends of the path plan initial point.

3.4. Results and discussion

3.4.1. Weed control on herbaceous crops: Spraying of herbicides

In this task, the entire work plan is known before the task is performed; therefore, it is possible to improve the following power components: SFC_v, *MR*, P_{PTO}, P_{hyd} and P_{el}. To conduct the tests, a small wheat crop with known coordinates and a known weed

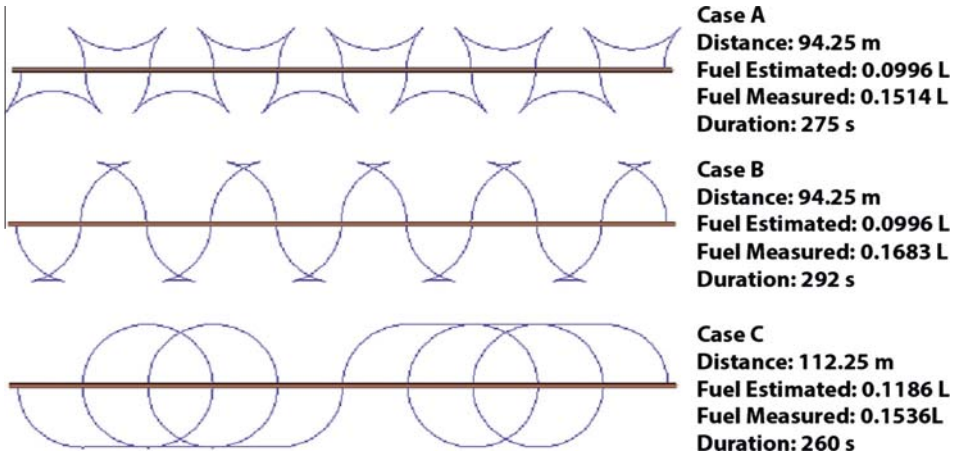

Fig. 15. Path of non-working distances with $d_{AB} < 2r_{min}$.

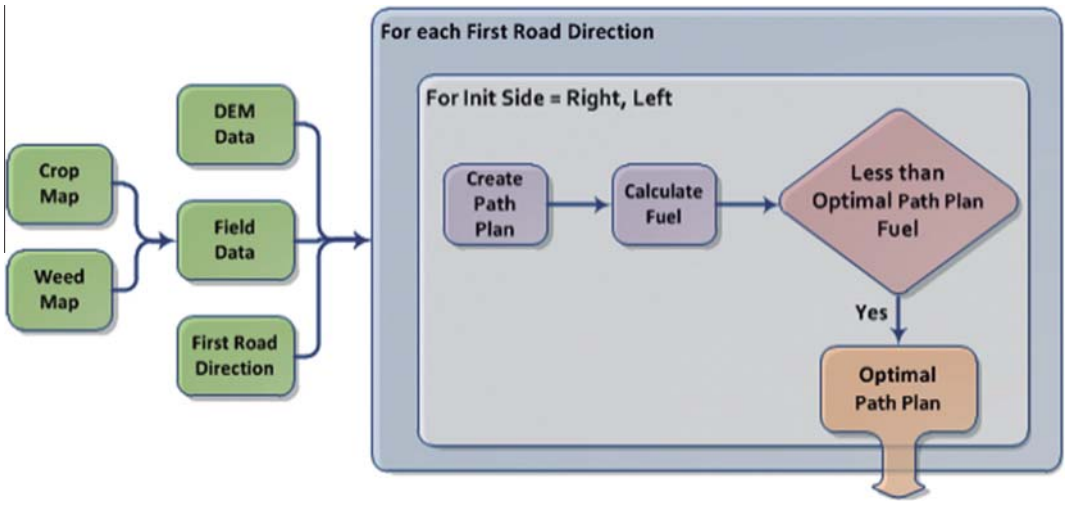

Fig. 16. Path plan selection.

map, as shown in Fig. 17, was used. The first step is to compute the path plan. In this test, we compute both the optimized and unoptimized paths. To perform the first step, we use the procure represented in Fig. 16, and we obtained the graph shown in Fig. 18, here we can observe that the minimum fuel consumption is obtained for a track angle of approximately 49° . Beginning at the right side, the fuel consumption is represented in Fig. 18, where the first point is indicated with an asterisk. In the worst case, the fuel consumed increases by approximately 53% with respect to the best case. Furthermore, the other power components are optimized when applying the criteria described above.

To analyze the reduction in the fuel consumption, this test compares a traditional method with the optimized method using the same GMU in both cases. Fig. 17 represents the path plan of both methods: in the traditional method the track angle is the one of the longest side (44°) and the path plan go over the whole crop. For the improved method, the track angle is calculated (49°) and the path plan is calculated such that the first nozzle (nearest to the starting point) opens at some time in each track (although the last track can be an exception). Fig. 19a shows the fuel consumed with respect to the distance traveled. The estimated data are the data computed using the consumption model, and the measured data are the data read from the real system. We can see that the rate of fuel consumption using the traditional method increases faster than does the improved one. A reduction of approximately 41% is obtained in the real system, and a reduction of 61% is obtained in the system model. In addition, we can see that the total distance also decreases for the improved method because we know the weed map before of treatment; therefore, it is possible to skip some rows with no weeds.

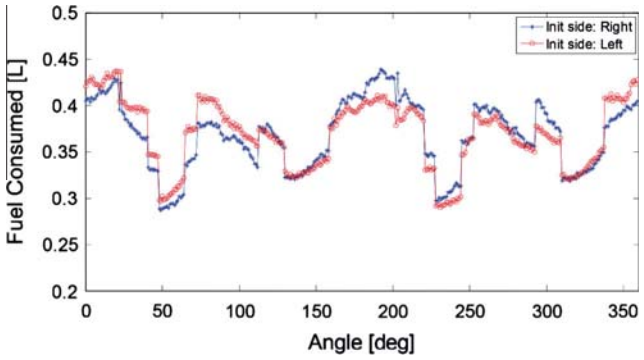

Fig. 18. Fuel consumption vs road angle for weed control on herbaceous crops.

Fig. 19b shows the fuel flow using the traditional and improved methods for spraying herbicides for weed-control treatments. In the traditional method, the PTO is activated, to the rated rpm, during all working distances, which greatly increases the power consumed; furthermore, the engine speed is much higher than necessary. For the non-working distances, where the PTO is deactivated, there are zones characterized by low fuel consumptions. In contrast, in the improved method, the PTO is deactivated when it is not used, resulting in a significant energy-use improvement, and the tracks without weeds are deleted, obtaining important *MR* losses and work time reduction.

There are important differences between the system model and the real system because the crops are situated in an urban zone

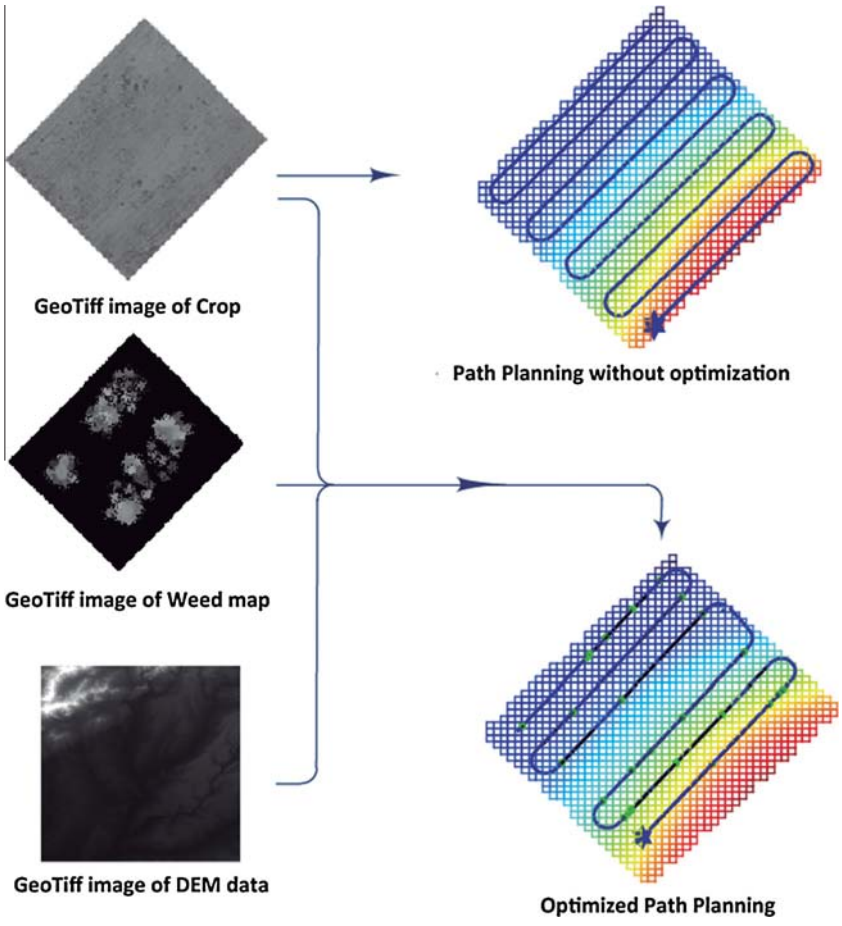

Fig. 17. Field data and path planning for weed control on herbaceous crops test.

close to an abrupt change in elevation, and the DEM data are not sufficiently accurate, resulting in differences between the estimated consumption spikes. Furthermore, the rpm control in the GMU is not effective, and when it is activated, the engine speed is set to the rated rpm, which is too high for the low power demanded by the sprayer implement. In addition, the quickest gears are disabled to limit the ground speed to 7 km/h, which does not allow for a good SFC optimization for low energy requirements, such as the non-working distances, including all routes to reach weeds.

3.4.2. Weed control for fire resistant crops with wide furrows: Plowing and fire treatment

To conduct this test, we used a small maize crop with known limits and DEM data obtained from the Internet, as shown in Fig. 20. In this task, the path planning must cover the entire field because the weed map is created during the treatment and because the track orientation angle is fixed by the row orientation. Therefore, for the path plan selection, we can only choose the first direction and the initial side. In addition, because this implement uses butane gas, whose weight is very low, for the thermal

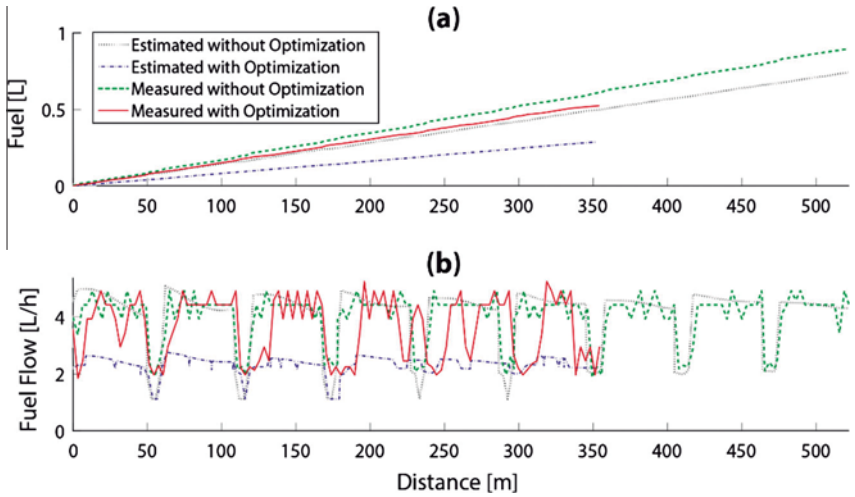

Fig. 19. Fuel data using the sprayer implement.

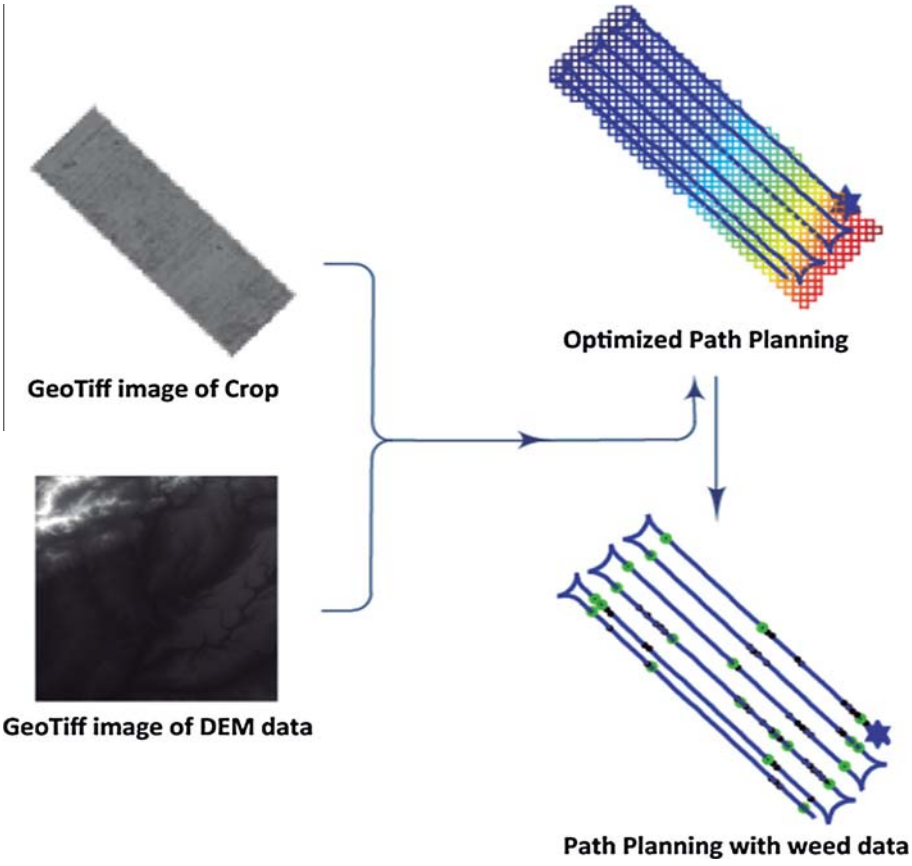

Fig. 20. Field data and path planning for weed control on fire resistant crops with wide grooves test.

Table 8
Fuel consumption for weed control for fire resistant crops with wide furrows.

1st track angle (°)	135.5°		315.5°	
Initial side	Right	Left	Right	Left
Fuel consumed (*L*)	0.4295	0.4308	0.4316	0.4316

treatment, the mass changes during application are almost negligible. Consequently, the optimization of the path plan does not provide substantial improvements, as shown in Table 8, where the difference between the worse and best case is only 0.49% of the total fuel used. Fig. 20 shows the optimized path plan over the DEM data and the path plan with the weed data obtained during the treatment, where the start is the first point. At the black points, there is a change in the nozzle status, and at the green points, all the nozzles are closed.

In addition to the thermal treatment in-row for the weed control treatment, this implement applies a physical treatment in the furrows as a row crop cultivator, which uses a substantial amount of energy. In addition, we can optimize this physical treatment, considering that this treatment must be applied to the four rows treated or over none of them and that the set-unset time is high, approximately 2–4 s. However, the time between from when we obtain the weed data until the treatment should be started is sufficient.

To analyze the reduction in fuel consumption, this test compares a traditional method with the optimized method using the GMU for both cases. Fig. 21a shows the fuel consumed with respect to the distance traveled. We can see that the fuel consumed using

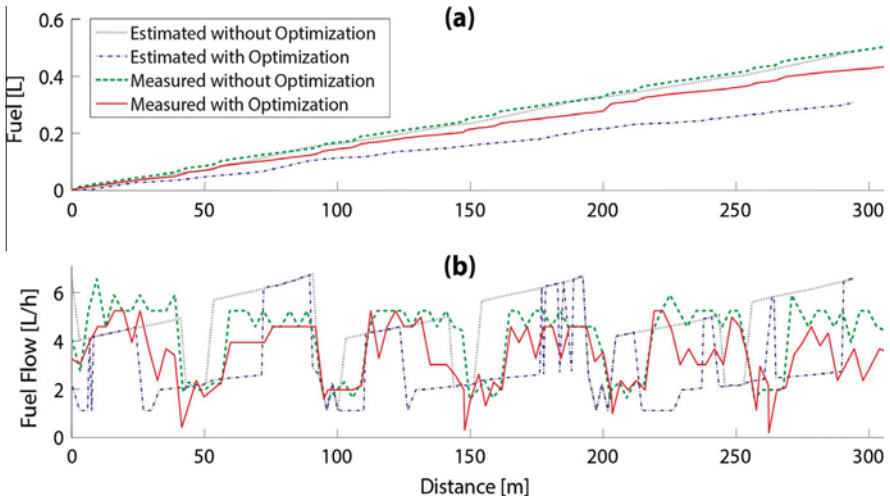

Fig. 21. Fuel data using flaming and row crop cultivator implement.

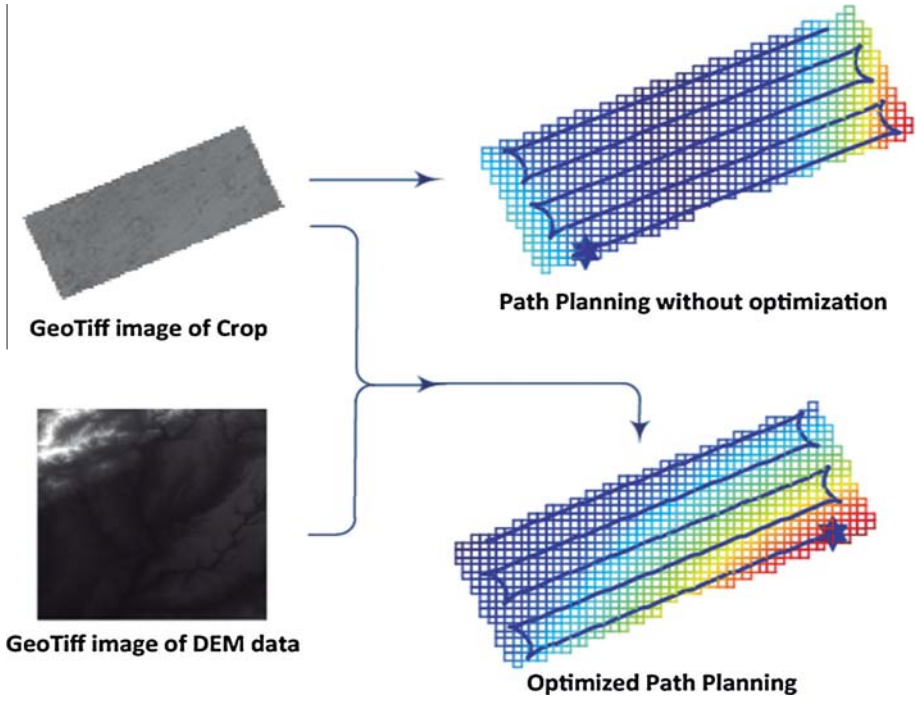

Fig. 22. Field data and path planning for the tests.

the traditional method increases faster than with the improved one. A reduction of approximately 13% in the real system and approximately 36% in the system model are obtained. Fig. 21b shows the fuel flow using the improved and unimproved methods of furrows plowing and thermal treatment for the weed-control treatment. In the uno improved method, the implement plows along all the working distances, with the consequent power demanded increase. We can see that for the non-working distances, where the implement is elevated, the fuel consumption is lower.

In the improved method, the implement is elevated when there is no weeds, resulting in a significant energy-use improvement, but because the weed map is not know in advance and because it is thus not possible to delete any rows, the total distance traveled and the time are similar for both cases.

For this application, we obtain similar data using the system model and the real system for the un improved method because the SFC adjustment with the drawbar force is very good in our GMU. However, this is not true for the improved method. This is because the response of the real system to moving the TPH is not very fast. Furthermore, in both cases, we can observe that the total distance is larger for the real system, which is because this implement is very heavy for our GMU and because the path tracking, especially for non-working distances (curves), is not very good. Besides we can observe that sometimes the fuel consumption is very low, this is because there is very strong changes on the power demand which generate big fluctuations on the fuel flow measurement system. Besides this is the application with the most demand power which leads the fuel flow is greater thus generating greater errors in the measure.

3.4.3. Pest control on trees: Fumigation using insecticides

In this task, the tracks of the path plan are fixed, and the plan is carried out by an autonomous implement that needs PTO power during all working distance. Therefore, we cannot perform a good reduction of the PTO power. In addition, we do not know the instantaneous PTO power demanded by the implement; therefore, the GMU must provide the maximum PTO power demanded by this implement at all times. Consequently, the SFC is not optimized either. Hence, we can improve *MR*, P_{hyd} and P_{el} following the methodology described above.

To conduct the tests, we used a small olive crop with known limits and the DEM data, which is obtained from the Internet, as shown in Fig. 22. In this task, there is an important mass loss during the treatment; thus, optimizing the path plan is very important. Because the fuel consumed on the positive slopes is bigger than that on the negatives slopes and because it is proportional to the system mass, it is important to choose a good path plan that results in a reduced total fuel consumption. However, considering that the track angles are fixed at the beginning, we cannot optimize the angle, and because the treatment must cover all trees, we cannot delete tracks either. Therefore, we can only choose the first direction and the initial side. In Table 9, we observe that the fuel increase in the worst case with respect to the best case is approximately 1.52%. This value is not excessive because the field is too small and because the treatment only uses approximately 4% of the total applied product.

To analyze the reduction in the fuel consumption using our GMU, this test compares the worst case with the best case, both represented in Fig. 22, where the start is the first point. Fig. 23a shows the fuel consumed with respect to the traveled distance for the worst and best cases for the pest control treatment. We can observe that the fuel consumed using the traditional method increases faster than does the improved method. Reductions of approximately 5% in the real system and of approximately 6% in the system model are obtained.

Fig. 23b shows the fuel flows for these cases, where we can observe that each of the two working distances have similar fuel flows. This is because the field is placed on a sloped terrain, and the working distances with higher flows correspond to positive slopes and the others to negative slopes. It is more prominent for the system model because the slopes in the DEM data obtained from the Internet are greater than the real one. In addition, the total fuel consumed in the real system is higher than in the model because the time is also longer. This is because in the real system, there are delays when the GMU changes direction,

Table 9
Fuel consumption for pest control on olives.

1st track angle (°)	135.5°		315.5°	
Initial side	Right	Left	Right	Left
Fuel consumed (*L*)	0.3577	0.3546	0.3523	0.3565

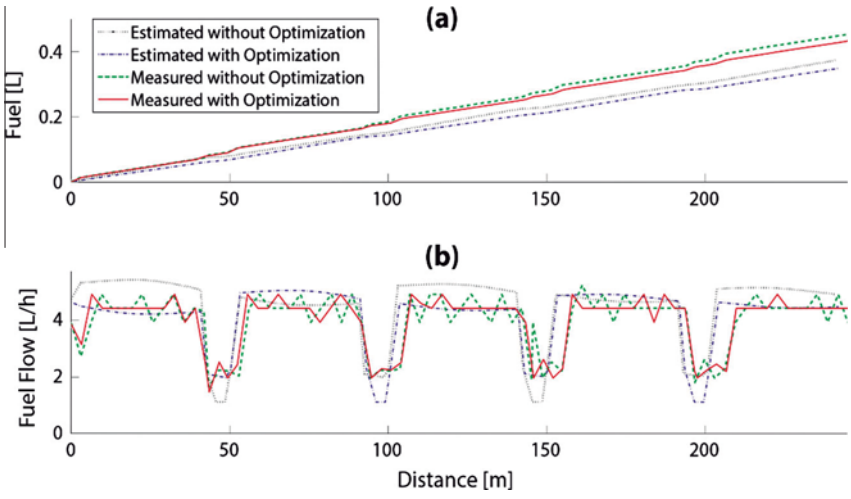

Fig. 23. Fuel data using the canopy sprayer implement.

sets/unsets the PTO, moves the TPH, etc. This is true for all tests performed.

4. Conclusions

This work demonstrates that it is very important to efficiently use engine power by adjusting the gear and throttle positions and that a good and fast control system can help reduce the fuel consumption and working time. Our GMU is a first prototype with some limitations, such as the ground speed being limited to 7 km/h and the PTO control, which can be addressed in the future.

Furthermore, it has been shown that prior knowledge of the field DEM data allows the path plan to be optimized, which is especially interesting for working on terrain slopes and for performing agriculture tasks using implements with payload variations, such as sprayers, whereby the motion reduction is minimized. The DEM data estimation can be obtained from the Internet, in our case from the NASA website (EOSDIS, 2014). We observed that the DEM data are not very accurate, but the data can be corrected using the elevation data obtained from the GMU GPS system, thus improving the optimization for future treatments.

In the three tasks analyzed, a selective treatment is performed; however, we observed that in the first case (Section 3.4.1), where the areas to be treated are known in advance, the fuel reduction is the best. Thus, we need a weed detection system that provides the weed data in advance with the consequent energy cost, which was not considered in this paper because we are sure that it is smaller than the energy savings achieved. In the second case (Section 3.4.2), we know the areas to be treated a few seconds before the treatment, but it is sufficient for applying some energy-saving actions to obtain an important energy reduction. Finally, in the last case (Section 3.4.3), an autonomous implement able to detect the areas to be treated a few milliseconds in advance is used. The implement does not allow the use of nearly any energy-saving actions, and the fuel reduction obtained is thus the lowest. It has the advantage of not requiring communication between the implement and the GMU.

The GMU consumption model implemented allows for the prediction of the GMU energetic behavior in different tasks and for following different path plans. The combination of this model with a three-dimensional representation of the field allows for the determination of the optimum path plan with respect to fuel consumption. In addition, if the weed map is available, it is possible to combine these data with our GMU model to obtain an important reduction in fuel consumption.

The theoretical studies and experiments conducted in this work reveal that for weed and pest control using robotic tractors with the actuated techniques of fuel reduction, it is possible to significantly reduce the energy requirements. Sowing tasks can be performed in addition to this type of energy reduction process, obtaining the best row orientation. It is especially interesting for cases similar to those analyzed at the Sections 3.4.2 and 3.4.3, where the task track orientation is fixed by the row orientation. This energy reduction significantly decreases fuel consumption and the CO_2 and NO_X atmospheric pollutant emissions.

Acknowledgments

The research leading to these results received funding from the European Union's Seventh Framework Programme [FP7/2007-2013] under Grant Agreement n° 245986.

References

ANSI/ASAE S296.4 DEC95 Agricultural Machinery Management Data, 1995. In: ASAE Standards. St. Josep, Michigan, pp. 118–120.

ASAE D497.4 FEB2003 Agricultural Machinery Management Data, 2003. In: ASAE Standards. St. Josep, Michigan, pp. 273–280.

ASAE D497.7 MAR2011 Agricultural Machinery Management Data, 2011. In: ASAE Standards. St. Josep, Michigan, pp. 372–380.

ASAE S313.3 FEB04 Soil Cone Penetrometer, 2004. In: ASAE Standards. St. Josep, Michigan, pp. 903–904.

Bochtis, D.D., Sørensen, C.G., 2009. The vehicle routing problem in field logistics Part I. Biosyst. Eng. 104, 447–457. http://dx.doi.org/10.1016/j.biosystemseng.2009.09.003.

Bochtis, D.D., Vougioukas, S.G., 2008. Minimising the non-working distance travelled by machines operating in a headland field pattern. Biosyst. Eng. 101, 1–12. http://dx.doi.org/10.1016/j.biosystemseng.2008.06.008.

Bochtis, D.D., Sørensen, C.G., Green, O., 2012. A DSS for planning of soil-sensitive field operations. Decision Support Syst. 53, 66–75. http://dx.doi.org/10.1016/j.dss.2011.12.005.

Carballido, J., Perez-Ruiz, M., Gliever, C., Agüera, M., 2012. Design, development and lab evaluation of a weed control sprayer to be used in robotic systems, In: Proceedings of the First International Conference on Robotics and Associated High-Technologies and Equipment for Agriculture. Presented at the Applications of automated systems and robotics for crop protection in sustainable precision agriculture, Pisa University Press srl, Pisa, Italy, pp. 23–29.

CNH America LLC, 2009. BOOMER 3040, 3045, 3050 CVT Service Manual Complete Contents.

EOSDIS. 2014. Nasa's Earth Observing System Data Information System [WWW Document], n.d. EOSDIS NASAs Earth Obs. Syst. <http://reverb.echo.nasa.gov> (accessed 18.07.13).

España, Real Decreto 61/2006, de 31 de enero, por el que se determinan las especificaciones de gasolinas, gasóleos, fuelóleos y gases licuados del petróleo y se regula el uso de determinados biocarburantes, 2006, Boletín Oficial del Estado, 17 de febrero de 2006, núm. 41, pp. 6342–6357.

Frasconi, C., Martelloni, L., Fontanelli, M., Raffaelli, M., Emmi, L., Pirchio, M., Peruzzi, A., 2014. Design and full realization of physical weed control (PWC) automatic machine within the RHEA project, in: Second International Conference on Robotics and Associated High-Technologies and Equipment for Agriculture and Forestry. Presented at the New trends in mobile robotics, perception and actuation for agriculture and forestry, PGM, Madrid, Spain, pp. 3–11.

Grečenko, A., 1968. Predicting the performance of wheel tractors in combination with implements. J. Agric. Eng. Res. 13, 49–63. http://dx.doi.org/10.1016/0021-8634(68)90120-0.

Grisso, R., Pitman, R., Perumpral, J.V., Vaughan, D., Roberson, G.T., Hoy, R.M., 2001. "Gear Up and Throttle Down" to Save Fuel. Virginia Cooperative Extension.

Grisso, R., Kocher, M., Vaughan, D., 2004. Predicting tractor fuel consumption. Biol. Syst. Eng. Pap. Publ.

Grisso, R.D., Vaughan, D.H., Roberson, G.T., 2006. Method for Fuel Prediction for Specific Tractor Models. In: 2006 ASAE Annual Meeting.

Grogan, J., Morris, D.A., Searcy, S.W., Stout, B.A., 1987. Microcomputer-based tractor performance monitoring and optimization system. J. Agric. Eng. Res. 38, 227–243. http://dx.doi.org/10.1016/0021-8634(87)90091-6.

Hameed, I.A., Bochtis, D.D., Sørensen, C.G., 2011. Driving angle and track sequence optimization for operational path planning using genetic algorithms. Appl. Eng. Agric. 27, 294–306.

Hameed, I.A., Bochtis, D.D., Sørensen, C.G., Jensen, A.L., Larsen, R., 2013. Optimized driving direction based on a three-dimensional field representation. Comput. Electron. Agric. 91, 145–153. http://dx.doi.org/10.1016/j.compag.2012.12.009.

Harris, H.D., 1992. Prediction of the torque and optimum operating point of diesel engines using engine speed and fuel consumption. J. Agric. Eng. Res. 53, 93–101. http://dx.doi.org/10.1016/0021-8634(92)80076-5.

Harris, H.D., Pearce, F., 1990. A universal mathematical model of diesel engine performance. J. Agric. Eng. Res. 47, 165–176. http://dx.doi.org/10.1016/0021-8634(90)80038-V.

International Energy Agency, 2013. Oil Information: Documentation For Beyond 2020 Files.

Jin, J., Tang, L., 2010. Optimal coverage path planning for arable farming on 2D surfaces. Trans. ASABE 53, 283–295.

Jin, J., Tang, L., 2011. Coverage path planning on three-dimensional terrain for arable farming. J. Field Robot. 28, 424–440. http://dx.doi.org/10.1002/rob.20388.

Larsen, W.E., 1981. Efficiency of utilization of four-wheel drive tractors. Agric. Energy ASAE Publ. 81, 417–421.

Mileusnić, Z.I., Petrović, D.V., Đević, M.S., 2010. Comparison of tillage systems according to fuel consumption. Energy 35, 221–228. http://dx.doi.org/10.1016/j.energy.2009.09.012.

Oksanen, T., Visala, A., 2009. Coverage path planning algorithms for agricultural field machines. J. Field Robot. 26, 651–668. http://dx.doi.org/10.1002/rob.20300.

Rahimi-Ajdadi, F., Abbaspour-Gilandeh, Y., 2011. Artificial Neural Network and stepwise multiple range regression methods for prediction of tractor fuel consumption. Measurement 44, 2104–2111. http://dx.doi.org/10.1016/j.measurement.2011.08.006.

RHEA. 2014. RHEA Project – EU [WWW Document], n.d. "Robot Fleets Highly Eff. Agric. For. Manag. <http://www.rhea-project.eu/> (accessed 30.10.13).
Sarri, D., Lisci, R., Rimediotti, M., Vieri, M., 2014. RHEA Airblast Sprayer: Calibration Indexes of the Airjet Vector Related to Canopy and Foliage Characteristics, In: Second International Conference on Robotics and Associated High-Technologies and Equipment for Agriculture and Forestry. Presented at the New Trends in Mobile Robotics, Perception and Actuation for Agriculture and Forestry, PGM, Madrid, Spain, pp. 73–81.
Titan Enterprises Ltd – Titan flow meters for oil, boiler and diesel fuel applications – PD400 oil flowmeter [WWW Document], 2014. URL <http://www.flowmeters.co.uk/> (accessed 20.02.14).

5 PUBLICACIÓN II:

Reducing air pollution with hybrid-powered robotic tractors for precision agriculture

M. Gonzalez-de-Soto, L. Emmi, C. Benavides, I. Garcia and P. Gonzalez-de-Santos

Biosystems Engineering, ISSN 1537-5110, vol. 143C, pp. 79-94

DOI: *http://dx.doi.org/10.1016/j.biosystemseng.2016.01.008*

Impact Factor (2014): 1.619

Category: Agriculture, Multidisciplinary: 9/56 (Q1)

Category: Agricultural, Engineering: 4/12 (Q2)

BIOSYSTEMS ENGINEERING 143 (2016) 79–94

Available online at www.sciencedirect.com

ScienceDirect

journal homepage: www.elsevier.com/locate/issn/15375110

Research Paper

Reducing air pollution with hybrid-powered robotic tractors for precision agriculture

Mariano Gonzalez-de-Soto [a,b,*,1,2], Luis Emmi [a,1], Carmen Benavides [b,2], Isaias Garcia [b,2], Pablo Gonzalez-de-Santos [a,**,1]

[a] Centre for Automation and Robotics (UPM-CSIC), Ctra CAMPO REAL km 0,2, 28500 Arganda del Rey, Madrid, Spain

[b] Escuela de Ingenierías Industrial e Informática, Universidad de León, Dept. de Ingeniería Eléctrica y de Sistemas y Automática, Campus de Vegazana s/n, 24071, León, Spain

ARTICLE INFO

Article history:
Received 7 August 2015
Received in revised form
8 January 2016
Accepted 20 January 2016
Published online xxx

Keywords:
Atmospheric emissions
Exhaust gasses
Hybrid power
Robotic tractor
Precision agriculture

A hybrid energy system used in robotic tractors for precision weed and pest control in agriculture is evaluated and its exhaust emissions compared with the use of an internal combustion engine as a single power source. The agricultural implements require power for hydraulic pumps and fans which, initially, was provided by a power take-off system (PTO), wasting a lot of energy. The objectives of this work were to design and assess a hybrid energy system including the removal of the alternators from the tractor and the modification of the agricultural implements to replace the PTO power with electric power, using small pumps and small fans. These changes improved energy use and reduced the atmospheric pollution emission from the internal combustion engine. The hybrid energy system used the original combustion engine of the tractor in combination with a new electrical energy system, which consisted of a hydrogen fuel cell. An analysis of the exhaust gases using the internal combustion engine as the single power source and using the hybrid energy system was carried out to compare the results obtained. The results showed a reduction in emissions of almost 50% for the best case.

1. Introduction

Non-road vehicles, such as agricultural machines, use large amounts of energy, usually fossil fuels and emit large amounts of pollution to atmosphere. Off-road internal combustion engines (ICEs) emit carbon dioxide (CO_2), nitrogen oxides (NO_X), carbon monoxide (CO), particulate matters (PM) and hydrocarbon (HC). CO_2 and NO_X are greenhouse gases, and they contribute to global warming. Furthermore, they can

* Corresponding author. Centre for Automation and Robotics (UPM-CSIC), Ctra CAMPO REAL km 0,2, 28500 Arganda del Rey, Madrid, Spain.
** Corresponding author.
E-mail addresses: mariano.gonzalez@car.upm-csic.es (M. Gonzalez-de-Soto), luis.emmi@car.upm-csic.es (L. Emmi), carmen.benavides@unileon.es (C. Benavides), isaias.garcia@unileon.es (I. Garcia), pablo.gonzalez@car.upm-csic.es (P. Gonzalez-de-Santos).
[1] Tel./fax: +34650015576; +34689876367; + 34918711900x221.
[2] Tel./fax: +34650015576; +34987291000x5395; +34987291000x5289.
http://dx.doi.org/10.1016/j.biosystemseng.2016.01.008
1537-5110/

List of symbols and acronyms

CO	Carbon monoxide
CO_2	Carbon dioxide
D	Implement draft force (kN)
E_{EES}	Energy demand supplied by the electrical energy system (kW h)
EES	Electrical energy system
E_{ICE}	Energy demand supplied by the internal combustion engine (kW h)
EMS	Energy management system
GPS	Global positioning system
HC	Hydrocarbon
HES	Hybrid energy system
HFC	Hydrogen fuel cell
ICE	Internal combustion engine
MR	Motion resistance (kN)
n	Number of tools
NO_X	Nitrogen oxides
P_{EES}	Power demand supplied by the electrical energy system (kW)
PEM	Proton exchange membrane
P_{ICE}	Power demand supplied by the internal combustion engine (kW)
$P_{IMP\ control}$	Electrical power of the implement control system (kW)
PM	Particulate matter
P_{Task}	Electrical power demand of the task (kW)
PTO	Power take-off
P_{Tool}	Electrical power of each implement tool (kW)
$P_{UGV\ control}$	Electrical power of the UGV control system (kW)
PV	Photovoltaic
PVGIS	Photovoltaic geographical information system
RDS	Row detection system
RTK	Real time kinematic
SFC_V	Specific fuel consumption volume (l kW h^{-1})
SHC	Specific hydrogen consumption (kg kW h^{-1})
TE	Total energy (kW h)
TPH	Three-point hitch
UGV	Unmanned ground vehicle
WDS	Weed detection system

cause health problems: NO_X may cause or worsen respiratory diseases, such as bronchitis or emphysema, and may also aggravate existing heart disease; CO binds to haemoglobin in the blood and can cause harmful health effects by reducing oxygen delivery to the body's tissues and organs (such as the brain and heart), reducing work capacity and mental skills; decreasing learning ability; causing headaches, nausea, and dizziness; and, at extremely high levels, can cause death. HCs are volatile organic compounds, such as xylenes, toluene, benzene and ethyl-benzene. These compounds can cause headaches, dizziness, loss of consciousness, etc. Furthermore, benzene is carcinogenic and increases the likelihood of leukaemia. Particle matter (PM) emitted from combustion engines is a complex mixture of liquid droplets and fine particles have a number of components, including sulphates and nitrates, metals, organic chemicals, and dust or soil particles. These particles can also affect the lungs or heart function causing serious health problems according to the US Environmental Protection Agency (EPA, 2015).

Some research analysing energy use and the pollution emitted by agricultural tractors has been carried out. Clements et al. (1995) analysed the energy used in weed control using herbicides and tillage and found that alternative weed control strategies can provide interesting energy savings. Hansson, Lindgren, and Norén (2001) compared different methods and calculated the average absolute and specific emission values from agricultural tractors. Considering the consequences of these emissions, we need to progressively reduce the use of hydrocarbon fuels. To achieve this, fossil fuels can be replaced by cleaner fuels or electrical systems. Dalgaard, Halberg, and Porter (2001) presented a model of fossil fuel use for Denmark and proposed the use of their model to simulate possible agricultural production scenarios in an effort to improve future techniques. Guzman and Alonso (2008) analysed energy use in Mediterranean agriculture and evaluated the contribution of the organic olive oil production towards improving energy efficiency and compared the results with respect to the conventional production. Soni, Taewichit, and Salokhe (2013) presented an analysis of the CO_2 emissions and energy consumption in agricultural task performed over rain fed crops. Peltre, Nyord, Bruun, Jensen, and Magid (2015) analysed how increasing soil organic carbon content decreased the draft force in ploughing and the consequent reductions in fuel consumption and emissions.

To date much research has studied alternative energy sources to the use of fossil fuels and ICEs. Biofuel is one of these alternatives. Gasparatos, Stromberg, and Takeuchi (2011), analysed the impact of biofuels on society and environment demonstrating that biofuels generate many impacts that must be considered. However, many works on alternative power sources propose the use of batteries; for example, Delucchi and Lipman (2001) analysed the lifecycle costs of battery-powered electric vehicles (that is, initial vehicle cost as well as operating and maintenance costs) to develop a detailed model of the lifecycle costs of electric vehicles. This model was compared to a gasoline ICE vehicle model and determined the battery properties needed to reduce the costs of electric vehicles to be economically competitive with ICE vehicles. Mousazadeh et al. (2010) looked at the various battery technologies available for use in solar-assisted plug-in hybrid electric tractors to be used in light-duty agricultural operations. This was extended by Mousazadeh et al. (2011) who carried out a life cycle analysis of a solar-assisted plug-in hybrid electric tractor and compared the results with that of a similar power output ICE tractor considering economic costs and environmental emissions. They determined that the life cycle costs of solar-assisted plug-in hybrid electric tractors are lower than those of ICEs.

Other important alternatives to batteries as the energy source in electric vehicles are fuel cells; usually, the same fuel can also be used by an ICE. For example, Mulloney (1993) proposed the use of environmentally benign fuel cells for power production, avoiding the use of fossil fuels for field crop production and distribution. They also presented an

engineering systems analysis of how such systems can mitigate pollution. Lutz, Larson, and Keller (2002) compared the theoretical maximum efficiency of a fuel cell to the efficiency of a Carnot cycle using the same fuel to determine the net reaction. They found that the maximum efficiency was quite similar in both systems, but in practice, a fuel cell exhibits higher efficiency because ICEs cannot operate at theoretical maximum efficiency. This would require a very high temperature, which would generate problems in terms of engine construction materials. Eaves and Eaves (2004), compared the manufacturing and refuelling costs of a fuel cell vehicle and a battery electric vehicle using an automobile model reflecting the largest segment of light-duty vehicles. They determined that a battery electric vehicle performs far more favourably in terms of cost, energy efficiency, mass, and volume. In another example of this type of researchy, Offer, Howey, Contestabile, Clague, and Brandon (2010) compared battery electric vehicles, hydrogen fuel cell electric vehicles and hydrogen fuel cell plug-in hybrid vehicles. They concluded that battery electric vehicles and hydrogen fuel cell plug-in hybrid vehicles have reasonably similar lifecycle costs. However, these costs are higher than the costs of ICEs (in 2010) but these costs could drop by 2030. These vehicles offer different advantages depending on driving pattern.

The approach presented in this paper was tested using agricultural autonomous vehicles developed within the RHEA project (http://www.rhea-project.eu/). During the development of this project, it was observed that during precision agriculture tasks, the ICE very frequently supplied more power than needed, particularly when the implement (a tool or utensil for doing work (Dictionary, 2015), in this case, agricultural work) uses PTO power. Thus, the objective of this work was to develop, implement and assess a hybrid energy system (HES) for robotic tractors used in precision agriculture. These agricultural vehicles were designed to work at low speed; thus, the aerodynamics and vehicle size do not present substantial problems. Furthermore, in many agriculture tasks the tractor needs to counterweight or increase its weight. Therefore, weight is usually not a problem. Taking advantage of these features, the proposed energy system combines the use of batteries, a hydrogen fuel cell, and photovoltaic (PV) cells with the original ICE of the tractor to achieve a substantial decrease in fossil fuel use and a consequent reduction in the emission of pollutants. This energy system allowed the tractor to increase the work capacity because the implement can incorporate its own motor decreasing the workload of the ICE of the tractor.

To carry out this work, the main objective was divided into the following sub-objectives:

- Analyse the main features of the used systems (Section 2.1).
- Implement an energy model to predict the energy requirements (Section 2.2).
- Analyse the energy demands of each subsystem and task (Section 3.1.1)
- Design and implement an HES that supplies the energy requirements of all of the different agriculture tasks accomplished (Section 3.1.2).
- Present the results obtained after conducting a series of field experiments to check the energy system and assess the pollutant emission reduction, comparing HES with the system based on the ICE (Section 3.2).

2. Materials and methodology

This section presents the system used and its main power features, focussing on obtaining an energy model. The aim was to develop a model that would allow the energy requirements of three agricultural tasks considered in this work to be analysed (weed control on fire-resistant crops with wide furrows, weed control on herbaceous crops and pest control in tree crops). According to the energy requirements, as system was designed and the size of the energy system specified.

2.1. *Systems*

In this work, an unmanned ground vehicle (UGV) and three different implements, one for each of agricultural tasks analysed were used. Here, the main features of this UGV are presented. It had a control system, an energy system and a fuel consumption measurement system. The system and the method used to measure the fuel consumption and estimate the exhaust gases from the ICE are described. The agricultural tasks and implements used in this work are presented; that is, a description of the changes in the implements to replace the PTO power by electric power as well as an enumeration of the implement power features, which were needed to design the energy model.

2.1.1. *Unmanned ground vehicle*

The UGV used in this work is based on the commercial vehicle CNHi Boomer 3050 CVT compact tractor. It inherits the main features from the original tractor that was modified and programmed using a special software package. The UGV was improved with an additional power system; a control system, which manages the main vehicle functions; and a safety system, which provides safety to the vehicle, the environment and the people involved (RHEA, 2014).

The UGV was equipped with a control system and four power systems: an ICE, a PV panel, a hydrogen fuel cell (HFC) and batteries. The group formed by the PV panel, the HFC and the batteries is referred as the electrical energy system (EES). Figure 1 shows the final aspect of the UGV used for the analysis and tests provided in this article. In this figure, the different subsystems whose main features are detailed in the following sections can be identified. Originally, the UGV used two alternators (12 V dc and 24 V dc), which were removed and replaced with appropriately designed and sized EES. In Section 3, the added energy system features (PV panel, hydrogen fuel cell and batteries) will be sized, justified and assessed.

2.1.1.1. UGV control system. The UGV control system (see Fig. 2) allowed an autonomous worker to apply an effective treatment with high precision. It was responsible for synchronising and processing all information selecting the best behaviour for the entire system depending on the current

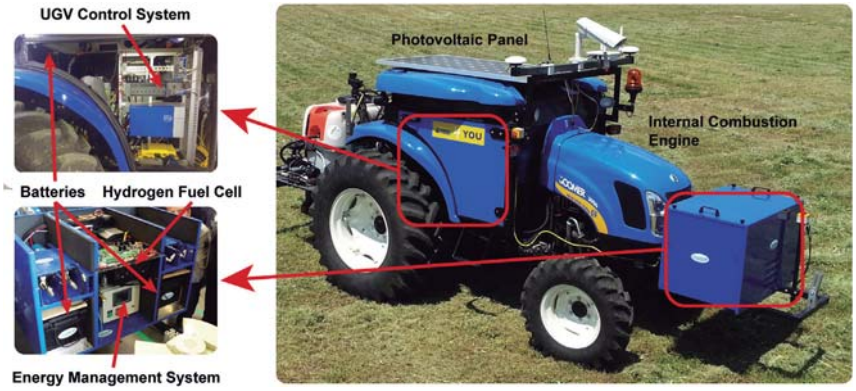

Fig. 1 – Unmanned ground vehicle (UGV).

working situation. This controller communicated with other subsystems via diverse electronic communication protocols (Ethernet, serial and CAN bus) and it interpreted the information coming from the external user and other devices (Emmi, Gonzalez-de-Soto, Pajares, Gonzalez-de-Santos, 2014a, b). The set of all of these systems (controllers, sensors and actuators) had an average power demand of approximately 170 W for 12 V dc devices and of approximately 260 W for 24 V dc devices.

The UGV was equipped with a positioning system that consisted of a GPS receiver; a Trimble Model BX982, with two antennas. This system used an RTK signal correction, provided by a base station, achieving an accuracy of approximately ±0.025 m. A second antenna was used to obtain the heading of the UGV even when the UGV was stationary (Carballido, Perez-Ruiz, Emmi, Agüera, & others, 2014).

A vision system, installed on-board the UGV, was used by the weed detection system (WDS), the row detection system (RDS) and the safety system. The RDS estimated rops rows and the WDS was able to identify weeds and crop plants even when they were contaminated with materials from the soil (Guerrero et al., 2013), (Montalvo et al., 2013).

The safety system comprised of an obstacle detection system based on a vision camera, a laser and a remote controller used by the operator. The laser on-board the vehicle was in charge of the lowest safety level and was configured to stop the vehicle motion when any type of obstacle in the UGV path was detected, considering the time to stop the vehicle (Garrido et al., 2012).

The work plan execution was supervised by a base station which generated the work plan and sent it to the UGV. When the UGV was working, this base station was responsible for monitoring the status of both the UGV and the agricultural implement in real-time and detecting failures (Conesa-Muñoz, Gonzalez-de-Soto, Gonzalez-de-Santos, & Ribeiro, 2015).

2.1.1.2. *Internal combustion engine*. The ICE could work as the only power source, providing the total power demanded by the agricultural task, or as a part of the HES, providing only the power to move the UGV with its implement. It preserved features from the original tractor, although the maximum ground speed has been limited to 7 km h^{-1} for safety reasons; thus some gears were disabled. The main ICE features are

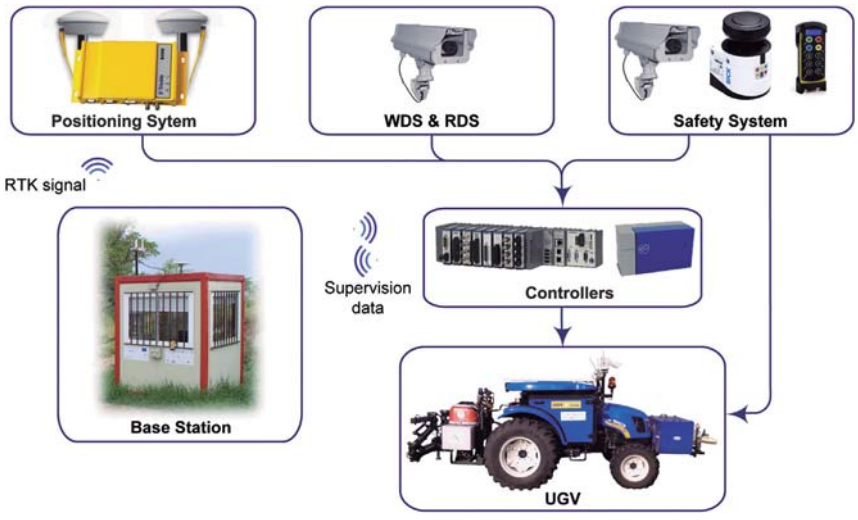

Fig. 2 – UGV control system.

Table 1 – Main features of the ICE. Source: (CNH America, 2009).

Feature	Value
Gross power	33.6 kW
Rated speed	2800 rpm
Idle speed	1050 rpm
Maximum speed	3050 rpm

compiled in Table 1. Figure 3 shows the ICE performance curves provide by the manufacturer, which were used to calculate the exhaust gas emissions and to implement the energy demand model. In this figure, torque, specific fuel consumption volume (SFC_v) and the power curve with respect to the ICE speed can be seen. These curves were used to estimate the ICE fuel consumption and the exhaust emissions.

2.1.1.3. *Hydrogen fuel cell*. An HFC was used because it provides good performance to generate electrical power (approximately 50%) and fairly rapid refuelling. It was situated in a box placed on the tractor muzzle, next to the hydrogen tanks, where there was enough space. A proton exchange membrane (PEM) fuel cell was selected and metal hydride tanks offered by the company Tropical S.A. (Athens, Greece), which has a power range from 0.5 to 5 kW with a specific hydrogen consumption (SHC) of approximately 0.74 N m^3 Kw h^{-1}. This value was used to estimate the hydrogen consumption (Tropical, 2015).

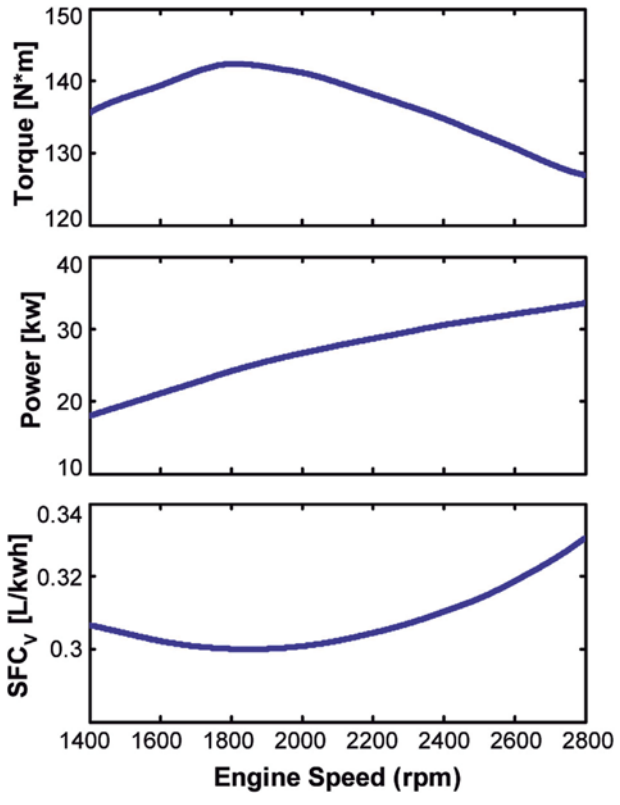

Fig. 3 – ICE performance curves. Source: (CNH America LLC, 2009).

2.1.1.4. *Photovoltaic panel*. The PV panel was used as an additional system for "free" energy, which charges the batteries whenever there is sufficient light; even when the UGV is in a garage. The panel was situated at the highest part of the UGV to minimise shadows. Only the antennas and the camera were higher to improve signal transmission and the area of view. The PV panel was set horizontally to collect solar power independently of orientation.

2.1.1.5. *Batteries*. Batteries were used to store excess electrical energy and to supply energy during high demand periods (for example during starting of the ICE) and to ensure that the vehicle's energy management system (EMS) had a continuous energy supply. Because the batteries were heavy, one group of batteries was placed over the rear axle to reduce the slippage in tasks requiring a draft force. Another battery bank was placed next to the HFC, hydrogen tanks and EMS, inside a box in the front part of the tractor and acts as counterweight, which is necessary to work with heavy implements.

2.1.1.6. *Energy management system*. The EMS was responsible for regulating and adapting the electrical power and supervising the electrical energy storage. This system consisted of a controller that managed the electrical energy flow from the HFC and PV systems. It collected data about the status of the battery and hydrogen tanks and controlled the power provided by the HFC.

2.1.2. *Fuel consumption measurement and calculation of the exhaust gas emissions*

A number of studies analysing exhaust gas emissions from ICEs have been carried out in recent years as part of the continuous interest in reducing the emissions of pollutants. Some of these works have been focused on agricultural machines. Lindgren and Hansson (2002) developed a mathematical model of a tractor and analysed the fuel consumption and engine emissions for different engine control strategies and engine transmission characteristics. Janulevičius, Juostas, and Pupinis (2013) measured the exhaust emissions and fuel composition in a real tractor during ploughing for different scenarios and correlated the results to the load factor of the tractor. These works concluded that the fuel consumption and the production of emissions depends on engine speed and load conditions. The main exhaust gas is CO_2, and its amount increases with ICE speed and the fuel consumption. The largest concentrations of CO, HC and PM are emitted when the ICE operates under a partial load and at a low speed. This contrasts to NO_x emissions which are the largest when the ICE load and speed are the highest which is when combustion temperatures are highest, improving combustion, and reducing CO, HC and PM generation.

In this work, the fuel consumption is measured using two PD400 flowmeters from Titan Enterprises Ltd. (Sherborne, Dorset, UK): One meter was installed in the fuel supply line, and the other in the return line. Fuel flow was obtained from the difference between the data measured in each flowmeter. The flowmeters had a measuring range of 1–60 L h^1. This was sufficient for the ICE used which had a maximum flow of

~30 L h^{-1}, and the rated flow of the fuel pump, which was approximately 12.54 L h^{-1}. The recommended temperature range was from 0 to 60 °C, which was slightly low for the return line requiring a small radiator to cool the returned fuel. The flowmeter accuracy was approximately ±2.5% with a low loss of pressure of 10 kPa (Titan, 2014). This fuel consumption measurement system was calibrated and validated by measuring the total mass of fuel consumed during different tests.

The exhaust gas emissions from the ICE were calculated considering the partial load and speed (work regime) of the ICE according to the ISO 8178 standard (ISO, 1996) and the fuel features specified in España (2006). To calculate the partial load, the values of wheel slippage were measured (the difference between the ground speed provided by GPS and the wheel speed provided by the control system), PTO speed, ICE speed, three-point hitch (TPH) position and terrain slope (obtained from the orthometric height in each point). Using this data and the equations of ASABE Standards, (ASAE, 2011), (ANSI/ASAE, 1995), (ASAE, 2004), (ASAE, 2003) the partial load of the ICE was calculated. With this partial load, the work regime of the ICE was obtained by interpolating the power curves of the ICE as shown in Fig. 3. With this data and the standard ISO 8178 the corresponding emission factor for each exhaust substance was estimated. The ISO standard defined the emissions factors of exhaust gasses for agricultural ICEs in eight individual work regimes, considering the maximum power and the manufacturing year of the ICE. For small ICEs, as in this case, the emission factors of NO_x and HC were joined, therefore the ISO standard defined the emission factors to calculate: CO, PM and NO_x + HC. Finally, the CO_2 emission was calculated using the chemical equation of combustion reaction (considering the other exhaust emission gasses calculated with the emission factor of the ISO standard) and the measured fuel consumption.

2.1.3. *Implements and tasks*

Three different agricultural tasks with their respective implements were considered: weed control using a flaming and a row crop cultivator implement, weed control with an herbicide patch sprayer, and pest control with a canopy sprayer. Figure 4 illustrates these three implements working in experimental fields and in the next sections the main features of each implement and their main requirements are described. Furthermore, the changes in the implements to use adequately the HES are described.

2.1.3.1. Weed treatment with a flaming and row crop cultivator implement. This task performed ploughing and thermal treatment using a particular mechanical-thermal machine. The WDS detected weed patches by processing the images from the camera in real time. The UGV was programmed to follow a predefined path, which fixes the initial and final point of each track (path followed by the vehicle through the treated crop). These were approximate points, and were corrected by the RDS. The area analysed in each image was a rectangle with a width of 3 m (4 rows) and length of 2 m. It was georeferenced with an accuracy of approximately 0.08 m and divided into square cells with 0.25-m sides (Emmi et al., 2014b).

The implement consists of a flaming and row crop cultivator. It performed mechanical treatment in the furrows (space between crop rows), as performed by a row crop cultivator, and a thermal in-row treatment for weed control. This flaming and row crop cultivator implement (see Fig. 4b) was used for crops with wide row spaces (approximately 750 mm) that can withstand high temperatures over short periods of times, such as maize, garlic, leek, and onion. It was controlled from the UGV, which was able to regulate the gas pressure of each burner separately in three stages: zero (off), low and high. Table 2 shows the basic features of this implement (Gonzalezde-Santos, Ribeiro, Fernadez-Quintanilla, Dorado, 2014).

Originally, this implement had two hydraulic cylinders to extend and retract the main bar, which was extended for working and retracted for transporting. These cylinders could be replaced by linear actuators with electrical motors (LINAK LA36, Guderup, Nordborg, Denmark), reducing the power demanded from the ICE and increasing the power demanded from the EES by a small amount because the main energy demand of this task was in the ploughing, which was supplied by the ICE. This implement used fuel gas for the burners, but we did not consider this fuel in the energy analysis, only the electrical power used to light these burner. This gas can be any type of biogas, whose combustion emissions are considered null.

2.1.3.2. Weed treatment with a herbicide patch sprayer. This task consists of the spraying of herbicides over the weed patches of herbaceous crops, such as wheat and barley. The WDS was an external system that took images using aerial robots and provides a weed map of the crop with a 272 cell size of 0.5 m. The path plan followed by the UGV was improved by applying a path planning calculation method, such as, for example, the method described in (Gonzalez-de-Soto, Emmi, Garcia, & Gonzalez-de-Santos, 2015), which obtained an important reduction in work time. This path plan fixed the point where selected nozzles were opened or closed, as well as the initial and final point of each track.

The implement used was a patch sprayer (see Fig. 4b) which was used to apply herbicide in the weed-control treatments. This implement is used for herbaceous crops, such as wheat or barley, with small row spaces (approximately 100–170 mm), and was able to activate each nozzle separately and regulate the total flow of the product applied. It had two electrical lineal actuators to extend and retract the spraying booms that are controlled by the main control system from the UGV. Table 2 presents the main features of this implement (Carballido, Perez-Ruiz, Gliever, & Agüera, 2012).

Originally, this implement used a main pump that worked with the PTO using the ICE power. The pump worked to rated power whenever a valve was open, it used a bypass line to return the product overflow, and therefore it wasted a large amounts of energy. To improve this system, this main pump was replaced by a series of small pumps, using one pump for each nozzle. The selected pump for this application was the model MG100 Micropump, (TCS Micropumps Ltd, Faversham, Kent, UK) which was able to

BIOSYSTEMS ENGINEERING 143 (2016) 79–94

Fig. 4 – Implements working: (a) Flaming and row cultivator, (b) Patch sprayer, and (c) Canopy sprayer.

regulate the flow to provide sufficient flow and pressure. Furthermore, this implement control system was able to regulate the main flow (the sum of each nozzle flow) to ensure and improve the correct operation. This change generated an significant reduction of the power demanded from the ICE and slightly increased the power demanded from the EES.

2.1.3.3. *Pest control with a canopy sprayer*. This task consists of spraying insecticides into tree canopies for pest control. The path plan only fixed the initial and final point of each track, and the UGV was responsible for designing the path to follow. The implement was an autonomous canopy sprayer (see Fig. 4c) that sprayed a pesticide solution over the tree canopies and blew the spray along the entire canopy. The

Table 2 – Main features of the implements. Source: (RHEA, 2014), (LINAK, 2015), (TCS, 2015.), (EBM-PAPST, 2015).

Implement	Feature	Value
Flaming and row crop cultivator	Power of implement controller	40 W (24 V)
	Number of burners (2 per row)	8
	Power of valves and sensors	<1 W
	Power of each ignitor	144 W (24 V)
	Linear actuator motor power (x2)	240 W (24 V)
Patch sprayer	Power of implement controller	40 W (24 V)
	Number of nozzles	12
	Nozzle nominal flow	0.757 L min^{-1}
	Nozzle nominal pressure	276 kPa
	Power of each pump	16.5 W (24 V)
	Power of flow control system	15 W (12 V)
	Motor power of each linear actuator (x2)	200 W (12 V)
Canopy sprayer	Power of implement controller	40 W (24 V)
	Number of diffusors	8
	Nozzle nominal flow (2 per diffusor)	0.4 L min^{-1}
	Nozzle nominal pressure	300 kPa
	Power of each pump	19 W (24 V)
	Power of flow control system	24 W (24 V)
	Air flow per nozzle	~30 m^3 min^{-1}
	Power of each fan	105 W (24 V)
	Ultrasonic sensors power	12 W (24 V)
	Motor power of each angle regulator (x4)	36 W (24 V)

redesigned canopy sprayer was designed to spray trees planted in rows spaced at approximately 4 m apart, for example in olive groves. The implement was autonomous and the main control system on the UGV only turned the implement on and off. It has eight diffusors separated by 0.6 m, four of which (the lower and upper) adapted the spray direction to the canopy from −15° to 15° with respect to its initial position. Each of these diffusors was equipped with two nozzles and one air outlet, and the implement control system was able to activate each diffusor separately. It used eight ultrasonic sensors to detect the tree canopy to activate the adequate diffusors and regulate the diffusors positions, and it is able to regulate the main flow of insecticide and air. Table 2 shows the main features of this implement (Sarri, Lisci, Rimediotti, & Vieri, 2014).

Similar to the patch sprayer, this canopy sprayer originally used the ICE power from the PTO to operate the main pump and the fan to disperse the pest control product throughout the tree canopy. In this study the implement was autonomous and the UGV main control did not know the instantaneous power requirements of the task. Thus, the pump and the fan worked at the rated power continuosly, wasting large amounts of energy. The system could be improved using a similar process to the previous case: replacing the main pump by a series of small pumps and the main fan by some small fans, using one pump and one fan in each diffusor. For this task, there were very similar requirements and therefore can the same pump model, MG100 Micro Pump could be used, and the axial compact fan EC W1G250-HH37-52 (ebm-papst Group, Mulfingen, Baden-Württemberg, Germany) was able to provide sufficient air flow. In this implement the main control was of product flow and air flow control was not necessary. The reduction of power demand from the ICE was the largest of the three cases, and the power demanded from the EES was also the largest.

2.2. Energy demand model

To estimate the total energy consumed in each agriculture task, the instantaneous power, the time and the relationship with the energy source were all required. The UGV had four energy sources: fuel, hydrogen, batteries and solar power although the instantaneous power provided by the sun cannot be regulated. In the energy demand model, two values were obtained: (a) the energy demand supplied by the ICE, the energy used to move the UGV and the implement, and (b) the electrical energy demand supplied by the EES. The total energy (TE) consumed could be calculated using

$$TE = E_{ESS} + E_{ICE}. \quad (1)$$

where E_{EES} is the energy supplied by the ESS and E_{ICE} the energy supplied by the ICE. To design and size the EES, the energy supplied by these systems can be calculated by

$$E_{EES} = \int_t P_{ESS}(t) = \int_t P_{UGV\ control}(t) + P_{IMP\ control}(t) + P_{Task}(t) \quad (2)$$

where P_{EES} is the instantaneous power demanded to the EES; $P_{UGV\ control}$ is the power used to supply the UGV control system described in the Section 2.1.1; $P_{IMP\ control}$ is the power consumed by the electrical control system of the implement: controllers, sensors, position actuator, etc.; and P_{Task} is the electrical power used to apply the treatment, whose values are defined

$$P_{Task} = nP_{Tool} \quad (3)$$

where n is number of tools active and P_{Tool} is the electrical power consumed by each tool. A tool is defined as a set of systems that can be activated separately to correctly apply the treatment in a given zone. With the flaming and row cultivator implement, a tool is the set of two burners and hoes used in each crop row, which use two ignitors (only to start) and two valves (only to change the status); in the patch sprayer, a tool is each nozzle, which used a pump; and in the canopy sprayer, a tool is the set of two nozzles and an air outlet of each diffusor, which use a pump and a fan.

Furthermore, we can estimate the energy provides by the ICE as

$$E_{ICE} = \int_t P_{ICE}(t) = \int_t [D(t) + MR(t)]v(t) \quad (4)$$

where v is the system speed (m s^{-1}); D is the implement draft force (kN), which depends on the dimensionless soil texture adjustment parameter and the machine-specific parameters; MR is the motion resistance (kN), which depends of the soil surfaces, terrain slope, wheel slip, total system mass and UGV tyres. This expression calculated the energy obtained from the ICE, it did not take into account the losses of mechanical and traction efficiency in the UGV (ASAE, 2011), (ANSI/ASAE, 1995), (ASAE, 2004), (ASAE, 2003).

3. Case studies

In this section, the energy requirements of each task are studied and the design process followed is analysed. The results obtained using this HES to perform the treatments to crops are described.

3.1. Energetic analysis

The energy requirements of each studied task were analysed using the energy model previously descrfibed. Using these data, the necessary features of the HES are presented and the real devices used in the HES are defined.

3.1.1. Energy demand

In this section, the electrical energy requirements supplied by the EES for the three agriculture tasks studied are analysed: pest control using insecticides, weed control using ploughing and flaming and weed control using herbicide. To carry out this energy estimation, a representation of real crops was used (see Fig. 5) where the experimental tests that are analysed in Section 3.2 are used. The model described in Section 2.2 was used to estimate the total energy consumed as maximum power demand and average power. Also, this power was split into two values: the power demanded by the 24-V dc systems and the one demanded by the 12-V dc systems.

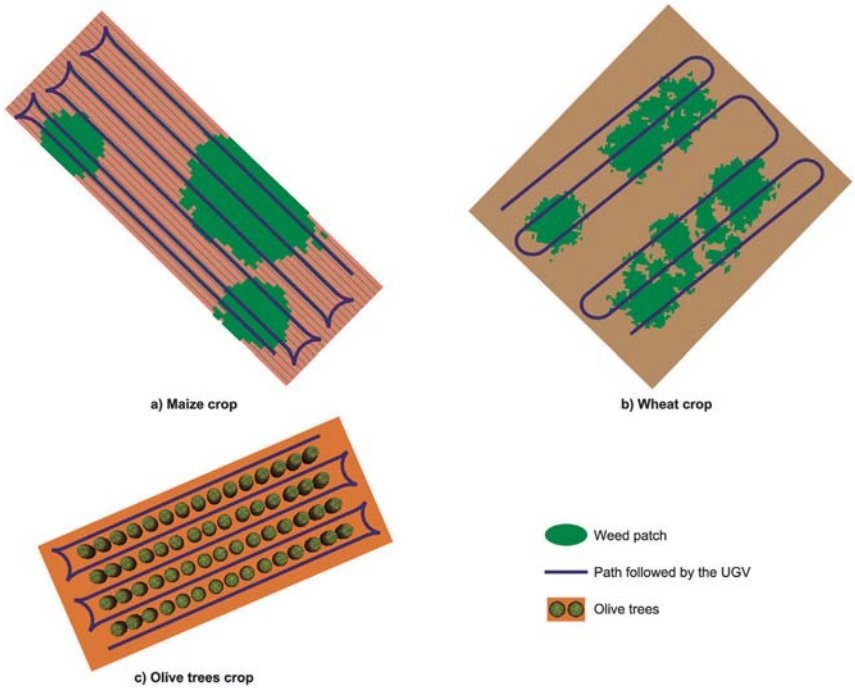

Fig. 5 – Test bench.

3.1.1.1. *Energy analysis in weed control using the flaming and row crop cultivator implement*. Figure 6 represents the electrical power demand of the 12-V dc devices, 24-V dc devices and the sum of both. For this task, it was observed that the demand from the 12-V dc devices was almost constant and that the demand of 24-V dc system had abrupt and very short peaks, which were generated by the burner ignitors. Table 3 presents the values of these peaks, and the average values of each represented power demand. The total hydrogen consumed during a working shift of 8 h was calculated, assuming that the HFC, described in Section 2.1.1, supplied all of the electrical energy. This task represented the lowest power demand from the EES because ploughing was supplied by the ICE, and the gas does not need power to work, only an ignition spark; thus, the EES is basically used to power the electrical control systems.

3.1.1.2. *Energy analysis in weed control using the patch sprayer*. Figure 7 illustrates the instantaneous power demand in the weed control task applying herbicides using the UGV with the patch sprayer. In this case, it can be observed that the power used by the 12-V dc systems was almost constant because they were mainly control systems but the power demanded by the 24-V dc systems had important variations that occurred when the pumps applied the treatment to weed patches. Table 3 presents the maximum values of the power demand, their average values and the total hydrogen consumed during a working day of 8 h. Values that, in general, increase with respect to the above cases.

3.1.1.3. *Energy analysis in pest control tasks using the canopy sprayer*. As in the other tasks, Fig. 8 shows the power demanded in pest control using the autonomous canopy

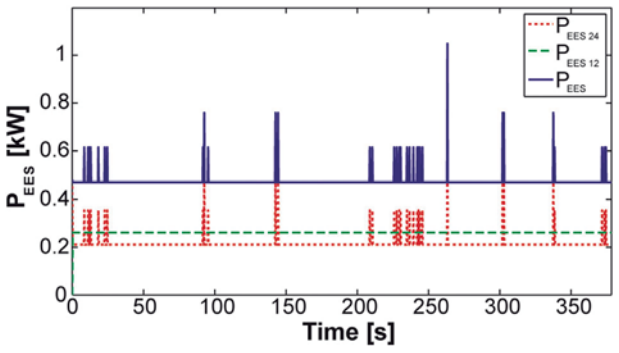

Fig. 6 – Power demands in weed control using the flaming and row crop cultivator implement.

Table 3 – Power and hydrogen consumed in each application.

	Implement		
	Flaming and row crop cultivator	Patch sprayer	Canopy sprayer
12 V average power	0.26 kW	0.28 kW	0.26 kW
24 V average power	0.22 kW	0.28 kW	0.90 kW
Total average power	0.48 kW	0.56 kW	1.16 kW
12 V maximum power	0.26 kW	0.40 kW	0.26 kW
24 V maximum power	0.79 kW	0.41 kW	1.39 kW
Total maximum power	1.05 kW	0.68 kW	1.65 kW
H_2 consumed (for 8 h)	2.43 Nm^3	2.84 Nm^3	5.96 Nm^3

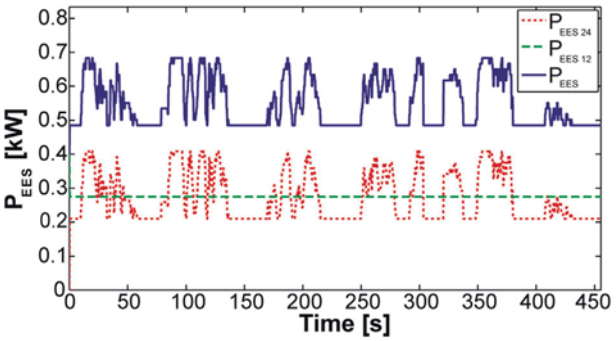

Fig. 7 – Power demands in weed control using the sprayer implement.

sprayer. These graphs are quite similar to the last analysed case, but with larger values in the power demanded of the 24-V systems, the only voltage used in this implement. These numerical values can be seen in Table 3 and compared to the above cases. As expected, this task had the highest power demand from the EES although the power demand from the 12-V dc systems was quite similar to the other three cases because it was used mainly by the control systems. Thus, the controllers had a quasi-constant power demand, and were not strongly influenced by the task performed.

3.1.2. *Hybrid energy system*

The energy system studied here used the original ICE of the tractor operating in parallel with the EES. Figure 9 presents the architecture of the HES. It can be seen that the ICE was used to provide motion, overcoming the MR and the possible draft forces generated by the implement, and the EES was used to power all electrical systems of the UGV. The ICE had enough power and autonomy for the task analysed in this work, but an EES needed to be designed to supply the electrical energy requirements of each agricultural task.

The EES used hydrogen as the main energy source with a small contribution from PV energy. It used batteries to adapt the power to the energy requirement and store the electric energy generated by the PV panel when it was not in use. The EES was designed according the maximum values in Table 3.

The hydrogen system was designed to supply the average power demanded by all electric system, control systems, sensors, actuators, etc. Therefore, an HFC with a minimum power of 1.16 kW and a hydrogen storage of at least 5.96 Nm^3 was required. The HFC used was based on TROPICAL TB-1000 model. It is an unregulated DC power system based on PEM fuel cell technology (FCgen-1020ACS, Ballard Power Systems, Burnaby, British Columbia, Canada). It has to be fuelled with pure hydrogen and is able to deliver up to 1.4 kW peak electrical power and 1.2 kW in nominal continuous power operation. Metal hydride tanks were used as a hydrogen storage system, and a minimum of 2 tanks with capacities of 3 Nm^3 was required. However, for further The PV panel used was a Module EGM-185 (EGing PV Co., Ltd, Jintan, Jiangsu, P.R.C), which had a power rating of 183 W with an efficiency of approximately 15%. In the test bench location (40°18′29″ N, 3°29′14″ W), this panel provided an average energy per day of 0.88 kWh, with a maximum of 1.46 kW h day^{-1} in July according the irradiation data available from the PV Geographical Information System of the Institute for Energy and Transport (PVGIS, 2015).

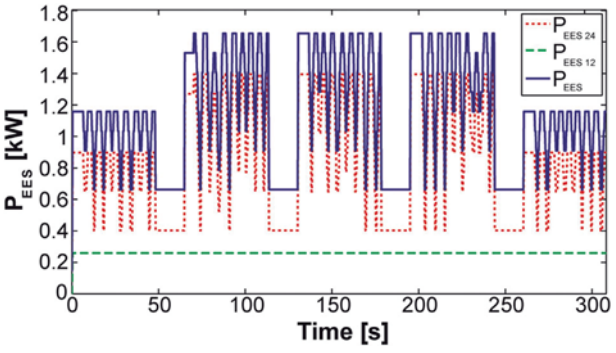

Fig. 8 – Power demand in pest control tasks using the canopy sprayer implement.

With respect to the batteries, deep-cycle lead-acid batteries were used which can be discharged using most of their capacity and supply current demands greater than the current provided by in the short term by the HFC. They were charged by both the HFC and PV panel and stored all unused PV energy. The batteries were divided into two banks: one bank to supply the 12-V dc systems and the other bank for the 24-V dc systems. Each group was formed by two batteries with 2.2 kW h of capacity; this capacity is enough to store the PV energy over several days of inactivity and sufficient to satisfy at sporadic instantaneous high energy demands, such as the ones shown in Fig. 8. Table 3 shows that the power demands of the 24-V dc systems are higher, but this does not consider the energy required to start the ICE. Furthermore, because deep-cycle batteries were used, two or more batteries in parallel were required to start the ICE.

The EMS is responsible for (a) regulating and adapting the power provided by the HFC and the PV panel; (b) assuring a minimum charge in the batteries; (c) obtaining the maximum PV power; and (d) supervising hydrogen storage, batteries status and PV power. It used two solar controllers with maximum power point tracking (MPPT SS-MPPT-15L, Morningstar, Inc., Chicago, Illinois, US) to obtain the maximum power from the PV panel: one for the 12-V batteries and another one for 24-V batteries. Two DC battery chargers (BCD1015, Analytic Systems Ware Ltd, Delta, British Columbia, Canada), were required to adapt the power from the HFC. Two chargers were required for each battery voltage. The EMS was equipped with a controller that managed the energy flow. The block diagram of the EMS is shown in Fig. 10, where C_{12V}, C_{24V} are the charges of the 12- and 24-V batteries, respectively; C12V min and C24V min are the minimum charge in these batteries with the HFC stopped and $C_{12V\ MAX}$ and $C_{24V\ MAX}$ are the maximum charges in these batteries with the HFC running. The values C12V min and C24V min are calculated to ensure correct operation during high energy demand periods. The $C_{12V\ MAX}$ and $C_{24V\ MAX}$ values were calculated to create a hysteresis cycle for the HFC operation with a value that is high enough to avoid excessive start/stop on the HFC but low enough to allow for the storage of the PV energy generated when the UGV was stationary.

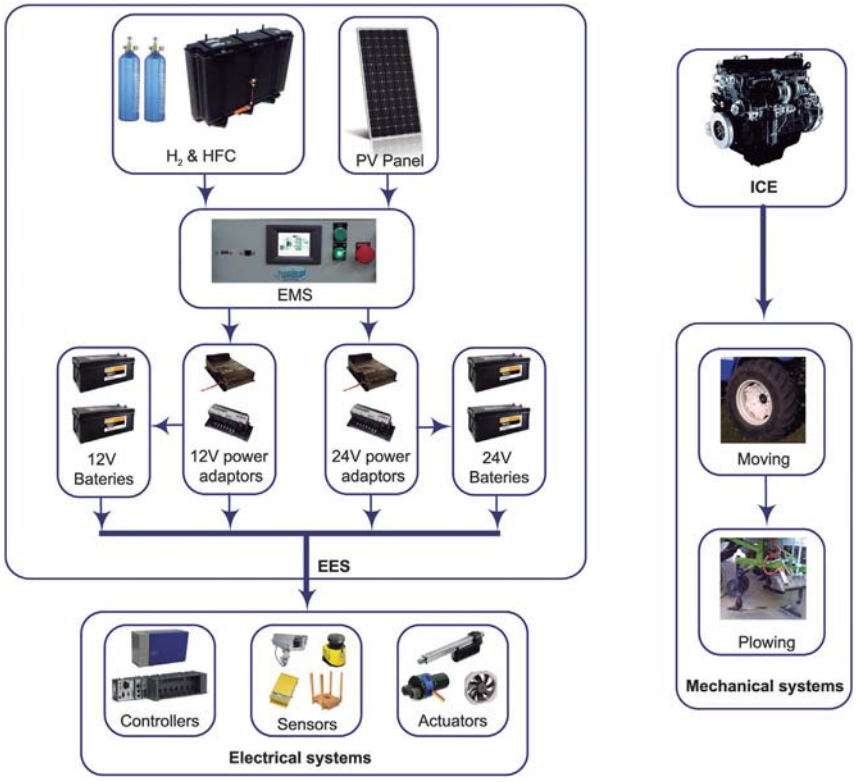

Fig. 9 – Hybrid energy system.

3.2. *Results and discussion*

In this section, the emission reductions obtained by using the HES in the UGV under real scenarios are presented. To analyse the results, the emissions using the UGV with the ICE as the only power system were compared with the UGV using the HES described in Section 3.1.2. The same UGV was used for all tests, and fuel consumption and emissions were measured as explained in Section 2.1.2. The experimental test benches were the crops represented in Fig. 5.

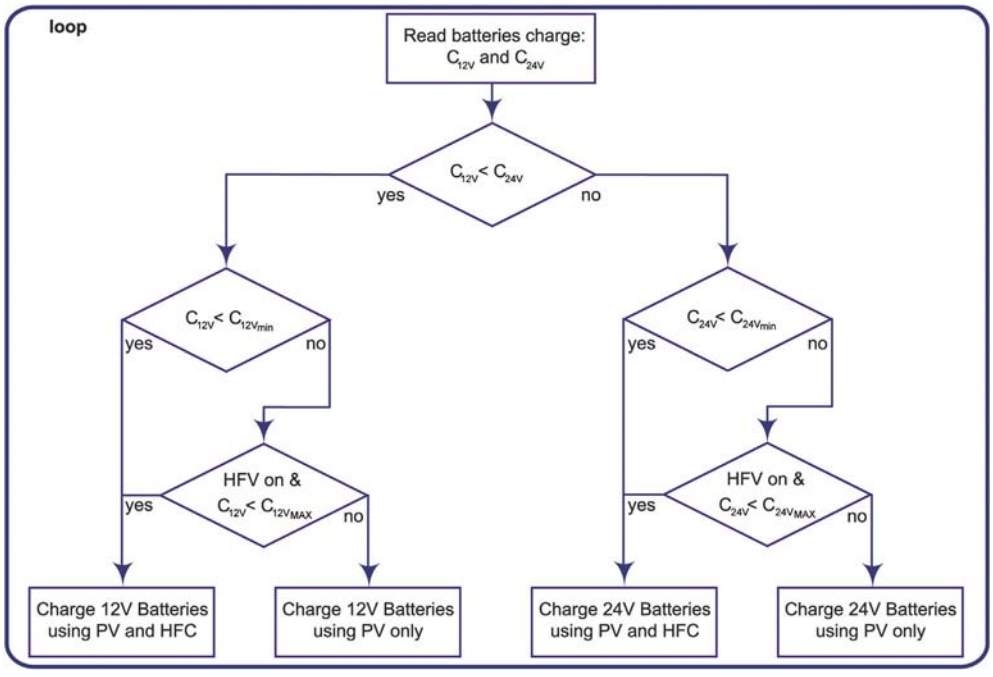

Fig. 10 – Block diagram of the flow energy control.

3.2.1. Hybrid power in weed control for fire resistant crops with wide furrows: ploughing and flame weed treatment

This test is performed over the maize crop shown in Fig. 5a, where the path followed by the UGV and the weed patch treated can be seen. As described in Section 2.1.3.1, the UGV detected the weed patches in real time, therefore, path planning covered the entire field. Although the burners were only activated over weeds patches, the hoes ploughed all furrows to control weeds and aerate the soil. Therefore, there was an important energy demand required to plough all tracks and exhaust gas flow increased, especially the CO_2, as can be see in Fig. 11a, which shows the exhaust gas flow emitted with respect to UGV position. This required energy to plough was the main demand and it was supplied by the ICE in both cases (i.e. using the ICE alone and using it with the HES). Therefore, the emission reduction obtained due by using the HES was low. As can be seen in Fig. 11 and in Table 4, the reduction of air pollution during this task was low, much lower than in the other analysed tasks, as will be seen in the next sections. The CO_2 emission showed only a small reduction due to the energy consumed by the ignitors of the flamers and the electric control system, although the energy consumed by the ignitors was almost negligible.

3.2.2. Hybrid power in weed control on herbaceous crops: spraying of herbicides

This test was performed over the wheat crop shown in Fig. 5b. From the weed map the path followed by the UGV to treat all weed patches can be seen. The weed map was known in advance of the treatment and therefore the path could be optimised to obtain energy reductions. In this case, the method described by (Gonzalez-de-Soto et al., 2015) was used to calculate the path. In Fig. 5b, all tracks had the same weed zone so that the track path direction was adapted to the shape of the weed patches.

Table 4 – Average values and comparison of exhaust gas emissions in weed control using the flaming and row crop cultivator implement.

	Units	CO_2	CO	HC + NO_X	PM
System with only ICE	g h^{-1}	11,320	113.2	147.8	12.6
	g kWh^{-1}	561	5.61	7.32	0.63
Hybrid system	g h^{-1}	10,355	112.9	147.5	12.6
	g kWh^{-1}	514	5.61	7.32	0.63
Exhaust gas reduction[a]	%	8.53	0.2	0.2	0.0

[a] With respect to the emissions per hour.

Figure 12 shows the instantaneous emissions of CO_2, CO, HC + NO_X and PM, and Table 5 shows their average values and the reductions obtained when using the HES. Figure 12a shows a significant reduction in CO_2 because the HES avoids the use of the PTO, resulting in a significant reduction in fuel consumption. Figure 12c presents the reduction of the emissions of HC and NO_X, but they are lower than the reduction in CO_2. This occurs because the NO_X concentration in the exhaust gasses decreases with the ICE speed but the concentration of HC increases. PM emissions were very similar in both cases (see Fig. 12d) because PM concentrations in exhaust gases increase as ICE speed decreases, as was the case here when the PTO was off or operating slowly. A similar result occurred with the CO, but to a lesser extent, as can be seen in Fig. 12b

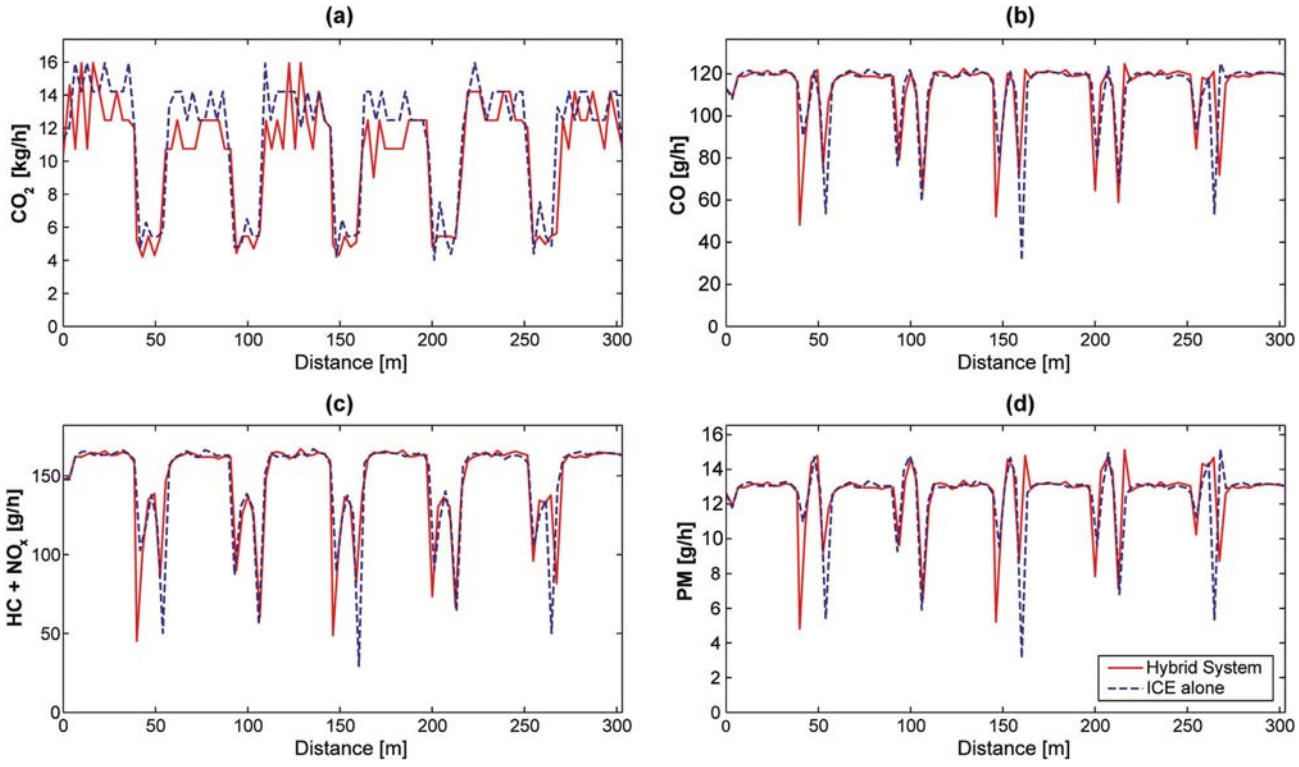

Fig. 11 – Exhaust gas emissions in weed control using the flaming and row crop cultivator implement.

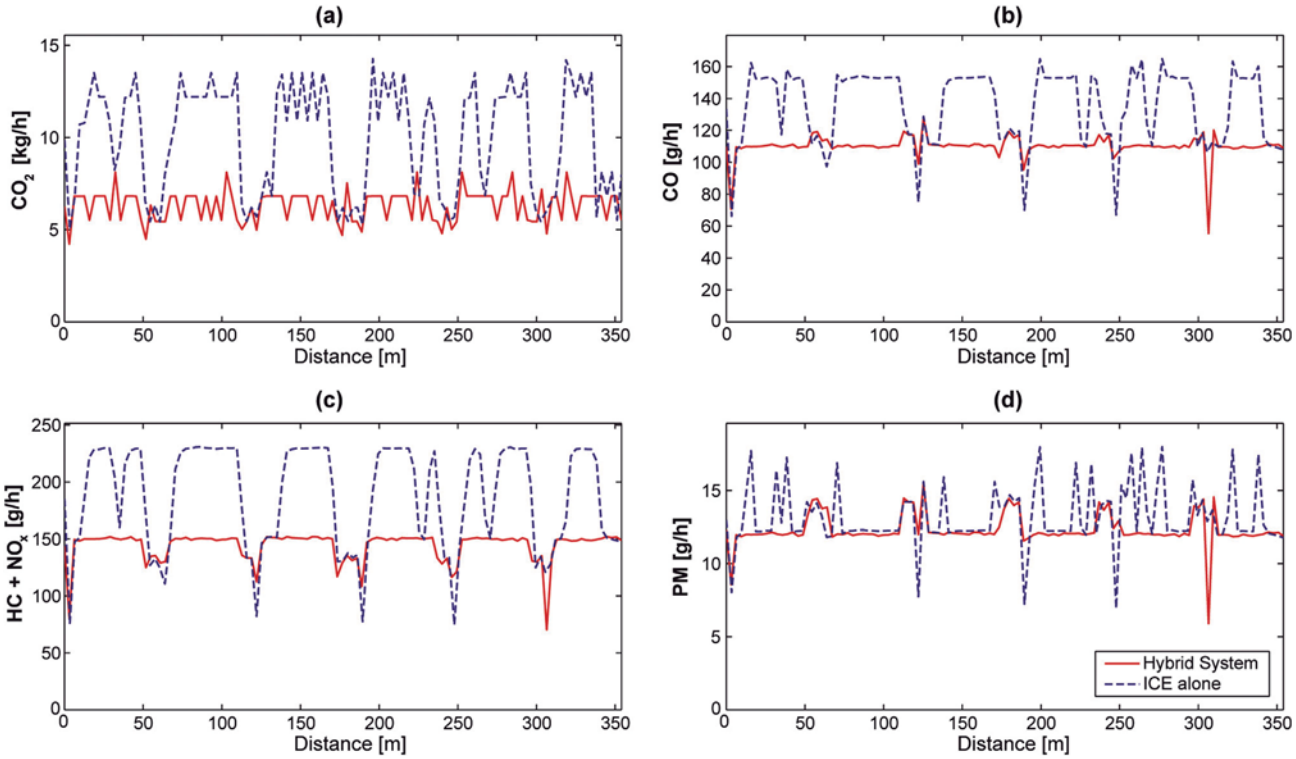

Fig. 12 – Exhaust gas emissions in weed control using the patch sprayer.

and in Table 5. It can be observed that the CO and PM emissions respect to the energy (g kW h^{-1}) increased when the HES was used due to the effect of decreasing ICE speed. In numerous works that analysed ICE exhaust gases, similar emission results have been obtained for these gases (Janulevičius et al., 2013; Lindgren & Hansson, 2002; Lindgren et al., 2011; Li, McLaughlin, Patterson, Burtt, & others, 2006; and Labeckas and Slavinskas, 2013).

3.2.3. *Hybrid power for the pest control on trees: fumigation using insecticides*

These tests were performed in the small olive grove shown in Fig. 5c, where the path followed by the UGV can be seen. As described in Section 2.1.3.3, the implement used for this task was an autonomous canopy sprayer, which detected and sprayed all trees along the track. The path must therefore pass along both sides of each tree in the crop.

Table 5 – Average values and comparison of the exhaust gas emissions in the weed control using the patch sprayer.

	Units	CO_2	CO	$HC + NO_X$	PM
System with only ICE	g h^{-1}	9860	133.4	185.2	13.0
	g kWh^{-1}	390	5.28	7.33	0.62
Hybrid System	g h^{-1}	6253	109.7	143.4	13.0
	g kWh^{-1}	317	5.57	7.29	0.51
Exhaust gas reduction[a]	%	36.6	17.8	22.6	5.4

[a] With respect to the emissions per hour.

As shown in Section 3.1.1, this implement demands the most energy from the EES of the three analysed implements and therefore the highest power demand reduction from the ICE was achieved. This reduction is shown in Fig. 13 and Table 6, where the highest reduction in the exhaust gases out of the three analysed tasks can be observed. The reduction in CO_2 emissions almost reached 50%. The results are quite similar to the previous case (herbicide spraying) but with greater reduction in emissions, except for PM emissions, which presents a lower emission reduction with canopy sprayer. This is because in this case, when the ICE supplied all of the energy requirements, its PM emissions were the lowest out of the three cases analysed. This occurred because the PTO operated at its rated power during the entire operation and the PM concentration in the ICE exhaust gases was at its lowest. In Table 6 it can be observed that CO and PM emissions with respect to energy (g kW h^{-1}) are again lower when the ICE is used alone since with the HES the ICE works at low speed. Although the concentration of CO and PM in the exhaust gases was the lowest for this ICE speed and load, the total of exhaust gases increased such that, using the ICE alone, the emissions (g h^{-1}) of CO and PM were greater than using the HES.

4. Conclusions

This work demonstrates that it is possible to combine current agricultural machines, which use ICEs for power, with new technologies that are based on clean energy sources to obtain significant reductions in the emission of atmospheric

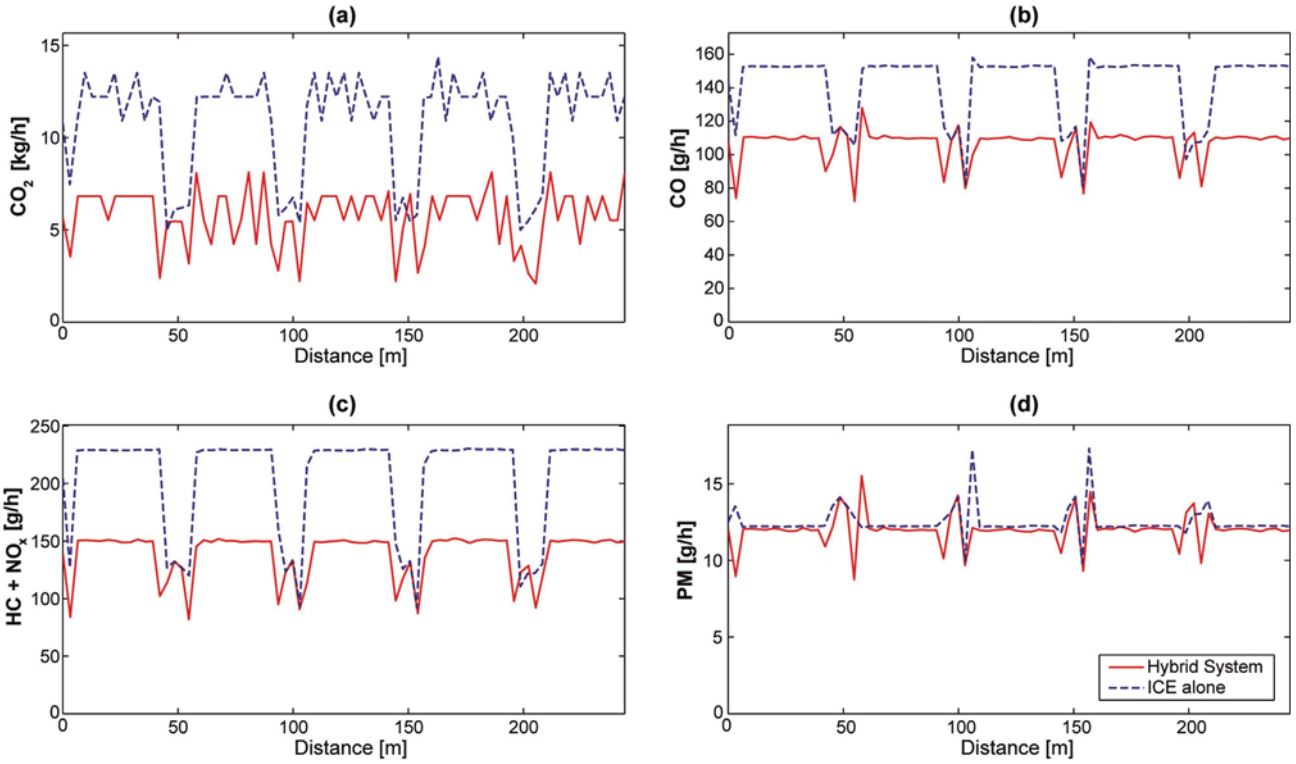

Fig. 13 – Exhaust gas emissions in pest control tasks using the canopy sprayer.

pollutants and greenhouse gases. This occurred by offloading the ICE and adding this load to an additional EES. This approach allows for the use of small agricultural tractors to move larger implements that have their own motors by the addition of an EES. This is especially interesting for agricultural tasks because, normally, the size and height are usually not problems for tractors. Furthermore, it is sometimes necessary to add weight to agricultural tractors to help reduce slippage or act as a counterweight. Agricultural tasks with draft force often require additional weight to reduce slippage. When draft force is negligible, but a heavy implement is used to apply a product, counterweights are required.

The technique of adding an EES appears very effective for tasks where the implement requires PTO power, as shown in Sections 3.2.2 and 3.2.3. The replacement of this PTO power is relatively simple; only small changes were required in the implement, as those described in Section 2.1.3. When the implement generated draft force, such as in ploughing, this technique was not as effective as in the case analysed in Section 3.2.1, but a reduction in the pollutant emissions was obtained from these robotic systems when the electric energy consumption was important.

The use of EES allows small electrical actuators to be used, which are able to apply the treatments in small areas consuming very little power. This use of distributed systems is especially interesting in precision agriculture, where the treatment is focused on the affected area, which is often smaller than the total area that the implement is able to treat. As found here, the use of a main motive power system can waste energy to carry out the same treatment. Furthermore, the losses from electrical energy transport are lower than the losses due to friction in mechanical energy transmission systems.

The greatest improvement is the results was obtained by the autonomous implement analysed in Section 3.2.3. In this case, the UGV did not know the instantaneous power requirements of the implement, and thus, for the case in which the ICE is the only power source, the ICE must supply the rated power to the implement, which is a very inefficient use of energy. However, with the HES, the implement uses the energy provided by the EES, and it is able to manage its energy, using only the required amount.

The theoretical studies and experiments conducted in this work reveal that the use of a HES in precision agriculture using robotic tractors improves the quality of the exhaust gasses and the energy use. Robotic tractors have increased electricity consumption compared to traditional tractors; therefore, it is very interesting to add an EES when the tractor is robotised

Table 6 – Average values and comparison of the exhaust gas emissions in pest control tasks using the canopy sprayer implement.

	Units	CO_2	CO	HC + NO_X	PM
System with only ICE	g h^{-1}	10,739	142.5	204.7	12.5
	g kWh^{-1}	378	5.01	7.19	0.44
Hybrid System	g h^{-1}	5640	107.1	139.3	12.0
	g kWh^{-1}	286	5.43	7.06	0.61
Exhaust gas reduction[a]	%	47.5	24.8	32.0	3.8

[a] With respect to the emissions per hour.

because the use of alternators increases the energy losses. Furthermore, an EES can be designed to supply some of the energy requirements of the agricultural task, as in this work. The HES achieved a significant reduction in atmospheric pollutant emissions, such as CO_2, CO, NO_X, HC and PM, which can cause environmental changes and health issues. This work has demonstrated that, currently, the use of this type of HES provides reliability and autonomy and that it can be used in all agricultural tasks with any tractor, offloading the ICE to a greater or lesser extent, which can be regarded as an intermediate step towards the use of completely clean energy systems.

Acknowledgements

The research leading to these results received funding from the European Union's Seventh Framework Programme [FP7/2007-2013] under Grant Agreement nº 245986.

REFERENCES

ANSI/ASAE. (1995). *S296.4 DEC95 Agricultural machinery management data* (pp. 118–120). St. Joseph, MI, USA: ASAE Standards.

ASAE. (2003). *D497.4 FEB2003 Agricultural machinery management data* (pp. 273–280). St. Joseph, MI, USA: ASAE Standards.

ASAE. (2011). *D497.7 MAR2011 Agricultural machinery management data* (pp. 372–380). St. Joseph, MI, USA: ASAE Standards.

ASAE. (2004). *S313.3 FEB04 Soil cone penetrometer* (pp. 903–904). St. Joseph, MI, USA: ASAE Standards.

Carballido, J., Perez-Ruiz, M., Emmi, L., Agüera, J., &, others. (2014). Comparison of positional accuracy between RTK and RTX GNSS based on the autonomous agricultural vehicles under field conditions. *Applied Engineering in Agriculture, 30*, 361–366.

Carballido, J., Perez-Ruiz, M., Gliever, C., & Agüera, M. (2012). Design, development and lab evaluation of a weed control sprayer to be used in robotic systems. In *Proceedings of the First International Conference on Robotics and Associated High-Technologies and Equipment for Agriculture. Presented at the Applications of automated systems and robotics for crop protection in sustainable precision agriculture* (pp. 23–29). Pisa, Italy: Pisa University Press srl.

Clements, D. R., Weise, S. F., Brown, R., Stonehouse, D. P., Hume, D. J., & Swanton, C. J. (1995). Energy analysis of tillage and herbicide inputs in alternative weed management systems. *Agriculture Ecosystems & Environment, 52*, 119–128. http://dx.doi.org/10.1016/0167-8809(94)00546-Q.

CNH America LLC. (2009). *BOOMER 3040, 3045, 3050 CVT service manual complete contents*.

Conesa-Muñoz, J., Gonzalez-de-Soto, M., Gonzalez-de-Santos, P., & Ribeiro, A. (2015). Distributed multi-level supervision to effectively monitor the operations of a fleet of autonomous vehicles in agricultural tasks. *Sensors, 15*, 5402–5428. http://dx.doi.org/10.3390/s150305402.

Dalgaard, T., Halberg, N., & Porter, J. R. (2001). A model for fossil energy use in Danish agriculture used to compare organic and conventional farming. *Agriculture Ecosystems & Environment, 87*, 51–65. http://dx.doi.org/10.1016/S0167-8809(00)00297-8.

Delucchi, M. A., & Lipman, T. E. (2001). An analysis of the retail and lifecycle cost of battery-powered electric vehicles. *Transportation Research Part D: Transport and Environment, 6*, 371–404. http://dx.doi.org/10.1016/S1361-9209(00)00031-6.

Dictionary - WordReference.com [WWW Document], URL http://www.wordreference.com/(accessed 6.5.15).

Eaves, S., & Eaves, J. (2004). A cost comparison of fuel-cell and battery electric vehicles. *Journal of Power Sources, 130*, 208–212. http://dx.doi.org/10.1016/j.jpowsour.2003.12.016.

EBM-PAPST [WWW Document], World market leader for energy-saving fans and motors. URL http://www.ebmpapst.com/en/ (accessed 30.4.15).

Emmi, L., Gonzalez-de-Soto, M., Pajares, G., & Gonzalez-de-Santos, P. (2014a). New trends in robotics for agriculture: integration and assessment of a real fleet of robots. *The Scientific World Journal*, 2014, 21. http://dx.doi.org/10.1155/2014/404059.

Emmi, L., Gonzalez-de-Soto, M., Pajares, G., & Gonzalez-de-Santos, P. (2014b). Integrating sensory/actuation systems in agricultural vehicles. *Sensors, 14*, 4014–4049. http://dx.doi.org/10.3390/s140304014.

EPA, U. S. Environmental Protection Agency [WWW Document]. URL http://www.epa.gov/(accessed 4.9.15).

España. (2006). *Real Decreto 61/2006, de 31 de enero, por el que se determinan las especificaciones de gasolinas, gasóleos, fuelóleos y gases licuados del petróleo y se regula el uso de determinados biocarburantes*. Boletín Oficial del Estado, 17 de febrero de 2006, núm. 41 (pp. 6342–6357).

Garrido, M., Ribeiro, A., Barreiro, P., Debilde, B., Balmer, P., Carballido, J., et al. (2012). Safety functional requirements for robot fleets for highly effective agriculture and forestry management (RHEA). In *Proceedings of the international conference of agricultural engineering*. Spain: CIGR-AgEng2012. Valencia. July 8-12.

Gasparatos, A., Stromberg, P., & Takeuchi, K. (2011). Biofuels, ecosystem services and human wellbeing: putting biofuels in the ecosystem services narrative. *Agriculture Ecosystems & Environment, 142*, 111–128. http://dx.doi.org/10.1016/j.agee.2011.04.020.

Gonzalez-de-Santos, P., Ribeiro, A., Fernadez-Quintanilla, C., & Dorado, J. (2014). Assessing a fleet of robots for herbicide applications. In *Proceedings International Conference of Agricultural Engineering. Presented at the International Conference of Agricultural Engineering*. Zurich, Switzerland: GEYSECO.

Gonzalez-de-Soto, M., Emmi, L., Garcia, I., & Gonzalez-de-Santos, P. (2015). Reducing fuel consumption in weed and pest control using robotic tractors. *Computers and Electronics in Agriculture, 114*, 96–113. http://dx.doi.org/10.1016/j.compag.2015.04.003.

Guerrero, J. M., Guijarro, M., Montalvo, M., Romeo, J., Emmi, L., Ribeiro, A., et al. (2013). Automatic expert system based on images for accuracy crop row detection in maize fields. *Expert Systems with Applications, 40*, 656–664. http://dx.doi.org/10.1016/j.eswa.2012.07.073.

Guzmán, G. I., & Alonso, A. M. (2008). A comparison of energy use in conventional and organic olive oil production in Spain. *Agricultural Systems, 98*, 167–176. http://dx.doi.org/10.1016/j.agsy.2008.06.004.

Hansson, P.-A., Lindgren, M., & Norén, O. (2001). PM – power and machinery: a comparison between different methods of calculating average engine emissions for agricultural tractors. *Journal of Agricultural Engineering Research, 80*, 37–43. http://dx.doi.org/10.1006/jaer.2001.0710.

ISO. (1996). *8178-4:1996–Reciprocating internal combustion engines – exhaust emission measurement – Part 4: test cycles for different engine applications* (International Organisation of Standardisation).

Janulevičius, A., Juostas, A., & Pupinis, G. (2013). Tractor's engine performance and emission characteristics in the process of

ploughing. *Energy Conversion and Management, 75*, 498–508. http://dx.doi.org/10.1016/j.enconman.2013.06.052.

Labeckas, G., & Slavinskas, S. (2013). Performance and emission characteristics of a direct injection diesel engine operating on KDV synthetic diesel fuel. *Energy Conversion and Management, 66*, 173–188. http://dx.doi.org/10.1016/j.enconman.2012.10.004.

Li, Y. X., McLaughlin, N. B., Patterson, B. S., Burtt, S. D., & others. (2006). Fuel efficiency and exhaust emissions for biodiesel blends in an agricultural tractor. *Canadian Biosystems Engineering/Le Genie des biosystems au Canada, 48*, 2.

LINAK [WWW Document], n.d.. Tecnológica Actuadores Lineales LINAK Actuadores SLuSpain Port. URL http://www.linak.es/ (accessed 28.4.15).

Lindgren, M., Arrhenius, K., Larsson, G., Bäfver, L., Arvidsson, H., Wetterberg, C., et al. (2011). Analysis of unregulated emissions from an off-road diesel engine during realistic work operations. *Atmospheric Environment, 45*, 5394–5398. http://dx.doi.org/10.1016/j.atmosenv.2011.06.046.

Lindgren, M., & Hansson, P.-A. (2002). PM – power and machinery: effects of engine control strategies and transmission characteristics on the exhaust gas emissions from an agricultural tractor. *Biosystems Engineering, 83*, 55–65. http://dx.doi.org/10.1006/bioe.2002.0099.

Lutz, A. E., Larson, R. S., & Keller, J. O. (2002). Thermodynamic comparison of fuel cells to the Carnot cycle. *International Journal of Hydrogen Energy, 27*, 1103–1111. http://dx.doi.org/10.1016/S0360-3199(02)00016-2.

Montalvo, M., Guerrero, J. M., Romeo, J., Emmi, L., Guijarro, M., & Pajares, G. (2013). Automatic expert system for weeds/crops identification in images from maize fields. *Expert Systems with Applications, 40*, 75–82. http://dx.doi.org/10.1016/j.eswa.2012.07.034.

Mousazadeh, H., Keyhani, A., Javadi, A., Mobli, H., Abrinia, K., & Sharifi, A. (2010). Evaluation of alternative battery technologies for a solar assist plug-in hybrid electric tractor. *Transportation Research Part D: Transport and Environment, 15*, 507–512. http://dx.doi.org/10.1016/j.trd.2010.05.002.

Mousazadeh, H., Keyhani, A., Javadi, A., Mobli, H., Abrinia, K., & Sharifi, A. (2011). Life-cycle assessment of a solar assist plug-in hybrid electric tractor (SAPHT) in comparison with a conventional tractor. *Energy Conversion and Management, 52*, 1700–1710. http://dx.doi.org/10.1016/j.enconman.2010.10.033.

Mulloney, J. A., Jr. (1993). Mitigation of carbon dioxide releases from power production via "sustainable agri-power": the synergistic combination of controlled environmental agriculture (large commercial greenhouses) and disbursed fuel cell power plants. Energy conversion and management. In *Proceedings of the International Energy Agency Carbon Dioxide Disposal Symposium 34* (pp. 913–920). http://dx.doi.org/10.1016/0196-8904(93)90036-A.

Offer, G. J., Howey, D., Contestabile, M., Clague, R., & Brandon, N. P. (2010). Comparative analysis of battery electric, hydrogen fuel cell and hybrid vehicles in a future sustainable road transport system. *Energy Policy, 38*, 24–29. http://dx.doi.org/10.1016/j.enpol.2009.08.040.

Peltre, C., Nyord, T., Bruun, S., Jensen, L. S., & Magid, J. (2015). Repeated soil application of organic waste amendments reduces draught force and fuel consumption for soil tillage. *Agriculture Ecosystems & Environment, 211*, 94–101. http://dx.doi.org/10.1016/j.agee.2015.06.004.

PVGIS - Photovoltaic Geographical Information System [WWW Document], JRCs Inst. Energy Transp. - PVGIS - Eur. Comm. URL http://re.jrc.ec.europa.eu/pvgis/(accessed 5.4.15).

RHEA Project - EU [WWW Document], "Robot Fleets Highly Eff. Agric. For. Manag. URL http://www.rhea-project.eu/(accessed 3.30.15).

Sarri, D., Lisci, R., Rimediotti, M., & Vieri, M. (2014). RHEA airblast sprayer: calibration indexes of the airjet vector related to canopy and foliage characteristics. In *Second International Conference on Robotics and Associated High-Technologies and Equipment for Agriculture and Forestry. Presented at the New trends in mobile robotics, perception and actuation for agriculture and forestry* (pp. 73–81). Madrid, Spain: PGM.

Soni, P., Taewichit, C., & Salokhe, V. M. (2013). Energy consumption and CO2 emissions in rainfed agricultural production systems of Northeast Thailand. *Agricultural Systems, 116*, 25–36. http://dx.doi.org/10.1016/j.agsy.2012.12.006.

TCS Micropumps [WWW Document], High Perform. Miniat. Pumps. URL http://www.micropumps.co.uk/(accessed 28.4.15).

Titan Enterprises Ltd - Titan flow meters for oil, boiler and diesel fuel applications - PD400 oil flowmeter [WWW Document], 2014. URL http://www.flowmeters.co.uk/pd_pd400om.php#data (accessed 20.2.15).

Tropical [WWW Document], Fuel Cell Power Gener. Hydrog. Technol. Electr. Automob. – Trop. SA Fuel Cell Hydrog. Technol. URL http://www.tropical.gr/index.php (accessed 24.4.15).

6 PUBLICACIÓN III:

Autonomous systems for precise spraying - Evaluation of a robotised patch sprayer

M. Gonzalez-de-Soto, L. Emmi, M. Perez-Ruiz, J. Aguera, and P. Gonzalez-de-Santos

Biosystems Engineering, ISSN 1537-5110

DOI: *http://dx.doi.org/10.1016/j.biosystemseng.2015.12.018*

Impact Factor (2014): 1.619

Category: Agriculture, Multidisciplinary: 9/56 (Q1)

Category: Agricultural, Engineering: 4/12 (Q2)

NOTA: A la fecha de presentación de la presente tesis doctoral, esta publicación aún no ha sido presentada en formato tradicional impreso, pero está disponible "*online*" en el formato "*article in press*" y puede ser citado como:

Gonzalez-de-Soto, M., Emmi, L., Perez-Ruiz, M., Aguera, J., and Gonzalez-de-Santos, P., Autonomous systems for precise spraying - Evaluation of a robotised patch sprayer, Biosystems Engineering (2016), http://dx.doi.org/10.1016/j.biosystemseng.2015.12.018

BIOSYSTEMS ENGINEERING XXX (2016) 1–18

Available online at www.sciencedirect.com

ScienceDirect

journal homepage: www.elsevier.com/locate/issn/15375110

Research Paper

Autonomous systems for precise spraying – Evaluation of a robotised patch sprayer

Mariano Gonzalez-de-Soto [a,d,*], Luis Emmi [a], Manuel Perez-Ruiz [b], Juan Aguera [c], Pablo Gonzalez-de-Santos [a]

[a] Centre for Automation and Robotics (UPM-CSIC), 28500 Arganda del Rey, Madrid, Spain
[b] School of Agricultural Engineering, University of Seville, Ctra. de Utrera, Km. 1, 41013 Seville, Spain
[c] Department of Rural Engineering, University of Cordoba, Campus Universitario Rabanales, 14071 Córdoba, Spain
[d] Department of Electrical Systems and Automation Engineering, School of Industrial Engineering and Informatics, University of León, Campus de Vegazana s/n, 24071 León, Spain

ARTICLE INFO

Article history:
Published online xxx

Keywords:
Precision spraying
Autonomous systems
Agricultural robot
Herbicide saving
Weed control

Advances in different technologies, such as global navigation satellite systems, geographic information systems, high-resolution vision systems, innovative sensors and embedded computing systems, are finding direct application in agriculture. These advances allow researchers and engineers to automate and robotise agricultural tasks no matter the inherent difficulties of the natural, semi-structured environment in which these tasks are performed. Following this current trend, this article aims to describe the development and assessment of a robotised patch spraty -20ying system that was devised for site-specific herbicide application in agricultural crops and is capable of working in groups or fleets of autonomous robots. The robotised patch sprayer consisted of an autonomous mobile robot based on a commercial agricultural vehicle chassis and a direct-injection spraying boom that was tailor-made to interact with the mobile robot. There were diverse sources (on-board and remote sensors) that can supply the weed data for the treatment. The main features of both the mobile robot and the sprayer are presented along with the controller that harmonised the behaviour of both main subsystems. Laboratory characterisation and field tests demonstrated that the system was reliable and accurate enough to accomplish the treatment over 99.5% of the detected weeds and treatment of the crop with no weed treated was insignificant; approximately 0.5% with respect to the total weed patches area, achieving a significant herbicide savings.

1. Introduction

In recent decades, research on weed-sensing technologies, sensor fusion and selective crop management with herbicides or others control treatments have progressed significantly (Jeon & Tian, 2009; Khot, Tang, Steward, & Han, 2008 and Lee et al., 2010). Particularly noteworthy is the improvement in the navigation capabilities of vehicles and agricultural implements by combining global navigation

* *Corresponding author*. Centre for Automation and Robotics (UPM-CSIC), 28500 Arganda del Rey, Madrid, Spain.
E-mail addresses: marianogds@outlook.com, mariano.gonzalez@car.upm-csic.es (M. Gonzalez-de-Soto).

http://dx.doi.org/10.1016/j.biosystemseng.2015.12.018
1537-5110/

Nomenclature

a	Equidistant spacing of the nozzles
D_c	Applied dose (l ha^{-1})
FCS	Frontal cell size (m)
GNSS	Global navigation satellite system
GPS	Global positioning system
LCS	Lateral cell size (m)
MWC	Minimum weed coverage
n_a	Number of active nozzles
NWT	Not weed treated (m^2)
p	Ratio, herbicide volume/volume water
PLC	Programmable logic controller
Q_{ch}	Injected herbicide flow (l min^{-1})
Q_n	Nominal workflow (l min^{-1})
Q_w	Total water flow (l min^{-1})
RHEA	Robot fleet for highly effective agricultural and forestry management
RTK	Real-time kinematic
v	Robot speed
WCM	Weed control map
WDS	Weed detection system
WNT	Weed not treated (m^2)
WPP	Weed patch perimeter (m)
WPPA	Weed patch perimeter angles (rad)

satellite system (GNSS) sensors with dynamic measurement units. Nevertheless, many of these studies have focused solely on individual developments with only individual components of the whole system being studied, tested and evaluated. For example, Blackmore, Griepentrog, Nielsen, Nørremark, and Resting-Jeppesen (2004) focused on the development of an autonomous tractor, whereas Wisserodt et al. (1999) concentrated on controlling a hoe. Nørremark, Griepentrog, Nielsen, and Søgaard (2008) attempted to develop intra-row weed management using a self-propelled, unmanned hoe that was composed of an autonomous vehicle and a cycloid hoe. The vehicle and the tool were controlled independently to follow a pre-planned task. Nonetheless, both of the subsystems had their own GNSSs, and therefore expensive components in the system were duplicated. These efforts revealed a need to simplify systems and to develop integrated autonomous agricultural equipment.

Recently, Berge, Goldberg, Kaspersen, and Netland (2012) presented a GPS guided autonomous robot for weed control in cereals based on machine vision, a system able of perform weed monitoring and spraying in the same operation. Also there are some commercial systems for the automatic weed control in agriculture, for example the "Robocrop Spot Sprayer" offered by "Garford Farm Machinery" (Garford, 2015).

The latest development is the use of multi-robot systems, or fleets of robots, for outdoor applications including applications that are related to agriculture, to perform tasks in a collaborative way (Vougioukas, 2012). This idea was introduced a few years ago (Bautin, Simonin, & Charpillet, 2011 and Bouraqadi, Fabresse, & Doniec, 2012), but the first real attempts were conducted only recently (RHEA, 2015). Improvement in the integration of individual components (acquisition, guidance, decision making and actuation) appears to be essential to establish fully autonomous agricultural systems. Furthermore, new developments must consider the specific requirements of the vehicles to be used as members of autonomous fleets.

The components that are required to build such a system come from different research areas and demand diverse disciplines (agronomy, robotics, automatic control, machine vision, etc.). Therefore, the integration task requires a multidisciplinary approach, whereby each discipline must address different technologies, operating systems, programming languages, methodologies, etc.

The main aim of this work is to describe and assess an attempt to configure a fully integrated path spraying technology for site-specific herbicide application in agricultural crops that is capable of being integrated into fleets of autonomous, heterogeneous robots.

This study is part of the results that were derived from the project RHEA – robot fleet for highly effective agricultural and forestry management, which is funded by the European Union through its Seventh Framework Programme. This project, which was devoted to developing a fleet of heterogeneous robots for agricultural specific-site treatment, configured a fleet of aerial robots based on a hex-rotor that was equipped with perception systems operating remotely (Peña, Torres-Sánchez, de Castro, Kelly, López-Granados, 2013 and Rabatel, Gorretta, & Labbé, 2014), and a fleet of ground vehicles based on a commercial agricultural vehicle chassis that were equipped with perception (Romeo et al., 2012) and actuation systems to operate in three scenarios: wheat and maize fields and olive orchards (Frasconi et al., 2014; Perez-Ruiz et al., 2014 and Sarri, Lisci, Rimediotti, & Vieri, 2014). These essential subsystems were complemented by other systems: a Mission Manager, which was in charge of generating the tasks (Conesa-Muñoz, Ribeiro, Andujar, Fernandez-Quintanilla, & Dorado, 2012); a Communication System to communicate between the robot and the base station (Drenjanac & Tomic, 2013); a Safety System to address safety issues for humans and animals; and a Location System to obtain the position of every vehicle with respect to the base station (Perez-Ruiz, Slaughter, Gliever, & Upadhyaya, 2012).

The RHEA fleet was fully operative by mid-year 2014 and generated positive results after successful demonstrations were conducted throughout the first half of that year. However, this article goes further in quantitatively assessing the performances of a specific subset of components comprising the unmanned ground vehicle (i.e. the robot), the sprayer prototype (i.e. the implement) and the relevant integration subsystems (i.e., the main computer and location system). The main objective of this work is to analyse a smart herbicide application system based on a direct-injection sprayer used for precision weed control. In this analysis the weed area not treated and the area without weeds treated was estimated according to the weed control map (WCM) and these values were measured using real systems. This system needs a WCM that is provided by a weed detection system (WDS) that can be used with on-board systems (in real time) or using external devices.

To achieve this objective, a description of the sprayer prototype is given in Section 2. The unmanned ground vehicle is described in Section 3 by focusing on the control structure that governed the robot and was comprised of the integration of diverse sensory systems, actuation systems and decision-making components to establish a fully autonomous agricultural system with the primary purpose of performing site-specific weed-control tasks while decreasing the use of agricultural inputs. Section 4 characterises the patch sprayer according to laboratory tests, and Section 5 illustrates the tests that were conducted using the whole system. These tests were conducted in the field in order to characterise, assess the whole system and agrochemical savings that can be achieved using this system compared to conventional broadcast applications. Finally, Section 6 summarises the main conclusions.

2. Precision spraying system

The basic principle of a smart herbicide application system is that a real-time machine vision system can detect weeds or use accurate prescription maps of weed infestations growing within the field (e.g., using a camera mounted on an unmanned aerial vehicle). When coupled to a rapid-response spray control system, the smart herbicide application system permits the selective application of post-emergence herbicides exclusively to the unwanted plant material. This smart spraying system (See Fig. 1) was fabricated with twelve high-speed solenoid valves (Model VC01, NTech Industries Inc, Ukiah, California, US), which were mounted on a stainless steel sprayer boom at a fixed spacing of 0.5 m. These solenoid valves consisted of an inlet for incoming liquid, a spray nozzle, a nozzle cap, an LED indicator, a 3-pin electrical connector (signal, negative and positive), and two captive screws. The boom sprayer was divided into twelve sections, each containing one solenoid valve. Each valve was energized by a 12-V d c source to allow the spraying from each section to be controlled independently. The LED indicated when the solenoid was open.

A commercial central direct-injection system (Model Sidekick Pro, Raven Industries Inc., Sioux Falls, SD, USA) was equipped with a water tank (200 l) and a separate container for the herbicide (15 l) for injection according the work plan developed by the base station and the WDS. This base station calculated the initial and final point of each track according to the crop dimensions (a track was defined as the crop section that is treated in each path followed by the vehicle through the crop) and the WDS fixed the point where a nozzle must be opened or closed. This data can be interpreted by the base station to improve the work plan when the WDS is an external device, or in real time when the WDS is on-board the vehicle. The controller (SCS-sidekick) unit was controlled by the *Actuation Controller* of the vehicle, as well as the signal inputs from various sensors. This *Actuation Controller* was part of the control architecture that was implemented on the autonomous vehicle and was a system that was commanded by a *Main Controller* in charge of supervision, communications and planning, as explained below. This *Main Controller* used the RTK-GNSS position and the application rate map information to determine the desired application rate. An intermediate connection box between the sprayer and the *Implement Controller* was created and installed to accommodate the signal sensors and to host the injection system controller and the programmable logic controller (PLC) device. The injection system controller supplied variable voltage to a gear motor to power the injector pump. This voltage caused the injector pump to turn at the appropriate speed to generate the desired flow rate for the herbicide. A sensor integrated into the system measured the flow rate of the herbicide from the injector pump speed. The controller used the herbicide flow rate from the pump speed to determine whether a change in the herbicide flow rate was needed. The herbicide flow rate was verified using a mini-flow meter. Figure 2 illustrates the final prototype assembly of the precision spraying system.

3. Unmanned ground vehicle

Given the characteristics of the precision spraying system regarding its size, weight, power requirements, among others, it was decided to use a medium-size agricultural tractor. The vehicle was designed to be a system that allows various types of agricultural implements to be interconnected or integrated easily with the vehicle for the execution of diverse agricultural tasks focused mainly (but not exclusively) on weed control tasks.

To meet the requirements of the site-specific spraying task, the unmanned ground vehicle was equipped with diverse high-tech perception and actuation systems, such as machine vision and laser for obstacle detection, real-time kinematic – global positioning system (RTK – GPS) for precise localisation, and a set of specialised sensors and actuators for the automation of the tractor.

For the control of the unmanned ground vehicle, a hybrid architecture was implemented (Emmi, Gonzalez-de-Soto, Pajares, & Gonzalez-de-Santos, 2014), where a *Main Controller* is in charge of receiving and performing the mission that is generated by an external operator, planning the correct behaviours that the vehicle and the implement must execute depending on the mission requirements and synchronising with the other subsystems on-board the vehicle.

3.1. *The vehicle*

The vehicle that was used for giving mobility and power to the automated sprayer system was a modified commercial tractor CNHi Boomer-3050 which was part of the RHEA project. This tractor has a 51-hp (37.3 kW) engine and an approximate mass of 1200 kg. The operator cabin was removed in order to build a more compact vehicle that housed computers and subsystems (See Fig. 3). The vehicle has one GPS receiver which needs two antennas to provide the position and orientation of the vehicle, these two GPS antennas were positioned in the upper part of the vehicle, as were the communication antennas and the camera. A laser system was placed in the front of the vehicle for obstacle detection.

The configuration that was used for the localisation system was an RTK-GNSS correction signal from a local base station (configured using a Trimble Model BX982 receiver, Sunnyvale, California, US) to obtain an RTK fixed quality accuracy. This GPS receiver configured as a base station can provide

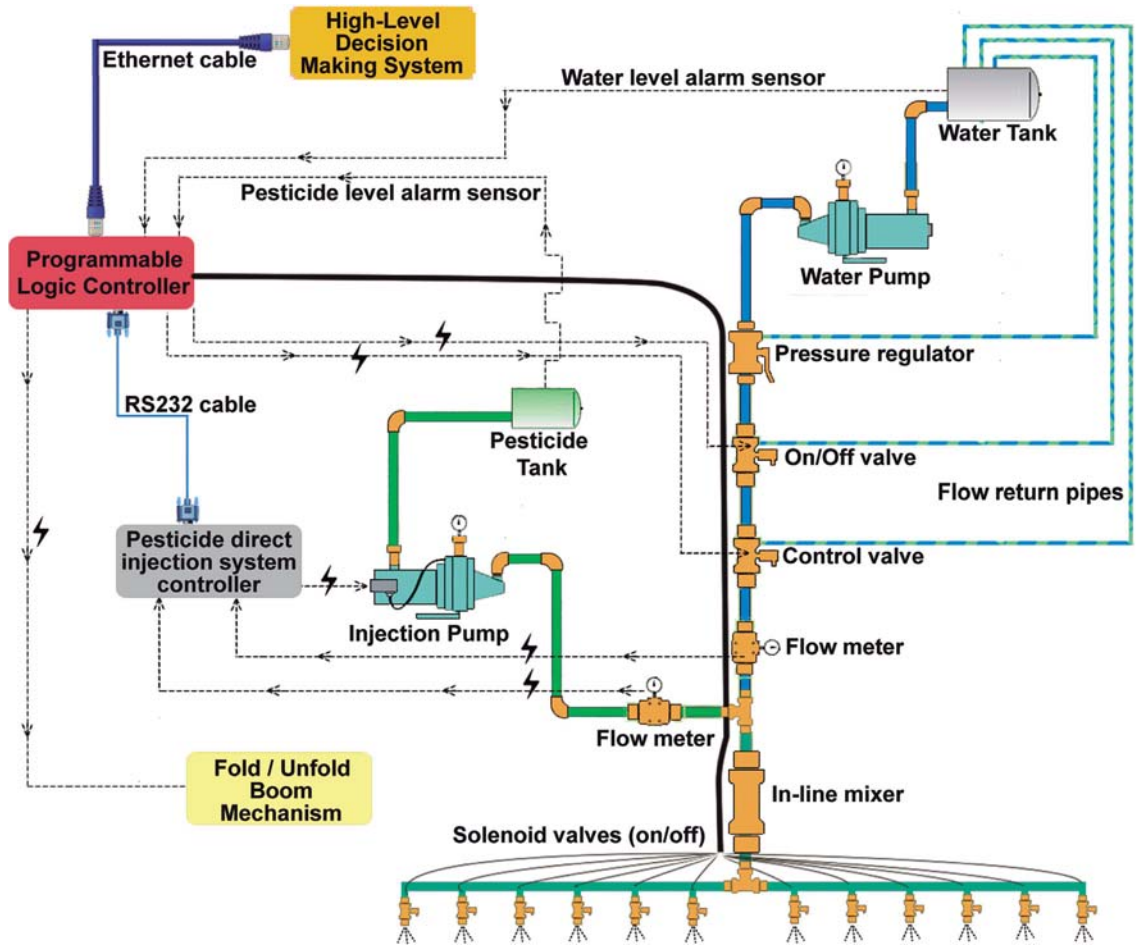

Fig. 1 – Simplified schematic diagram of the fundamental spraying components.

correction signal to multitude of GPS receivers, or it can be replaced by other different source of GPS correction signal. The unmanned ground vehicle also had on-board Trimble Model BX982 receiver, which communicated directly (via serial interface) with the main controller as well as other distributed systems that required information on the vehicle location. The GNSS receiver output (See Fig. 3) was configured as the "NMEA-0183 PTNL, AVR" string message, which contains the latitude and longitude geographic coordinates and the yaw angle (in degrees) (Carballido, Perez-Ruiz, Emmi, & Agüera, 2014).

Regarding the safety of the vehicle and the entire system, a set of parallel processes at different risk levels were implemented to prevent collisions (a) between the fully autonomous agricultural system (the unmanned ground vehicle and the smart spraying system) and other vehicles that are working simultaneously on the same field and (b) between the fully autonomous agricultural system and various obstacles that can be found in farm fields.

The laser system on-board the vehicle was in charge of the lowest safety level and was configured to pause the vehicle motion (overriding the *Main Controller* commands) when an obstacle is detected in a specified "danger zone" (which was defined depending on the current vehicle speed and the time that the vehicle took to stop before colliding with the obstacle) (Garrido et al., 2012). The machine vision system was in charge of the middle safety level, preventing an obstacle from reaching the "danger zone" of the laser (Hödlmoser, Bober, Kampel, & Brandstötter, 2011). The top safety layer involved cooperative behaviours among the diverse vehicles that are working in the same field at the same moment and are capable of sharing GNSS coordinates. Therefore, a master supervisor was implemented that receives these GNSS positions, evaluates possible future collision situations, and then prevents these situations by commanding the vehicles to pause at various mission points (Emmi et al., 2014).

All of these subsystems were integrated by the *Main Controller*, which was based on a CompactRIO-9082, (National Instruments Corporation, Austin-Texas-USA) running the LabVIEW Real-Time operative system (National Instruments Corporation, Austin-Texas-USA). This system was selected because it offers powerful stand-alone and networked execution for deterministic, real-time applications and is designed for extreme ruggedness, reliability, and I/O flexibility, which is appropriate for the integration of different sensory and actuation systems in precision agriculture autonomous applications.

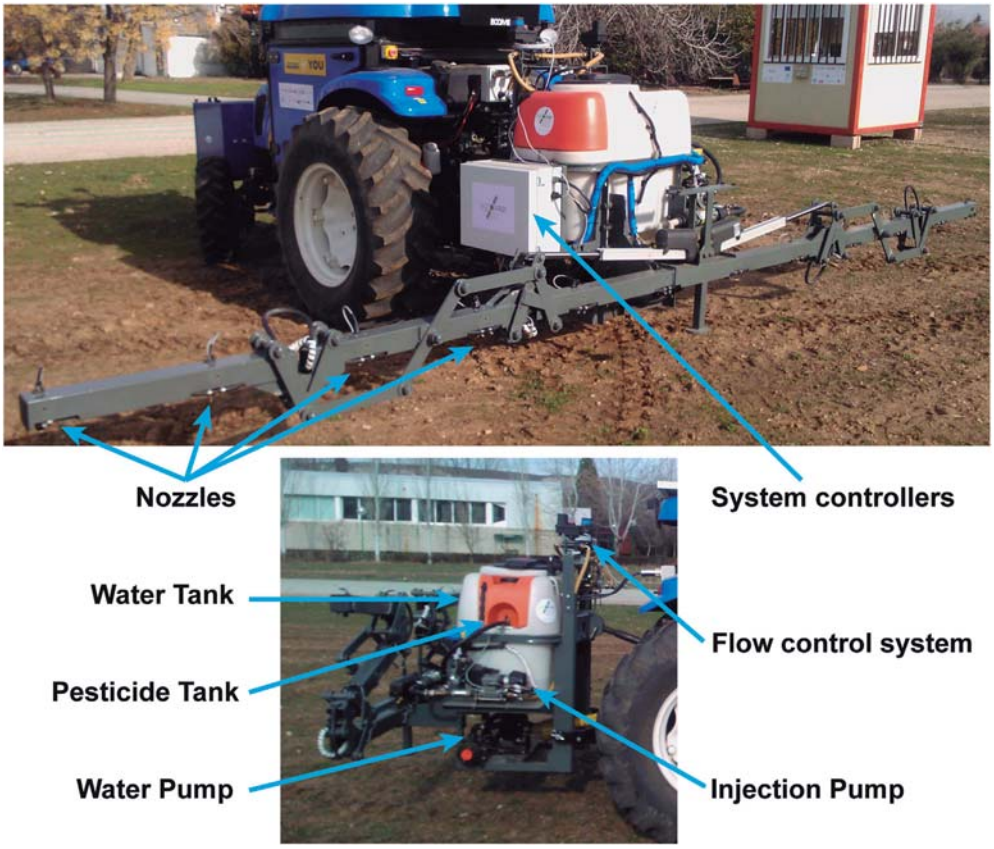

Fig. 2 – Smart spraying system and its main components.

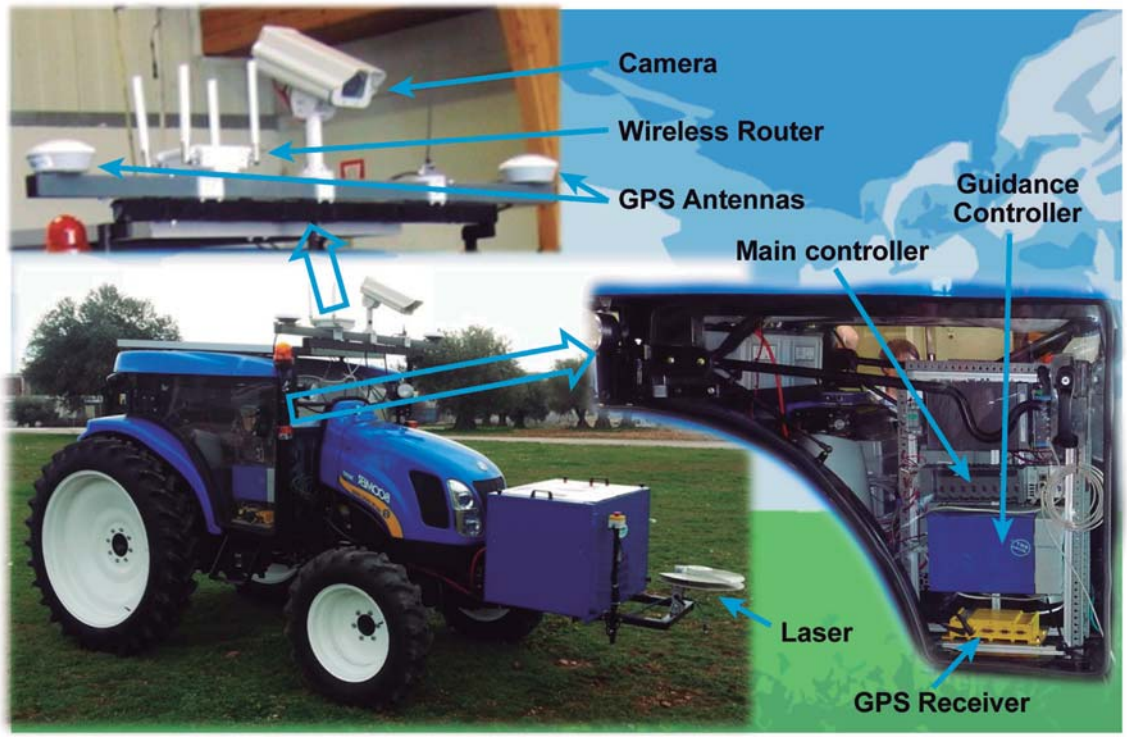

Fig. 3 – Unmanned ground vehicle; layout of the on-board sensors and communications antennas; layout of the on-board computer systems inside the cabin of the vehicle.

3.2. Control systems

As previously mentioned, the autonomous vehicle and the smart spraying system were controlled based on a hybrid architecture (See Fig. 4), its core based on a *Main Controller* in charge of synchronising and processing the information coming from the different sensors and the external operator and selecting the best behaviour for the entire system depending on the current situation, the environment perceived and the general mission to be performed. The *Main Controller* communicated with the other subsystems via diverse communication protocols (Ethernet, serial and CAN bus) and was also in charge of supervising the correct operation of the sensors and actuators. Furthermore, the *Main Controller* was responsible for a) interpreting the information coming from the base station; b) evaluating the reliability of sensors and actuators; c) creating an action plan to be executed by the actuation system (in this case the smart spraying system); d) communicating with external users (who can take the control) and other devices; and e) supervising the execution of the general mission.

In this type of application, the information on the weed spatial distribution can be provided to the autonomous systems for precise spraying by diverse sources, from on-board and remote sensors, or unmanned aerial vehicles, or satellite information. In this case the WDS was used in real time, using the on-board camera, for crop with wide furrows (corn, garlic, onions…) and an external WDS for crop with close furrows (cereals). External devices can provide better weed data for cereals crops than the on-board system, and when there is a WCM before of the treatment they can improve the patch plan significantly. The weed spatial distribution was processed prior to application, and a grid map was generated containing the dose, the type of herbicide and the location of the weed patches (Lee et al., 2010). Based on this map, a mission was generated using diverse algorithms seeking, among other things, low herbicide consumption and high performance. The *Main Controller* on-board the vehicle received and processed this information, and the correct behaviour of the system was defined, which was expressed as (a) a set of trajectories referring to GPS positions (that must be followed by the autonomous vehicle) and (b) a series of GPS locations in which both the states of the nozzles and the dose of the treatment were set.

The trajectory contained information on the starting point and the ending point of the field, the turns that the vehicle must perform to continue with the treatment in the same field, and the speed along the path. This path-following task was performed by the *Actuation Controller*, which was a peripheral system of the *Main Controller*. In addition, the *Actuation Controller* was in charge of the communication between the vehicle and the implement, in which a PLC is responsible for activating the nozzles and controlling the valves for the water, herbicide flow and mixture.

4. Spray laboratory test procedures

4.1. Description, parameters and variables

In laboratory experiments, the direct injection controller was used to control the rate of chemical injection. For ratio rate control, which is usually intended for handgun operation, the chemical injection rate was set in proportion to the flow of water leaving the system. In this way, the direct injection controller received continuous, up-to-date flow

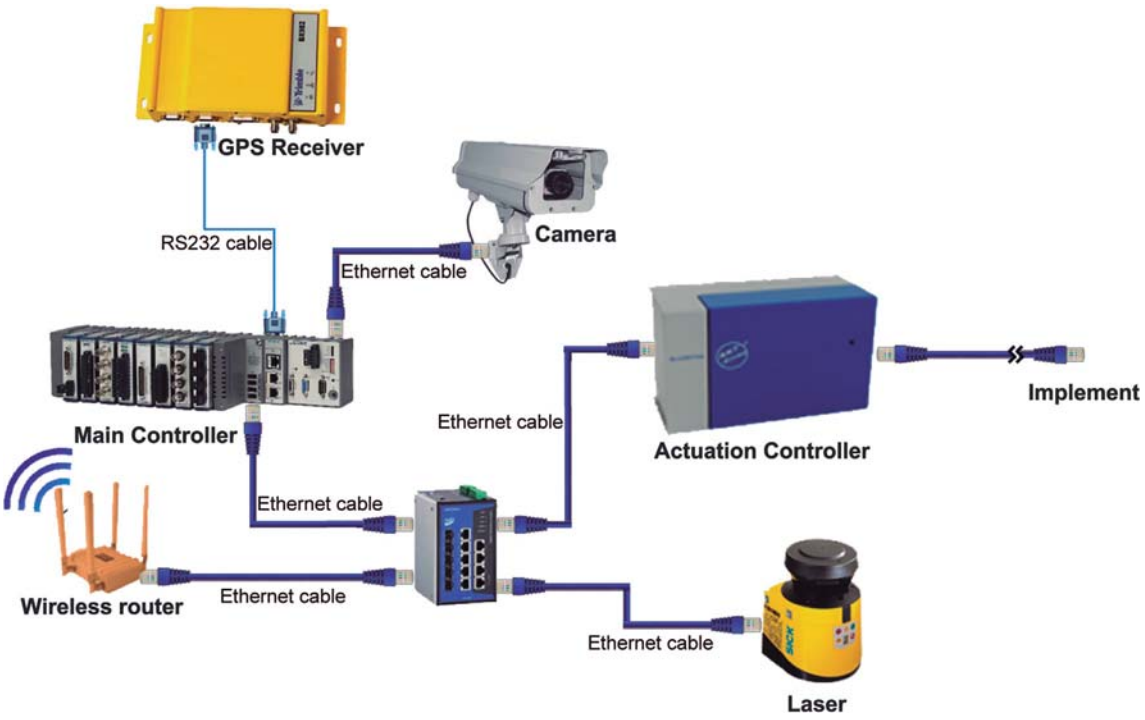

Fig. 4 – Schematic diagram of the control architecture on-board the autonomous vehicle.

meter data and adjusted the amount of injected herbicide accordingly.

The solenoid nozzles required a nominal working pressure of 276 kPa and applied a nominal workflow (Q_n) of 0.757 l min^{-1}. Q_w is the total water flow as measured by the flow meter that travelled to the set of nozzles that opened at each time and adjusted the injected herbicide flow (Q_{ch}) so that the ratio p = *herbicide volume/volume water* was constantly maintained at the value that was entered in the controller.

The total flow per active nozzle applied was the sum of the water flow plus the herbicide flow at the moment of application. For the proper operation of the spray nozzles, the total flow rate per nozzle must be maintained at a constant nominal value. This requirement implies a higher throughput at a given working pressure, which causes the droplet size to be too small, making the drops more susceptible to drift. In contrast, a lower nominal flow rate results in a too large droplet size, which reduces the plant surface covered per unit volume applied as well as the effect of the active material on the plant.

The applied dose (D_c) was defined as the volume of herbicide to be applied per unit area treated, expressed in l ha^{-1}. This value must be adjusted continuously according to the needs of each plot area and kept constant until further changes are required, regardless of the speed variations that the robot shifts through or the number of active nozzles (n_a).

D_c is the target variable to control, and its value should come mission-defined for each part of the plot to be treated, similar to active nozzles. Control of D_c was accomplished by adjusting the parameters of the actuators to which the system had access (control parameters): the total water flow rate Q_w and the ratio p. Table 1 defines the parameters used in the laboratory tests.

4.2. Relationship between the parameters and variables

The flow that was provided by the injection pump is computed as follows:

$$Q_h = \frac{1}{60} C_T D_h \tag{1}$$

Table 1 – Definition of the parameters and units that were used in the laboratory tests.

Constants	
$a = 0.50$ m	Equidistant spacing of the nozzles
$Q_n = 0.757$ l min^{-1}	Nominal nozzles flow
Control Parameters	
Q_w (l min^{-1})	Water flow
Q_h (l min^{-1})	Herbicide flow
p (ml l^{-1})	Herbicide volume/water volume
Variables	
v (m s^{-1})	Robot speed
n_a	Number of nozzles opened
Controlled variable	
D_h (l ha^{-1})	Applied herbicide doses
Intermediate variables	
Q_h (l min^{-1})	Injected herbicide flow
C_T (ha h^{-1})	Machine field capacity

It is known that

$$C_T = \frac{9}{25} v n_a a \tag{2}$$

Thus,

$$Q_h = \frac{3}{500} v n_a a D_h \tag{3}$$

Furthermore, the total water flow to be applied is

$$Q_w = n_a Q_n - Q_h = n_a \left(Q_n - \frac{3}{500} v a D_h \right) \tag{4}$$

and the proportion p is

$$p = 1000 \frac{Q_h}{Q_w} \tag{5}$$

Considering the above expressions yields

$$p = \frac{3000 v a D_h}{500 Q_n - 3 v a D_h} \tag{6}$$

4.3. Q_w, Q_h and p values in simulated robot speed

The injection pump had a minimum injection rate of 29.6 ml min^{-1}. This minimum means that the herbicide to be applied must be located in the auxiliary tank and diluted so that the injected flow conditions meet the required minimum but are not less than that value. These conditions were the minimum speed of work and a single nozzle open. Given the values of a and Q_n that were previously expressed, for a herbicide application rate of 8 l ha^{-1} and considering a range of speeds of 1.11–2.22 m s^{-1}. Figure 5 shows the values of Q_w, Q_h and p with respect to the speed value for each open nozzle. As we can see in the Eqs. (3) and (4), Q_w, Q_h are directly proportional to n_a; therefore, its total values increment with the number of open nozzles. Nevertheless, as we can see in Eq. (6), the p value is independent of n_a, and its value only changes with v.

5. Outdoor tests

In this section, we analyse the ability of each nozzle of the spraying system to apply the treatment over a simulated wheat crop using the real integrated system (*Unmanned Ground Vehicle* and *Implement*) with the whole aforementioned control system.

5.1. Experimental test bench

The tests were conducted over a hard, paved surface with three simulated weed patches limited by straight lines that were drawn on the pavement. These patches were parallelogram-shaped weed patches that allowed the measurement of the deviation of each nozzle as well as the analysis of behaviour of the system for three different angles in the weed patch perimeter. Figure 6a shows the scheme of this WCM where we can see the three weed patch perimeter angles (WPPA) that were chosen: $WPPA = atan(0)$, $WPPA = atan(0.5)$, and $WPPA = atan(1)$. The WPPA is an angle between 0 and $2^{-1}\pi$, whose value is $|WPPA' - 2^{-1}\pi|$, where

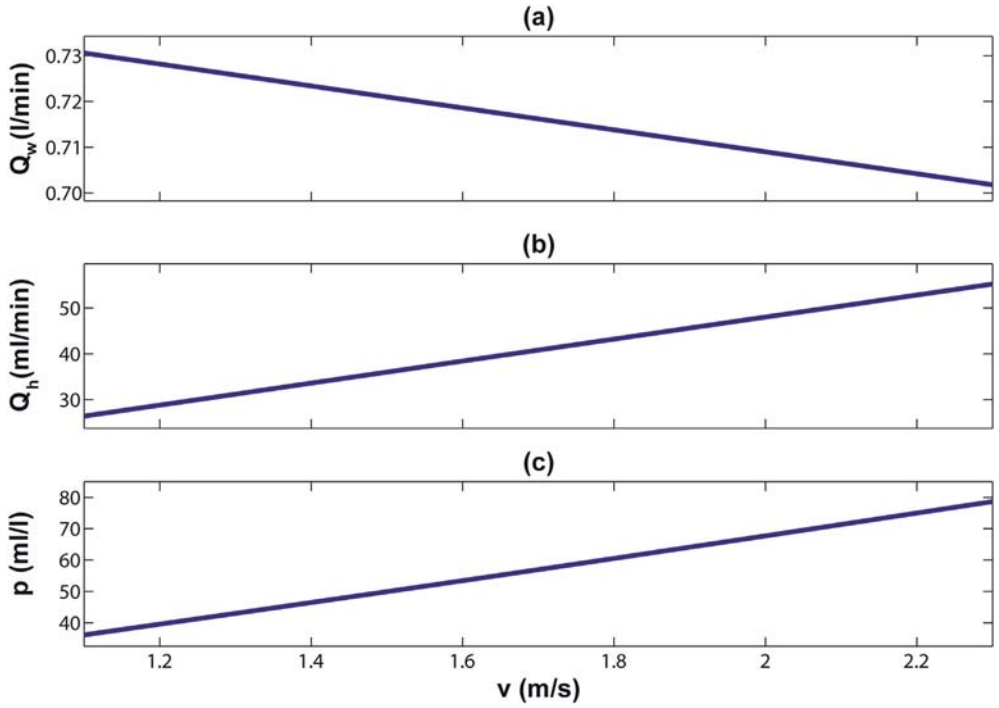

Fig. 5 – (a) Water flow, (b) Herbicide flow and (c) Herbicide/Water with respect to the speed for each open nozzle.

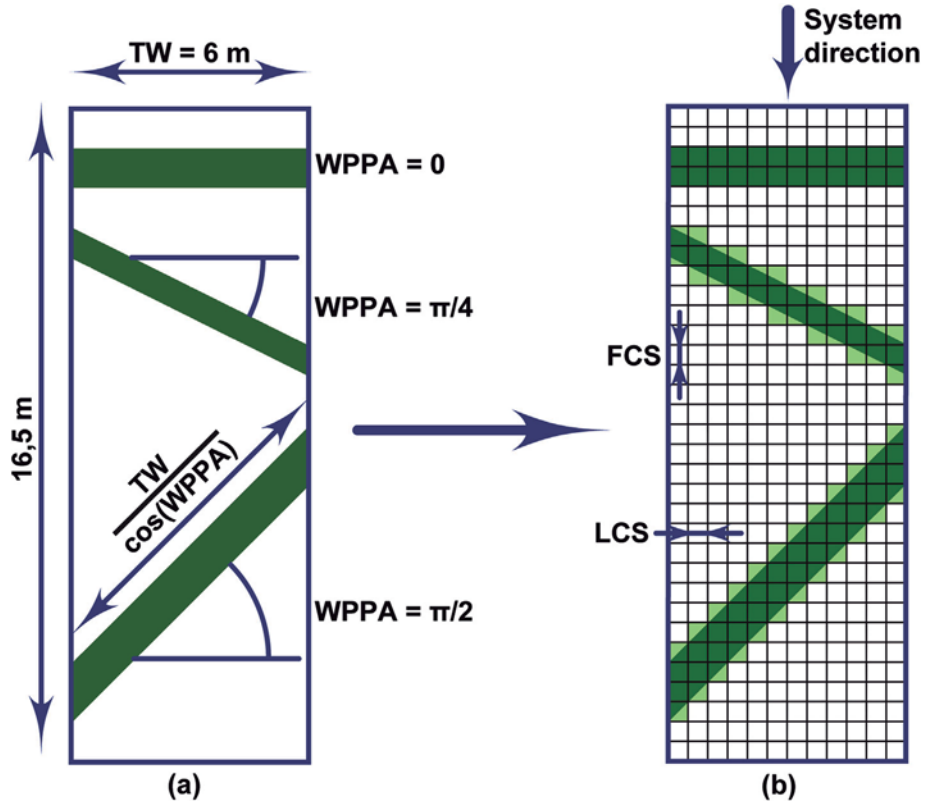

Fig. 6 – Weed control map of the crop. (a) True weed patches. (b) Weed control map.

WPPA′ is the angle between the weed patch limit line and the perpendicular line straight to the *Unmanned Ground Vehicle* trajectory. The three selected angles are critical for analysing the behaviour of the system.

For the purposes of this study, the area to be treated was homogenously divided into cells. A cell was approximately the area that is covered by a single nozzle. Thus, the width of the cell, lateral cell size(LCS), was set to 0.5 m, which is the lateral

size of the surface that is treated by each nozzle in each track, matching the distance between the nozzles of the sprayer boom. The system had a lag time of approximately 0.5 s, which is the average time from a nozzle-status-change command being sent to that change being completed. Therefore, considering that the system speed was approximately 0.83 m s^{-1} for all tests conducted, the minimum distance between some nozzle-status changings is 0.41 m. Thus, this distance was the length of the cell, frontal cell size (FCS), and was set to FCS = 0.5 m to ensure that the treatment covered all of the detected weeds.

Figure 6a represents the scheme of the scenario, and Fig. 6b illustrates the 0.5-m grid of the WCM that was obtained from this scenery. This scenario consists of a single track. To generate the gridded WCM, the area of weed patch was increased; this zone was called the not weed treated (NWT). Approximating the weed patch perimeter (WPP) to straight lines in each WCM cell, the minimum NWT value is given by the following:

$$\begin{aligned}
&0 \le WPPA < a\tan\left(\frac{LCS}{TW}\right) \Rightarrow 0 \le NWT < \frac{1}{2} LCS\, WPP_{WPPA} \cos(WPPA)\\
&a\tan\left(\frac{LCS}{TW}\right) \le WPPA \le \frac{\pi}{4} \Rightarrow NWT = \frac{1}{2} LCS\, WPP_{WPPA} \cos(WPPA)\\
&\frac{\pi}{4} < WPPA \le \left[\frac{\pi}{2} - a\tan\left(\frac{FCS}{TW}\right)\right] \Rightarrow NWT = \frac{1}{2} FCS\, WPP_{WPPA} \cos(WPPA)\\
&a\tan\left(\frac{FCS}{TW}\right) < WPPA \le \frac{\pi}{2} \Rightarrow 0 \le NWT < \frac{1}{2} FCS\, WPP_{WPPA} \cos(WPPA)
\end{aligned} \tag{7}$$

where WPP_{WPPA} is the section of the patch perimeter length with the corresponding WPPA (see Fig. 6a).

This WCM was generated by obtaining the weed coverage of each cell. The weed coverage was the percent of the soil surface that was covered by weeds; if this value was lower than minimum weed coverage (MWC), then the cell was considered to be weed-free. Otherwise, the cell was considered as a weed cell. Therefore, the mean of the maximum NWT was calculated as follows:

$$NWT = (1 - MWP)\frac{1}{2}(LCS + FCS) WPP_{WPPA} \cos(WPPA) \tag{8}$$

Furthermore, this MWC generates some weed areas that were not treated, and this zone was called the weed not treated (WNT) zone. The mean of the maximum WNT was as follows:

$$WNT = MWP\frac{1}{2}(LCS + FCS) WPP_{WPPA} \cos(WPPA) \tag{9}$$

In numerous works that analyse weed detection systems and an MWC of approximately 15% is considered a typical value if a cell is infested (Montalvo et al., 2013), (Gerhards & Christensen, 2003), (Torres-Sanchez, López-Granados, de Castro, & Peña, 2014). Considering a fixed MWC of 15%, the NWT and WNT were estimated with respect to the WPP. The data obtained for these calculations are presented in Table 2 for WPPA values between 0 and π rad, where $WPP' = WPP\cos(WPPA)$.

To assess these data in the working system, weed patches were marked over a pavement as shown in Fig. 7a, where the green lines were the weed patch limits and the white lines were the lines to be treated by each nozzle. The water in the sprayer was dyed to better mark the treatment (water) on the ground, and the white lines help to obtain a measurement accuracy of approximately ±0.025 m. Figure 7b shows how the system applied the product over the pavement and white lines when the nozzles were opened. As shown in the figure, the lateral distribution of applied product was too narrow for broadcast coverage because the spray boom was intentionally fixed to a lower than the appropriate height to improve the measurements; that is, as the nozzles were closer to the white lines, the marks of the limits were better defined.

Table 2 – Theoretical NWT and WNT values for the sprayer implement.

WPPA		Theoretical NWT		Theoretical WNT	
Min	Max	Min	Max	Min	Max
0	0.083	0	0.425WPP′	0	0.075WPP′
0.083	$4^{-1}\pi$	0.250WPP′	0.425WPP′	0	0.075WPP′
$4^{-1}\pi$	3.058	0.250WPP′	0.425WPP′	0	0.075WPP′
3.058	$2^{-1}\pi$	0	0.425WPP′	0	0.075WPP′

Fig. 7 – Test pavement: (a) general vision, and (b) the system working over the simulated weed patch.

5.2. *Tests assessment and discussion*

This section presents the result of the tests for each WPPA chosen; each test was performed three times. To assess the test results, we measured the distance from the weed patch to the treatment start or end with an accuracy of approximately ±0.025 m, and thus, the area with weeds not treated and the area that is treated but without weeds treated was calculated

for each case. This area was calculated with respect to the grid of the WCM and with respect to the true weed zone as well.

In these tests, the average delay time of the whole system control was known in advance and was approximately 0.4 s, and the control system was adapted to compensate for this delay.

5.2.1. *Case 1. Weed patch angle: 0 rad*

In this test, the WCM exactly matched the true weed patch because the start and the end of the weed patch were set in multiples of FCS. Figure 8 shows the scheme of these tests, where it can be seen that the theoretical NWT is null (because the WCM matches the true weed distribution). An analysis of this figure showed that the weed zone that was not treated was quite small but somewhat larger towards the ends of the boom. This effect was due to the rapid pressure drop caused by the sudden opening of all of the nozzles. Additionally, the treatment outside of the weed zone was smaller than the weed zone that was not treated because nozzles can close faster than they can open.

Figure 9 illustrates in more detail the points at which each nozzle should have opened and closed and the points at where they actually did. These data allow the calculation of the average distance that was travelled by the system from the instant when the nozzles should have opened until the point they did; this value is approximately 0.093 m with a standard deviation of approximately 0.061 m. A similar calculation was performed for closing the nozzles and the average distance was approximately 0.007 m with a standard deviation of approximately 0.069 m.

The true NWT and WNT were calculated using the test results with an accuracy of approximately ±0.15 m^2 Table 3 shows the values that were obtained for these tests. In this table, it was observed that, in the worst case, the WNT was 0.775 m^2, which was 12.9% of the weed patch, and the maximum NTW is 0.250 m^2, which was 4.2% of the weed patch. In the best case the WNT was 0.575 m^2, which was 9.6% of the weed patch, and the minimum NTW was 0.075 m^2, which was 1.3% of the weed patch. These results were considered quite good considering the small size of the simulated weed patch, and in any event, these proportionate values would decrease as the weed patch size increases.

5.2.2. *Case 2: Weed patch angle: $4^{-1}\pi$ rad*

In these tests, to generate the WCM, we generated a theoretical NWT of 3 m^2, which is 45% of our weed patch. The start and the end of the weed patch were situated in multiples of the FCS to minimise this theoretical NWT, and WPPA = $4^{-1}\pi$ rad was chosen to open the nozzles in pairs.

Figure 10 shows the scheme of these tests where we can see that the theoretical NWT occupied a considerable area. When this figure was analysed it was observed that the weed zone that was not treated was quite small and evenly distributed among each nozzle because, in this case, the nozzles opened progressively. The treatment outside of the weed zone was smaller than the weed zone that was not treated, similar to the previous case.

Figure 11 represents in more detail the actual open and closed positions of each nozzle and the desired positions. The average error was approximately 0.056 m with a standard deviation of approximately 0.077 m; for the turn-off process, this error was approximately 0.019 m with a standard deviation of approximately 0.056 m. These results represented a small improvement compared to the previous case because the nozzles were opened stepwise and the pressure drop was much lower.

Using these test results, the true NWT and WNT were calculated with an accuracy of approximately ±0.008 m^2 and ±0.150 m^2, respectively, considering the true weed patch, which in this case was known. These results are shown in Table 4. In this table, it can be observed that a very important reduction in the WNT is obtained with respect to case 1, with

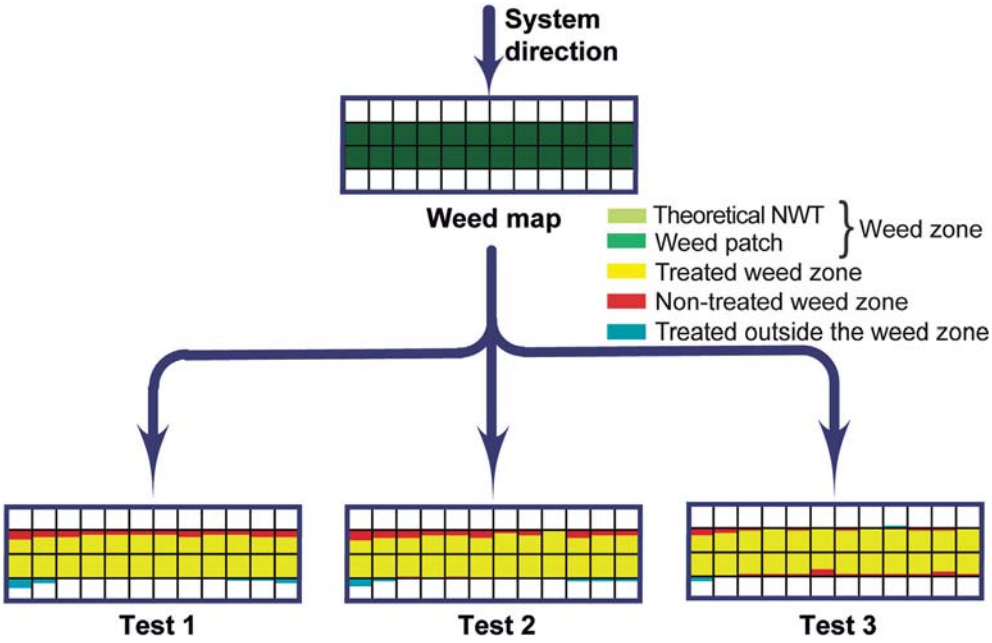

Fig. 8 – Scheme of the data in the tests over the weed patch with angle 0 rad.

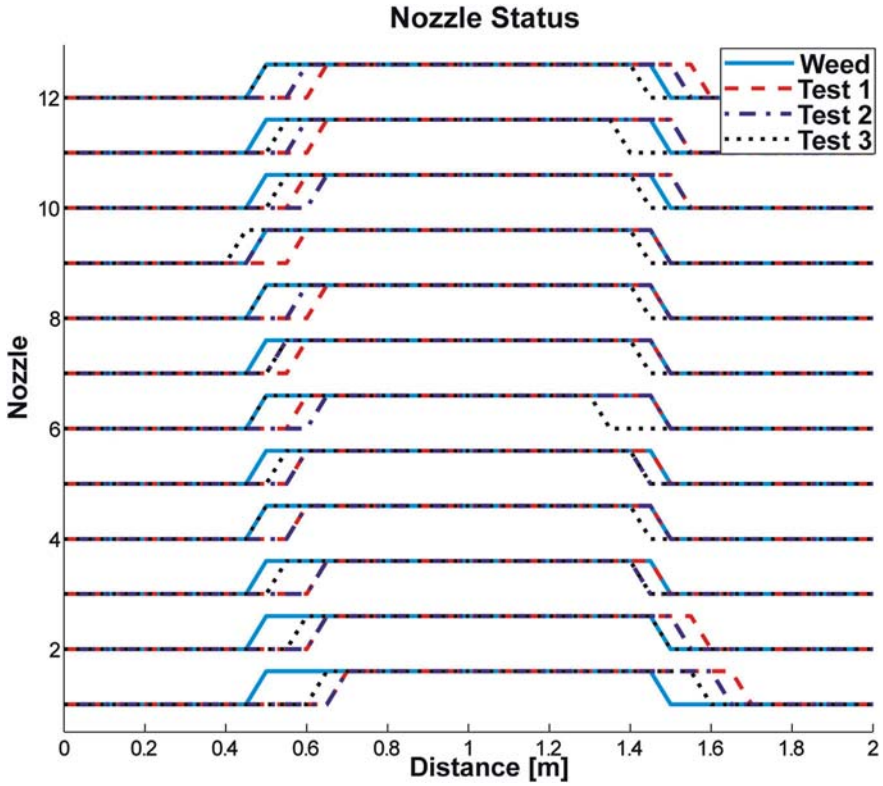

Fig. 9 – Result from the tests over the weed patch with angle 0 rad.

WPPA = 0 rad. The largest WNT was 0.018 m^2, which is 0.3% of the weed patch, and the smallest WNT was nil. However, the NWT presents a sharp increase, its minimum value was 2.536 m^2, which was 37.8% of the weed patch, and it had a maximum value of 3.254 m^2, which was 48.5% of the weed patch. This result occurred because the theoretical NWT value that was required to generate the gridded WCM was significantly higher than in case 1, but this percent value decreased when the weed patch size increased.

In addition, the NWT and WNT was calculated considering the gridded WCM with an accuracy of approximately ±0.150 m^2, and these results are shown in Table 4. In this case, the results were quite similar to those in case 1, with a small improvement in the WNT because the nozzles were opened gradually, and there was no sudden pressure drop.

5.2.3. *Case 3: Weed patch angle: $2^{-1}\pi$ rad*

In these tests, the theoretical NWT was the same as that in the previous case, 3 m^2, but now it represented 35% of the weed patch because the patch was larger. As in the previous cases, the start and end of the weed patch were set in multiples of FCS to minimise the theoretical NWT, and the WPPA was $2^{-1}\pi$ rad to open the nozzles one by one.

Figure 12 shows the scheme of these tests, and it can be seen that the theoretical NWT was less noticeable than that in the previous case but still had a significant area. In this figure, it can be seen that the weed zone that was not treated was quite small (as before) and evenly distributed among the nozzles. The treatment outside of the weed zone was also smaller than the weed zone that was not treated. In this case, these error zones, NWT and WNT, were less noticeable because although its area was roughly equal to that in case 2, the weed patch surface was larger, and therefore, this error represents a lower percentage of the surface area.

Figure 13 shows in detail where each nozzle was opened and closed and where they should have done so. As in the previous cases, we calculated the average error value, which was approximately 0.068 m with a standard deviation of approximately 0.032 m. For the turn-off process, this error was approximately 0.019 m with a standard deviation of approximately 0.051 m. These values were similar to those that were obtained in the case with WPPA = $4^{-1}\pi$ rad.

As in the previous cases, the true NWT and WNT were calculated using the test results. When the true weed patch sizes were considered, which are known in these cases, an accuracy of approximately ±0.150 m^2 and <±0.004 m^2 for NWT and for WNT values, respectively, was achieved. Table 5 shows these values, where NWT values are close to the obtained values in case 2, with WPPA = $4^{-1}\pi$ rad, and the WNT values are slightly lower. The biggest WNT was 0.002 m^2,

Table 3 – Measured NWT and WNT values on the tests over the weed patch with angle 0 rad (±0.15 m^2).

Action	Measured WNT			Measured NWT		
	Test 1	Test 2	Test 3	Test 1	Test 2	Test 3
Open	0.775	0.675	0.250	0.000	0.000	0.025
Close	0.00	0.050	0.325	0.250	0.175	0.050
Total	0.775	0.725	0.575	0.250	0.175	0.075

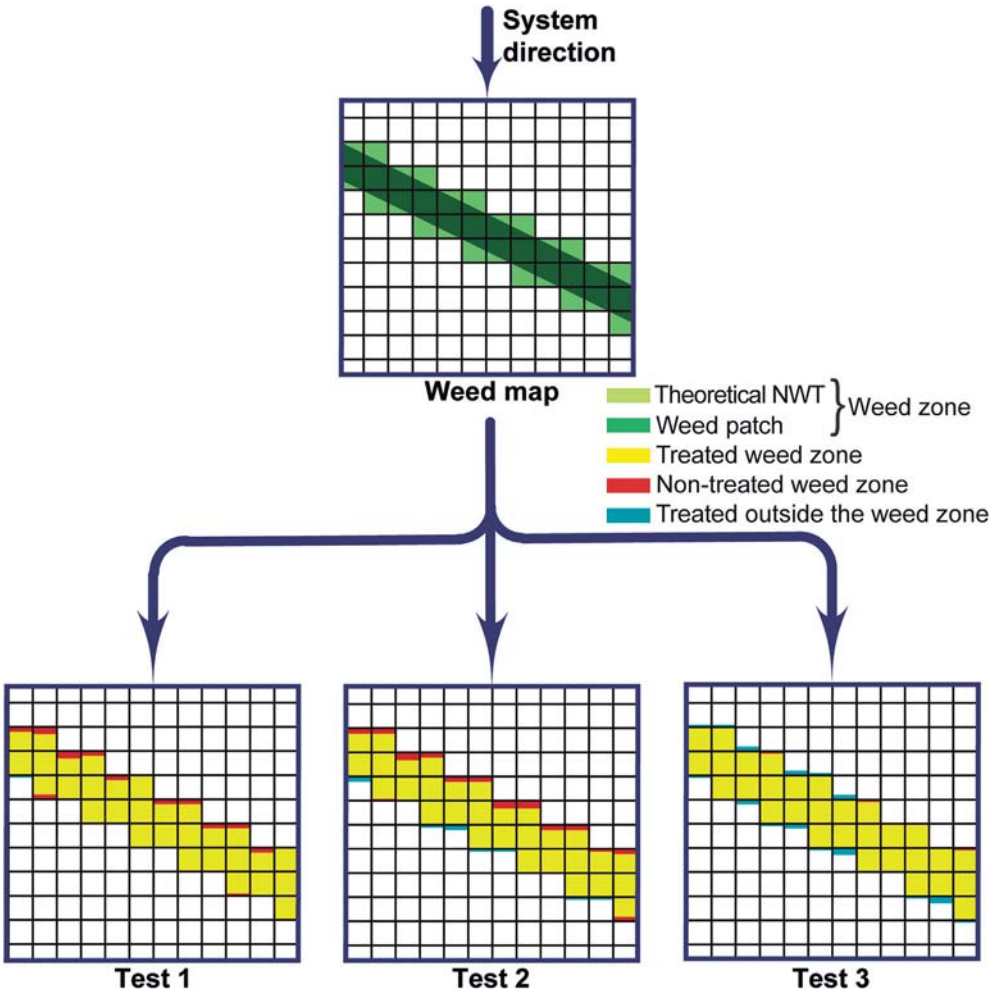

Fig. 10 – Scheme of the data in the tests over the weed patch with angle $4^{-1}\pi$ rad.

which was 0.02%, a negligible value, of the weed patch, and the minimum was nil. However, in this case, as in case 2, the NWT had values that were not negligible. The maximum NWT value was 2.843 m^2, which was 33.5% of the weed patch, and its minimum value was 2.542 m^2, which was 30.0% of the weed patch. This result occured for the same reason as in case 2. In this case, the weed patch surface area was larger than that in case 2; therefore, the percent values were lower.

The NWT and WNT values were also calculated with respect to the gridded WCM with an accuracy of approximately ±0.150 m^2 (Table 5). These data were similar in the three analysed cases, with a small difference in case 1 in which all of the nozzles were opened at once, causing an increased delay, albeit slight, in the two nozzles at each end of the spray boom.

5.3. *General assessment of the robotic system*

These tests reveal that the behaviour of the entire system was very good for the parameters that were used for the evaluation. Eqs. (7)–(9) revealed that if the grid step is reduced (LCS and/or FCS) the system behaviour can improve and reduce NWT and WNT values.

Using these data, NWT and WNT theoretical values can be estimated for any weed patch as the mean of the maximum and minimum values given that the WPPA is distributed equitably among all of its possible values when applying the following equations:

$$WNT = \sum_i P_i K_{WNT_i} WPP \int_{WPPA_i}^{WPPA_{i+1}} \cos(WPPA)\, dWPPA \tag{10}$$

$$NWT = \sum_i P_i K_{NWT_i} WPP \int_{WPPA_i}^{WPPA_{i+1}} \cos(WPPA)\, dWPPA \tag{11}$$

where i is the number of different WPPA ranges to be considered, P_i is the probability of each of these ranges, K_{WNTi} is the constant corresponding to the range i to calculate WNT, and K_{NWTi} is the constant corresponding to the range i to calculate NWT. For the WNT calculation, the possible very small patches away from the detected patch perimeters can be disregarded. In the case of a homogenous weed concentration being slightly lower than the MWC (worst case, which is highly unlikely), the WNT would increase up to values very

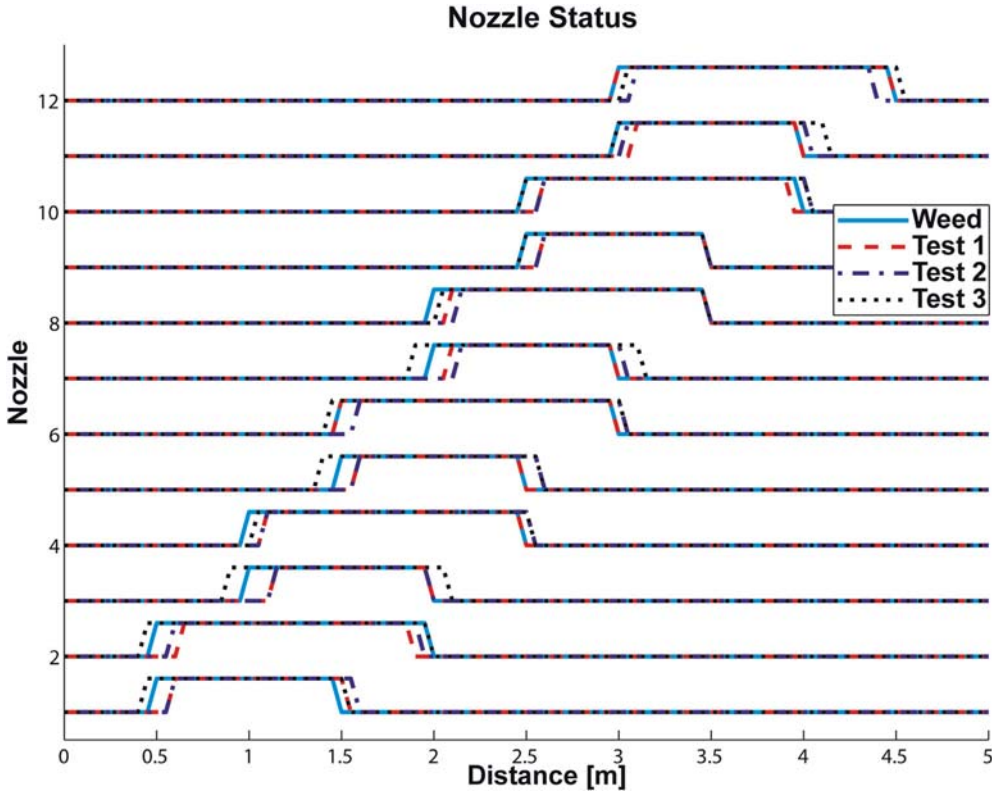

Fig. 11 – Result for the tests over the simulated weed patch with angle $4^{-1}\pi$ rad.

close to MWC, that is the percentage of crop surface with no detected weed.

Given that the test results demonstrate that the system worked correctly for the defined parameters, these parameters can be used to estimate the NWT and WNT values for any weed patch by replacing these parameter values in Eqs. (10) and (11).

Normally, winter crops, such as wheat, have low or medium weed coverages of between 0% and 66% (Kwon et al., 2013), (Steinsiek, Oliver, & Collins, 1982), (Gerhards, Wyse-Pester, & Johnson, 1997), (Lemieux, Cloutier, & Leroux, 1992). For example, let us consider a crop of 10,000 m^2 with a low weed distribution consisting of five nearly circular weed patches whose radii are approximately 5, 8, 9, 15 and 18 m, and the weed is to be removed from these patches. These weed patches represent 22.6% of the crop surface, and it is estimated that our system would treat 23.1% of the crop surface. Furthermore, it can be estimated that the WNT is approximately 0.5% and that the NWT is approximately 0.8%. Therefore, in this hypothetical case, this spraying system would have achieved the treatment of approximately 99.5% of the weed-infested area using 76.9% less product than a conventional spraying system applying the herbicide uniformly.

In these results, the NWT parameter is low and it could be decreased more by reducing the size of the treated cell (0.5 m × 0.5 m), which would entail an increase in the number of nozzles on the boom. Furthermore, the cell size can be reduced by improving the system delays, reducing the FCS value, or using more precise (less area of action) and more narrowly spaced nozzles, thereby reducing the LCS value.

Furthermore, in the performed tests, it was discovered that when the tractor moved at a speed of 0.83 m s^{-1}, the average

Table 4 – Measured NWT and WNT values (m^2) for the tests over the weed patch with angle $4^{-1}\pi$ rad.

	Action	Measured WNT			Measured NWT		
		Test 1	Test 2	Test 3	Test 1	Test 2	Test 3
With respect to the real weed patch (±0.004)	Open	0.018	0.019	0.000	1.170	1.112	1.566
	Close	0.000	0.000	0.000	1.466	1.566	1.688
	Total	0.018	0.019	0.000	2.536	2.678	3.254
With respect to the weed map (±0.150)	Open	0.550	0.650	0.075	0.000	0.000	0.225
	Close	0.075	0.075	0.000	0.025	0.225	0.375
	Total	0.625	0.725	0.075	0.025	0.225	0.600

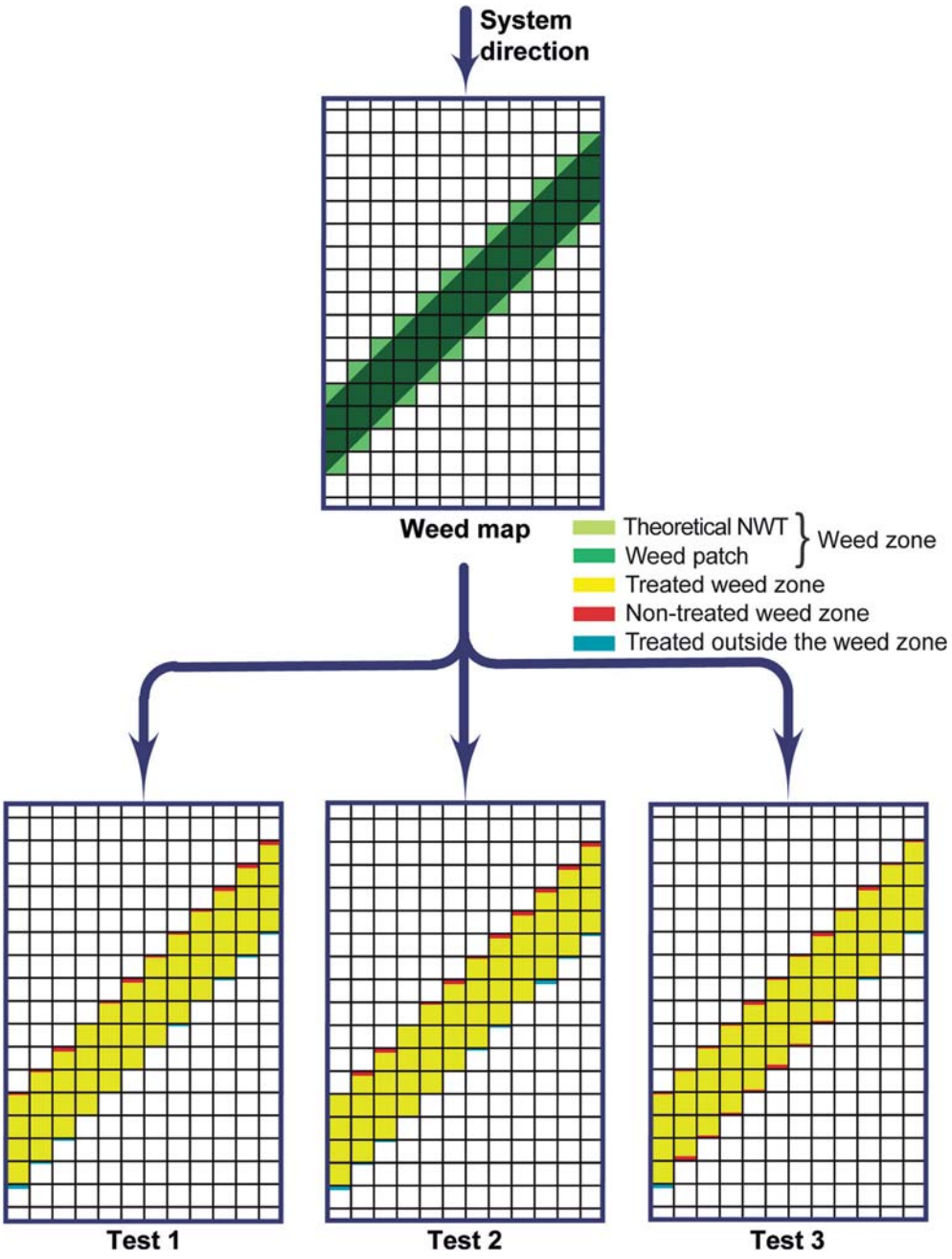

Fig. 12 – Scheme of the data in the tests over the weed patch with angle $2^{-1}\pi$ rad.

distance error to apply the treatment is of approximately 0.044 m with a standard deviation of approximately 0.066 m. Furthermore, the average error was larger for switching on the nozzles (ca. 0.072 ± 0.061 m), whereas for switching off the treatment, the average error was smaller (ca. 0.015 ± 0.059 m). Therefore, the system behaviour to switch off the treatment was better than that to switch it on. Moreover, the average distance error is very low and can be considered as a small offset, which is expected to tend toward 0 by increasing the number of tests; otherwise, it can be corrected easily by adjusting the system delays. The standard deviation value was also quite low, as this value represents the error to switch on/off the treatment, wherein values can be maintained below 0.010 m.

5.4. *Demonstration in wheat field*

In the final demonstration of the RHEA project, this system was used in a real wheat crop with controlled weed patches several times, and it was shown that it worked correctly. Figure 14c illustrates the wheat crop in which the demonstration was conducted. Figure 14a shows the system applying the treatment over a weed patch, and in Fig. 14b, it can be seen that the system stopped treatment outside of the weed patch. Finally, Fig. 14d shows how the results were evaluated; the water-sensitive paper is spotted by water when the treatment is on. To obtain the error, the weed patch was limited using stakes and ropes fixed in the crop, and the error was calculated measuring the distance between these weed patch limits

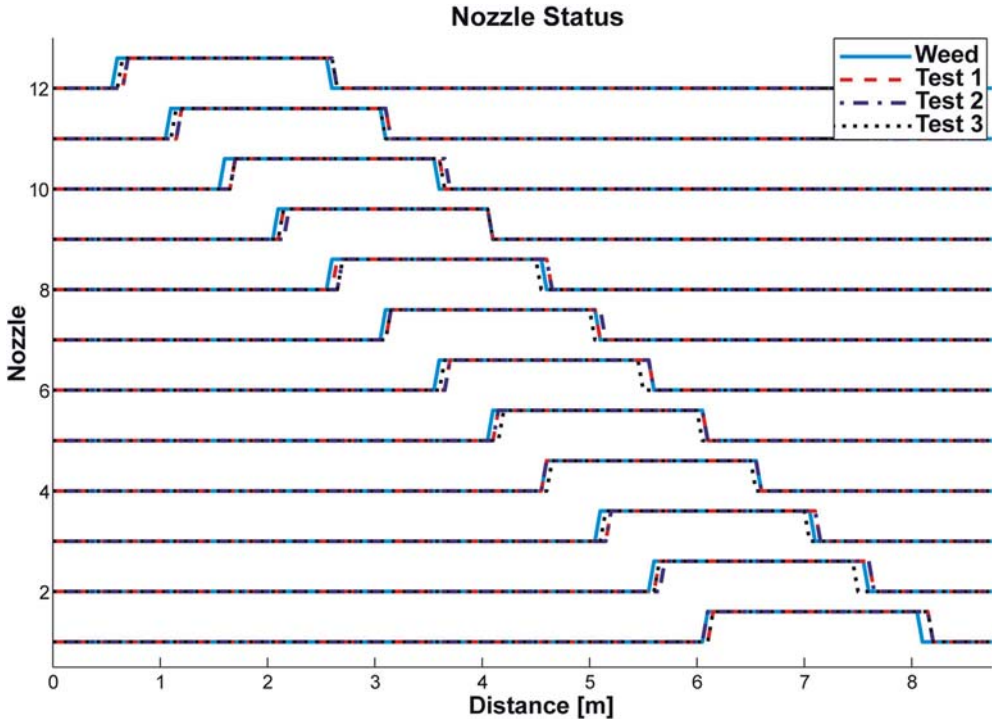

Fig. 13 – Results in the tests over the weed patch with an angle of $2^{-1}\pi$ rad.

and the spot over the sensitive paper. A video of this demonstration is available in the URL "http://youtu.be/WeAtUeoAYi0".

In this demonstration the WCM was provided by an external WDS. Two aerial robots took the crop images that were processed by a computer to get the WCM. This computer created the work plan (that included the WCM) and sent it to the vehicle which follow the defined work plan to perform the weed control treatment. The wheat height was approximately 10–15 cm, and the WDS considered weeds to be all detected plants that were not wheat. The evaluations performed in this demonstration showed that the vehicle followed quite right the defined routes, with a maximum deviation of approximately 7 cm. With respect to the accuracy of the herbicide spraying, more than 95% of the area of the weed patches was treated, therefore the WNT was lower than 5%, a little bit higher than expected and the NWT was also higher than expected (Gonzalez-de-Santos, Ribeiro, Fernadez-Quintanilla, & Dorado, 2014). This deviation appeared to be due to new errors inserted by the use of an external WDS; the position accuracy of this external WDS was lower than the accuracy provides by the GPS used in the vehicle.

The result of this demonstration confirmed that the system works quite well and that the use of this type of system confers important reductions of herbicide products with the attendant potential decreases in environmental contamination.

6. Conclusions

This article describes the design, development and experimental tests (both laboratory and field) of a robotised patch spraying system that was devoted to site-specific herbicide application in cereals. The robotised patch sprayer was based on a tractor, a spraying boom, a location system and a centralised controller that coordinate the subsystem functions to configure a fully autonomous system.

The patch spraying system increased the accuracy in the herbicide application substantially and thus can be used in

Table 5 – Measured NWT and WNT values on the tests over the weed patch with angle $2^{-1}\pi$ rad.

	Action	Measured WNT			Measured NWT		
		Test 1	Test 2	Test 3	Test 1	Test 2	Test 3
With respect to the real weed patch (±0.004)	Open	0.000	0.001	0.001	1.132	1.093	1.151
	Close	0.000	0.000	0.001	1.700	1.750	1.391
	Total	0.000	0.001	0.002	2.832	2.843	2.542
With respect to the weed map (±0.150)	Open	0.400	0.450	0.375	0.000	0.000	0.000
	Close	0.000	0.000	0.225	0.200	0.250	0.100
	Total	0.400	0.450	0.600	0.200	0.250	0.100

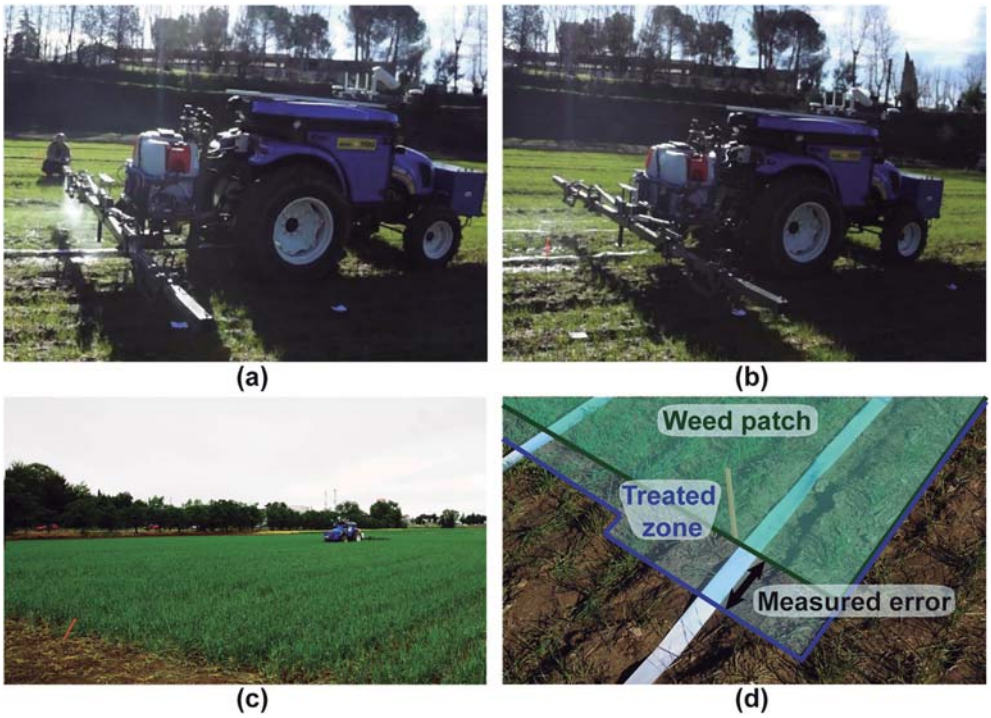

Fig. 14 – The spraying system working over a wheat crop. (a) System treating a weed patch. (b) System outside of weed patches. (c) Wheat crop. (d) Evaluation of result using water-sensitive tape.

precision farming to implement site-specific management techniques for the variable-rate application. In this system, fixed-duration pulses through solenoid valves actuated individual nozzles. The next step is to use electrochemical conductivity sensors on the nozzles to estimate the concentration of an injected spray solution in real time. This implementation will help to monitor the applied concentration at nozzle level and to determine the maps of herbicide use.

The tractor, based on a commercial agricultural vehicle, provided all of the requested features regarding mechanical power, electrical power, energetic autonomy, manoeuvrability and reliability. This autonomous robot, along with the location system based on GNSS technology and the controller, exhibited an accuracy of approximately ±0.07 m following predetermined trajectories, good enough for working on traditional wide-row crops.

Considering that the main objective of this article is not the description and characterisation of every system component but the assessment of the entire system working as a test bed. The tests that were conducted on a hard level surface demonstrated that the intended robot can provide an important reduction in herbicide use compared to traditional methods. Herbicide savings depend on weed abundance and distribution; in general, winter crops have low to medium weed coverages (i.e., between 0% and 66%). Therefore, the use of these types of systems is very interesting in these crops because for a weed concentration of approximately 33%, herbicide savings can be close to 66%.

The experiments revealed that if a good WCM is used (the WCM can be created in real-time by an on-board WDS or previously to the treatment by an external WDS.), this new implement can treat approximately 99% of the detected weeds. And, the area of not infested crop treated is insignificant, appreciable amounts of herbicides can be saved reducing soil and groundwater pollution.

In this work, this system for weed control in agricultural crop using herbicides was analysed. It could be used for other pest control tasks using suitable pesticides and for other agricultural tasks, for example fertilisation tasks using liquid fertilizer where the concentration applied could be varied according to the requirements of the different zones of the crops.

Acknowledgements

The research leading to these results has received funding from the European Union's Seventh Framework Programme [FP7/2007–2013] under Grant Agreement nº 245986. The RHEA consortium was formed by Centre for Automation and Robotics, Institute of Agricultural Sciences and Institute for Sustainable Agriculture from CSIC; CogVis Software and Consulting GmbH; FTW Forschungszentrum Telekommunikation Wien GMBH; Cyberbotics SARL; Universita di Pisa; Universidad Complutense de Madrid; Tropical S.A.; Soluciones Agricolas de Precision S.L.; Escuela Tecnica Superior de Ingenieros Agronomos and Escuela Tecnica Superior de Ingenieros Industriales from Universidad Politecnica de Madrid; Airrobot Gmbh & Co Kg; Universita Degli Studi di Firenze; Institut National de Recherche en Sciences et Technologies Pour L'environnement et L'agriculture (IRSTEA); Case New Holland Industrial; Bluebotics SA; and C.M. SRL.

REFERENCES

Bautin, A., Simonin, O., & Charpillet, F. (2011). Towards a communication free coordination for multi-robot exploration. In *Proceedings of the 6th national conference on control architectures of robots. Grenoble, France*.

Berge, T. W., Goldberg, S., Kaspersen, K., & Netland, J. (2012). Towards machine vision based site-specific weed management in cereals. *Computers and Electronics in Agriculture, 81*, 79–86. http://dx.doi.org/10.1016/j.compag.2011.11.004.

Blackmore, B. S., Griepentrog, H. W., Nielsen, H., Nørremark, M., & Resting-Jeppesen, J. (2004). Development of a deterministic autonomous tractor. In *Proceedings of the CIGR international conference, Beijing, China*.

Bouraqadi, N., Fabresse, L., & Doniec, A. (2012). On fleet size optimization for multi-robot Frontier-based exploration. In *Proceedings of the 7th national conference on control architectures of robots. Nancy, France*.

Carballido, J., Perez-Ruiz, M., Emmi, L., & Agüera, J. (2014). Comparison of positional accuracy between RTK and RTX GNSS based on the autonomous agricultural vehicles under field conditions. *Applied Engineering in Agriculture, 30*, 361–366.

Conesa-Muñoz, J., Ribeiro, A., Andujar, D., Fernandez-Quintanilla, C., & Dorado, J. (2012). Multipath planning based on a NSGA-II for a fleet of robots to work on agricultural tasks. In *WCCI 2012 IEEE world congress on computational intelligence, congress of evolutionary computation (CEC)* (pp. 2236–2243).

Drenjanac, D., & Tomic, S. D. K. (2013). Middleware challenges in robotic fleets for precision agriculture. *Journal of Mechanics Engineering and Automation, 3*, 702–714.

Emmi, L., Gonzalez-de-Soto, M., Pajares, G., & Gonzalez-de-Santos, P. (2014). New trends in robotics for agriculture: integration and assessment of a real fleet of robots. *The Scientific World Journal, 2014*, 1–21.

Frasconi, C., Martelloni, L., Fontanelli, M., Raffaelli, M., Emmi, L., Pirchio, M., et al. (2014). Design and full realization of physical weed control (PWC) automated machine within the RHEA project. In *Proceedings of the 2nd international conference on robotics and associated high-technologies and equipment for agriculture and forestry (RHEA-2014), Madrid, Spain, May 21–23* (pp. 3–11).

Garford Farm Machinery Ltd | News: Latest News [WWW Document], n.d. URL: http://www.garford.com/news_latest.html (accessed 01.23.15).

Garrido, M., Ribeiro, A., Barreiro, P., Debilde, B., Balmer, P., Carballido, J., et al. (2012). Safety functional requirements for robot fleets for highly effective agriculture and forestry management (RHEA). In *Proceedings of the international conference of agricultural engineering, CIGR-AgEng2012. Valencia, Spain. July 8–12*.

Gerhards, R., & Christensen, S. (2003). Real-time weed detection, decision making and patch spraying in maize, sugarbeet, winter wheat and winter barley. *Weed Research, 43*, 385–392.

Gerhards, R., Wyse-Pester, D. Y., & Johnson, G. A. (1997). Characterizing spatial stability of weed populations using interpolated maps. *Weed Science*, 108–119.

Gonzalez-de-Santos, P., Ribeiro, A., Fernadez-Quintanilla, C., & Dorado, J. (2014). Assessing a fleet of robots for herbicide applications. In *Proceedings international conference of agricultural engineering. Presented at the international conference of agricultural engineering, GEYSECO, Zurich, Switzerland*.

Hödlmoser, M., Bober, C., Kampel, M., & Brandstötter, M. (2011). Vehicle guidance implemented on a single-board computer. In *Proceedings of the robotics and associated high-technologies and equipment for agriculture, 187–196. Montpellier, France*.

Jeon, H. Y., & Tian, L. F. (2009). Direct application end effector for a precise weed control robot. *Biosystems Engineering, 104*, 458–464.

Khot, L. R., Tang, L., Steward, B. L., & Han, S. (2008). Sensor fusion for improving the estimation of roll and pitch for an agricultural sprayer. *Biosystems Engineering, 101*, 13–20.

Kwon, Y.-S., Chung, N., Bae, M.-J., Li, F., Chon, T.-S., Kim, M.-H., et al. (2013). Evaluation of global warming effects on the geographical distribution of weeds in paddy fields by characterizing germination time and morphological factors. *Ecological Informatics, 17*, 94–103. http://dx.doi.org/10.1016/j.ecoinf.2013.06.007. Special issue of the 7th International Conference on Ecological Informatics, 13–16 December 2010, Ghent, Belgium: "Unravelling complexity and supporting sustainability".

Lee, W. S., Alchanatis, V., Yang, C., Hirafuji, M., Moshou, D., & Li, C. (2010). Sensing technologies for precision specialty crop production. *Computers and Electronics in Agriculture, 74*, 2–33.

Lemieux, C., Cloutier, D. C., & Leroux, G. D. (1992). Sampling quackgrass (Elytrigia repens) populations. *Weed Science*, 534–541.

Montalvo, M., Guerrero, J. M., Romeo, J., Emmi, L., Guijarro, M., & Pajares, G. (2013). Automatic expert system for weeds/crops identification in images from maize fields. *Expert Systems with Applications, 40*, 75–82. http://dx.doi.org/10.1016/j.eswa.2012.07.034.

Nørremark, M., Griepentrog, H. W., Nielsen, J., & Søgaard, H. T. (2008). The development and assessment of the accuracy of an autonomous GPS-based system for intra-row mechanical weed control in row crops. *Biosystems Engineering, 101*, 396–410.

Peña, J. M., Torres-Sánchez, J., de Castro, A. I., Kelly, M., & López-Granados, F. (2013). Weed mapping in early-season maize fields using object-based analysis of unmanned aerial vehicle (UAV) images. *PLoS ONE, 8*, e77151.

Perez-Ruiz, M., Gonzalez-de-Santos, P., Ribeiro, A., Fernandez-Quintanilla, C., Peruzzi, A., Vieri, M., et al. (2014). Highlights and preliminary results for autonomous crop protection. *Computers and Electronics in Agriculture, 110*, 150–161.

Perez-Ruiz, M., Slaughter, D. C., Gliever, C. J., & Upadhyaya, S. K. (2012). Automatic GPS-based intra-row weed knife control system for transplanted row crops. *Computers and Electronics in Agriculture, 80*, 41–49.

Rabatel, G., Gorretta, N., & Labbé, S. (2014). Getting simultaneous red and near-infrared band data from a single digital camera for plant monitoring applications: theoretical and practical study. *Biosystems Engineering, 117*, 2–14.

RHEA. (2015). *A robot fleet for highly effective agriculture and forestry management*. http://www.rhea-project.eu.

Romeo, J., Pajares, G., Montalvo, M., Guerrero, J. M., Guijarro, M., & Ribeiro, A. (2012). Crop row detection in maize fields inspired on the human visual perception. *The Scientific World Journal, 2012*.

Sarri, D., Lisci, R., Rimediotti, M., & Vieri, M. (2014). RHEA airblast sprayer: calibration indexes of the airjet vector related to canopy and foliage characteristics. In *Proceedings of the 2nd international conference on robotics and associated high-technologies and equipment for agriculture and forestry (RHEA-2014), Madrid, Spain, May 21–23, pp. 73–84*.

Steinsiek, J. W., Oliver, L. R., & Collins, F. C. (1982). Allelopathic potential of wheat (*Triticum aestivum*) straw on selected weed species. *Weed Science*, 495–497.

Torres-Sanchez, J., López-Granados, F., de Castro, A., & Peña, J. M. (2014). Multitemporal weed mapping using UAV imagery for early site-specific control: the case of wheat as a narrow row crop. In *Second international conference on robotics and associated high-technologies and equipment for agriculture and forestry. Presented at the new trends in mobile robotics, perception and*

actuation for agriculture and forestry, PGM, Madrid, Spain, pp. 269–278.

Vougioukas, S. G. (2012). A distributed control framework for motion coordination of teams of autonomous agricultural vehicles. *Biosystems Engineering, 113*, 284–297.

Wisserodt, E., Grimm, J., Kemper, M., Kielhorn, A., Kleine-Hartlage, H., Nardmann, et al. (1999). Gesteuerte Hacke zur Beikrautregulierung innerhalb der Reihe von. Pflanzenkulturen [Controlled Hoe for Weeding within Crop Rows]. In *Tagung Landtechnik 1999/VDI-MEG* (pp. 155–160). Düsseldorf, Germany: VDI-Verlag.

7 PUBLICACIÓN IV:

Integrating sensory/actuation systems in agricultural vehicles

L. Emmi, M. Gonzalez-de-Soto, G. Pajares, and P. Gonzalez-de-Santos

Sensors, ISSN 1424-8220, vol. 14, no. 3, pp. 4014–4049, 2014.

DOI: *http://dx.doi.org/10.3390/s140304014*

Impact Factor (2014): 2.245

Category: Instruments & Instrumentation: 10/56 (Q1)

Category: Chemistry, Analytical: 31/71 (Q2)

Category: Electrochemistry: 14/28 (Q2)

NOTA: La investigación llevada a cabo para esta publicación se engloba en un proyecto de ámbito más amplio, parte de cuyos resultados fueron reflejados en el texto de otra tesis doctoral con formato tradicional [11]. Dicha tesis refleja una parte de la investigación enfocada a contribuir en la configuración informática para el control y manejo de flotas de robots en agricultura de precisión, claramente separada del objetivo y los resultados de la investigación reflejados en el presente documento. En cualquier caso, dado que se compartió y se utilizó el mismo material y los experimentos en ambas investigaciones, se podrán encontrar aquí ciertas informaciones (en el texto, las tablas y los resultados) que aparecen también en la tesis doctoral mencionada.

Sensors **2014**, *14*, 4014-4049; doi:10.3390/s140304014

OPEN ACCESS

sensors

ISSN 1424-8220

www.mdpi.com/journal/sensors

Article

Integrating Sensory/Actuation Systems in Agricultural Vehicles

Luis Emmi [1,*], Mariano Gonzalez-de-Soto [1], Gonzalo Pajares [2] and Pablo Gonzalez-de-Santos [1]

[1] Centre for Automation and Robotics (UPM-CSIC), Arganda del Rey, Madrid 28500, Spain; E-Mails: mariano.gonzalez@car.upm-csic.es (M.G.-S.); pablo.gonzalez@car.upm-csic.es (P.G.-S.)

[2] Department of Software Engineering and Artificial Intelligence, Faculty of Informatics, University Complutense of Madrid, Madrid 28040, Spain; E-Mail: pajares@ucm.es

***** Author to whom correspondence should be addressed; E-Mail: luis.emmi@car.upm-csic.es; Tel.: +34-91-871-1900; Fax: +34-91-871-7050.

Received: 7 January 2014; in revised form: 11 February 2014 / Accepted: 13 February 2014 / Published: 26 February 2014

Abstract: In recent years, there have been major advances in the development of new and more powerful perception systems for agriculture, such as computer-vision and global positioning systems. Due to these advances, the automation of agricultural tasks has received an important stimulus, especially in the area of selective weed control where high precision is essential for the proper use of resources and the implementation of more efficient treatments. Such autonomous agricultural systems incorporate and integrate perception systems for acquiring information from the environment, decision-making systems for interpreting and analyzing such information, and actuation systems that are responsible for performing the agricultural operations. These systems consist of different sensors, actuators, and computers that work synchronously in a specific architecture for the intended purpose. The main contribution of this paper is the selection, arrangement, integration, and synchronization of these systems to form a whole autonomous vehicle for agricultural applications. This type of vehicle has attracted growing interest, not only for researchers but also for manufacturers and farmers. The experimental results demonstrate the success and performance of the integrated system in guidance and weed control tasks in a maize field, indicating its utility and efficiency. The whole system is sufficiently flexible for use in other agricultural tasks with little effort and is another important contribution in the field of autonomous agricultural vehicles.

Keywords: agricultural autonomous system; computer-vision; precision agriculture

1. Introduction

Autonomous outdoor navigation of vehicles with integrated sensor and actuation systems was proposed in the 1920s, but it was first realized in the 1980s, when the technology was mature enough to allow for actual tests [1]. Currently, there exists a growing interest in the field with significant progress [2]. NavLab was one of the first and more outstanding vehicles capable of navigating in a real, dynamic environment with the help of machine vision, a range finder and heavy computing power onboard the vehicle [3]. A few years later, some researchers tried to automate agricultural vehicles by using different concepts and techniques. Erbach *et al*. [4] proposed a static system based on radio beacons to triangulate the vehicle's position for steering purposes. A similar system using cameras in the field to track a visual mark on the vehicle was also used to determine the position of the tractor [5]. Although this system was successful, researchers returned to the NavLab philosophy by putting cameras onboard the vehicle. The static vision system evolved toward mobile equipment that was able to identify the environment and use its features for vehicle steering purposes. This technique led several researchers [6,7] to develop controllers for autonomous agricultural tractors to track straight crop rows.

A different approach, based on GPS (Global Positioning System), was proposed by O'Connor *et al*. [8] at around the same time. These authors demonstrated how an autonomous vehicle equipped with a carrier phase GPS with four antennas can provide both position and heading in the field with accuracy high enough to accomplish agricultural tasks. Since then, GPS has been adopted as the typical technique for measuring and controlling a vehicle's position and heading, and it has been included in some commercial systems [9]. Nevertheless, research is still ongoing, and new approaches using GPS for the autonomous guidance of tractors have recently been proposed [10].

Although GPS technology provides good accuracy for guiding agricultural vehicles, machine vision has been shown to be crucial to identify environmental particularities and obstacles; therefore, both techniques started to be merged in the 2000s and became the standard approach for agricultural vehicles [11]. Specifically, camera-based systems have been developed for guidance as the main task [12,13] and for weed and crop discrimination, where guidance was a consequence [14–19]. Guidance and detection tasks require sensors and elements to be conveniently arranged, adjusted, and calibrated onboard the vehicle for accuracy during implementation [20,21].

Apart from the problems of making a vehicle autonomous, an agricultural system needs to be equipped with the proper implements to carry out farming tasks such as tilling, planting seeds, weed control, fertilizing, applying pesticide, mowing, and harvesting. This is a step forward in the automation of agricultural systems, which this article's authors are focused on. There are two basic types of implements depending on whether they are carried or towed by the vehicle. The positioning accuracy of the former type depends on the positioning accuracy of the perception system and the vehicle, and most current developments fall in this topic. The latter depends on the accuracy of the perception system, the positioning accuracy of the vehicle, as well as the positioning accuracy of the implement steering mechanism. Some attempts have been made in positioning this type of system by using two GPS antennas, one located on the vehicle and the other on the implement. For example, Nørremark *et al*. [22] developed an unmanned hoeing system for intra-row weed management based on real-time kinematic (RTK) GPS techniques. The system was composed of an autonomous vehicle

and a side-shifting arrangement fixed to a weed implement. Both the vehicle and implement were equipped with RTK-GPS; thus, the two subsystems provided their own position to allow the vehicle to follow predefined GPS paths and the implement to act on every plant, whose positions were obtained automatically during seeding. Other effective actuation systems (cultivator and sprayer) have also been developed with mechanical control based on the RTK-GPS perception system [23].

One important concern in agriculture is productivity, where agricultural tasks have to be carried out with accuracy, maximum performance, and minimal resources. This situation means that the integration of the aforementioned systems (the vehicle and the implement) must be carried out under an architecture with an effective and reliable design to meet all requirements, specifically the expected real-time performance. Thus, the architecture is a crucial issue, where all subsystems are to be coordinated. Suprem *et al*. [24] highlighted the importance of the effective integration of sensors, computers, and actuators. There has been a great emphasis on the development of the individual elements but not so much on their integration; note that integration is particularly crucial in agricultural vehicles where the ideal situation is to design flexible and open systems for more than one agricultural application, as mentioned by [25], with the aim of making full use of agricultural vehicles for a wide range of agricultural applications. Accordingly, Garc á-P érez *et al*. [26] proposed a hybrid agent-based architecture for agricultural purposes, where perception and actuation tasks are integrated and conveniently coordinated.

Slaughter *et al*. [27] reviewed systems in autonomous robots for agricultural tasks and identified four main subsystems: guidance, weed detection and identification, precision actuation, and mapping. Guidance and weed detection and identification are based on RTK-GPS and imaging sensors. Actuation systems are focused on precise control where weeding is a specific agricultural treatment [28], based on micro-sprays, cutting tools or thermal and electrocution devices. Mapping is the process of applying information obtained at a previous stage to the application; Bak and Jakobsen [29] obtained a map during sowing, which was used during the treatment of weeds. These four subsystems are also described in [2].

On the other hand, Rovira-Mas [30,31] proposed an open architecture for intelligent autonomous vehicles, based on a three-layer (safety, information and machine actuation) structure. The safety layer is responsible for all security aspects concerning the vehicle and the user's integrity. The information layer (perception) is in charge of processing all data supplied by the set of sensors onboard the tractor. Finally, the actuation layer (action and decision making) executes the decisions made according to the intelligent processes. All of these layers are interrelated to fulfill the difficult agricultural requirements. It is clear that, for the progress of agricultural autonomous vehicles, it is necessary to follow an architectural model based on such schemes with the required flexibility and scalability to expand the range of the vehicle's applications while simultaneously achieving adequate robustness and efficiency. Rovira-Mas [30] developed the perception system in depth, emphasizing the sensor deployment under a specific configuration for real-time purposes, as well as analyzing the following four important properties: flexibility, scalability, robustness, and efficiency.

Based on the above considerations, we propose an architecture that integrates the above four subsystems (guidance, weed detection and identification, precision actuation, and mapping) while covering the above-mentioned four properties (flexibility, scalability, robustness, and efficiency). This process is achieved with the proposed scheme displayed in Figure 1. It consists of three main modules:

sensing, acting, and decision making. Sensing is in charge of collecting information from the environment through the set of sensors available (imaging, inertial systems, and GPS). The information must be appropriate for guidance, weed/crop detection and identification, and mapping. Sensors are adapted according to tasks to be carried out, and new sensors could be added when required, such as range finders for safety navigation (flexibility). Depending on the agricultural application, each sensor can be replaced by similar sensors with different specifications (scalability). The harsh environmental conditions must be determined by sensors (robustness). All sensors must be able to provide data to be synchronized for real-time implementation (efficiency). The Decision-Making System is in charge of processing the information through specific procedures and algorithms for guidance, weed detection and identification, and mapping. The hardware/software components are designed with the aim of receiving all available information supplied by the sensors, which can be activated/deactivated conveniently (flexibility, scalability). These components control all data and processes to guarantee that they are received on time (robustness) with the required coherence for real-time applications (efficiency). After this, decisions are made to be transmitted (messages) to the perception and/or actuation systems when required. Control actions are applied either for navigation or on the agricultural implements for specific tasks, such as weeding. Different implements should be possible, and different parts of the implements can be activated or deactivated (flexibility and scalability). Implements must act with the highest precision as possible for site-specific applications (robustness and efficiency). All subsystems are linked with the appropriate communication protocol. The proposed architectural design with the separated functionalities and properties is the main contribution of this paper. The open architecture allows the same robot to be used for different agricultural applications with little effort, one of the main demands of manufacturers and farmers. We have successfully tested this design in maize fields with a high degree of performance.

Figure 1. Architectural design: perception (sensing), actuation, and decision making.

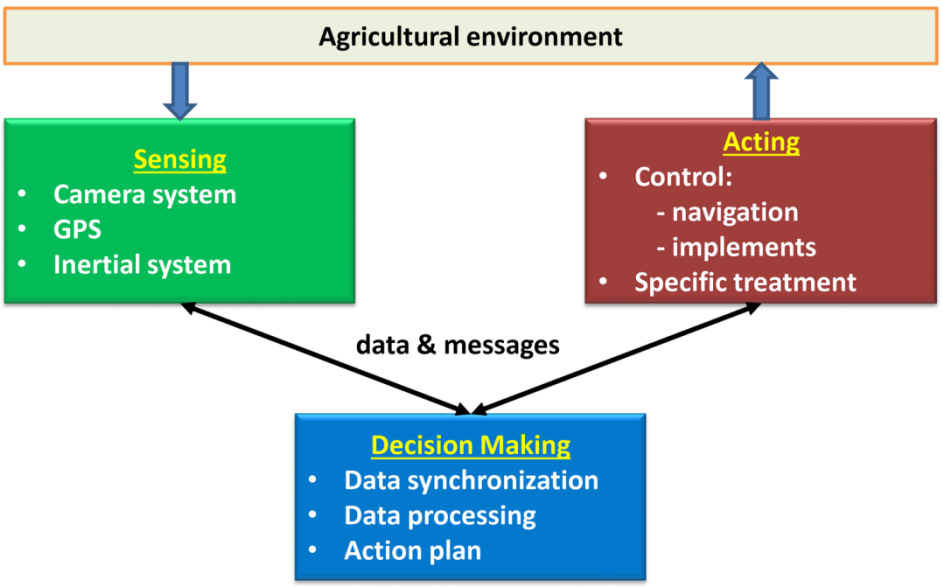

Thus, this paper aims to configure a whole system integrating perception, actuation, and decision making as subsystems for an agricultural autonomous system working on real wide-row crops (see Figure 2). Our proposed architecture is designed for weed control in maize fields [32], but it should be

suitable, using the same vehicle with its architecture, for other agricultural purposes such as cereal treatments or even for seeding.

Figure 2. Perception, decision making, and actuation in an agricultural vehicle.

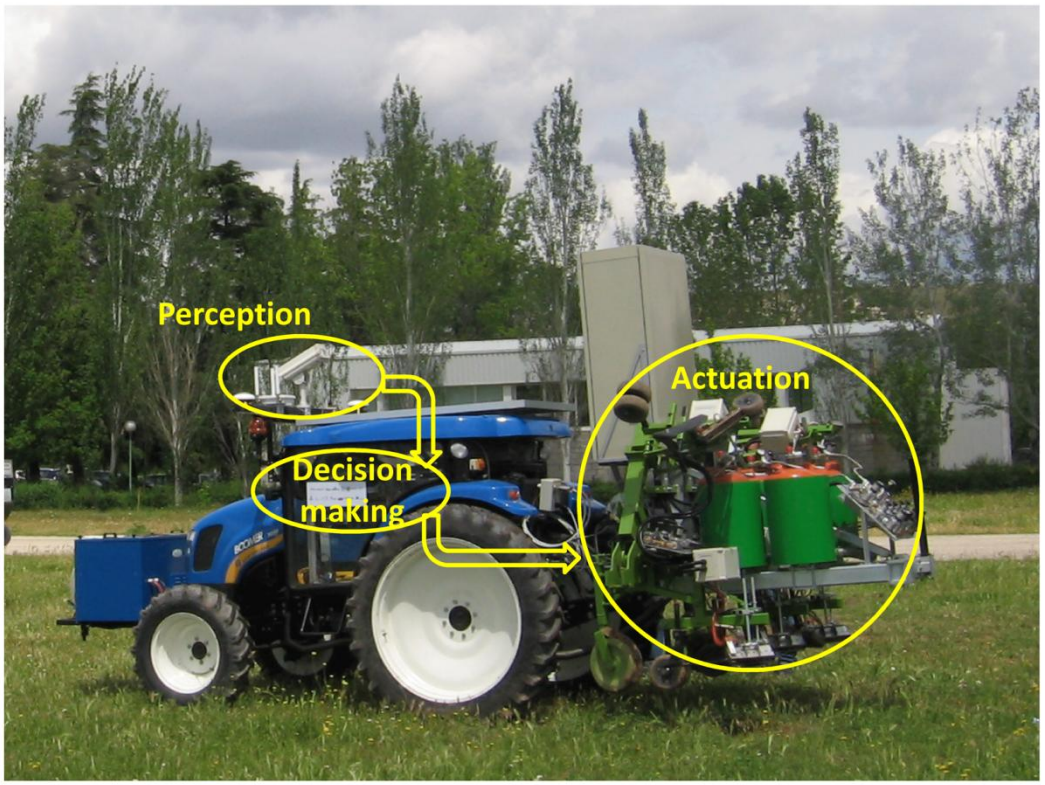

The paper is organized as follows: Section 2 presents the perception system that relies on machine vision. Its main tasks are row identification and weed detection. Section 3 briefly describes the actuation system. Then, the integration of the perception and actuation as well as the decision-making mechanisms are explained in Section 4. Experiments have been conducted in a real maize field with an autonomous vehicle that is a part of the RHEA project (robot fleets for highly effective agriculture and forestry management) in which the subsystems introduced in this article are integrated; Section 5 details those experiments and discusses some results. The conclusions are finally drawn in Section 6.

2. Perception System: Localization and Weed Detection

The perception system is designed for crop/weed identification with two main goals: row following and weed discrimination for site-specific treatment. Crop row detection is the basis for both weed discrimination and guidance and requires the localization and identification of the rows (straight line equations) in the image. This section is devoted to the specification of the perception system, the steps for data processing, and the properties of the system architecture.

2.1. Description of the Perception System

The perception system consists of three main sensors: color camera, Inertial Measurement Unit (IMU), and RTK-GPS (consisting of two antennas: one for XYZ positioning and the other for heading

calculations). Figure 3a displays the main sensors on-board the vehicle based on a commercial tractor chassis. The camera and IMU are embedded into a housing with a fan controlled by a thermostat for cooling purposes, assuming that some agricultural tasks are conducted under high working temperatures, above 50 ℃. The housing is IP65 protected to work in harsh environments (exposure to dust, drops of liquid from sprayers, *etc*.). Additional to the appointed sensors, the perception system also comprises a wireless communication device, to enable the user for remotely controlling and monitoring the entire system. Figure 4 displays the assemblage of these parts.

Figure 3. (**a**) Sensors on-board the tractor; (**b**) Region of Interest (ROI) for the vision system.

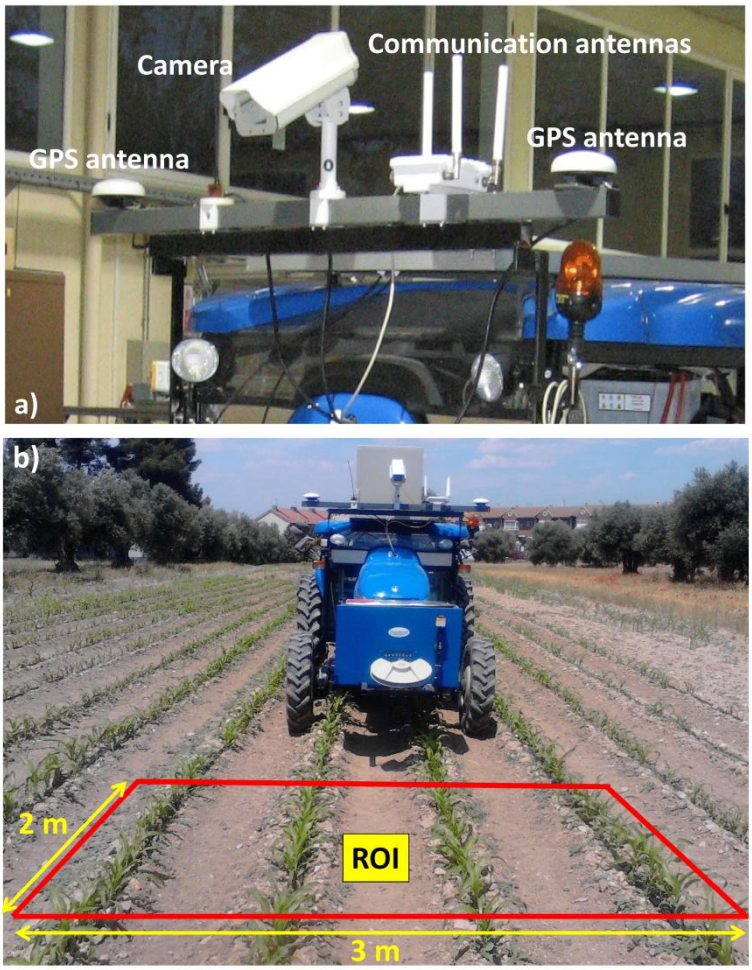

The camera-based sensor is the SVS4050CFLGEA model from SVS-VISTEK [33] and is built with the CCD Kodak KAI 04050M/C sensor with a GR Bayer color filter; its resolution is 2,336 by 1,752 pixels with a 5.5 by 5.5 μm pixel size. This camera is Gigabit Ethernet compliant connected to the Main Controller (see Section 4). The IMU (see Figure 4), of LORD MicroStrain® Sensing Systems (Williston, VT, USA) is a 3DM-GX3®-35 high-performance model miniature Attitude Heading Reference System (AHRS) with GPS [34]. It is connected via RS232 to the Main Controller and provides information about pitch and roll angles. Both the camera and IMU are robust enough and exhibit sufficient capabilities for real-time performance, required for agricultural tasks. The GPS receiver is the Trimble® BX982 GNSS receiver, supporting two antennas for precise heading calculation, mounted on the lateral ends of the vehicle (see Figure 3a). The goal is to apply specific treatments in the Region of

Interest (ROI) in front of the tractor, which is a rectangular area 3 m wide and 2 m long (see Figure 3b). It covers four crop rows in the field. This area starts at 3 m with respect to a virtual vertical axis traversing the center of the image plane in the camera, i.e., where the scene is imaged.

Figure 4. Perception system: sensors and equipment.

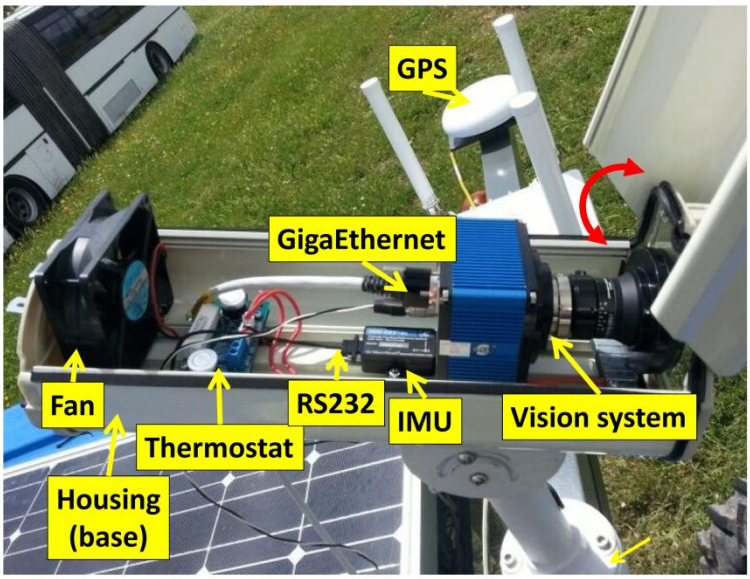

Figure 5. Camera system geometry.

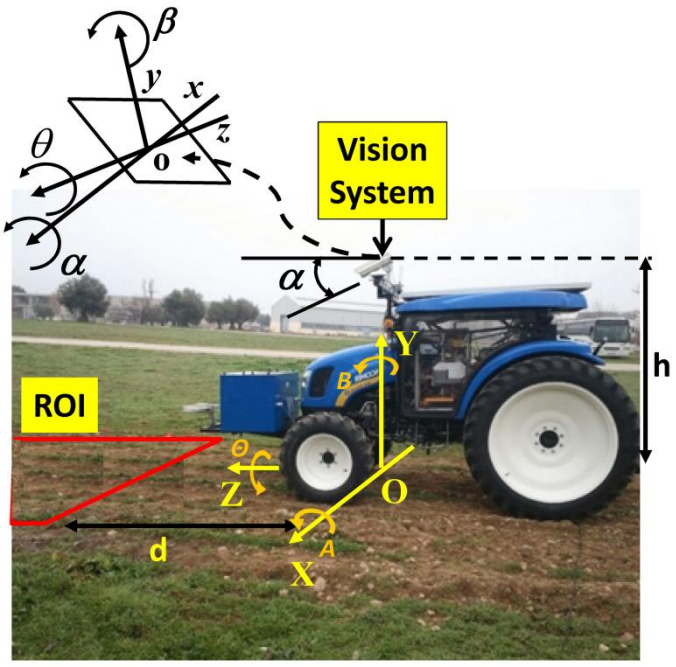

Figure 5, displays the camera system geometry [17]. *OXYZ* is the reference frame located in the ground with its axes oriented as displayed, aligned with the reference axis of the GPS system; h is the height from *O* to the origin *o* of the reference frame *oxyz* attached to the camera; roll (θ), pitch (α), and yaw (β) define the three degrees of freedom of the image plane with respect to the referential system; d is the distance from the beginning of the ROI measured perpendicular to X axis.

2.2. Characteristics of the Perception System

Four properties have been identified as basic requirements for the perception system integrated into the proposed architectural design:

(a) Flexibility/Modularity

The perception system consists of the elements described above with a direct communication link to the Decision-Making System running on the Main Controller. Different sensors can be connected via GigaEthernet and RS232 communication ports, which are standard interfaces. Any sensor can be connected/disconnected without restrictions other than the physical capacity of the Main Controller (see Section 4). The operations of linkage and decoupling can be carried out via software, without affecting the remaining modules or the operability. This procedure allows a multi-sensor arrangement according to the required agricultural tasks. Some crop line detection algorithms do not need the IMU, and when this happens, this sensor is simply ignored and then activated when required. This method avoids important disruptions to the designed systems and at the same time proves the flexibility and modularity of the proposed architecture.

(b) Scalability

Sensors and their corresponding drivers can be added to increase the amount of work according to the demanded agricultural tasks. Again, the unique restriction is the limitation of the number of ports available in the Main Controller, which can be easily expanded. So, we could add a multispectral or thermal camera for plant discrimination or a stereoscopic vision-based system with a GigaEthernet connection for object detection for safety purposes. Different cameras with higher resolutions are accepted when required. Regarding the processing of data provided by the sensors, the Decision-Making System implemented in the Main Controller allows for high-performance processing.

(c) Robustness

The camera-based system is robust enough to support the adverse outdoor agricultural environments with sufficient physical and electronic protections. It is designed to withstand mechanical vibrations from the tractor's engine, soil roughness, extreme temperatures, and high variability in illumination. Additionally, the camera is equipped with an UV/IR filter to cut spectral ultraviolet and infrared radiation, which considerably affects the image quality. The IMU is encapsulated and calibrated to provide stable values.

(d) Real-Time/Performance

The perception system, particularly the camera, is arranged onboard the tractor to cover the region of interest where the specific actuation is to be applied. It is placed closed to the center of gravity to minimize vibrations and undesired mechanical effects. The image acquisition is controlled through the exposure time, again with the aim of achieving high quality images. The data processing for crop/weed detection and guidance is designed under specific modules, programmed as dynamic-link libraries (DLL) in C++, and embedded in the Main Controller. The modules are optimized to work in real-time for the proposed specific treatment.

2.3. Process: Integration of Information

The vehicle is programmed to follow a pre-defined plan or general mission (see Figure 6). The mission consists of a set of waypoints that are established based on GPS coordinates, which define the beginning (starting points) and end positions (target points) for crossing the field. For this particular case, the information from the mission contains some uncertainty, so that the start and end points may not match the corresponding crop line's center. This requires the use of the crop row detection system to correct this uncertainty presented in the general mission.

Figure 6. Example of path planning in the maize field.

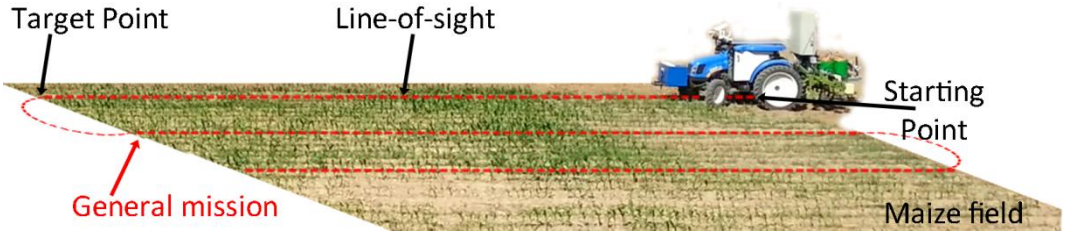

In addition to the crop row detection, the perception system delivers information on the weed infestation in the field, allowing the computation of the percentage of weed presence inside the ROI. To do this, the ROI is divided into rectangular sections 0.375 m wide (corresponding to split in two the inter-row space, with the objective to identify the infestation on each side of the crop row) and 0.25 m long (which corresponds to the minimum resolution for the execution of the treatment). The size of these sections is adjusted based on the characteristics of the actuation system that performs the treatment (see Section 3.1). The procedure is as follows:

(1) The operation speed set for this type of treatment is defined as 0.83 m/s (3 km/h).
(2) The pre-defined plan determines the traversal order of the waypoints to be visited, including starting and target points.
(3) Between two waypoints inside the field, the vehicle follows the line-of-sight.
(4) The camera captures images at frame rates up to ten images per second.
(5) The system reads the GPS coordinates at a rate of 10 Hz and captures an image whenever the vehicle moves within 2 m on the field, which is the length of the ROI.
(6) The camera vision system processes each image to identify four crop lines. The IMU provides information about extrinsic camera parameters, pitch (α) and roll (θ), so that, together with the remaining extrinsic and intrinsic parameters, four expected crop lines are identified. The expected crop lines serve as guidelines to determine the real crop lines [17].
(7) Based on the relative positioning of the two central crop lines identified with respect to the center of the image, if deviations occur between the detected crop lines and the line-of-sight, the lateral deviation and heading are corrected to align the tractor with the real crop lines in the field.
(8) The detected crop lines are used to determine the weed coverage inside the ROI, based on the green densities around the crop lines and between adjacent crop lines [19].

Georeferencing Images

Because the raw image received from the camera is transmitted by Ethernet (non-deterministic procedure), the image analysis process consumes a specific amount of time and the actuation point (implement elements that perform the treatment) is located several meters behind the ROI, an element for synchronization and georeferencing is needed to maintain a real-time performance and high-accuracy treatment. To accomplish this synchronization, each image captured is associated with a GPS position, and a map for weed coverage is created that is referenced to GPS coordinates.

3. Sensing/Actuating in Crops

Actuation in crops, which is the primary objective in agriculture, is normally performed by implements or devices towed/pulled by tractors that provide energy and motion. Implements are tools composed of simple sensors to obtain the status of the crop and simple actuators to perform simple actuation such as opening/closing valves, moving prismatic cylinders, *etc*. Most of these sensors/ actuators are controlled by using PLCs or similar devices. If sophisticated sensor systems such as a machine vision system or range finders are required, they are provided as external devices as indicated in Section 2.

3.1. Description of the Actuation System

Although the proposed system can be applied to a large number of implements, we will specify the system for a particular mechanical-thermal machine [32], which is devoted to weed control (see Figure 7a) in flame-resistant crops such as maize, onion, and garlic. This implement is pulled by the autonomous tractor, and the Main Controller is in charge of decision making and synchronizing the activation of the treatment as well as managing the lateral position of the implement with respect to the vehicle's position.

Figure 7. (**a**) Mechanical-thermal machine; (**b**) Implement steering actuator (implement front view); (**c**) Main frame (implement rear view).

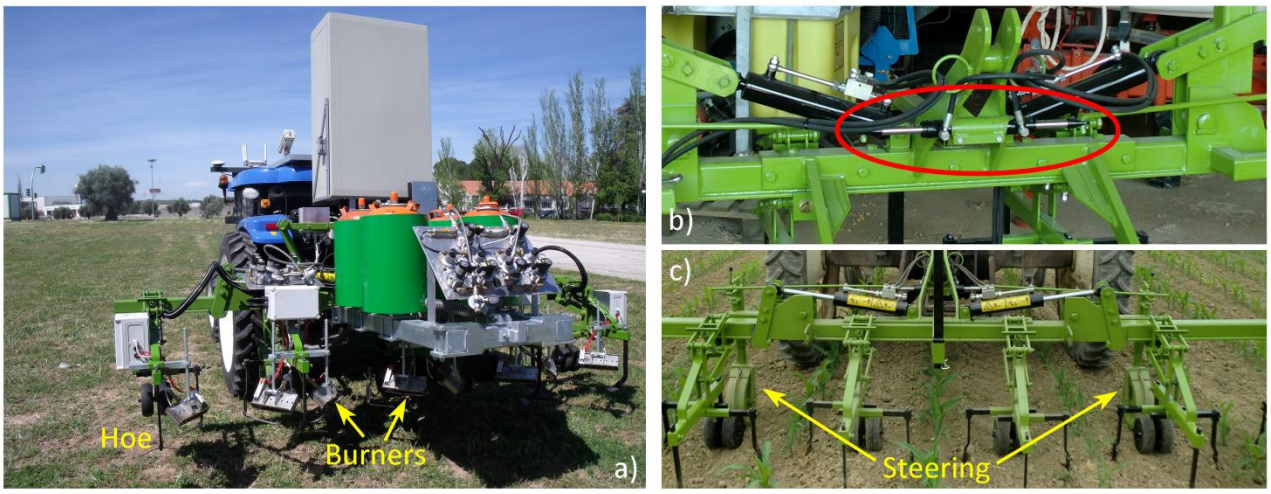

This specific implement consists of four couples of burners, about 0.25 m long, attached to a main frame (see Figure 7a) to address four successive crop rows. The objective of the burners is to perform selective treatment in the intra-row space. The treatment in the inter-row space is achieved by mechanical actuation, i.e., specialized hoes (see Figure 7a). Every burner's flame intensity depends on the weed coverage identified by the weed detection system presented in Section 2 [35]. The control of the ignition of the burners is performed by the Actuation Controller, which receives the action messages from the Main Controller.

Given that the implement contains two different elements to perform weed control, and given the possible risk of crop damage, an adequate degree of accuracy in positioning the burners and mechanical elements is needed. This step is performed by a guidance system, which is in charge of executing small adjustments in the lateral position of the implement with respect to the vehicle. This lateral positioning system consists of a linear actuator (central double rod hydraulic cylinder, see Figure 7b) that modifies the angle of the steering wheels, allowing the operative machine to move laterally with respect to the vehicle (see Figure 7c). This cylinder features a displacement of ±0.031 m, exerts a force of 2,000 N, and is powered by the hydraulic system of the vehicle. The lateral control of the implement is performed directly by the Main Controller through the controller area network (CAN) bus communication system onboard the autonomous vehicle.

Figure 8. Lateral-position sensor setup. (**a**) Assembly diagram of the sensory system between the implement and the vehicle; (**b**) Structure of the sensory system; (**c**) Photo of actual sensory system.

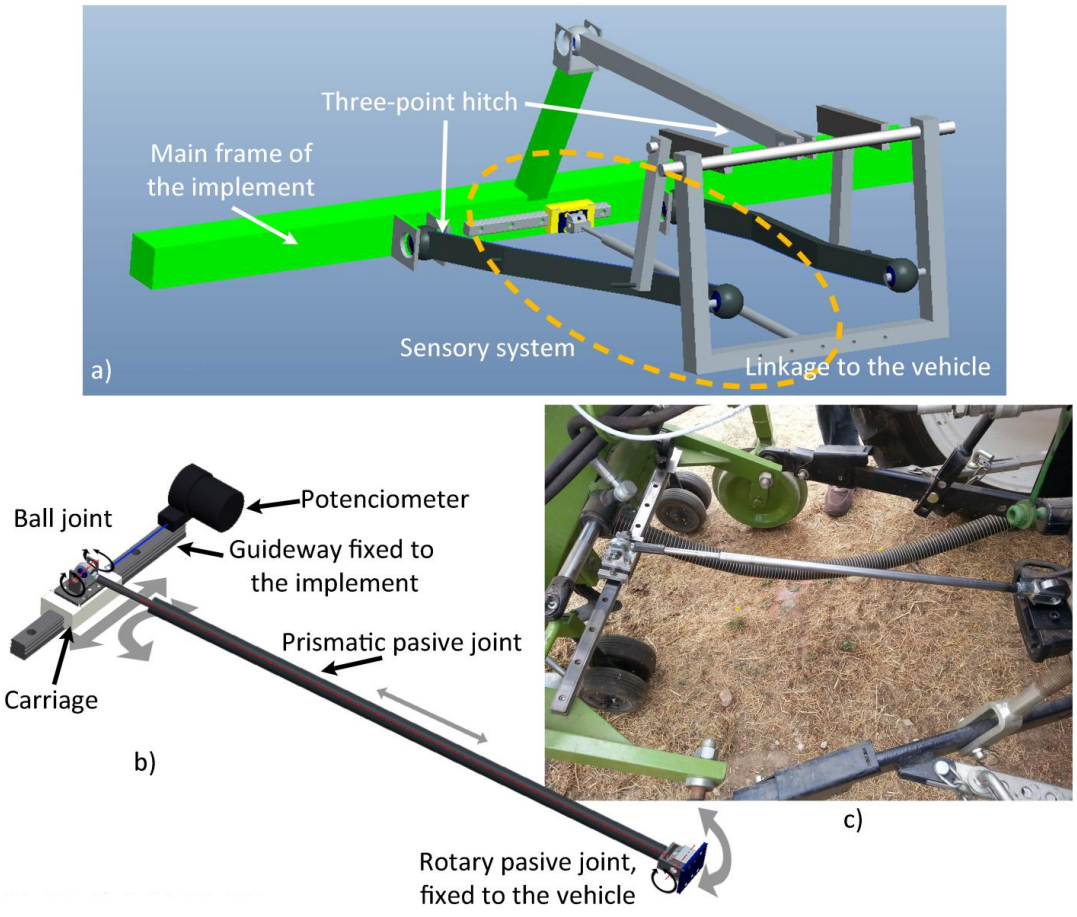

3.1.1. Lateral-Position Sensor

The positioning device for measuring the lateral displacement of the implement with respect to the vehicle is composed of a passive mechanism and a positioning sensor. The passive mechanism relies on a telescopic arm that joins the vehicle's rear to the implement main frame (see Figure 8b). The end of the arm is fixed to the vehicle through a passive rotary joint, with the rotation axis perpendicular to the arm. The other end is fixed to a carriage through a ball joint. The carriage can slide over a linear guide. A cable-pull potentiometer (JX-PA-20-N14-13S-125) is fixed to the carriage so that the sensor can measure the displacement of the implement. Thus, the positioning device measures the relative displacement of the implement with respect to the vehicle in a direction perpendicular to the vehicle's longitudinal axis. Figure 8b shows the basic scheme of the sensory system, and Figure 8a,c illustrate how it is placed between the implement and the vehicle. In addition to the lateral-position sensor for measuring the displacement of the implement with respect to the vehicle, an encoder (JX-EP-20-N14-110-25C) was placed in the hydraulic cylinder that modifies the angle of the steering wheels for more precise control of the implement guidance.

3.1.2. Measuring the Implement Lateral Position with Respect to the Vehicle

Based on the three-point hitch geometric model and the sensory system setup, it is possible to relate the potentiometer measurements with the actual lateral displacement of the implement. Figure 9 shows a schematic model of the three-point hitch for connecting the implement, where Δd is the difference in the potentiometer measurement and ΔX is the real implement displacement with respect to the center of the vehicle. Based on the geometric model of the three-point hitch, Equation (1) and Equation (2) represent the positions of the points *Pl* and *Pr* with respect to the central reference axis *h* (see Figure 9). Equation (3) represents the position of the point *Pr* as a function of θ (see Figure 9), which represents the excursion angle of the three-point hitch left arm. Equation (4) represents the implement center axis *i*, as a function of *Pr* and *Pl*. Given the geometric model of the link between the three-point hitch and the implement and knowing the dimensions of the arms and the range of θ (see Figure 9), it can be calculated that, in the case of implement maximum excursion, the real displacement ΔX, described in Equation (5) is 0.17% greater than the measured displacement Δd, described in Equation (7), which is negligible.

$$(X_{Pl} - (Xh - a/2))^2 + (Y_{Pl} - Yh)^2 = L^2 \quad (1)$$

$$(X_{Pr} - (Xh + a/2))^2 + (Y_{Pr} - Yh)^2 = L^2 \quad (2)$$

$$(X_{Pl}, Y_{Pl}) = \left((Xh - a/2) - L \cdot \cos\theta\,, Yh - L \cdot \sin\theta\right) \quad (3)$$

$$(Xi, Yi) = (Pl + Pr)/2 \quad (4)$$

$$\Delta \mathrm{X} = Xh - Xi \quad (5)$$

$$\Delta Y = (Yh - \left(\sqrt{1 - D^2}\right) \cdot L - Yi \quad (6)$$

$$\Delta \mathrm{d} = \sqrt{\Delta \mathrm{X}^2 + \Delta \mathrm{Y}^2} \quad (7)$$

Figure 9. Schematic model of the three-point hitch for connecting the implement.

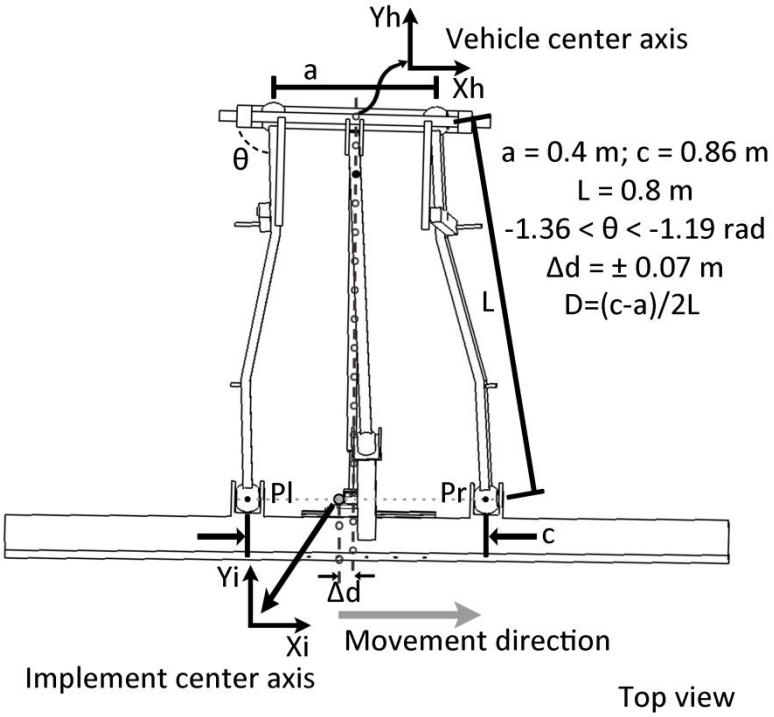

3.2. Characteristics of the Actuation System

Following the properties described for the perception system in Section 2, the actuation system exhibits the following characteristics:

(a) Flexibility/modularity

The actuation system consists of a main frame and simple actuators that apply a given process to the crop. In this sense, the main frame and the related positioning systems can be used for a large number of crops, and the specific actuators (burners, nozzles, *etc*.) can be easily changed for different crops. As agricultural vehicles normally provide electric and hydraulic power, there are many different types of actuators that can be used in these devices. This makes the actuation system have little dependence on the type of crop to be treated.

(b) Scalability

The number of electrical, hydraulic or pneumatic actuators (relays, prismatic cylinders, *etc*.) that can be connected depends on the number of I/O channels provided by the Main Controller. The specific controller used in this work (see Section 4) allows the designers to use a large number of I/O channels that can be even cascade-connected, which makes the number of I/O ports nearly unlimited. Scalability is thus a minor problem.

(c) Robustness

As the actuation systems consist of a main frame made of steel and a number of commercial actuators that are rugged enough for use in industrial and natural environments, the system exhibits high robustness.

(d) Real-time/Performance

The lateral positioning of the main frame requires a simple PID controller that does not require high computing power, and signals are activated normally through a CAN bus that has few delays. However, hydraulic valves can have a slow response, jeopardizing the control performance. Thus, real-time performance in actuation systems is critical and must be carefully designed.

3.3. Process: Integration of Information

The actuation system consists of two main tasks: (a) controlling the activation/deactivation of the burners and (b) controlling the lateral positioning of the main frame with respect to the vehicle. The first piece of information comes directly from the vision system (camera-based sensor and processing), which informs the exact points where the treatment must be applied based on a weed coverage matrix. The second piece of information comes from the location system (GPS), which indicates the position in which the implement must be a few seconds later, depending on the vehicle's speed, position with respect to the crop lines, and the variations of the heading.

4. Perception-Actuation Integration and Decision Making

The perception system is connected and integrated under the Decision-Making System that runs in the Main Controller. Moreover, a part of the actuation system, which is in charge of the implement lateral control, is also integrated under the Decision-Making System. The Decision-Making System is primarily responsible for synchronizing the information coming from the different sensors, to associate the same reference system for each piece of information. Thus, the relationship between what is perceived and where and when the actuation is needed is created.

Other important tasks of the Decision-Making System are as follows: (a) the interpretation of the information; (b) the evaluation of its reliability; (c) the creation of an action plan to be executed by the actuation system; and (d) the supervision of the development of the general mission. Figure 1 displays a schematic of the conceptual architecture followed by the interaction between the perception system, the Decision-Making System, and the actuation system.

4.1. Description of the Decision-Making System

The Decision-Making System is in charge of collecting the information provided by the sensors about the environment, producing the actuation plan, and monitoring the execution of the various tasks that make up the general mission. The information must be synchronized, processed, interpreted, and arranged for decision making for the controllers and actuators with the purpose of actuations over agricultural fields. This system is also in charge of sending messages to the sensors and actuators to demand specific behaviors on the corresponding devices. All of these processes run within the Main Controller, which consists of a CompactRIO-9082, with a 1.33 GHz dual-core Intel Core i7 processor, including an LX150 FPGA with a Real-Time Operating System. LabVIEW Real-Time [36] from National Instruments, release 2011, is used as the development environment.

Making Decisions Based on the Reliability of the Information of the Perception System.

Although the commercial devices in the perception system are very trustworthy, some disturbances may occur from the interaction with the environment that can affect the quality of the acquired information. Some of these disturbances include a decrease in the GPS precision or the loss of a message, as well as disturbances in the image due to reflections or lighting changes. Such disturbances can be detected in real time, and based on the degree of influence of the disturbance, an estimation of the reliability of such information can be made.

The failure, loss or alteration of information directly affects the precision with which the treatment is performed at that instant in time, given that in this type of application, the vehicle is in motion and the treatment is being fulfilled based on that movement. For example, in the case of low reliability in the generation of a weed cover map in a small section of the mission, it is better to apply the treatment with the worst-case scenario rather than returning to that specific area.

4.2. Characteristics of the Decision-Making System

Based on the above considerations, this paper proposes a design that meets the above requirements under LabVIEW [36], where the four properties identified as appropriate for architectural design in agricultural robots can be summarized as follows:

(a) Flexibility/modularity

The Decision-Making System receives/sends data from/to the perception and actuation systems when required. They are directly connected to the corresponding devices, and these data are mapped as variables in LabVIEW. All processing and control modules are written as subVIs (functions) that are linked together. The image processing module is a DLL developed in C++ and is also written as a subVI. This means that all modules can be easily replaced, added or removed according to the specific needs of each agricultural application.

(b) Scalability

The architectural design achieves a high level of scalability because the system can grow simply by adding new functionalities embedded as new modules and connected with internal links.

(c) Robustness

cRIO supports a high range of working temperatures (0 ℃ to +55 ℃), with ingress protection IP20 and operational humidity up to 90%. This computer supports operational sinusoidal vibrations up to 500 Hz at 5 G. The system has been tested in real, harsh agricultural conditions and can accomplish real tasks with extraordinary robustness. LabVIEW has also been tested successfully in different robotics systems including autonomous agricultural robots. Part of this feature is achieved by suppressing the external links of communication between the different modules in charge of the different devices. Only local protocols are required to arrange ordered data coming from the different systems.

(d) Real-time/Performance

LabVIEW is specifically designed for running under a real-time operating system. It allows remote communications via Wi-Fi, where limits are established by the Wi-Fi network and not by LabVIEW. This program is suitable for communications with a base station.

4.3. Process: Integration of Information

The Decision-Making System is in charge of three main tasks: (a) perception and actuation synchronization; (b) trajectory planning; and (c) weed coverage map interpretation.

The Decision-Making System knows the general mission to be performed, and based on that assignment, the plan that meets the most optimal execution (shortest distance) is fulfilled. This planning consists of sub-paths where the vehicle follows straight or curved lines, linking a starting and a final point. The RTK-GPS is the main sensory system to close the control loop for path following and is corrected when necessary by the camera-based system. The Decision-Making System sends the planned sub-path to the actuation system, which is in charge of the path following.

Along each sub-path, the Decision-Making System commands the perception system to acquire images in coordination with the navigation speed. Each order is triggered every two meters in front of the tractor along each sub-path. This measurement is fixed by the length of the ROI, and the exact positions are provided by the GPS. Full area coverage should be guaranteed to avoid gaps and uncovered areas.

5. Results

Various experiments have been conducted to assess the performance of the proposed architecture. The experiments have been carried out in the experimental fields at the CSIC-CAR facilities in Arganda del Rey, Madrid, Spain, on different dates, during May/June/July and October 2013, and additional calibration tests were carried out in December 2013. We have tested our whole system in two different maize fields with sizes of 15 m by 60 m and 18 m by 48 m, i.e., with sufficient lengths to travel along different paths. During the first phase, both the perception and actuation systems were verified separately, and during the second phase, the systems were checked together under the supervision of the Decision-Making System.

5.1. Perception System Assessment Tests

As mentioned previously, the operation speed defined for this application was 0.83 m/s (3 km/h) and the ROI was defined to be 3 m wide and 2 m long. These parameters mean that every 2.4 s, the perception system must be able to provide all required data processed and ordered, i.e., with correct synchronization between them. We have analyzed more than 5,000 images with the corresponding GPS and IMU data. A first set of tests was carried out to verify that the data acquisition was synchronized and on time. A second set of tests was intended to verify the accuracy of guidance and weed detection.

5.1.1. Execution Time Tests: Data Acquisition and Processing

Table 1 displays the average time spent in the process of image acquisition and interpretation, beginning with image capture and transmission to the availability of data by the decision-making algorithms. The camera sensor time is split into two parts. The first part is the image acquisition time, which includes the exposure time required to excite the sensor and the time for image transmission to the Main Controller until it is available for the Decision-Making System. The second part is the image processing averaged time, where the computational time differs depending on the density of greenness (crop/weeds) existing in each image.

Table 1. Averaged times required by the perception system until data are available for control and actuation.

	Camera Sensor			GPS	IMU	Synchronization (Next Treatment Segment)
	Image Acquisition	Image Processing	Perception (Sub-Total)	Acquisition	Acquisition	
Average Time (ms)	50	250–300	300–350	1	1	2.4 s
Refresh Rate (Hz)	10	3.3	2	10	50	-

From the results in Table 1, we can see that the time spent for the perception system (subtotal column) is below the required 2.4 s. Moreover, we have time enough to increase the tractor's speed when required and depending on the specific agricultural task. Minimum frequencies are defined for refreshing data, although normally, the information of the processed image is available when the vehicle travels the operation area segment.

5.1.2. Synchronization Tests: Georeferencing an Image

After confirmation of the ability by the Main Controller to complete the treatment throughout the work area within the time requirements without losing information, the next element to be evaluated is the accuracy of the information obtained by the perception system related to positions on the field, based on the vision system setup in Figure 5. Given the situation presented in Section 2.3.1, the synchronization of one acquired image with respect to a GPS position is not a trivial task and introduces an error associated with the non-deterministic transmission process. The simplest solution is to store the last GPS position available just before sending the command to the camera to acquire an image. This creates an uncertainty regarding whether the acquired image corresponds to the stored GPS position or to a subsequent position, taking into account the age of the stored GPS data, among other factors. A set of tests was carried out following this synchronization approach, where we can draw two interpretations: one related to the error associated with georeferencing the weed coverage matrix (longitudinal error), and another interpretation of the error related to the deviation between the detected crop lines and the line-of-sight supplied by the perception system (lateral error).

(a) Computing the Longitudinal Error: Weed Coverage Matrix Georeferencing

Given the vision system setup described in Figure 5, the image acquired was calibrated to associate a point (pixel) in the image as a displacement (in meters) with respect to the reference frame *OXYZ* presented in Section 2.1, shown in Equation (8):

$$l(y) = 4.539\,E^{-6} \cdot y^2 - 0.0136 \cdot y + 6.822 \quad (8)$$

This equation is only valid for pixels with the *y* coordinate aligned at the center of the image and within ±1 m from the start of the ROI presented in Figure 5. This calibration has an associated error of ±0.02 m, due to human inaccuracy when selecting the correct pixel and vehicle vibrations transmitted to the frame onto which the camera is fixed.

Using the vision system characterization, a set of tests was conducted where a series of marks were drawn in a plane soil (see Figure 10) 1 m apart from each other and the vehicle followed a straight line over the marks (approximately 12 m at 0.83 m/s) and acquired images at a rate of 10 fps. Subsequently, the images where the marks were within the valid area were selected and compared with the real location of each mark. The mean square error between the theoretical position of each mark and the estimated position was 0.08 m. This result coincides with the distance between two consecutive GPS positions (at working speed). Taking into account that no synchronization element was implemented except for the matching of the frequency for the GPS and image acquisition, this experimental result validates the assumption that the acquired image must be within ±0.08 m of its associated GPS position in the longitudinal axis.

Figure 10. The test conducted for computing the longitudinal error of the vision system. Image acquired and diverse zooms. (**a**) Original image; (**b**) 200% zoom; 1 m apart between marks; (**c**) 800% zoom; mark location: pixel(y) = 1,103.

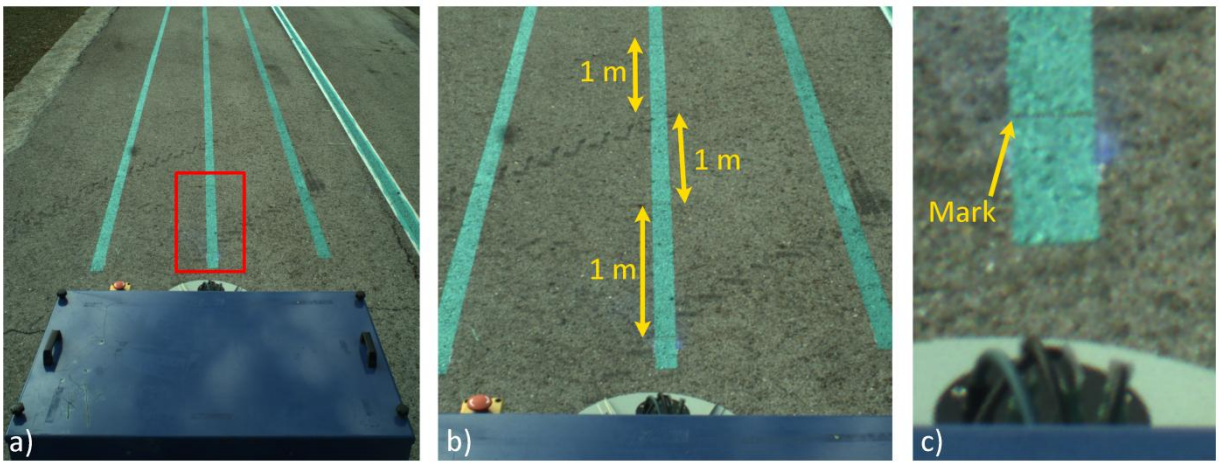

(b) Computing the Lateral Error: Row Crop Line Detection

Regarding the error associated with the measure of the lateral displacement of the line-of-sight related to the crop lines detected by the perception system, this error is directly related to changes in the heading of the vehicle in the instant in time when the image is acquired. This heading variation is due to the process of image georeferencing, which entails a translation of the GPS position acquired in that instant in time (corresponding to the position of the CCD sensor, see Figure 5) to the beginning of

the ROI. To estimate the associated error, a set of tests was conducted where the vehicle crossed the maize field several times, and using the information generated by the perception system, small adjustments for row following were executed (which generated changes in the heading). Figure 11 illustrates one of the recording changes in the heading of the vehicle, and Table 2 shows the results of all sets. Equation (9) defines the variations in the lateral deviation of the line-of-site based on the variations of the heading:

$$\Delta d = \sin(\Delta \varphi) \cdot L \tag{9}$$

where L is the distance between the beginning of the ROI and the main coordinate system of the vehicle (which corresponds to the rear axle) and has an associated error of ±0.08 m from the georeferencing procedure.

Figure 11. Example of heading variations with respect to the theoretical value when the vehicle is crossing the maize field.

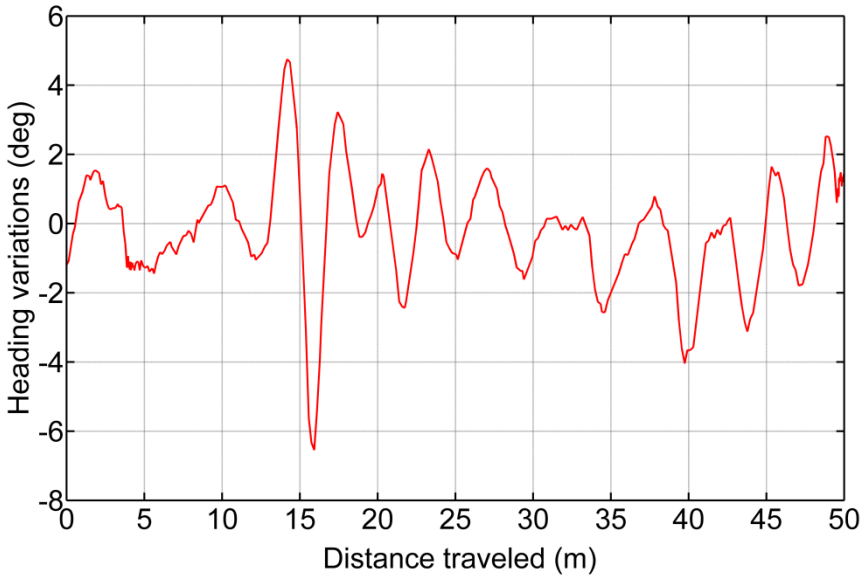

Table 2. Standard deviations of the variations of the heading and the error associated with the calculation of the lateral displacement of the line-of-sight related to the crop lines detected by the perception system.

	Standard Deviation of the Variation of the Heading *Δφ* (deg)	**Error associated with the Measurement of the Lateral Deviation *Δd*, (m)**
Set 1	0.36	0.03
Set 2	0.26	0.03
Set 3	0.24	0.02
Set 4	0.32	0.03
Set 5	0,18	0.012
Total	0.27	0.03

5.1.3. Image Processing Tests

(a) Correcting the Vehicle Trajectory with Row Detection

Crop line detection is a crucial task for guidance and weed detection. The first test consists of the analysis of the correct line detection and the tractor's trajectory correction when required. We have randomly selected 400 images acquired during the May/June and October 2013 tests at the CSIC-CAR facilities in Arganda del Rey (Madrid, Spain). The images were acquired over several days under different illumination conditions, i.e., cloudy, sunny days, and days with high light variability. Each processed image is associated with the GPS and IMU data as well as the corrected value for guidance. Given the crop lines, we chose the two central crop lines and determined the correction by computing the deviation of the central line with respect to an imaginary vertical line that divides the image into two equal halves. This deviation was computed in pixels and transformed to a distance based on image calibration [17].

Figure 12a,b display a sequence of two images acquired during the execution of a straight trajectory following a planned path. Figure 13a,b display the corresponding processed images with the crop lines detected in the ROI. As previously mentioned, the crop lines also serve as local corrections when path planning deviations occur. The tractor in Figure 13a undergoes a slight deviation from the planned trajectory. Indeed, we can see that the upper right corner in the box, belonging to the tractor, is very close to the rightmost crop row and that this box is misaligned with respect to the four crop lines detected in the image displayed in Figure 13a. This misalignment is corrected and can be observed in the subsequent image (see Figure 13b), where the box is better centered relative to the crop lines. This correction is carried out without delays as expected under the proposed architecture. The situation displayed in the above images was normal in our experiments because the tractor navigates on rough agricultural fields with some irregularities.

Figure 12. Consecutive original images acquired by the perception system. (**a**) Deviations of the tractor with respect to the crop lines; (**b**) Correction of this deviation.

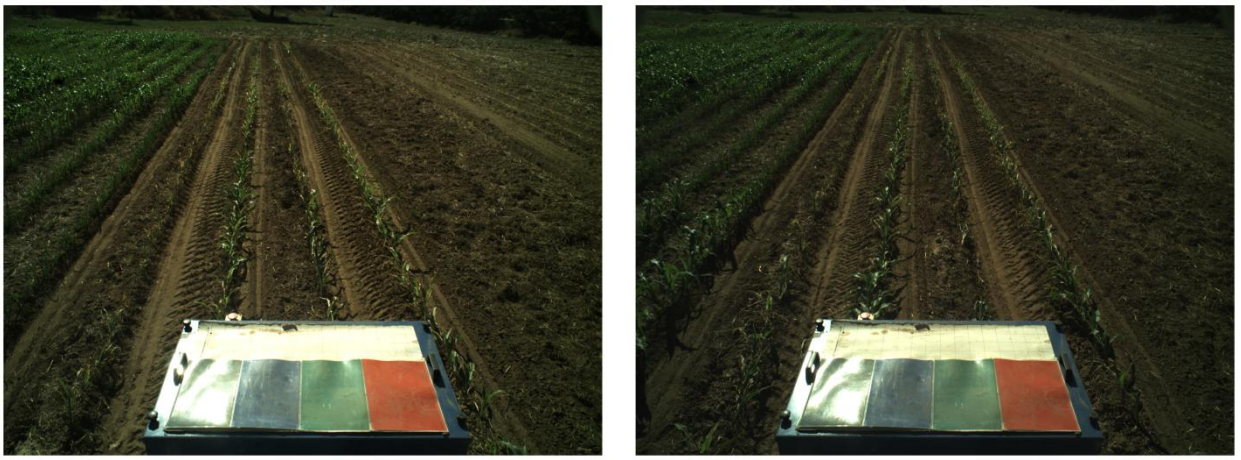

a) b)

Figure 13. Processed images with the detected crop lines corresponding to images in (**a**) and (**b**) in Figure 12 respectively.

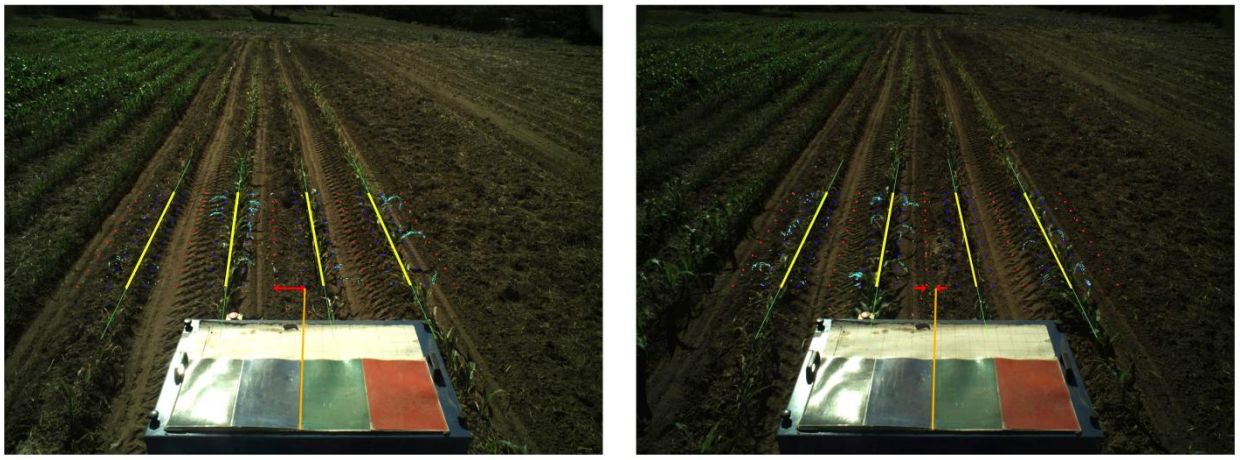

From the set of the 400 selected images, we have verified the corrections ordered by the vision system, assuming that corrections below 0.03 m are ignored and that the path following continues with the GPS. After each correction, we verified that the tractor in the next image in the sequence is conveniently positioned. We have verified that on average, a correction has been demanded for 30% of the images (120 images). From these, we have verified that the tractor was correctly positioned on 89% of the subsequent images. For the remaining images, the correction was erroneously demanded. In this case, the path following based on GPS assumed full responsibility of the guidance.

In Figure 14, the comparison between the use of the information provided by the row detection system and using only GPS for crossing the maize field is illustrated, where it is noteworthy that the row detection system slightly improves the row following, taking into account that the theoretical path to be followed using only the GPS system corresponds to the center of the row by which the two results are compared. It is worth noting that the crop rows at the end of the experimental field were slightly damaged (the last 10 m), due to the large number of tests performed, and in this area, the vision system for row detection produced a large number of errors.

Figure 14. Comparison of the vehicle guidance in a maize field, represented as the lateral error of the rear axle with respect to the theoretical center of the rows.

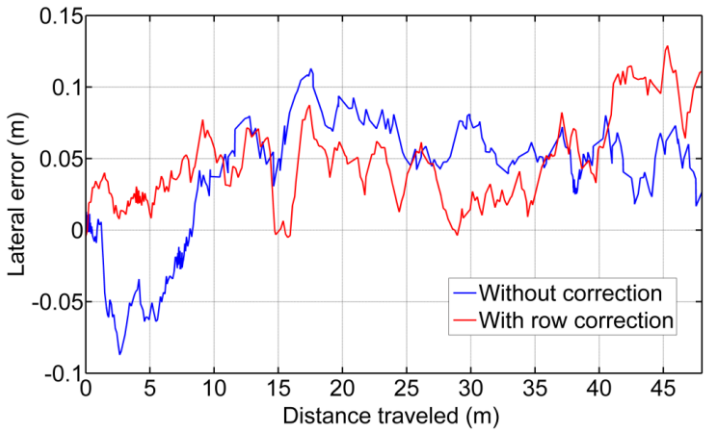

Figure 15. Consecutive images along a sub-path with the detected crop lines (yellow); parallel lines to the left and right crop lines (red); horizontal lines covering 0.25 m in the field.

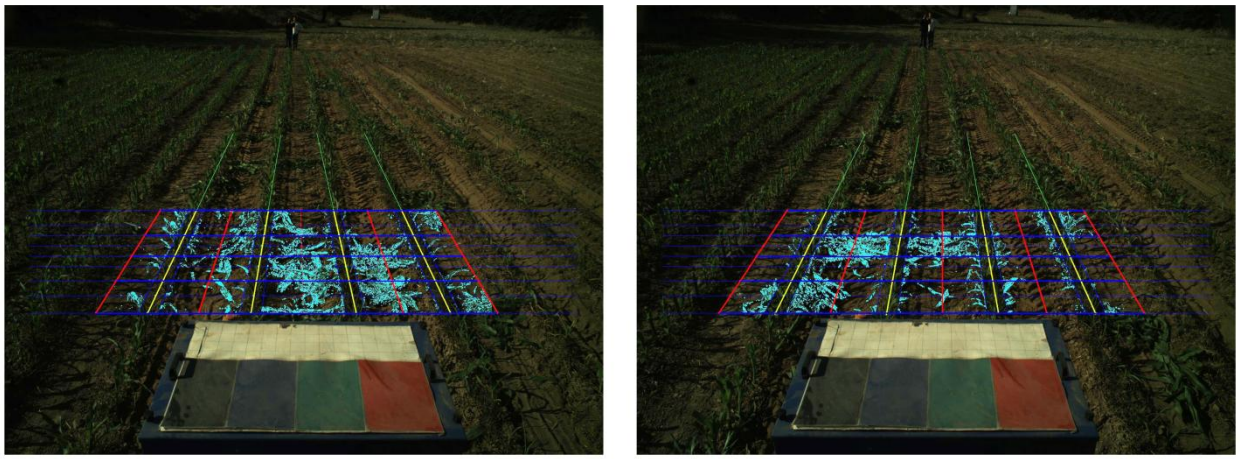

a) b)

(b) Weed Detection

For each image, we also compute and store a density matrix of weeds associated with the image. This matrix contains low, medium, and high density values. It is assumed the camera is calibrated and arranged conveniently considering intrinsic and extrinsic parameters [17]. Figure 15 illustrates two consecutive images along a sub-path. They contain three types of lines defining the cells required for computing the density matrix as follows:

(1) Once the crop lines are identified, they are confined to the ROI in the image (yellow lines), which covers fixed positions in the image.
(2) To the left and right of each crop line, parallel lines are drawn (red). They divide the inter-crop space into two parts.
(3) Horizontal lines (in blue) are spaced conveniently in pixels so that each line corresponds to a distance of 0.25 m from the base line of the spatial ROI in the scene.
(4) The above lines define 8 × 8 trapezoidal cells, each trapezoid with its corresponding area *Aij* in pixels. For each cell, we compute the number of pixels identified as green pixels, *Gij*, (drawn as cyan pixels in the image). We exclude the pixels close to the crop lines with a margin of tolerance, which represents 10% of the width of the cell along horizontal displacements. This is because this margin contains mainly crop plants but not weeds. The weed coverage for each cell is finally computed as $d_{ij} = A_{ij}/G_{ij}$. The different d_{ij} values compose the elements of the density matrix.

From a set of 200 images, we have classified the coverage with three levels (Low, $dij \leq 33\%$, Medium, $33\% < dij \leq 66\%$, and High, $dij > 66\%$). These percentages are checked against the criterion of an expert, who determines the correct classification. We have obtained a 91% success rate.

5.2. Sensing/Actuation System Test

To measure and validate the accuracy of the sensory system, several tests were performed with the following results:

5.2.1. Computing the Error Associated with the Sensory System in Measuring the Lateral Displacement of the Implement with Respect to the Vehicle

(a) Static Tests: Accuracy of the Acquisition Module

This trial consisted of acquiring static position measurements from the potentiometer when the implement was placed and anchored at three different displacements with respect to the vehicle. Figure 16 illustrates these three positions as three sets of data. In Set 1 the implement was placed almost in the maximum displacement to the right; in Set 2 the implement was placed almost in the maximum displacement to the left; and, in Set 3 the implement was placed almost aligned with the longitudinal axis of the tractor. This test confirms the proper operation of both the potentiometer and carriage displacement systems and states that the potentiometer measurements have a mean absolute error of ±0.0003 m, given by the standard deviation of the diverse sets (see Table 3).

Figure 16. Measuring the position of the sensor in static tests.

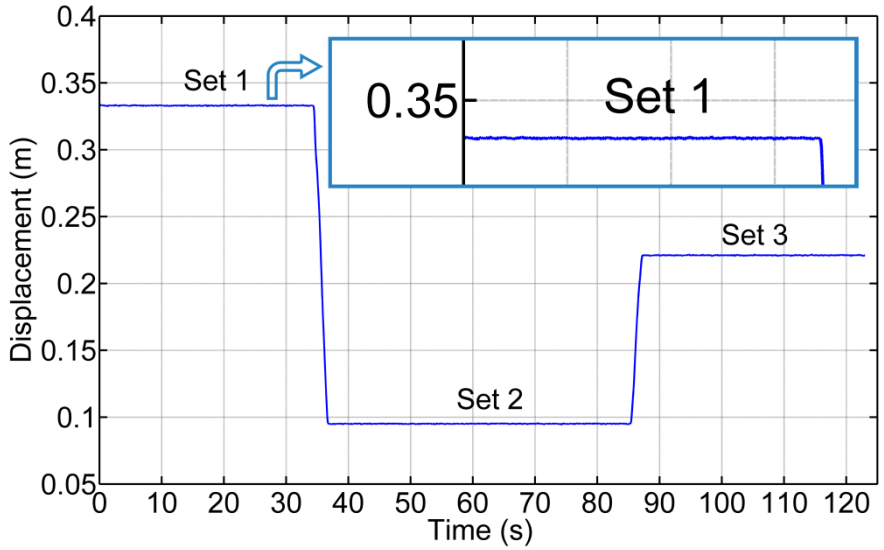

Table 3. Standard deviation and variance of the data presented in Figure 16.

	Standard Deviation (m)	Variance (m^2)
Set 1	0.000256897	6.59961E-08
Set 2	0.000224263	5.02939E-08
Set 3	0.00025533	6.51932E-08

(b) Deflection Test: Measuring the Error Added by the Rod Bending and the Junctions

Because the sensory system has a 1 m long arm, the deflection of the arm generates a measurement error. Additionally, the link between the arm and the two joints in both ends has a certain degree of backlash. To measure the error added by this deflection/backlash, the implement was fixed relative to

the vehicle and an external force was added to the carriage, generating deflection of the materials and measuring the maximum ranges. Figure 17 shows diverse sets of forces applied to the carriage: Set 1 and Set 3 forces the system to the right, and Set 2 and Set 4 force it to the left. This test does not seek to develop a model of the deflection of the materials that make up the sensory system but instead aims to determine, in the worst case, how much such deflections/backlash affects the final lateral displacement measurement of the implement with respect to the vehicle. Moreover, maintaining a certain degree of deflection in the sensory system reduces the number of system blocks and breaks. The total error due to arm deflection and backlash of the joints is ±0.004 m. (See Table 4).

Figure 17. Measuring the position of the sensor where external forces are flexing the sensorial system.

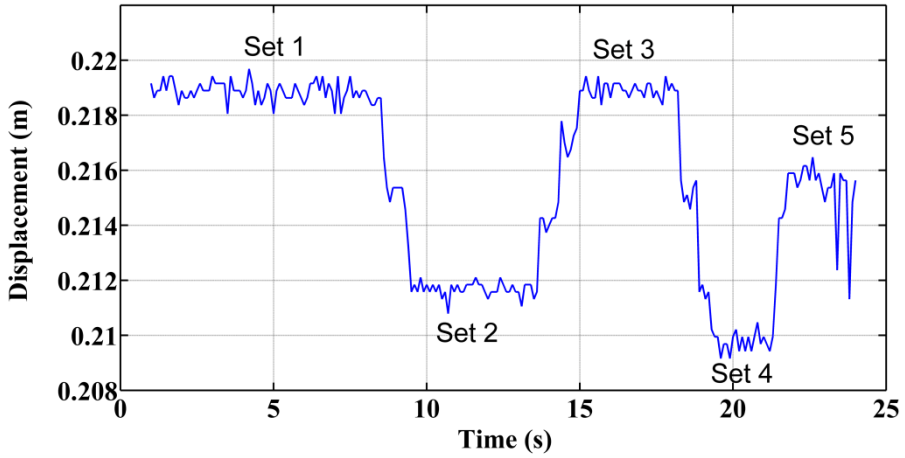

Table 4. Mean displacement values of the sensory system due to material flexing.

	Mean Value (m)
Set 1	0.2189 ± 0.0003
Set 2	0.2117 ± 0.0003
Set 3	0.2189 ± 0.0003
Set 4	0.2087 ± 0.0003

(c) Dynamic Tests: Measuring the Error of the Entire Sensory System While the Vehicle is in Motion

A final test was conducted to measure the variations in displacement while the implement is modifying its lateral position with respect to the vehicle and the vehicle is following a straight line at 0.83 m/s. This test defines how much the sensor dynamics affect the control of the lateral displacement. To validate the entire system, a Sick Laser LMS100 pointing to a 0.03 m wide bar located at the center of the implement was installed at the bottom of the vehicle. The laser detects the bar as a peak in the readings, and by measuring the movement of that peak in the transverse axis, it was possible to determine with very high accuracy the position of the implement with respect to the center of the vehicle. Both the laser information and the potentiometer information were related and synchronized with the GPS. Given that the laser was configured to have an opening angle between beams of 0.25 degrees and the bar was 1.2 m apart from the Laser, this validation system had a

resolution of 0.0052 m. Figure 18 illustrate the results where the laser measurements are compared with the potentiometer measurements. The mean absolute error calculated was ±0.004 m.

Figure 18. Comparison of the readings of the Laser compared with the output of the potentiometer.

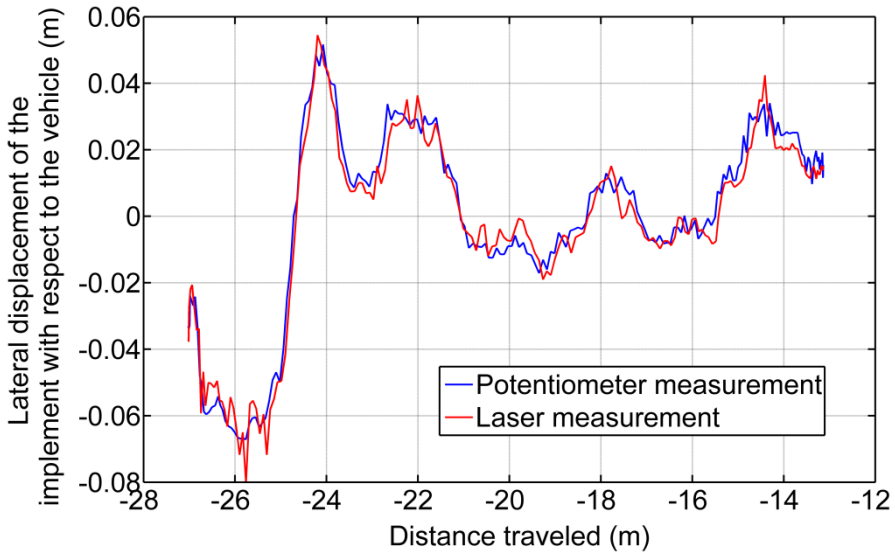

Figure 19. Schematic diagram of the PID controller in cascade configuration for controlling the lateral displacement of the implement with respect to the vehicle.

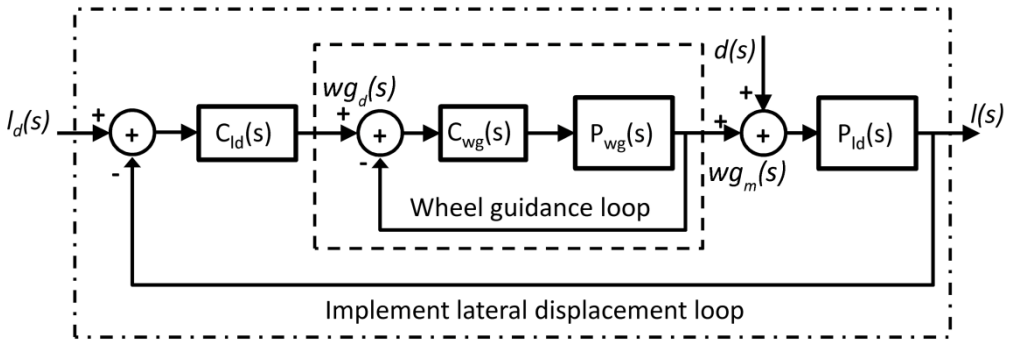

5.2.2. Results of the Control for the Adjustment of the Implement Lateral Displacement with Respect to the Vehicle

For lateral control of the implement, two PID controllers in cascade configuration were implemented (see Figure 19). The first controller ($C_{wg}(s)$) is responsible for adjusting the hydraulic piston that defines the position of the steering wheels of the implement. The desired position of the steering wheels is given by $wg_d(s)$, and the current position of the steering wheels, which is measured by the encoder (see Section 3.1.1), is given by the variable $wg_m(s)$. The second controller ($C_{ld}(s)$), given a desired setpoint of the lateral displacement of the implement ($l_d(s)$), generates the desired steering signal. Figure 20 presents the response of both controllers, where the vehicle was moving in a straight line at 0.28 m/s. The response time of the wheel guidance controller was set based on the system that it replaced (an operator with a steering wheel), and the response time of the implement lateral controller depended on the speed of the vehicle.

Figure 20. Time response of the two PID controllers.

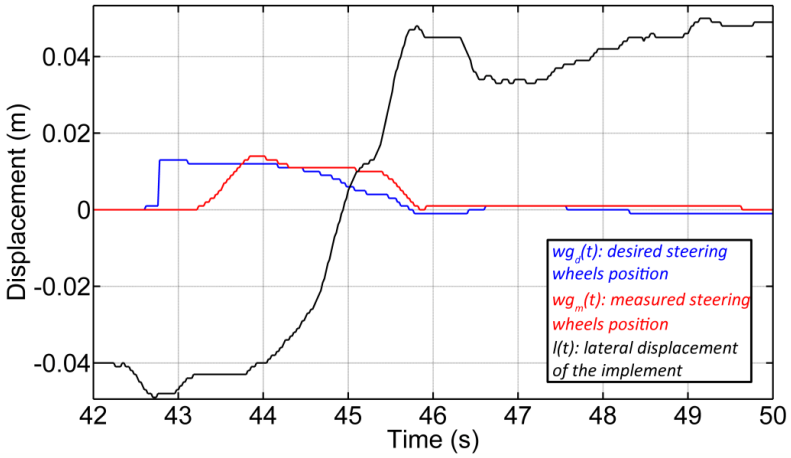

Figure 21. Experimental results of the implement lateral displacement control with three different setpoints.

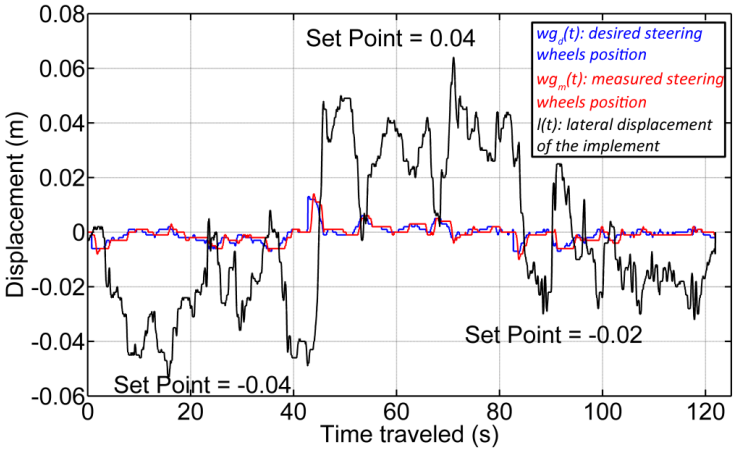

Figure 21 illustrates an example of the implement lateral-position control with three diverse setpoints. Although it is observed that the implement is not maintaining the desired position for each setpoint due to disturbances from the soil ($d(s)$), the results obtained are encouraging. We have been able to keep the implement around the desired position with a mean absolute error of 0.01 m for a complex and heavy system with a very important dynamic response.

5.2.3. Calculation of Delays in the Thermal Treatment

As a final test of each individual element presented in this article, the calculation of delays associated with the treatment for weed control is presented. A set of tests was performed to detect in which GPS position the burners turn on and off, using an Internet protocol camera (IP camera), model Axis 211M, mounted on the back of the implement pointed to a couple of burners (set at a rate of 10 fps). The method to associate an image with a GPS position is the same synchronization approach presented in Section 5.1, which has an error of ±0.1 s. For conducting such tests, a straight path was defined, and within that path, a set of points where the burners were turned on and off consecutively

was selected (see Table 5). The same criterion used by [35] was applied to determine in which image the burner could be considered ignited or extinct.

Figure 22. Example of the image sequence used for the calculation of the delay of the thermal treatment. (**a**) Detection of the ignition starting; (**b**) Detection of flame on the ground; (**c**) Detection of the withdrawal of the flame; (**d**) Detection of the total extinction of the burner.

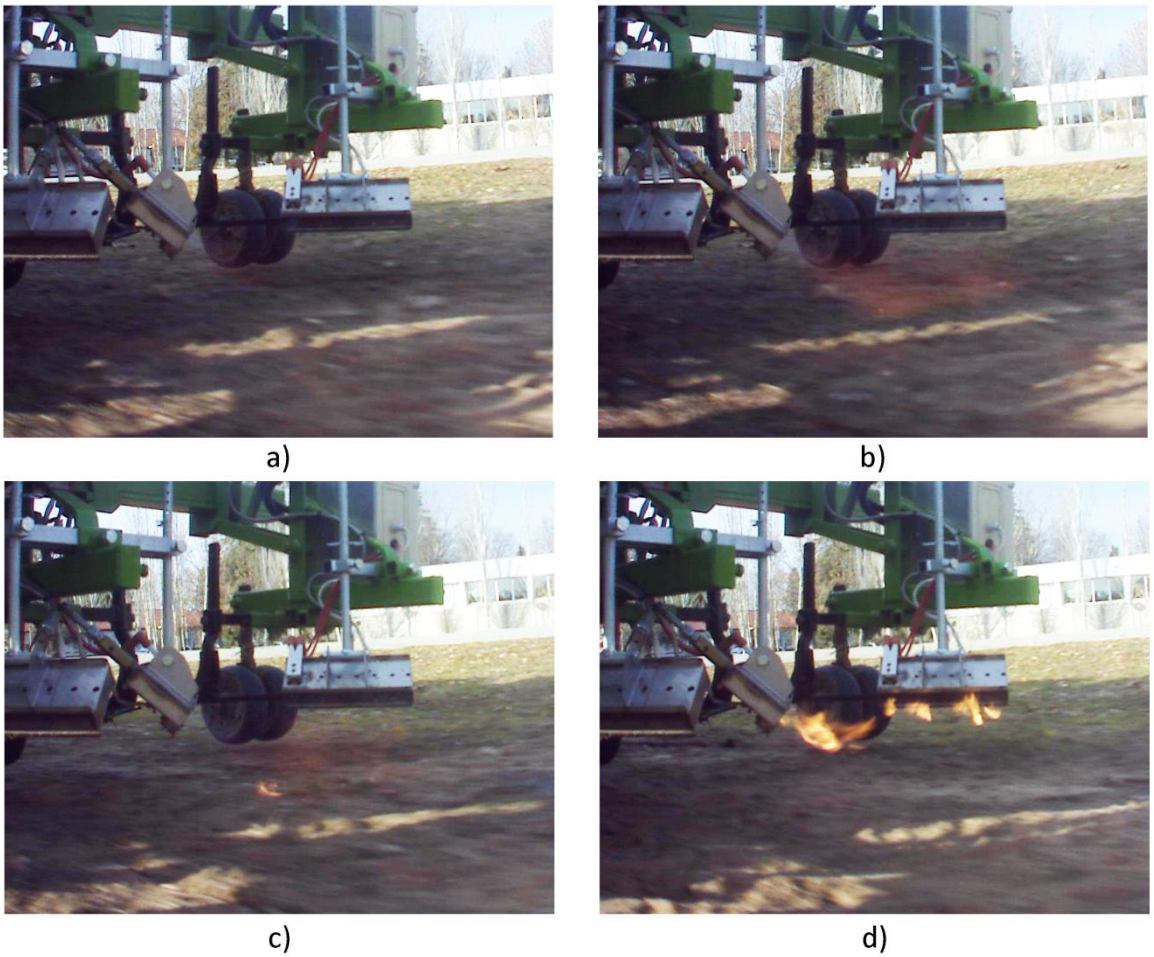

Figure 22a represents the time right when the burners start to turn on. After three consecutive frames (approximately 0.3 s), the burners are operating 100%, corresponding to Figure 22b, where a uniform combustion throughout the burners can be observed. Regarding the extinction of the burners, Figure 22c represents the time right when the burners start to turn off (where the uniform combustion begins to fail). And, after five consecutive frames (approximately 0.5 s), there is no combustible pressure in the system, and the last remnants are consumed, representing the situation of Figure 22d.

Based on the observation of the acquired images, it was possible to calculate the associated delays of the treatment activation. Each selected image had an associated GPS position, and the position where the command was sent (desired position) was compared to the position where the action for ignition/extinction was effective (real position) for calculating the associated delay (see Table 5). The treatment is considered to begin when the flame makes contact with the soil (see Figure 22b). On the other hand, the treatment is considered to end when the flame stops making contact with the soil (see Figure 22c). In addition, a consumption of fuel in the transition stages presented in Figure 22 can be

observed, so these transitions are taken into account when carrying out the study of delays in the system and the comparison between the activation of the actuation system and savings in the product used for the treatment.

With the calculation of the associated delays for both the ignition (0.7 s) and the extinction (1 s) of the burners, the Decision-Making System can adjust the coordinates where such commands must be sent given an operational speed to increase the effectiveness of the treatment.

Table 5. Relative UTM positions where the ignition and extinction commands were sent, the associated relative UTM positions where the action was detected, and the produced delays.

		Desired Position (Relative)		Real Position (Relative)		Time Delay
		X (m)	Y (m)	X (m)	Y (m)	(s)
Set 1	Ignition	−7.48	−3.36	−7.87	−3.36	0.8
		−12.49	−3.14	−12.85	−3.13	0.6
		−17.46	−2.90	−17.78	−2.88	0.5
		−22.45	−2.67	−22.96	−2.64	0.8
	Extinction	−10.00	−3.25	−10.54	−3.21	0.8
		−14.93	−3.04	−15.63	−2.97	1.1
		−19.93	−2.78	−20.63	−2.75	1.1
		−24.93	−2.55	−25.74	−2.50	1.3
Set 2	Ignition	−8.51	−2.78	−9.22	−2.73	0.8
		−13.53	−2.51	−13.96	−2.48	0.6
		−18.47	−2.15	−18.99	−2.11	0.7
		−23.48	−1.70	−24.01	−1.65	0.7
	Extinction	−11.00	−2.64	−11.76	−2.62	0.9
		−16.01	−2.35	−16.91	−2.29	1.2
		−20.98	−1.92	−21.63	−1.87	0.9
	Mean Delay of Ignition =	***0.7 s***		***Mean Delay of Extinction =***		***1.0 s***

Figure 23. (**a**) The path of the vehicle recorded following the pre-defined mission; (**b**) Error between the trajectory followed by the vehicle and an estimation of the position of the center line of the central rows for each sector.

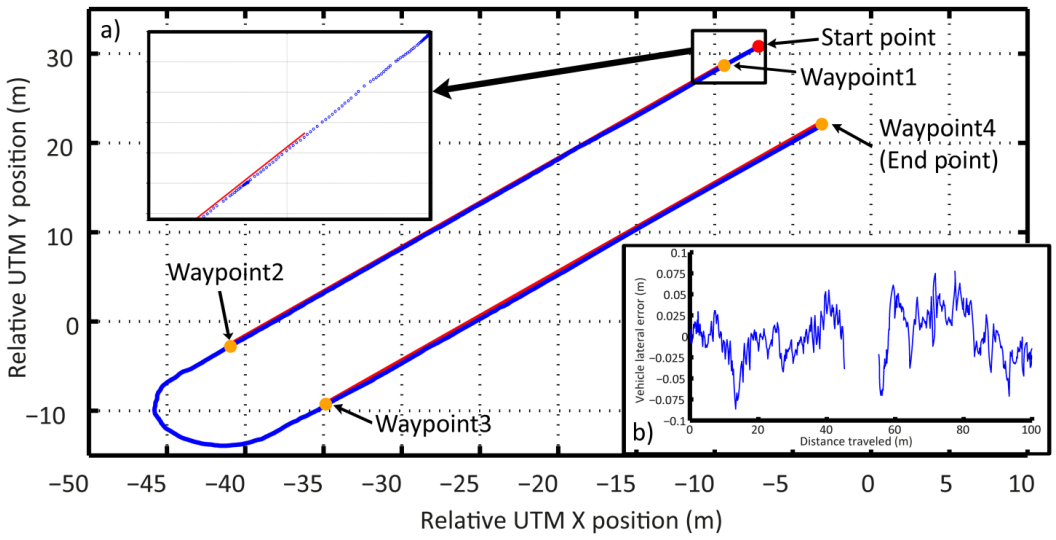

5.3. Perception/Actuation and Decision Making

With the aim to present a complete working system, a general test that involved the coordination between the perception system and the actuation was executed. Given that the system was designed for selective weed control, this final test was used to assess the ability of the system in performing this task.

The whole agricultural system was scheduled to follow a pre-defined plan along the maize field, consisting of the following four waypoints (see Figure 23), which was part of the general mission to be accomplished. The other part of the mission is the execution of the weed control treatment by weed coverage detection, synchronization, and actuation. The primary objective of the mission was to follow the waypoints without putting the crop at risk and to execute an effective treatment in the areas where the weed coverage was higher than the minimum permitted coverage. The Decision-Making System was in charge of this primary objective, based on the information provided by the perception system with the actuation system.

5.3.1. Path Following Test: Deviation Errors

The pre-defined path (the four waypoints—red lines) represents the start and end of each pass through the field. The path was selected with a certain degree of uncertainty, i.e., did not correspond exactly to a centered and parallel line between the two central rows. This represents the mapping proposed in [2,27]. Therefore, the perception system must identify the misalignment of the followed path (line-of-sight) with respect to the row crops. Table 6 presents each of the relative UTM coordinates where the row detection system generated an output (every 2 m of distance traveled) and the correction parameter over the line-of-sight followed. Sector 1 corresponds to the straight line that connects waypoint 1 with waypoint 2; Sector 2 corresponds to the straight line that connects waypoint 3 with waypoint 4. Figure 23b illustrates the difference between the trajectory of the vehicle and an estimated position of the center line of the central rows for both Sector 1 and Sector 2.

Table 6. Relative UTM positions where the perception system generated an output correction value.

Sector 1			**Sector 2**		
Points (Relative UTM)		**Correction**	**Points (Relative UTM)**		**Correction**
X (m)	**Y (m)**	**(m)**	**X (m)**	**Y (m)**	**(m)**
−6.31	31.86	0.19	−38.17	−12.48	0.24
−7.67	30.47	0	−36.85	−11.22	0.28
−9.08	29.02	−0.11	−35.54	−10.08	0.30
−10.46	27.61	0	−34.29	−8.78	0.22
−11.06	27.01	0	−33.26	−7.82	−0.09
−12.43	25.68	0	−31.80	−6.48	0
−13.89	24.21	0	−30.45	−5.13	0
−15.42	22.68	0	−29.20	−3.86	0
−16.66	21.48	0.06	−27.84	−2.50	0
−18.02	20.13	−0.31	−26.33	−1.02	0.07
−19.46	18.76	0	−24.90	0.38	0
−20.74	17.43	−0.14	−23.60	1.65	0
−22.14	15.98	0	−22.24	2.98	0.11

Table 6. *Cont*.

Sector 1			Sector 2		
Points (Relative UTM)		Correction	Points (Relative UTM)		Correction
X (m)	Y (m)	(m)	X (m)	Y (m)	(m)
−23.59	14.56	0	−20.81	4.44	0
−24.92	13.23	0	−19.49	5.70	0
−26.21	11.95	0	−18.12	7.03	0
−27.62	10.52	0	−16.78	8.38	0
−29.00	9.19	0	−15.54	9.65	0
−30.23	7.94	−0.12	−14.14	11.08	0
−31.68	6.49	0	−12.66	12.48	0
−32.94	5.25	0	−11.29	13.87	0
−34.34	3.81	−0.16	−9.86	15.28	0
−35.77	2.40	0	−8.51	16.68	0.06
−37.24	0.88	0	−6.98	18.18	0.09

In this test, the corrections were not made based on the same magnitude as indicated by the row detection system but were decreased by a factor related to the phenological stage of the maize plants, given that the width of the plants could affect the precise detection of the rows (for this test, the phenological stage of the maize was between 5 and 7 leaves with collar). This factor was adjusted to decrease the abrupt changes in the heading of the vehicle given the corrections that must be performed; however, the time and distance needed to converge in following the row crops were increased.

5.3.2. Weed Control Test: Amount of Product Applied in the Treatment

The second part of the mission presented in Figure 23 was the execution of the weed control in the maize field by a mechanical-thermal treatment. To do this, each time an image was acquired by the perception system, a weed density matrix was given. This matrix is interpreted by the Decision-Making System to plan the ignition and extinction of the burners. Each matrix cell contains the weed density information (d_{ij}) of either the left side or the right side of each crop row, in an area of 0.375 m wide by 0.25 m long. Given that the thermal treatment is performed in the intra-row space, the action is executed by each couple of burners. Therefore, the matrix must be processed to define the state of each couple of burners at each instant in time.

Figure 24 illustrates the interpretation of the weed matrices and the resultant weed coverage map for the entire mission, when all coverage matrices are joined consecutively. It can be seen that in many cases, the treatment is only necessary in one cell, i.e., in the intra-row space with an area of 0.25 m wide by 0.25 m long, which represents precisely the minimum area defined for treatment. Given the georeferencing errors, the communication delays, and the electro-mechanical limitations of the entire system (limitations of the perception system, the Main Controller, and the actuation system), it is impossible to accurately fulfill the ignition and extinction of the treatment for the worst cases (only one cell). Therefore, to execute an effective treatment, the burners must be turned on early enough to ensure that the desired area is being treated properly. Given the delays calculated in the previous test, the original weed coverage map becomes the map presented in Figure 25.

Figure 24. Resulting weed coverage map based on the weed density matrices and the interpretation of the three density levels.

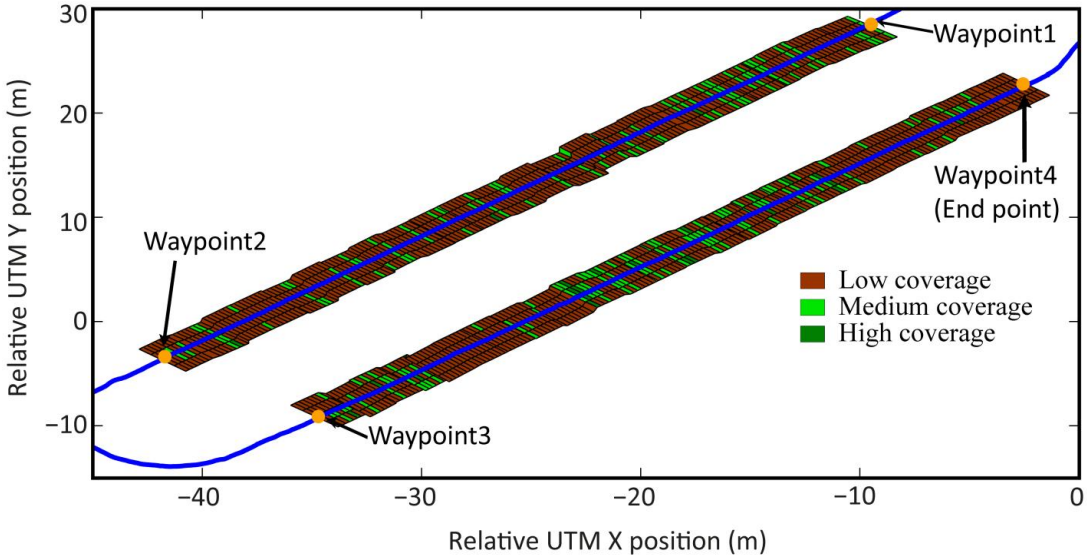

Figure 25. Resulting map of the burner's actuation based on the original weed coverage matrices and the delays associated with the ignition and extinction of the burners.

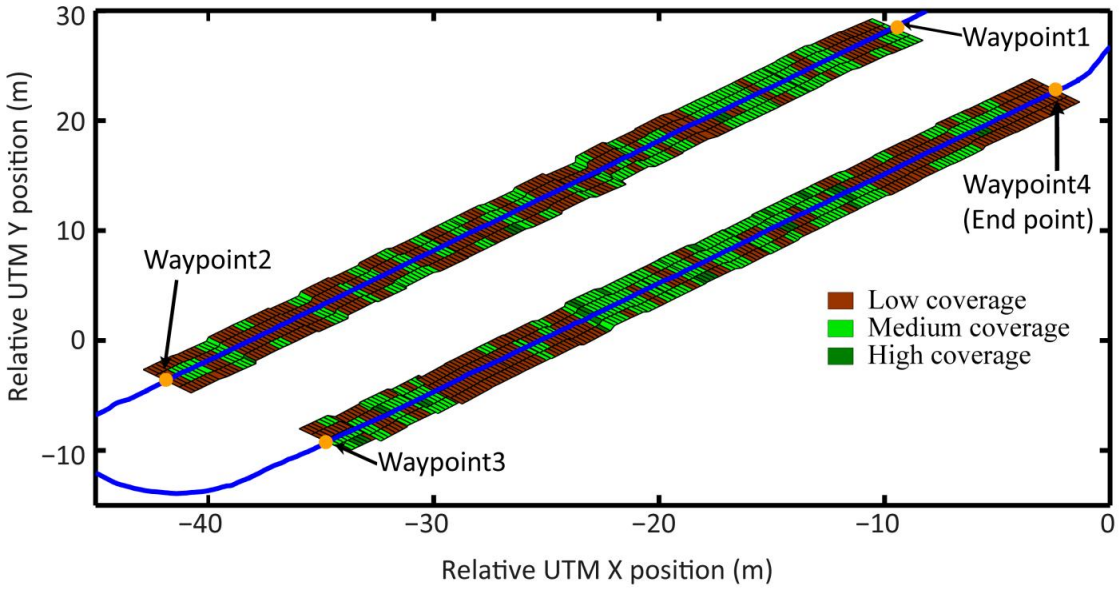

These electro-mechanical and communication limitations lead to the increase in the use of product for weed control (in this case, LPG). Table 7 presents a comparison of the use of product between a hypothetical treatment (Situation 1) following this mission but without the use of the perception system for weed detection (assuming full weed coverage in the entire mission) and the real treatment (Situation 3) executed with the resulting weed coverage map presented in Figure 25. Table 7 also presents the use of product in a hypothetical treatment (Situation 2) where there are no electro-mechanical and communication limitations.

Table 7. Comparison of the use of product for selective weed control.

		Area (m^2)	Percentage of the Coverage Area	Total Distance Traveled by the Four Pairs of Burners When Ignited (*Td*)	Total Operating Time Of the Burners (*Tt*)	Total Consumed Product (Kg) [35]	Percentage of Product Spared
Situation 1	Total Burners treatment area	95.4	-	381.8 m	916.3 s	0.65	-
Situation 2	Low coverage weed detected	16.3	17.1%	65.3 m	156.6 s	0.17	85.1%
	High coverage weed detected	1.4	1.5%	5.8 m	13.8 s	0.02	
Situation 3	Low coverage treated area	39.1	41%	156.3 m	375 s	0.41	65.1%
	High coverage treated area	2.6	2.8%	10.5 m	25.2 s	0.04	

4. Conclusions

The configurations of the perception, the decision-making, and the actuation system have been defined to make up an autonomous vehicle for agricultural applications and, more specifically, for weed control in wide-row crops.

The described perception system has two important tasks: (a) the detection of the crop rows for guiding the vehicle in the field and (b) the detection of weed coverage to perform selective weed control. Based on the tests conducted, the perception system has been shown to be flexible, scalable, robust, and with a suitable level of real-time performance for the application for which it was designed.

Commercial devices were used with standard communication protocols for exchanging messages and interaction between them; the system has proven its reliability for a large number of working hours; the processing algorithms have proven to be quite flexible and scalable, with the ability to adapt to different situations for both the system itself and the environment perceived.

The image acquisition and data processing capabilities have been presented, as well as the required times associated with each task performance and the limitations of each system. The errors associated with the integration of information between image acquisition and GPS positions have been characterized, where positioning the weed coverage matrix has an associated error of ±0.08 m, and the lateral displacement of the path followed with respect to the center of the crop rows has an associated error of ±0.03 m. Both errors are perfectly manageable because the actuation system, i.e., the burners, has a working length of 0.25 m, allowing for a certain degree of flexibility in planning, and allows for minor adjustments on where the burners should be turned on and off. Possible future work to improve the georeferencing of images is the use of an external trigger to synchronize the capture of images, a capability already incorporated in the GPS, the Main Controller, and the camera.

Crop row detection is a crucial task for guidance and weed detection. The proposed method achieves acceptable results with 89% of successful corrections in path following. Additionally, the high weed detection rate (91%) verifies the real-time performance of the proposed approach. This has

been achieved under different illumination conditions and different crop growth stages, verifying the robustness and efficiency of the whole system.

A lateral-position sensor device has been designed and integrated into the mechanical-thermal machine to execute the control of the lateral displacement of the implement with respect to the vehicle. The device has proven to be robust enough to work in difficult working conditions (given the amount of dust and water) and with sufficient reliability and accuracy for accurate control. Moreover, the controller designed for executing this task, although it meets the desired characteristics, requires a major adjustment for better rejection of disturbances coming from the contact of the implement with the ground.

The delays associated with the activation of the treatment were computed, i.e., the ignition and extinction of the burners. Given the architecture of the Decision-Making System and the Actuation Controller, in addition to the electro-mechanical delay of the relays and igniters, both the ignition time delay (0.7 s) and the extinction time delay (1 s) were measured. To ensure an effective treatment, the planning of the activations of the burners must take into account these delays, which leads to a higher amount of applied product. However, the tests conducted have shown that selective treatment remains, and depending on the coverage of the weeds in the field and the proximity between patches of weeds, there may be higher or lower product savings. Future work can focus on improvements to reduce the delays associated with communication between the Decision-Making System and the actuation computer. These two elements can be integrated into the same computer, a capability that can be fulfilled by the current Main Controller.

The integration of the sensors and actuators presented in this article has been positively assessed by the RHEA consortium. The experimental results obtained with individual vehicles make the incorporation of this design into a fleet of robots promising, which is the main future objective of the authors.

The proposed architecture, with three main systems, is designed for weed control in maize fields, but thanks to its flexible and open design, the same vehicle can be used for different agricultural tasks. The unique requirement requires the adaptation of new elements and related processes for the intended task. For example, these systems could be used for site-specific treatments in garlic or other crops with different row widths.

Acknowledgments

The research leading to these results has been funded by the European Union's Seventh Framework Programme (FP7/2007-2013) under Grant Agreement No. 245986. The authors thank all of the RHEA partners for supporting this work in many different ways. Additionally, the authors wish to make a special acknowledgment to Andrea Peruzzi and his research group of the Agricultural Machinery and Farm Mechanization, Department of Agriculture, Food and Environment (DAFE), University of Pisa, Italy, for the confidential information provided.

Authors Contributions

The work presented here was carried out in collaboration between all authors. Luis Emmi, Gonzalo Pajares and Pablo Gonzalez-de-Santos defined the research theme. Luis Emmi designed the architecture for the integration and synchronization of the perception, actuation, and decision

making as subsystems for an agricultural autonomous system working on real wide-row crops. Gonzalo Pajares developed the algorithms for crop and weed detection. Luis Emmi and Mariano Gonzalez-de-Soto developed and implemented the algorithms for the integration and test execution. Luis Emmi analyzed and discussed the results obtained. All authors have contributed to, seen and approved the manuscript.

Conflicts of Interest

The authors declare no conflict of interest.

References

1. Li, M.; Imou, K.; Wakabayashi, K.; Yokoyama, S. Review of research on agricultural vehicle autonomous guidance. *Int. J. Agric. Biol. Eng.* **2009**, *2*, 1–16.
2. Auat Cheein, F.A.; Carelli, R. Agricultural robotics: Unmanned robotic service units in agricultural tasks. *IEEE Ind. Electron. Mag.* **2013**, *7*, 48–58.
3. Hebert, M.; Kanade, T. Outdoor Scene Analysis Using Range Data. In Proceedings of the IEEE International Conference on Robotics and Automation, San Francisco, CA, USA, 7–10 April 1986; pp. 1426–1432.
4. Erbach, D.C.; Choi, C.H.; Noh, K. Automated Guidance for Agricultural Tractors. In *Automated Agriculture for the 21st Century*; ASAE: Washington, DC, USA, 1991.
5. Noguchi, N.K.; Terao, H. Development of an agricultural mobile robot using a geomagnetic direction sensor and image sensors. *J. Agric. Eng. Res.* **1997**, *67*, 1–15.
6. Billingsley, J.; Schoenfisch, M. Vision-guidance of agricultural vehicles. *Auton. Robots* **1995**, *2*, 65–76.
7. Gerrish, J.B.; Fehr, B.W.; van Ee, G.R.; Welch, D.P. Self-steering tractor guided by computer vision. *Appl. Eng. Agric.* **1997**, *13*, 559–563.
8. O'Connor, M.; Bell, T.; Elkaim, G.; Parkinson, B. Automatic Steering of Farm Vehicles Using GPS. In Proceedings of the 3rd International Conference on Precision Agriculture, Minnesota, MI, USA, 23–26 June 1996.
9. Rekow, A.K.W.; Ohlemeyer, H. Automated Headland Turns the Next Step in Automated Agricultural Machines. In *Landtechnik*; Technik AgEng: Hannover, Germany, 2007; pp. 199–209.
10. Gomez-Gil, J.; Alonso-Garcia, S.; Gómez-Gil, F.J.; Stombaugh, T. A simple method to improve autonomous GPS positioning for tractors. *Sensors* **2011**, *11*, 5630–5644.
11. Stentz, A.; Dima, C.; Wellington, C.; Herman, H.; Stager, D. A system for semi-autonomous tractor operations. *Auton. Robot.* **2002**, *13*, 87–104.
12. Rovira-Más, F.; Zhang, Q.; Reid, J.F.; Will, J.D. Machine vision based automated tractor guidance. *Int. J. Smart Eng. Syst. Des.* **2003**, *5*, 467–480.
13. Kise, M.; Zhang, Q. Development of a stereovision sensing system for 3D crop row structure mapping and tractor guidance. *Biosyst. Eng.* **2008**, *101*, 191–198.
14. Gée, Ch.; Bossu, J.; Jones, G.; Truchetet, F. Crop/weed discrimination in perspective agronomic images. *Comput. Electron. Agric.* **2008**, *60*, 49–59.

15. Zheng, L.; Zhang, J.; Wang, Q. Mean-shift-based color segmentation of images containing green vegetation. *Comput. Electron. Agric.* **2009**, *65*, 93–98.
16. Jones, G.; Gée, Ch.; Truchetet, F. Assessment of an inter-row weed infestation rate on simulated agronomic images. *Comput. Electron. Agric.* **2009**, *67*, 43–50.
17. Romeo, J.; Guerrero, J.M.; Montalvo, M.; Emmi, L.; Guijarro, M.; Gonzalez-de-Santos, P.; Pajares, G. Camera sensor arrangement for crop/weed detection accuracy in agronomic images. *Sensors* **2013**, *13*, 4348–4366.
18. Montalvo, M.; Pajares, G.; Guerrero, J.M.; Romeo, J.; Guijarro, M.; Ribeiro, A.; Ruz, J.J.; de la Cruz, J.M. Automatic detection of crop rows in maize fields with high weeds pressure. *Expert Syst. Appl.* **2012**, *39*, 11889–11897.
19. Guerrero, J.M.; Guijarro, M.; Montalvo, M.; Romeo, J.; Emmi, L.; Ribeiro, A.; Pajares, G. Automatic expert system based on images for accuracy crop row detection in maize fields. *Expert Syst. Appl.* **2013**, *40*, 656–664.
20. Xue, J.; Zhang, L.; Grift, T.E. Variable field-of-view machine vision based row guidance of an agricultural robot. *Comput. Electron. Agric.* **2012**, *84*, 85–91.
21. Rovira-Más, F.; Zhang, Q.; Hansen, A.C. Design of Intelligent Systems. In *Mechatronics and Intelligent Systems for Off-Road Vehicles*; Springer: London, UK, 2010; pp. 249–269.
22. Nørremark, M.; Griepentrog, H.W.; Nielsen, J.; Søgaard, H.T. The development and assessment of the accuracy of an autonomous GPS-based system for intra-row mechanical weed control in row crops. *Biosyst. Eng.* **2008**, *101*, 396–410.
23. Perez-Ruiz, M.; Carballido, J.; Agüera, J.; Rodríguez-Lizana, A. development and evaluation of a combined cultivator and band sprayer with a row-centering RTK-GPS guidance system. *Sensors* **2013**, *13*, 3313–3330.
24. Suprem, A.; Mahalik, N.; Kim, K. A review on application of technology systems, standards and interfaces for agriculture and food sector. *Comput. Stand. Interfaces* **2013**, *35*, 355–364.
25. Blackmore, B.S.; Stout, W.; Wang, M.; Runov, B. Robotic Agriculture—The Future of Agricultural Mechanisation? In Proceedings of the 5th European Conference on Precision Agriculture, Uppsala, Sweden, 9–12 June 2005; pp. 621–628.
26. García-Pérez, L.; García-Alegre, M.C.; Ribeiro, A.; Guinea, D. An agent of behaviour architecture for unmanned control of a farming vehicle. *Comput. Electron. Agric.* **2008**, *60*, 39–48.
27. Slaughter, D.C.; Giles, D.K.; Downey, D. Autonomous robotic weed control systems: A review. *Comput. Electron. Agric.* **2008**, *61*, 63–78.
28. Pedersen S.M.; Fountas S.; Blackmore S. Agricultural Robots–Applications and Economic Perspectives. In *Service Robot Applications*; Takahashi, Y., Ed.; InTech: Rijeka, Croatia, 2008; pp. 369–382.
29. Bak, T.; Jakobsen, H. Agricultural robotic platform with four wheel steering for weed detection. *Biosyst. Eng.* **2004**, *87*, 125–136.
30. Rovira-Más, F. Sensor architecture and task classification for agricultural vehicles and environments. *Sensors* **2010**, *10*, 11226–11247.
31. Rovira-Más, F. General Architecture for Intelligent Agricultural Vehicles. In Proceedings of Robotics, Clermont-Ferrand, France, 3–4 September 2010.

32. Peruzzi, A.; Frasconi, C.; Martelloni, L.; Fontanelli, M.; Raffaelli, M. Application of Precision Flaming to Maize and Garlic in the RHEA Project. In Proceedings of the 1st International Conference on Robotics and Associated High-technologies and Equipment for Agriculture, RHEA-2012, Pisa, Italy, 19–21 September 2012; pp. 55–60.
33. SVS-VISTEK. The Focal Point of Machine Vision. Available online: http://www.svs-vistek.com/ (accessed on 8 January 2014).
34. MicroStrain Sensing Systems. Available online: http://www.microstrain.com/inertial/3dm-gx3-35 (accessed on 8 January 2014).
35. Frasconi, C.; Fontanelli, M.; Raffaelli, M.; Martelloni, L.; Peruzzi, A. Sensor Based LPG Management System for Application of Precision Flaming. In Proceedings of the 1st International Conference on Robotics and Associated High-technologies and Equipment for Agriculture, RHEA-2012, Pisa, Italy, 19–21 September 2012; pp. 67–72.
36. National Instruments. Available online: http://spain.ni.com/ (accessed on 8 January 2014).

8 RESULTADOS Y DISCUSIÓN

Los resultados obtenidos en la investigación llevada a cabo y recogidos en las publicaciones que conforman esta tesis doctoral demuestran que utilizar robots y sistemas automatizados para agricultura de precisión aplicando las técnicas adecuadas reduce considerablemente las sustancias contaminantes emitidas a la atmosfera y vertidas sobre los suelos agrícolas. En esta sección se enumeran y discuten los resultados principales obtenidos en cada una de las publicaciones presentadas.

8.1 Resultados en la reducción de contaminantes atmosféricos mediante la optimización de combustible utilizando tractores robotizados para el control de malas hierbas e insectos

En la primera publicación, "*Reducing fuel consumption in weed and pest control using robotic tractors*" (capítulo 4), se ha presentado un análisis del consumo de las UMTs y una metodología para reducir este consumo y llevar a cabo las distintas tareas agrícolas de forma eficiente. Los principales resultados obtenidos en el trabajo realizado son:

- Se han determinado los aspectos y características de la UMT, de los implementos utilizados y de las tareas consideradas que son necesarios tener en cuenta para estimar el consumo de combustible.

- Se ha diseñado e implementado un sistema de medida del flujo instantáneo de combustible consumido por un tractor. Este sistema utiliza dos medidores de flujo modelo PD400 [80] y tiene en cuenta las características del combustible definidas en el Real Decreto 61/2006 [81]. Además, se ha logrado una precisión en la medida de ±5%, para lo cual fue necesaria una calibración y comparación con otras técnicas de medida; en este caso, se ha medido la cantidad total de combustible empleado y se ha comparado con el resultado calculado a partir de los datos proporcionados por el medidor de flujo, siendo el tiempo una variable conocida.
- Se ha obtenido un modelo de consumo de combustible de la UMT basado en los estándares de la ASABE (sociedad americana de ingenieros agrícolas y biológicos) [82], [83], [84], [85], que permite estimar del consumo instantáneo y total para cada tarea al igual que analizar cada uno de los componentes de la demanda energética en las distintas partes de la tarea agrícola realizada.
- Se ha diseñado una metodología para obtener la representación del terreno en tres dimensiones. Para ello se han utilizado coordenadas UTM, respecto al geoide estándar WGS84 (Sistema Geodésico Mundial 1984), para referenciar las posiciones dentro del cultivo. La tercera dimensión se ha obtenido a partir de imágenes georreferenciadas con los datos de elevación del MDT (modelo digital de terreno), en este caso, disponibles en la página web de la NASA [86].
- Se ha definido una metodología de trabajo que reduce el valor de cada componente de la demanda energética. Las componentes consideradas han sido:
    - *El consumo especifico de combustible*: se ha determinado que un uso adecuado de las marchas (relación de transmisión entre el motor y las ruedas) y la posición del acelerador (directamente relacionada con la velocidad del motor) permite ahorrar hasta un 50% de combustible cuando el motor trabaja a potencias medias.
    - *La resistencia de movimiento*: se ha obtenido que aligerar la masa del sistema reduce esta resistencia, siempre y cuando esta masa sea suficiente para evitar un deslizamiento excesivo de las ruedas al realizar la tarea agrícola, ya que al disminuir la masa se incrementa el deslizamiento. El

tamaño y la presión de las ruedas también influye en estos valores de resistencia de movimiento y deslizamiento. Se ha obtenido que en tareas agrícolas, con suelos relativamente blandos, el uso de ruedas grandes reduce tanto el deslizamiento como la resistencia de movimiento. El último parámetro considerado para reducir esta resistencia ha sido el plan de rutas de la tarea. En esta publicación se han considerado las pendientes del terreno y la variación de masa del sistema a lo largo del tratamiento (debida principalmente al producto aplicado). Para ello se ha simulado cada posible plan de trabajo seleccionando el de menor consumo de combustible. Los resultados obtenidos muestran que se consiguen ahorros de hasta el 60% según el modelo teórico, valor que se queda en un nada despreciable 41% al medirlo sobre el sistema real.

- *La energía de labranza*: nos referimos con este término a la energía necesaria para llevar a cabo los distintos trabajos de preparación de la tierra de cultivo. En este caso se ha obtenido que ajustar adecuadamente la profundidad del arado y la velocidad permite reducir esta energía. Para arados profundos esta energía crece proporcionalmente con el cubo de la velocidad, en la tarea considerada en esta tesis doctoral se trata de un arado ligero en el que la proporcionalidad es respecto al cuadrado de la velocidad. Además el implemento considerado está equipado con un sistema de ajuste de profundidad en cada una de las herramientas de arado que permite optimizar la profundidad de arado para cada herramienta por separado y con ello la energía empleada. El sistema de arado de este implemento solo se puede deshabilitar elevando todo el implemento, es decir, permite arar los cuatro surcos que abarca o ninguno, por lo que para reducir el consumo podemos elevar el implemento cuando no hay mala hierba en ningún surco de la calle y bajarlo en caso contrario.
- *La energía de la TDF* (toma de fuerza, también llamada PTO por sus siglas en inglés Power Take-Off): Esta toma de fuerza proporciona energía al implemento para el trabajo correspondiente, en este caso para las bombas de agua y ventiladores. Al tratarse de sistemas automatizados para agricultura de precisión esta potencia no es constante e incluso existen periodos de

tiempo en los que esta potencia es innecesaria, y por tanto una forma de reducir el consumo es desactivar la TDF cuando no sea necesaria. Este sistema tiene dos marchas (normal y económica), por lo que ajustando adecuadamente estas marchas así como las revoluciones de esta toma también se logra un mejor uso del combustible.

- *La energía del sistema hidráulico*: los implementos considerados en esta tesis doctoral no hacen gran uso del sistema hidráulico, tan solo el implemento cultivador con tratamiento térmico lo utiliza para abrir y cerrar sus brazos laterales. Para reducir la energía consumida por este sistema se reduce el uso de esta opción, utilizándolo únicamente al principio y al final de la tarea. Esta energía también se emplea en la conexión tripuntal para elevar y bajar los implementos, por lo que, aunque no es una componente significativa, para reducir consumos se puede ajustar el rango de este movimiento al mínimo.
- *La energía eléctrica*: aquí tenemos la energía consumida por los diferentes controladores, sensores y actuadores eléctricos del sistema. Esta energía se reduce desactivando los aparatos cuando no son necesarios.

- Se ha determinado que el uso de un radio de giro mínimo y de maniobras marcha atrás, cuando este radio de giro no permite una maniobra simple, reduce la energía perdida por la resistencia de movimiento. Se ha de considerar que el radio de giro fijado como mínimo ha de permitir un rango suficiente para que el sistema de control de trayectoria pueda ajustar el ángulo de las ruedas directrices compensando posibles deslizamientos.
- Se ha comparado el consumo de combustible del tratamiento tradicional con la metodología de reducción de combustible descrita obteniendo los resultados expuestos a modo de resumen en la Tabla 1 (en el capítulo 4 se puede encontrar el consumo instantáneo para los diferentes casos). Para ello se han considerado tanto los datos obtenidos a partir del modelo energético del sistema y la representación tridimensional del terreno como los datos obtenidos experimentalmente utilizando los sistemas reales sobre cultivos reales. En la Tabla 1 puede observarse que los resultados teóricos son mejores que los experimentales. Esto se debe en parte a que

el MDT obtenido no es muy preciso, ya que la zona de pruebas está próxima a una población lo cual genera errores en la estimación de las elevaciones, y además, al tratarse de un primer prototipo de la UMT, su respuesta y funcionamiento aun es mejorable. A continuación se analizan y discuten los resultados obtenidos en las tres tareas consideradas para esta publicación:

- Utilizando el implemento sulfatador automatizado para el control de malas hierbas en cereales se ha obtenido que es posible reducir en gran medida el consumo de combustible aplicando las técnicas adecuadas. Esto es porque en este caso se tienen todos los datos de la tarea antes de comenzarla, por lo que es posible obtener un plan de trabajo con un grado de optimización muy elevado, en el cual se optimizan todas las componentes de la demanda energética. El hecho de conocer la distribución de los parches de malas hierbas a priori nos permite eliminar las posibles calles sin malas hierbas reduciendo el combustible y el tiempo empleado. Al tratarse de cultivos herbáceos con surcos estrechos (de 10 a 12 cm), en los que el tractor necesariamente ha de pisar el cultivo, también podemos ajustar el ángulo de

Tabla 1. Resultados en la optimización de combustible

Tarea	Método	Consumo de combustible calculado	Consumo de combustible experimental
Control de malas hierbas con herbicida	No optimizado	*0,74 L*	*0,90 L*
	Optimizado	*0,29 L*	*0,53 L*
	Reducción	*61 %*	*41 %*
Control de malas hierbas con tratamiento térmico y arado	No optimizado	*0,48 L*	*0,50 L*
	Optimizado	*0,31 L*	*0,43 L*
	Reducción	*36 %*	*13 %*
Control de plagas de insectos con insecticida	No optimizado	*0,37 L*	*0,45 L*
	Optimizado	*0,35 L*	*0,43 L*
	Reducción	*6 %*	*5 %*

las calles a cualquier valor para reducir el combustible. Además, considerando el valor medido del "índice de cono" del terreno (medida indicativa de la dureza de suelo [84]), el MDT, el mapa de malas hierbas y la masa del sistema en cada punto del plan de trabajo es posible estimar la resistencia de movimiento para optimizar dicho plan. Como podemos ver en la Tabla 1, aplicando todas estas técnicas es posible reducir el consumo de combustible por encima del 60% según el modelo teórico y, aunque este valor es menor en el caso experimental, sigue siendo superior al 40%.

- En el caso del implemento cultivador con tratamiento térmico automatizado para el control de malas hierbas se han obtenido resultados menos favorables. Esto se debe a que en este caso el mapa de distribución de malas hierbas no es conocido previamente a la tarea, ya que se detectan en tiempo real, por lo que es necesario recorrer todo el campo haya o no hierba. Y además el ángulo de las calles viene definido por el de las líneas de cultivo, por lo que solo es posible elegir dicho ángulo, aunque si se ha utilizado algún algoritmo similar para la siembra este ángulo ya estaría optimizado. En este caso la reducción más importante se genera al elevar el implemento en las zonas sin hierba ya que la mayor demanda energética es la generada por la fuerza de tracción en el proceso de aricado. Como se observa en la Tabla 1 esta metodología logra una reducción del 36 % en el análisis teórico que se queda en un 13 % al llevarlo a la práctica.
- Por último, utilizando el implemento fumigador autónomo para el control de plagas de insectos en un campo de olivos se ha obtenido una reducción de combustible notablemente más baja que en los casos anteriores. Esto se debe a que al tratarse de un implemento autónomo en el que la UMT tiene una información muy escasa sobre tratamiento las posibilidades de reducción son bastante inferiores, básicamente, tan solo podemos optimizar el plan de rutas considerando el MDT. Además, en este caso la TDF ha de funcionar a potencia nominal a lo largo de toda la calle, para que el implemento siempre disponga de suficiente potencia (la UMT desconoce la demanda instantánea), lo que incrementa notablemente el consumo. En la

Tabla 1 podemos ver que la reducción teórica lograda es tan solo del 6 % quedándose en un 5 % para el caso experimental.

8.2 Resultados en la reducción de contaminantes atmosféricos utilizando potencia hibrida en tractores robotizados para agricultura de precisión

Respecto al uso de alternativas al MCI basadas en fuentes energéticas limpias cabe destacar el uso de sistemas de potencia hibrida analizado en la publicación "Reducing air pollution with hybrid-powered robotic tractors for precision agriculture" (capítulo 5) cuyos principales resultados han sido:

- Se han determinado las características energéticas de la UMT necesarias para dimensionar un sistema hibrido de energía basado en el MCI original del tractor, una pila de hidrógeno, un panel fotovoltaico y baterías.
- Se han determinado las cantidades de CO_2, NO_x ,CO, HC y PM emitidas por el MCI de la UMT considerando las mediciones del flujo de combustible y la norma ISO8178 que define los factores de emisión para calcular las emisiones de los MCI en maquinaria agrícola considerando la antigüedad, potencia y régimen de trabajo del MCI (rpm y carga del motor) [87]. Para calcular la carga del motor se consideran las características del sistema y del terreno, se mide la velocidad del MCI (rpm), el deslizamiento (diferencia entre la velocidad de las ruedas y la del sistema GPS), la potencia de la TDF y el movimiento de la conexión tripuntal; con estos datos obtenidos experimentalmente, se aplican las ecuaciones de los estándares ASABE [82], [83], [84], [85].
- Se ha demostrado que es factible eliminar la alimentación de la TDF y del sistema hidráulico al implemento. Para ello se han calculado los requerimientos energéticos de los tres implementos considerados (cultivador con tratamiento térmico, sulfatador y fumigadora de árboles) para llevar a cabo cada tarea agrícola correspondiente y se han enumerado los cambios necesarios que consisten en reemplazar los sistemas que necesitan estas fuentes de potencia por sistemas eléctricos, reduciendo así la carga del MCI e incrementando la demanda de energía eléctrica. Los cambios más importantes propuestos han sido dos: (1) Sustitución de

las bombas de agua principales por pequeñas bombas eléctricas, utilizando una por cada boquilla del implementos para sulfatar cereales y una por cada dos boquillas del implemento para fumigar árboles (ya que este implemento tiene dos boquillas en cada difusor); (2) Reemplazo del ventilador principal del implemento fumigador de árboles utilizando un pequeño ventilador eléctrico en cada difusor.

- Se ha desarrollado un modelo de demanda energética para estimar las diferentes componentes energéticas de cada tarea. Esta demanda ha sido agrupada en dos partes, la potencia demandada por los sistemas eléctricos y el resto de demanda energética. Esta última demanda agrupa la potencia necesaria para vencer la resistencia de movimiento (considerando las pendientes y demás características del terreno y de las ruedas) y la fuerza de tracción generada por la labranza realizada con el implemento sobre el terreno (en el caso que corresponda). Por otro lado, la potencia eléctrica demandada abarca el abastecimiento de los sistemas de control, los sensores y los actuadores eléctricos, considerando las pequeñas bombas de agua y ventiladores añadidos en los implementos correspondientes.
- Se ha obtenido el valor medio de la potencia demandada a cada uno de los sistemas de abastecimiento energético (el sistema eléctrico y el MCI), al igual que de los posibles valores de pico que han de abastecer. Estos valores se han calculado realizando las correspondientes simulaciones para analizar la potencia total e instantánea demandada en cada una de las tres tareas. En estas simulaciones se ha utilizado el modelo energético desarrollado y una representación tridimensional de los campos de pruebas con la distribución de las malas hierbas, para los cultivos de trigo y de maíz, y de los árboles, para el cultivo de olivos. En estas simulaciones se ha obtenido que para el control de malas hierbas con aricado y tratamiento térmico la potencia eléctrica demandada es la más baja de las tres y casi constante, ya que, básicamente, se utiliza para los controladores, sensores y pequeños actuadores. Sin embargo, esta aplicación es la que más potencia mecánica demanda, ya que es la única que realiza una labranza del terreno. Por otro lado, para la fumigación de pesticidas en árboles se ha obtenido la mayor demanda eléctrica, ya que el implemento utilizado es el que más actuadores eléctricos (sensores de ultrasónico, bombas, ventiladores, etc.) emplea para aplicar el tratamiento. En la aplicación de

herbicidas se obtienen resultados parecidos a los de la fumigación de árboles pero con valores más bajos, ya que este implemento demanda menor potencia.

- Se ha diseñado y dimensionado un sistema híbrido de abastecimiento energético considerando el peor caso (el de mayor demanda) de los resultados obtenidos en la las simulaciones de demanda energética. Este sistema híbrido diseñado consta de dos partes principales, un MCI y un sistema de energía eléctrica:
    - El MCI abastece la potencia necesaria para vencer la resistencia de movimiento y la posible fuerza de tracción generada cuando el implemento lleva a cabo algún tipo de labranza del terreno (no se considera ninguna potencia eléctrica ya que el alternador original del tractor ha sido eliminado). La única de las tres aplicaciones consideradas que realiza una labranza del terreno es el control de malas hierbas con el implemento cultivador y de tratamiento térmico, implemento que ha sido dimensionado considerando la potencia del vehículo tractor, por lo que no es necesaria ninguna consideración adicional.
    - El sistema de energía eléctrica abastece a todos los dispositivos que utilizan este tipo de energía. Este sistema se diseña considerando las peores condiciones (con los requerimientos más exigentes) obtenidas en las simulaciones de demanda energética realizadas. Estos valores, principalmente, se han obtenido para la aplicación de pesticidas en árboles. Este sistema de abastecimiento energético está formado por una pila de hidrógeno, baterías de plomo-acido con ciclo profundo, un panel fotovoltaico y un sistema de gestión y control de energía. La pila de combustible utilizada ha sido una pila de hidrógeno tipo PEM (membrana de intercambio de protones) con 1,2 kW de potencia nominal, dimensionada para poder abastecer la potencia eléctrica media trabajando de forma continua durante toda la tarea, aunque puede ser desactivada cuando se considere innecesaria. El sistema de acumulación de hidrógeno es dimensionado para permitir trabajar de forma continuada al menos una jornada de ocho horas. Para los instantes de tiempo en los que la demanda de potencia es muy elevada se utilizan las baterías de plomo-ácido, las cuales forman dos bancos de baterías, uno de 12 V y otro de 24 V,

dimensionados para que puedan suministrar la potencia suficiente. Estas baterías también se encargan de alimentar los sistemas de control cuando el sistema está en reposo y la pila es innecesaria al igual que de suministrar potencia para la puesta en marcha del MCI. Se trata de unas baterías de ciclo profundo que permiten acumular la energía generada por el panel fotovoltaico. Este panel, con una potencia de 183 W, proporciona una energía gratuita que permite cargar las baterías siempre que haya luz, compensando las posibles descargas en largos periodos de inactividad sin consumir hidrógeno. En el lugar donde se han realizado las pruebas, este panel puede proporcionar una energía media de 1,46 kWh cada día, según los datos de radiación proporcionados por el Instituto de Energía y Transporte [88]. Por último, el sistema de gestión y control de energía se encarga de controlar el flujo de energía eléctrica, asegurando una carga mínima en los dos bancos de baterías, para abastecer posibles picos de corriente, como el arranque del MCI, activando la pila de hidrógeno cuando es necesaria y desactivándola para reservar capacidad en las baterías donde acumular la energía fotovoltaica generada.

- Se ha medido el combustible consumido y los datos necesarios para calcular las emisiones en una serie de pruebas experimentales sobre campos reales. Estas medidas se han realizado, por un lado, utilizando el sistema hibrido diseñado y, por otro lado, utilizando MCI como única fuente de potencia, con los alternadores necesarios y utilizando la TDF, para así poder comparar los resultados y estimar los beneficios medioambientales que se pueden lograr con el uso de este tipo de sistemas. Los campos de pruebas utilizados han sido los mismos cuyas representaciones en tres dimensiones se utilizaron en las simulaciones para obtener la estimación de la demanda energética. Los sustancias emitidas consideradas en este análisis han sido: CO_2, CO, la suma de HC + NO_x y PM; en la Tabla 2 se recogen los resultados del cálculo de estas sustancias emitidas a la atmósfera en ambos casos, además del porcentaje en la reducción obtenida al utilizar el sistema de potencia hibrido (en el capítulo 5 se pueden ver estos valeres mas detallados). A continuación se hace una descripción de los resultados en cada una de las tres tareas analizadas:

Tabla 2. Resultados en la reducción de contaminantes atmosféricos utilizando potencia hibrida

Tarea	Sistema de energía	CO_2 (kg/h)	CO (g/h)	HC + NO_X (g/h)	PM (g/h)
Control de malas hierbas con tratamiento térmico y arado	MCI	*11.32*	*113.2*	*147.8*	*12.6*
	Hibrido	*10.36*	*112.9*	*147.5*	*12.6*
	Reducción	*8.53 %*	*0.2 %*	*0.2 %*	*0.0 %*
Control de malas hierbas con herbicida	MCI	*9.86*	*133.4*	*185.2*	*13.0*
	Hibrido	*6.25*	*110.0*	*143.4*	*12.3*
	Reducción	*36.6 %*	*17.8 %*	*22.6 %*	*5.4 %*
Control de plagas de insectos con insecticida	MCI	*10.74*	*142.5*	*204.7*	*12.5*
	Hibrido	*5.64*	*107.1*	*139.3*	*12.0*
	Reducción	*47.5 %*	*24.8 %*	*31.9 %*	*3.8 %*

- En el control de malas hierbas en un cultivo de maíz utilizando el implemento cultivador con tratamiento térmico se ha obtenido que el sistema hibrido propuesto no aporta una gran reducción en la emisión de contaminantes, como se aprecia en la Tabla 2. Esto se debe a que el sistema hibrido propuesto no quita mucha carga al MCI en tareas de labranza, como es la llevada a cabo en el espacio entre líneas de cultivo por este implemento. Además, en este implemento, la energía necesaria para aplicar el tratamiento térmico ya está acumulada en las bombonas de gas, el cual se almacena presurizado (la energía y emisiones de la combustión de este gas no se consideran en esta publicación). Tan solo se aprecia una reducción significativa en las emisiones de CO_2 debida básicamente a la liberación de la pequeña carga que imponían los alternadores eléctricos al MCI. Sin embargo, esto es inapreciable en el resto de emisiones, ya que la variación del régimen de trabajo (rpm y carga) del MCI es muy pequeña y este se mantiene dentro del mismo rango fijado por la norma ISO 8178, la cual define unos factores de emisiones según unos ciertos rangos en el régimen de trabajo del motor.

- Respecto al uso del implemento sulfatador automatizado para el control de malas hierbas, se ha obtenido una reducción apreciable en los cuatro valores analizados. En este caso, la liberación de carga en el motor es muy considerable por lo que se obtiene una importante reducción de consumo de combustible fósil con la consiguiente reducción en el CO_2, más de un 36 %, como puede verse en la Tabla 2. Las otras emisiones presentan menor reducción, ya que el factor de emisiones de CO, HC y PM se incrementa al disminuir la velocidad (rpm) en los MCIs, especialmente el del PM, que como podemos observar en esta tabla tan solo se reduce algo más de un 5%. Según otros estudios, sabemos que el NO_X incrementa con la temperatura del MCI, es decir al aumentar la carga y la velocidad, por lo tanto, en este experimento, su reducción probablemente haya sido superior, incluso, a la del CO_2 (36%), pero al tratarse de un motor pequeño la norma ISO 8178 proporciona un único factor de emisión para la unión de HC + NO_x y como el comportamiento en la emisión de HC es contrario se obtiene una reducción inferior.
- Por último, en el caso del implemento fumigador de árboles sobre el campo de olivos es en el que se ha logrado mayor reducción global de emisiones. Ya que este implemento es el que más potencia del sistema eléctrico requiere y por tanto es el caso en el que existe mayor liberación de carga al MCI al utilizar el sistema hibrido de energía. En la Tabla 2 puede verse que el CO_2 se reduce casi a la mitad, al igual que sucedió con el combustible fósil empleado. Las otras emisiones presentan un comportamiento similar al caso anterior. Cabe destacar, que al utilizar el sistema hibrido, la concentración de CO, HC+NO_X, y PM en los gases expulsados por el MCI se incrementa, pero el flujo total de gas disminuye en mayor magnitud, motivo por el cual se reducen todas las emisiones por unidad de tiempo.

8.3 Resultados en la reducción de contaminantes químicos mediante el uso de sistemas fumigadores inteligentes

Para la reducción en el uso de productos químicos en agricultura, los cuales pueden ser considerados contaminantes del medio ambiente, se propone el uso de sistemas de

precisión que permiten optimizar la aplicación de estos productos centrándolos y dosificándolos según las necesidades del cultivo. En esta tesis doctoral se propone el uso de un sistema inteligente para sulfatar con precisión analizado en la publicación "*Autonomous systems for precise spraying - Evaluation of a robotised patch sprayer*" (capítulo 6). Los resultados obtenidos en el trabajo realizado para esta publicación son:

- Se han determinado las características de un implemento fumigador de precisión describiendo sus componentes y sistemas de control al igual que su funcionamiento y estructura. Este sistema inteligente está equipado con un sistema de control de la concentración de pesticida en la mezcla por lo que tiene un tanque para el agua y otro para el pesticida. También incorpora un sistema de control de flujo para regular el caudal total del producto pulverizado. Consta de doce boquillas con sus respectivas electroválvulas que permiten activarlas individualmente. Todo ello es controlado por un PLC (controlador lógico programable) el cual es comandado por el controlador principal situado en la UMT.
- Se ha definido un sistema de control principal para comandar y supervisar el implemento al igual que las características generales de una UMT y de los distintos sistemas de los que consta. Este sistema de control utiliza un mapa con el posicionamiento de los parches de malas hierbas que permite tratar únicamente las zonas infestadas, este mapa puede ser generado a partir de las imágenes tomadas por la cámara incorporada en la UMT o bien por algún otro sistema (externo a la UMT) de detección de malas hierbas. Para el caso de cultivos con surcos estrechos, como los cereales, los sistemas externos, basados principalmente en drones, pueden proporcionar mejores datos al tomar las imágenes perpendicularmente al plano de cultivo. Sin embargo, para cultivos con surcos anchos, como maíz, cebolla, remolacha, etc. las imágenes tomadas por la cámara de abordo permiten crear un mapa de malas hierbas lo suficientemente preciso.
- Se han determinado los valores de las variables a considerar para realizar un correcto tratamiento llevando a cabo una serie de pruebas y experimentos de laboratorio. Para ello se define el caudal y la presión de cada una de las boquillas al igual que las ecuaciones a aplicar para calcular la concentración de pesticida y el caudal total (variables controladas) según la velocidad del vehículo, el número de boquillas activas y la dosis que se desea aplicar.

- Se han obtenido los resultados de una serie de pruebas empíricas realizadas en un banco de pruebas plasmado sobre suelo asfaltado para medir la superficie infestada de malas hierbas que no es fumigada así como la superficie que a pesar de no estar infestada sí que es fumigada:
    - Para ello, se ha definido un entorno de pruebas formado por tres parches de malas hierbas con forma de paralelogramo con límites laterales no definidos, y con los límites frontales (respecto a la UMT) con ángulos

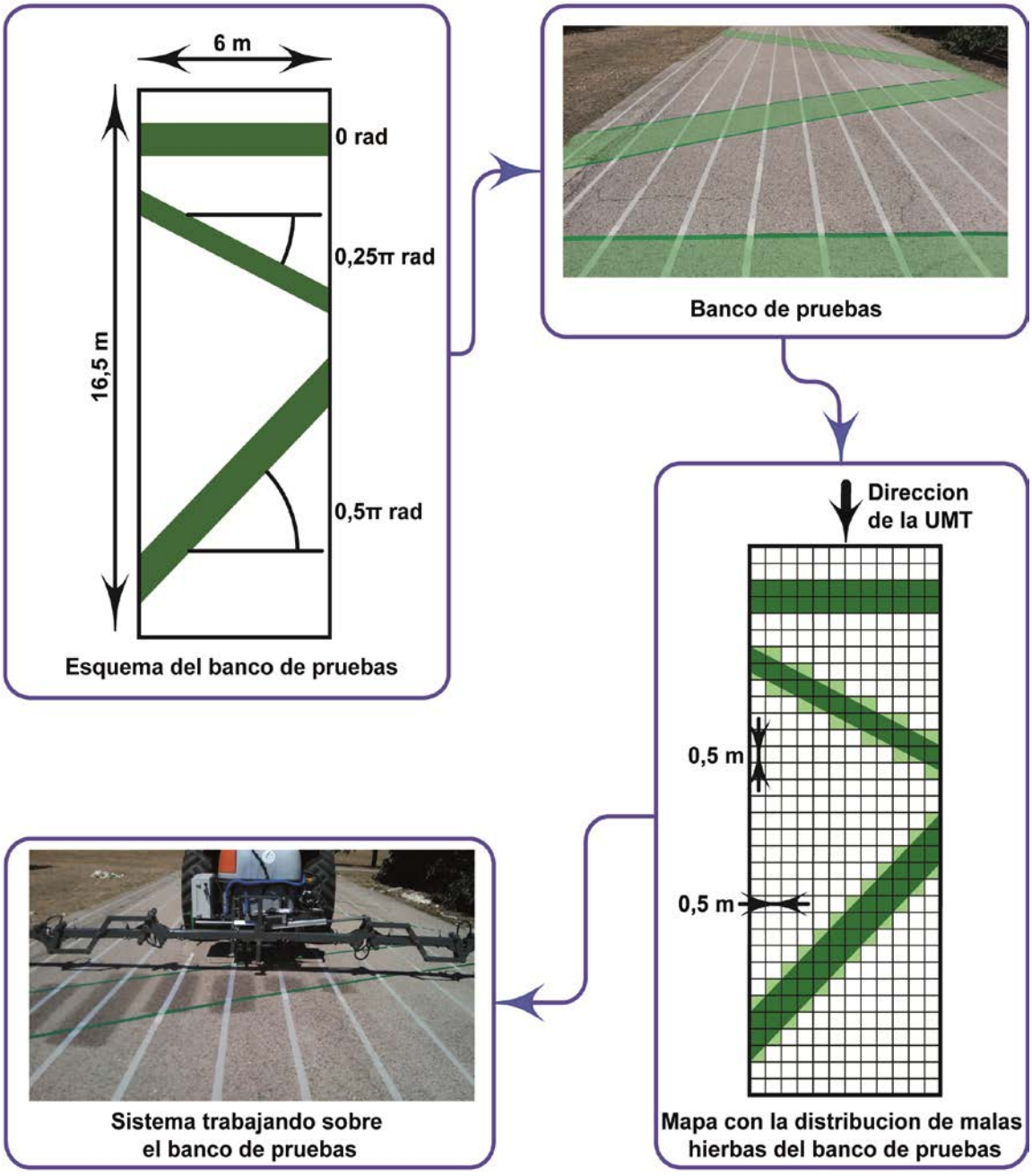

Figura 5. Distribución de malas hierbas en el banco de pruebas

(respecto a la perpendicular de la ruta de la UMT) de 0, 0,25π y 0,5π radianes respectivamente (ver Figura 5). Estos parches se han representado sobre suelo asfaltado utilizando cintas para delimitarlos y así poder tomar las correspondientes medidas. Considerando que las boquillas están distanciadas 0,5 metros, y que el sistema necesita unos 0,5 metros para cambiar el estado de alguna válvula (a 0,83 m/s), es necesario hacer una cuadrícula con celdas cuadradas de 0,5 metros de lado para representar el mapa de malas hierbas. Estos ángulos obligan a abrir y cerrar todas las válvulas al mismo tiempo en el parche orientado a 0 radianes, abrirlas y cerrarlas de dos en dos en el parche orientado a 0,5 radianes y de una en una para el parche de orientado a1 radian. Al obtener la cuadrícula, ya se genera una zona infestada no tratada que puede variar desde 0 hasta 0,075 veces el perímetro del parche en el peor caso, como se observa en la Tabla 3 (considerando que una celda está infestada si la cobertura de mala hierba es superior al 15% y la resolución mencionada).

  - Considerando la cuadrícula con la distribución de malas hierbas definida, se obtuvo un plan de trabajo para el sistema de fumigación inteligente que consistía en tratar los diferentes parches de malas hierbas representados en el suelo. La Tabla 3 recoge los valores máximos y mínimos de las superficies dentro de cada parche real (sin cuadricular) no fumigadas así como de las zonas fuera de estos parches que han sido fumigadas utilizando el sistema real sobre los parches representados en el suelo (en el capítulo 6 se pueden encontrar estos valores más detallados). Estos valores se han calculado considerando el ángulo de la línea que limita el parche y la distancia medida desde el límite de la mancha dejada por el sistema fumigador al aplicar el producto, el cual previamente fue tintado para mantener y mejorar la visibilidad de esta marca, hasta el límite del parche delimitado sobre el asfalto. Estas medidas han sido tomadas midiendo sobre el suelo con una precisión de ±2,5 cm.

- Se ha definido un modelo matemático para poder estimar la superficie infestada no tratada en un campo de cultivo al igual que de la superficie no infestada tratada, este modelo considera el rango de error determinado a partir de la evaluación de los

Tabla 3. Rangos de error al aplicar herbicidas utilizando el sistema inteligente para sulfatar

Caso	Superficie	Mínimo[1]	Máximo[1]
Al hacer la cuadricula[3]	*No tratada[2]*	*0*	*0,075*
	Tratada[3]	*0*	*0,425*
Parche de 0 radianes	*No tratada[2]*	*0,048*	*0,065*
	Tratada[3]	*0,006*	*0,021*
Parche de 0,5 radianes	*No tratada[2]*	*0,000*	*0,002*
	Tratada[3]	*0,211*	*0,271*
Parche de 1 radian	*No tratada[2]*	*0,000*	*0,000*
	Tratada[4]	*0,212*	*0,237*

[1]Con respecto al perímetro del parche de malas hierbas, para obtener la superficie habría que multiplicar este valor por la longitud del perímetro
[2]Superficie infestada con malas hierbas no tratada
[3]El nivel en la concentración de malas hierbas para considerar que una celda está infestada es del 15%
[4]Superficie no infestada con malas hierbas tratada

resultados obtenidos en el uso de este sistema para sulfatación inteligente de malas hierbas. Estas ecuaciones parten de la premisa de que el mapa de malas hierbas del cultivo es conocido por lo que se conoce la longitud de los perímetros de los distintos parches de malas hierbas así como su forma. Utilizando estas ecuaciones se puede estimar que en un campo de trigo con una superficie de 10.000 m^2 y una infestación de malas hierbas distribuida en 5 círculos con 5, 8, 9, 15 y 18 metros de radio, lo que representa el 22,6 % del cultivo (la infestación típica en los cultivos de invierno, como el trigo, suele estar entre el 0 y el 66%). Este sistema sería capaz de tratar el 99,5% de estos parches ahorrando el 76,9% del herbicida que utilizaría un sistema tradicional.

- Para finalizar, se han presentado los resultados de una demostración real del sistema sobre un campo de trigo. En esta demostración la información sobre el posicionamiento de los parches de malas hierbas fue proporcionada por un sistema externo que emplea drones para la adquisición de las imágenes las cuales son analizadas en un ordenador encargado de generar el plan de trabajo con el mapa de

distribución de malas hierbas que se envía a la UMT para que lleve el tratamiento. En esta demostración se obtuvo que el sistema es capaz de tratar más del 95% de la superficie de los parches de malas hierbas y que la zona tratada fuera de estos parches representa un porcentaje insignificante respecto a la superficie total de cultivo. Por lo que estos resultados demuestran un funcionamiento general del sistema correcto. Además, este implemento se puede utilizar para cualquier otro tipo de aplicación de pesticidas líquidos en agricultura al igual que en tareas de fertilización que utilicen productos líquidos con el consiguiente ahorro económico y reducción de sustancias químicas vertidas sobre el suelo. También cabe considerar que, al llevar a cabo un tratamiento selectivo según las necesidades del cultivo, la proporción de producto aplicado que es absorbido por las plantas es mayor con el consiguiente incremento en la biodegradación de los pesticidas reduciendo su infiltración al nivel freático del suelo y, con ello, la contaminación de las aguas subterráneas.

8.4 Resultados en la reducción de contaminantes químicos utilizando sistemas robotizados y técnicas de agricultura de precisión para aplicar alternativas a los productos químicos

Para finalizar esta sección de resultados, se presentan los resultados obtenidos en el uso de sistemas alternativos a los tratamientos con productos químicos para el control de plagas en agricultura, sistema que puede ser utilizado en agricultura ecológica. Para ello se consideran los resultados de la publicación "*Integrating sensory/actuation systems in agricultural vehicles*" (capítulo 7) cuyo enfoque principal, como podemos deducir de su título, no ha sido analizar este tipo de alternativas, sino analizar la integración de un sistema de control del vehículo e implemento agrícola, así como de los correspondientes sensores y actuadores, en un sistema controlador principal. Sin embargo también presenta ciertos análisis y resultados del uso de un tratamiento térmico, el cual puede emplear fuentes renovables como metano u otro tipo de biogás, para el control de malas hierbas en cultivos capaces de soportar este tipo de tratamientos. A continuación se exponen los resultados más relevantes obtenidos en el trabajo documentado en esta publicación:

- Se ha definido un sistema de adquisición de datos que proporciona la concentración de malas hierbas y posiciona los surcos de cultivo en tiempo real. Este sistema

utiliza una cámara situada en la parte superior de la UMT con una pequeña inclinación hacia el suelo que permite ir tomando imágenes de la zona de cultivo situada unos metros por delante del implemento. Estas imágenes se georreferencian utilizando los datos proporcionados por el sistema GPS y los cálculos trigonométricos necesarios (considerando la posición y orientación de la cámara). Posteriormente, algunas de estas imágenes, tomadas cada 2 metros, son tratadas centrándose en el área correspondiente a una porción de cultivo con forma rectangular de 2 m de longitud y 3 m de anchura, lo que equivale a los 4 surcos tratados por el implemento. Los datos proporcionados por este sistema permiten hacer un tratamiento de las zonas infestadas con malas hierbas así como corregir la trayectoria seguida por la UMT para no pisar las líneas de cultivo.

- Se han determinado las características del implemento cultivador con tratamiento térmico automatizado que se ha empleado en las pruebas. Consta de ocho quemadores que tratan cuatro líneas de cultivo y de rejas cultivadoras que llevan a cabo un aricado en el espacio entre estas líneas de cultivo. Estos quemadores están dispuestos de forma que cada línea de cultivo es tratada por dos de ellos, uno por cada lado. El implemento consta de un controlador (PLC) que se comunica con el controlador principal del UMT y permite activar cada pareja de quemadores por separado con dos posibles presiones en el gas combustible. Además, este implemento incorpora un sistema de control de posición lateral basado en dos ruedas directrices del cual se han definido los distintos componentes así como su funcionamiento.

- Se han determinado las características más relevantes del sistema de control principal en el cual se lleva a cabo todo el procesamiento de las imágenes y se genera el plan de actuación que ha de llevar a cabo el tratamiento. Este sistema está basado en un controlador en tiempo real modelo CompactRIO-9082 que ejecuta los algoritmos desarrollados en LabView.

- Se ha obtenido el tiempo de adquisición y procesado de cada imagen el cual está comprendido entre 0,6 y 0,7 segundos. Este valor se ha determinado a partir de una serie de pruebas experimentales para evaluar el funcionamiento del sistema detector de malas hierbas y líneas de cultivo en las que se ha evaluado la rapidez del sistema. Teniendo en cuenta que el área de interés analizado en cada imagen cubre

dos metros de la calle tratada y que la velocidad del sistema es de 0,83 m/s (3 km/h) se obtiene que el tiempo máximo de procesado es 2,4 segundos, mayor de 0,7 por lo que no supone ningún problema. También se ha determinado el error en el proceso de georreferenciación de las imágenes obteniendo que este error es de ±0,08 m en el posicionamiento frontal y ±0,03 m en el posicionamiento lateral (respecto a la línea seguida por la UMT). Para finalizar la evaluación de los resultados en estas pruebas, se han analizado los resultados obtenidos en el sistema de seguimiento de surcos y detección de malas hierbas, obteniendo que el sistema de seguimiento de surcos proporciona una precisión de ±0,05 m en la corrección lateral de la trayectoria, y que el error generado en la corrección de la dirección de la trayectoria es excesivo, por lo que se emplea únicamente para la corrección lateral ya que la dirección proporcionada en el plan de trabajo es lo suficientemente exacta para no necesitar corrección. Respecto a la detección de malas hierbas, el sistema analiza el porcentaje de pixeles verdes que hay en el espacio entre líneas de cultivo, dividendo el área analizada en celdas de 0,375 × 0,25 m, descartando una pequeña franja correspondiente a la línea de cultivo en cada una de estas celdas. Analizando estos resultados, se ha obtenido que el sistema es capaz de detectar el 91% de las malas hierbas.

- Se ha obtenido que el sistema de control de posicionamiento lateral es capaz de compensar pequeñas desviaciones de la UMT, de entorno a unos ±7 cm, con una precisión de ±4 cm. Estos valores han sido calculados a partir de una serie de pruebas utilizando el sistema de control de posicionamiento lateral del implemento.
- Se ha obtenido que el tiempo medio de encendido de los quemadores es de 0,7 s, y que su tiempo medio de apagado es de 1 s. Para calcular estos valores, se han realizado una serie de experimentos en los que se ha medido el tiempo desde que se manda la orden de encendido hasta que éste está completamente operativo y desde que se manda la orden de apagado hasta que la llama desaparece completamente. Para ello se ha empleado una cámara conectada al controlador principal que va capturando imágenes del quemador.
- Se ha determinado que el sistema de detección de líneas de cultivos proporciona datos de corrección adecuados en el 89% de los casos. Este dato se ha obtenido a partir de una serie de pruebas realizadas sobre un campo de maíz donde una

estación base proporciona un plan general que fija el punto inicial y el final de cada calle que ha de recorrer la UMT para llevar a cabo la tarea. El sistema de detección de surcos corrige la trayectoria, sin variar la dirección, ya que como explicamos anteriormente la precisión en el cálculo de esta dirección es peor que la proporcionada por la estación base. Las correcciones más importantes se producen al inicio de cada una de las calles para ajustarse a los surcos, ya que los datos proporcionados por la estación base se calculan geométricamente lo que puede conllevar desvíos laterales de varios centímetros, tras esta fase inicial las correcciones son mínimas, lo que demuestra que la dirección seguida es suficientemente precisa.

- Se ha definido el ahorro de producto combustible al utilizar el sistema de detección de malas hierbas. Para ello, se han llevado a cabo dos ensayos en dos escenarios diferentes, los cuales se han comparado con el supuesto caso en el que no hubiese sistema de detección de malas hierbas y los quemadores fueran continuamente encendidos a alta presión de gas, obteniendo los resultados recogidos en la Tabla 4 a partir de una serie de pruebas empíricas (estos datos se pueden encontrar en más detalle dentro del capítulo 7). En estos experimentos, al interpretar los datos de malas hierbas se realiza un redimensionamiento de las celdas para ajustarlas a las capacidades de los quemadores, se fija la distancia mínima (a 0.83m/s) entre cambios sucesivos del estado de los quemadores a 0,5 m y se define una celda por

Tabla 4. Uso de producto combustible en el control de malas hierbas mediante tratamiento térmico

Caso	Superficie poco infestada [1]	Superficie muy infestada [2]	Porcentaje de producto consumido [3]
Caso 1	*0 m^2 (0 %)*	*95,4 m^2 (100 %)*	*100 %*
Caso 2	*16,3 m^2 (17,1 %)*	*1,4 m^2 (1,5 %)*	*14,9 %*
Caso 3	*39,1 m^2 (41 %)*	*2,6 m^2 (2,8 %)*	*34,9 %*

[1] Superficie sobre la que se activan los quemadores en baja presión de gas.
[2] Superficie sobre la que se activan los quemadores en alta presión de gas.
[3] Con respecto a considerar que no se utiliza sistema de detección de malas hierbas y todo el tratamiento se hace con los quemadores en alta presión de gas.

cada línea de cultivo, siendo 0,75 × 0,5 m el tamaño de las celdas resultantes. Como puede verse en la Tabla 4, con el uso de estos sistemas se obtienen reducciones significativas, logrando un ahorro en el combustible empleado superior al 85% y al 65% en los casos 2 y 3, respectivamente.

9 CONCLUSIONES

Considerando los resultados obtenidos en las publicaciones de investigación realizadas y compendiadas en la presente tesis doctoral podemos destacar que la robótica y la automatización ofrecen multitud de técnicas y alternativas a tener en cuenta a la hora de reducir el uso de combustibles fósiles y de productos químicos en agricultura, los cuales generan gran cantidad de sustancias nocivas para el medio ambiente y están alterando gravemente las condiciones de nuestro planeta Tierra dando lugar a graves trastornos en los seres vivos que lo habitan y en el entorno que los rodea. Estas sustancias son perjudiciales para nuestra propia salud y bienestar, ya que pueden estar presentes en el aire que respiramos, en el agua que bebemos e incluso en los alimentos de los que nos nutrimos dando lugar a enfermedades y trastornos cada vez más habituales en la sociedad actual. Las siguientes secciones resumen las principales conclusiones obtenidas a partir de las publicaciones compendiadas en esta tesis doctoral.

9.1 Conclusiones respecto a la reducción de emisiones reduciendo el consumo de combustible en tareas agrícolas automatizadas

CONCLUSIÓN PRIMERA: Para optimizar el plan de trabajo respecto al combustible empleado en la realización de una tarea agrícola es necesario simular las posibles soluciones, para lo cual es muy importante tener un buen modelo de consumo del sistema

así como del terreno de cultivo a tratar. Obtener la representación tridimensional del terreno permite considerar las pendientes y obtener una estimación más precisa en las distintas opciones consideradas. Esto es especialmente interesante para aplicaciones en las que existe una importante variación en la masa del sistema, tales como fertilización, aplicación de pesticidas, recolecta de productos, etc. Para lograr un buen uso del combustible también es importante considerar aspectos más triviales como utilizar un ajuste entre la relación de transmisión (marcha) y la posición del acelerador adecuado para la potencia demandada, usar unas ruedas con la presión, las dimensiones y el dibujo adecuados, ajustar la masa, afinar la profundidad de arado, regular el uso de todos los sistemas y desactivarlos siempre que sea posible.

CONCLUSIÓN SEGUNDA: El uso de sistemas de adquisición de datos para determinar las zonas infestadas en tareas de control de plagas en agricultura mejora el uso de los recursos energéticos. Sin embargo, el uso de implementos autónomos que incorporan estos sistemas de adquisición para agricultura de precisión puede implicar derroches de energía muy elevados. Esto se produce principalmente cuando el tractor suministra potencia al implemento a través de la TDF y la comunicación entre ambos es muy escasa (el sistema de control del tractor desconoce los requerimientos energéticos del implemento). Esto obliga al tractor a mantener una velocidad constate en la TDF para que el implemento disponga siempre de potencia suficiente malgastando gran cantidad de energía, ya que el implemento necesita sistemas *bypass* para liberar posibles excesos de potencia, además de la imposibilitar un buen ajuste en la velocidad del MCI.

9.2 Conclusiones respecto a la reducción de emisiones mediante la inserción de sistemas de potencia basados en fuentes de energía limpia para sistemas agrícolas robotizados

CONCLUSIÓN TERCERA: Las modificaciones necesarias en implementos agrícolas para que puedan utilizar sistemas de potencias basados en fuentes energéticas limpias son relativamente sencillas. Lo más conveniente es el uso de actuadores eléctricos (bombas, ventiladores, cilindros, etc.) ya que ofrecen un rendimiento elevado y un rango de potencias muy amplio. Esto es especialmente interesante en implementos que utilizan la TDF en los cuales se puede reducir significativamente la energía demandada al MCI (hasta

casi un 50% en los casos analizados) permitiendo el uso de pequeños tractores combinados con grandes implementos.

CONCLUSIÓN CUARTA: Los sistemas eléctricos basados en fuentes limpias, los cuales liberan de carga al MCI reduciendo el consumo de combustible fósil, son los más interesantes en agricultura de precisión ya que permite usar multitud de actuadores con un rango de potencias muy amplio y un rendimiento muy alto. Esto es especialmente interesante en sistemas robotizados para agricultura de precisión ya que hacen posible el uso de pequeños actuadores distribuidos para un tratamiento independiente de cada zona de cultivo con un buen rendimiento energético, ya que se elimina la necesidad de sistemas *bypass* para liberar posibles excesos en la potencia suministrada que derrochan gran cantidad de energía (los sistemas agrícolas de precisión que utilizan la TDF suelen tener una bomba principal y válvulas, por lo que requieren de una línea *bypass* para aliviar posibles excesos de presión). La incorporación de sistemas de energía eléctrica basados en fuentes de energía limpia (baterías, pilas de combustible, paneles solares, etc.) es especialmente factible en cualquier vehículo agrícola ya que en estos sistemas el volumen (aerodinámica) y la masa no suelen representar problemas, incluso puede ser necesario incrementar la masa en ciertas ocasiones.

CONCLUSIÓN QUINTA: El uso de sistemas eléctricos en implementos autónomos facilita una mejor gestión energética sin necesidad de comunicación entre el implemento y el vehículo tractor. Además, los implementos pueden incorporar sus propias fuentes de energía, para autoabastecerse parcial o completamente.

9.3 Conclusiones respecto a la reducción de contaminantes hídricos utilizando sistemas robotizados para reducir el uso de productos químicos agrícolas

CONCLUSIÓN SEXTA: El uso de sistemas de agricultura de precisión para el control de malas hierbas reduce significativamente la cantidad de herbicida vertido sobre suelos agrícolas que va a parar a las aguas subterráneas. Estos sistemas son capaces de tratar en torno al 99% de la superficie infestada detectada sulfatando un porcentaje insignificante del resto de la superficie del cultivo, además, la proporción de herbicida absorbido por las plantas es muy alta, ya que las zonas infestadas tienen más plantas, lo cual mejora la

biodegradación logrando una reducción muy importante en el herbicida que va a parar a las aguas subterráneas.

CONCLUSIÓN SÉPTIMA: Esta técnica de adaptar el producto aplicado a las necesidades del cultivo se puede extender a otras tareas agrícolas, como cualquier tipo de control de plagas con pesticidas, tareas de fertilización, etc., con la consiguiente reducción de sustancias químicas vertidas sobre suelo agrícola.

9.4 Conclusiones respecto a la reducción en la contaminación hídrica por productos químicos agrícolas utilizando técnicas alternativas

CONCLUSIÓN OCTAVA: La aplicación de tratamientos térmicos para el control de malas hierbas es una opción alternativa a los herbicidas para los cultivos resistentes a estas dosis de calor (maíz, ajos, cebollas, etc.). El combustible empleado no genera contaminación hídrica y puede ser algún tipo de biogás cuya combustión no contribuye a la contaminación atmosférica. Esta técnica puede ser empleada en agricultura ecológica, en agricultura sostenible y en agricultura de conservación.

CONCLUSIÓN NOVENA: La robótica y la automatización ofrecen grandes posibilidades y expectativas para el desarrollo de técnicas agrícolas respetuosas con el entorno y el medio ambiente en las que es necesario seguir trabajando e investigando.

10 CONCLUSIONS

Considering the obtained results in the research publications conducted and encapsulated in this doctoral dissertation, we highlight that robotics and automation offer many techniques and alternatives that we must consider in order to reduce the use of fossil fuels and chemicals products in agriculture, which generates a large amount of dangerous substances for the environment and can seriously alter the conditions of our planet Earth leading to serious disorders in living beings that inhabit it and in the surrounding environment. These substances are harmful to our own health and well-being, because they can be present in the air we breathe, the water we drink and even the foods that nourish us causing diseases and disorders increasingly common in current society. The following sections summarize the main conclusions obtained from the publications presented in this doctoral dissertation.

10.1 Conclusions regarding the reduction of emissions by reducing fuel consumption in automated agricultural tasks

FIRST CONCLUSION: To optimize the work plan with respect to fuel consumption in an agricultural task, we need to simulate the possible solutions, for which it is very important to have a good consumption model of the system and a good representation of the crop to treat. A three-dimensional representation of the terrain allows us to consider the

slopes as well as to obtain an accurate estimation for the different options. This is especially interesting for applications where there are significant variations in the system mass, such as fertilization, pesticide application, product harvesting, etc. To achieve a good use of the fuel it is also important to consider trivial aspects as using a fit between the transmission ratio (gear) and the throttle position adequate to the power demand, using wheels with appropriate pressure, dimensions and drawing, adjusting the system mass, tuning the depth of plowing, regulating the use of all systems and deactivating it whenever it is possible.

SECOND CONCLUSION: Using data acquisition systems to determine the infested areas in pest control tasks in agriculture improves the use of energy resources. However, the use of autonomous implements for precision agriculture which incorporate these acquisition systems can involve very high waste of energy. This occurs mainly when the tractor provides power to the implement through the PTO and the communication between both is very scarce (the control system in the tractor does not know the energy requirements of the implement). This implies that the tractor has to maintain the PTO speed constant to supply the energy requirements of the implement at any time wasting a lot of energy, because the implement needs some bypass systems to release possible power excess, furthermore it precludes a good adjust of the engine speed.

10.2 Conclusions regarding emission reductions by inserting power systems based on clean energy sources for robotic agricultural systems

THIRD CONCLUSION: The necessary modifications in agricultural implements for using power systems based on clean energy sources are relatively simple. Using electric actuators (pumps, fans, cylinders, etc.) is a very good option because they offer high performance and a very broad power range. This is especially interesting for implements that use the PTO in which case the energy demanded to the engine can be reduced significantly (up to nearly 50% in the analyzed cases) allowing the use of small tractors combined with large implements.

FOURTH CONCLUSION: The electrical systems based on clean energy sources, which decrease the engine load reducing fossil fuel consumption, are the most interesting

in precision agriculture because they allow the use of many actuators with a wide power range and very high performance. This is especially interesting in robotic systems for precision agriculture because they allow the use of small actuators distributed for independent treatment of each crop area with a very good energy efficiency because it removes the need of using bypass systems to release each possible power excess which wastes a lot of energy (precision farming systems that use the PTO usually have a main pump and valves, thus requiring a bypass to alleviate possible pressure excess). Incorporating power systems based on clean energy sources (batteries, fuel cells, solar panels, etc.) is especially feasible in any agricultural vehicles because in these systems the volume (aerodynamic) and mass usually represent no problem, even sometimes we need to increase the mass.

FIFTH CONCLUSION: Using electrical systems in autonomous implements facilitate a better energy management without communication between the implement and the tractor unit. Furthermore, the implements can incorporate their own energy sources to be partially or completely self-sufficient.

10.3 Conclusions regarding the reduction of water contaminants using robotic systems to reduce the use of agricultural chemicals

SIXTH CONCLUSION: Using precision agricultural systems for weed control reduces significantly the amount of herbicide sprayed over agricultural soils which goes to groundwater. These systems are capable of treating approximately 99% of the detected infested surface spraying an insignificant percentage of the remainder crop surface, furthermore, the proportion of herbicide absorbed by plants is very high, because the infested areas have more plants, improving the biodegradation to achieve a very important reduction in the herbicide that goes to groundwater.

SEVENTH CONCLUSION: This technique based on adjusting the product applied to crop requirements can be extended to other agricultural tasks, such as any type of pest control with pesticides, fertilizers, etc., with the consequent reduction of chemical substances sprayed over agricultural surfaces.

10.4 Conclusions regarding the reduction of water pollution by agricultural chemicals using alternative techniques

EIGHTH CONCLUSION: The application of heat treatments for weed control is an alternative option to herbicides for the crops which are resistant to these small heat doses (corn, garlic, onions, etc.). The fuel burnt does not generate water pollution and can be any type of biogas whose combustion does not contribute to air pollution. This technique can be used in organic farming, sustainable agriculture and conservation agriculture.

NINTH CONCLUSION: Robotics and automation offer great potential and expectations for the development of agricultural techniques respectful with the soil and the environment in which we need to continue working and researching.

11 TRABAJO FUTURO

A la hora de optimizar el plan de trabajo se ha visto que las alturas del terreno obtenidas a partir de información disponible en internet presentan un rango de error que puede superar el metro, lo que nos lleva a considerar la posibilidad de mejorar los datos del MDT. Por lo que un trabajo futuro sería considerar la mejora en la precisión de estos datos. Una posibilidad sería llevar a cabo el registro de los datos de altura proporcionado por el sistema GPS de precisión mientras se lleva a cabo alguna tarea sobre el terreno, esto se limitaría a la zona de trabajo y requiere mucho tiempo, por lo que queda abierta la posibilidad en la investigación y mejora de otras técnicas.

En esta tesis doctoral se ha propuesto y analizado la posibilidad de utilizar un sistema de potencia hibrido para reemplazar parte de la energía obtenida a partir de combustibles fósiles por otras fuentes limpias. Sin duda, los sistemas de potencia híbridos que ya podemos encontrar en el mercado constituyen un paso intermedio y necesario para este cambio. Sin embargo un objetivo a largo plazo, cada día más necesario, es desarrollar sistemas agrícolas que utilicen fuentes de energía 100% limpias y respetuosas con el medio ambiente.

La idea presentada en el uso de herbicidas se puede extender al uso de cualquier otra sustancia química utilizada tanto en agricultura como en otras áreas. Dentro de la

agricultura se puede aplicar a cualquier tratamiento para el control de plagas mediante pesticidas, para lo cual sería necesario desarrollar un sistema de adquisición capaz de detectar las infestaciones de cada plaga correspondiente, como pueden ser insectos, hongos, parásitos, roedores, etc. Otra tarea agrícola a considerar es la fertilización de los terrenos, en la que se podría desarrollar un sistema que permita obtener las distintas deficiencias en nutrientes que presenta cada parte de un cultivo para así poder aplicar a cada parte del cultivo los nutrientes necesarios en la dosis adecuada.

Un área agrícola en el que la robótica puede aportar mejoras muy importantes y que está en una demanda creciente es el de la agricultura ecológica en la que el uso de cualquier tipo de producto de síntesis química está terminantemente prohibido. Utilizando tecnología robótica y visión artificial se pueden desarrollar sistemas capaces de llevar a cabo tareas de tipo mecánico para el control de las plagas que pueden dañar los cultivos, respetando las premisas impuestas para la obtención de productos calificados como ecológica. Esto conllevaría una eliminación completa de los pesticidas vertidos en campos agrícolas con la consiguiente mejora en la calidad de las aguas subterráneas y en la biodiversidad del terreno. También cabe destacar que estas técnicas, tal vez con alguna pequeña adaptación, se pueden extender a otros tipos de agricultura también respetuosas con el entorno y el medio ambiente, como la agricultura sostenible y la agricultura de conservación.

REFERENCIAS

[1] FAO, Agricultura mundial: hacia los años 2015/2030. Informe resumido. Roma, Italia: FAO - Organización de las Naciones Unidas para la Alimentación y la Agricultura, 2002.

[2] U. EPA, «US Environmental Protection Agency». [En línea]. Disponible en: http://www.epa.gov/. [Accedido: 09-abr-2015].

[3] «Troposfera.org || Portal de Calidad del Aire - Inicio». [En línea]. Disponible en: http://www.troposfera.org/. [Accedido: 26-may-2015].

[4] «Terra.org - Ecología práctica». [En línea]. Disponible en: http://www.terra.org/. [Accedido: 26-may-2015].

[5] UCM, «El Ciclo Del Agua», Universidad Complutense de Madrid Facultad de Educación - Dpto. Didáctica de las Ciencias Experimentales. [En línea]. Disponible en: http://pendientedemigracion.ucm.es/info/diciex/proyectos/agua/index.html. [Accedido: 25-may-2015].

[6] FAO, Lucha Contra la Contaminación Agrícola de los Recursos Hídricos. (Estudio FAO Riego y Drenaje - 55), E.D. Ongley. GEMS/Water Collaborating Centre Canada Centre for Inland Waters Burlington, Canadá: FAO - Organización de las Naciones Unidas para la Alimentación y la Agricultura, 1997.

[7] «Dictionary - WordReference.com». [En línea]. Disponible en: http://www.wordreference.com/. [Accedido: 05-jun-2015].

[8] «RHEA Project - EU», "Robot Fleets for Highly Effective Agriculture and Forestry Management". [En línea]. Disponible en: http://www.rhea-project.eu/. [Accedido: 30-oct-2013].

[9] SEAE, «SEAE - Sociedad Española de Agricultura Ecológica». [En línea]. Disponible en: http://www.agroecologia.net. [Accedido: 17-jul-2015].

[10] FAO, «Organic Agriculture: Agricultura Orgánica Inicio». [En línea]. Disponible en: http://www.fao.org/organicag/oa-home/es/. [Accedido: 20-jul-2015].

[11] L. A. Emmi, «Contributions to the configuration of fleets of robots for precision agriculture», 2014.

[12] «New Holland Agriculture». [En línea]. Disponible en: http://agriculture.newholland.com/uk/en/Pages/homepage.aspx. [Accedido: 09-ene-2014].

[13] CNH America LLC, «BOOMER 3040, 3045, 3050 CVT SERVICE MANUAL COMPLETE CONTENTS». 2009 CNH America LLC, 2009.

[14] A. Grečenko, «Predicting the performance of wheel tractors in combination with implements», J. Agric. Eng. Res., vol. 13, n.º 1, pp. 49-63, mar. 1968.

[15] Z. I. Mileusnić, D. V. Petrović, y M. S. Đević, «Comparison of tillage systems according to fuel consumption», Energy, vol. 35, n.º 1, pp. 221-228, ene. 2010.

[16] J. Grogan, D. A. Morris, S. W. Searcy, y B. A. Stout, «Microcomputer-based tractor performance monitoring and optimization system», J. Agric. Eng. Res., vol. 38, n.º 4, pp. 227-243, dic. 1987.

[17] W. E. Larsen, «Efficiency of utilization of four-wheel drive tractors», Agric. Energy ASAE Pub, vol. 81, n.º 4, pp. 417-421, 1981.

[18] H. D. Harris, «Prediction of the torque and optimum operating point of diesel engines using engine speed and fuel consumption», J. Agric. Eng. Res., vol. 53, pp. 93-101, sep. 1992.

[19] R. Grisso, R. Pitman, J. V. Perumpral, D. Vaughan, G. T. Roberson, y R. M. Hoy, «"Gear Up and Throttle Down" to Save Fuel», en Virginia Cooperative Extension, 2001.

[20] D. D. Bochtis y S. G. Vougioukas, «Minimising the non-working distance travelled by machines operating in a headland field pattern», Biosyst. Eng., vol. 101, n.º 1, pp. 1-12, sep. 2008.

[21] D. D. Bochtis y C. G. Sørensen, «The vehicle routing problem in field logistics part I», Biosyst. Eng., vol. 104, n.º 4, pp. 447-457, dic. 2009.

[22] I. A. Hameed, D. D. Bochtis, y C. G. Sørensen, «Driving angle and track sequence optimization for operational path planning using genetic algorithms», Appl. Eng. Agric., vol. 27, n.º 6, pp. 294-306, 2011.

[23] T. Oksanen y A. Visala, «Coverage path planning algorithms for agricultural field machines», J. Field Robot., vol. 26, n.º 8, pp. 651–668, 2009.

[24] J. Jin y L. Tang, «Optimal coverage path planning for arable farming on 2D surfaces», Trans. ASABE, vol. 53, n.º 1, pp. 283-295, 2010.

[25] J. Jin y L. Tang, «Coverage path planning on three-dimensional terrain for arable farming», J. Field Robot., vol. 28, n.º 3, pp. 424–440, 2011.

[26] D. D. Bochtis, C. G. Sørensen, y O. Green, «A DSS for planning of soil-sensitive field operations», Decis. Support Syst., vol. 53, n.º 1, pp. 66-75, abr. 2012.

[27] A. Gasparatos, P. Stromberg, y K. Takeuchi, «Biofuels, ecosystem services and human wellbeing: Putting biofuels in the ecosystem services narrative», Agric. Ecosyst. Environ., vol. 142, n.º 3-4, pp. 111-128, ago. 2011.

[28] M. A. Delucchi y T. E. Lipman, «An analysis of the retail and lifecycle cost of battery-powered electric vehicles», Transp. Res. Part Transp. Environ., vol. 6, n.º 6, pp. 371-404, nov. 2001.

[29] H. Mousazadeh, A. Keyhani, A. Javadi, H. Mobli, K. Abrinia, y A. Sharifi, «Evaluation of alternative battery technologies for a solar assist plug-in hybrid electric tractor», Transp. Res. Part Transp. Environ., vol. 15, n.º 8, pp. 507-512, dic. 2010.

[30] H. Mousazadeh, A. Keyhani, A. Javadi, H. Mobli, K. Abrinia, y A. Sharifi, «Life-cycle assessment of a Solar Assist Plug-in Hybrid electric Tractor (SAPHT) in comparison with a conventional tractor», Energy Convers. Manag., vol. 52, n.º 3, pp. 1700-1710, mar. 2011.

[31] J. A. Mulloney Jr., «Mitigation of carbon dioxide releases from power production via "sustainable agri-power": The synergistic combination of controlled environmental agriculture (large commercial greenhouses) and disbursed fuel cell power plants», Energy Convers. Manag., vol. 34, n.º 9-11, pp. 913-920, sep. 1993.

[32] S. Eaves y J. Eaves, «A cost comparison of fuel-cell and battery electric vehicles», J. Power Sources, vol. 130, n.º 1-2, pp. 208-212, may 2004.

[33] S. Ahlgren, A. Baky, S. Bernesson, Å. Nordberg, O. Norén, y P.-A. Hansson, «Tractive power in organic farming based on fuel cell technology – Energy balance and environmental load», Agric. Syst., vol. 102, n.º 1-3, pp. 67-76, oct. 2009.

[34] G. J. Offer, D. Howey, M. Contestabile, R. Clague, y N. P. Brandon, «Comparative analysis of battery electric, hydrogen fuel cell and hybrid vehicles in a future sustainable road transport system», Energy Policy, vol. 38, n.º 1, pp. 24-29, ene. 2010.

[35] A. E. Lutz, R. S. Larson, y J. O. Keller, «Thermodynamic comparison of fuel cells to the Carnot cycle», Int. J. Hydrog. Energy, vol. 27, n.º 10, pp. 1103-1111, oct. 2002.

[36] J. Zheng, X. Liu, P. Xu, P. Liu, Y. Zhao, y J. Yang, «Development of high pressure gaseous hydrogen storage technologies», Int. J. Hydrog. Energy, vol. 37, n.º 1, pp. 1048-1057, ene. 2012.

[37] N. A. Kelly y R. Girdwood, «Evaluation of a thermally-driven metal-hydride-based hydrogen compressor», Int. J. Hydrog. Energy, vol. 37, n.º 14, pp. 10898-10916, jul. 2012.

[38] A. Lebon, J. Carrete, L. J. Gallego, y A. Vega, «Ti-decorated zigzag graphene nanoribbons for hydrogen storage. A van der Waals-corrected density-functional study», Int. J. Hydrog. Energy, vol. 40, n.º 14, pp. 4960-4968, abr. 2015.

[39] J. D. Luscier, W. L. Thompson, J. M. Wilson, B. E. Gorham, y L. D. Dragut, «Using digital photographs and object-based image analysis to estimate percent ground cover in vegetation plots», Front. Ecol. Environ., vol. 4, n.º 8, pp. 408-413, 2006.

[40] C. M. Onyango y J. A. Marchant, «Segmentation of row crop plants from weeds using colour and morphology», Comput. Electron. Agric., vol. 39, n.º 3, pp. 141-155, ago. 2003.

[41] A. Tellaeche, X. P. BurgosArtizzu, G. Pajares, A. Ribeiro, y C. Fernández-Quintanilla, «A new vision-based approach to differential spraying in precision agriculture», Comput. Electron. Agric., vol. 60, n.º 2, pp. 144-155, mar. 2008.

[42] W. S. Lee, V. Alchanatis, C. Yang, M. Hirafuji, D. Moshou, y C. Li, «Sensing technologies for precision specialty crop production», Comput. Electron. Agric., vol. 74, n.º 1, pp. 2-33, oct. 2010.

[43] J. M. Guerrero, G. Pajares, M. Montalvo, J. Romeo, y M. Guijarro, «Support Vector Machines for crop/weeds identification in maize fields», Expert Syst. Appl., vol. 39, n.º 12, pp. 11149-11155, sep. 2012.

[44] M. Montalvo, J. M. Guerrero, J. Romeo, L. Emmi, M. Guijarro, y G. Pajares, «Automatic expert system for weeds/crops identification in images from maize fields», Expert Syst. Appl., vol. 40, n.º 1, pp. 75-82, ene. 2013.

[45] A. Ribeiro, C. Fernández-Quintanilla, J. Barroso, M. C. García-Alegre, y J. V. Stafford, «Development of an image analysis system for estimation of weed pressure.», en Precision agriculture'05. Papers presented at the 5th European Conference on Precision Agriculture, Uppsala, Sweden., 2005, pp. 169-174.

[46] A. Tellaeche, X. P. Burgos-Artizzu, G. Pajares, y A. Ribeiro, «A vision-based method for weeds identification through the Bayesian decision theory», Pattern Recognit., vol. 41, n.º 2, pp. 521-530, feb. 2008.

[47] M. Guijarro, G. Pajares, I. Riomoros, P. J. Herrera, X. P. Burgos-Artizzu, y A. Ribeiro, «Automatic segmentation of relevant textures in agricultural images», Comput. Electron. Agric., vol. 75, n.º 1, pp. 75-83, ene. 2011.

[48] F. López-Granados, «Weed detection for site-specific weed management: Mapping and real-time approaches», Weed Res., vol. 51, n.º 1, pp. 1-11, 2011.

[49] M. Montalvo, G. Pajares, J. M. Guerrero, J. Romeo, M. Guijarro, A. Ribeiro, J. J. Ruz, y J. M. Cruz, «Automatic detection of crop rows in maize fields with high weeds pressure», Expert Syst. Appl., vol. 39, n.º 15, pp. 11889-11897, nov. 2012.

[50] J. M. Guerrero, M. Guijarro, M. Montalvo, J. Romeo, L. Emmi, A. Ribeiro, y G. Pajares, «Automatic expert system based on images for accuracy crop row detection in maize fields», Expert Syst. Appl., vol. 40, n.º 2, pp. 656-664, feb. 2013.

[51] R. Gerhards y H. Oebel, «Practical experiences with a system for site-specific weed control in arable crops using real-time image analysis and GPS-controlled patch spraying», Weed Res., vol. 46, n.º 3, pp. 185-193, jun. 2006.

[52] M. Nørremark, H. W. Griepentrog, J. Nielsen, y H. T. Søgaard, «The development and assessment of the accuracy of an autonomous GPS-based system for intra-row mechanical weed control in row crops», Biosyst. Eng., vol. 101, n.º 4, pp. 396-410, dic. 2008.

[53] L. R. Khot, L. Tang, B. L. Steward, y S. Han, «Sensor fusion for improving the estimation of roll and pitch for an agricultural sprayer», Biosyst. Eng., vol. 101, n.º 1, pp. 13-20, sep. 2008.

[54] H. Y. Jeon y L. F. Tian, «Direct application end effector for a precise weed control robot», Biosyst. Eng., vol. 104, n.º 4, pp. 458-464, dic. 2009.

[55] T. W. Berge, S. Goldberg, K. Kaspersen, y J. Netland, «Towards machine vision based site-specific weed management in cereals», Comput. Electron. Agric., vol. 81, pp. 79-86, feb. 2012.

[56] Greenpeace España, «Agricultura ecológica». [En línea]. Disponible en: http://www.greenpeace.org/espana/es/Trabajamos-en/Transgenicos/Soluciones-y-demandas/Agricultura-ecologica/. [Accedido: 17-jul-2015].

[57] «Agricultura Ecológica». [En línea]. Disponible en: http://www.agricultura-ecologica.com/. [Accedido: 17-jul-2015].

[58] REGLAMENTO (CE) nº 889/2008 DE LA COMISIÓN de 5 de septiembre de 2008 por el que se establecen disposiciones de aplicación del Reglamento (CE) nº834/2007 del Consejo sobre producción y etiquetado de los productos ecológicos, con respecto a la producción ecológica, su etiquetado y su control. 2008.

[59] H. S. Sandhu, S. D. Wratten, y R. Cullen, «Organic agriculture and ecosystem services», Environ. Sci. Policy, vol. 13, n.º 1, pp. 1-7, feb. 2010.

[60] Y. Zhang, E. S. Staab, D. C. Slaughter, D. K. Giles, y D. Downey, «Automated weed control in organic row crops using hyperspectral species identification and thermal micro-dosing», Crop Prot., vol. 41, pp. 96-105, nov. 2012.

[61] M. J. Colloff, E. A. Lindsay, y D. C. Cook, «Natural pest control in citrus as an ecosystem service: Integrating ecology, economics and management at the farm scale», Biol. Control, vol. 67, n.º 2, pp. 170-177, nov. 2013.

[62] A. Datta y S. Z. Knezevic, «Chapter Six - Flaming as an Alternative Weed Control Method for Conventional and Organic Agronomic Crop Production Systems: A Review», en Advances in Agronomy, vol. 118, D. L. Sparks, Ed. Academic Press, 2013, pp. 399-428.

[63] G.-Y. Ye, Q. Xiao, M. Chen, X. Chen, Z. Yuan, D. W. Stanley, y C. Hu, «Tea: Biological control of insect and mite pests in China», Biol. Control, vol. 68, pp. 73-91, ene. 2014.

[64] M. Garfinkel y M. Johnson, «Pest-removal services provided by birds on small organic farms in northern California», Agric. Ecosyst. Environ., vol. 211, pp. 24-31, dic. 2015.

[65] FAO, «Agricultura sostenible - Organización de las Naciones Unidas para la Alimentación y la Agricultura». [En línea]. Disponible en: http://www.fao.org/post-2015-mdg/14-themes/sustainable-agriculture/es/. [Accedido: 20-jul-2015].

[66] «Agricultura Sostenible». [En línea]. Disponible en: http://www.agriculturasostenible.org/v_portal/apartados/apartado.asp. [Accedido: 20-jul-2015].

[67] «Instituto de Agricultura Sostenible - CSIC», Instituto de Agricultura Sostenible. [En línea]. Disponible en: http://www.ias.csic.es/. [Accedido: 20-jul-2015].

[68] «i·ambiente», i·ambiente. [En línea]. Disponible en: http://www.i-ambiente.es/. [Accedido: 20-jul-2015].

[69] D. A. G. Kurstjens, «Precise tillage systems for enhanced non-chemical weed management», Soil Tillage Res., vol. 97, n.º 2, pp. 293-305, dic. 2007.

[70] R. Kathiresan, «Integration of elements of a farming system for sustainable weed and pest management in the tropics», Crop Prot., vol. 26, n.º 3, pp. 424-429, mar. 2007.

[71] G. C. Rains, D. M. Olson, y W. J. Lewis, «Redirecting technology to support sustainable farm management practices», Agric. Syst., vol. 104, n.º 4, pp. 365-370, abr. 2011.

[72] J. R. Reeve, L. Carpenter-Boggs, y H. Sehmsdorf, «Sustainable agriculture: A case study of a small Lopez Island farm», Agric. Syst., vol. 104, n.º 7, pp. 572-579, sep. 2011.

[73] B. S. Chauhan, S. Ahmed, T. H. Awan, K. Jabran, y S. Manalil, «Integrated weed management approach to improve weed control efficiencies for sustainable rice production in dry-seeded systems», Crop Prot., vol. 71, pp. 19-24, may 2015.

[74] FAO, «Conservation agriculture». [En línea]. Disponible en: http://www.fao.org/ag/ca/. [Accedido: 17-jul-2015].

[75] AEAC.SV, «Asociación Española Agricultura de Conservación Suelos Vivos». [En línea]. Disponible en: http://www.agriculturadeconservacion.org/. [Accedido: 20-jul-2015].

[76] M. Farooq, K. C. Flower, K. Jabran, A. Wahid, y K. H. M. Siddique, «Crop yield and weed management in rainfed conservation agriculture», Soil Tillage Res., vol. 117, pp. 172-183, dic. 2011.

[77] B. S. Chauhan, R. G. Singh, y G. Mahajan, «Ecology and management of weeds under conservation agriculture: A review», Crop Prot., vol. 38, pp. 57-65, ago. 2012.

[78] A. A. Bajwa, «Sustainable weed management in conservation agriculture», Crop Prot., vol. 65, pp. 105-113, nov. 2014.

[79] K. Ramesh, «Chapter Four - Weed Problems, Ecology, and Management Options in Conservation Agriculture: Issues and Perspectives», en Advances in Agronomy, vol. 131, D. L. Sparks, Ed. Academic Press, 2015, pp. 251-303.

[80] «Titan Enterprises Ltd - Titan flow meters for oil, boiler and diesel fuel applications - PD400 oil flowmeter», 2014. [En línea]. Disponible en: http://www.flowmeters.co.uk/pd_pd400om.php#data. [Accedido: 20-feb-2014].

[81] España, Real Decreto 61/2006, de 31 de enero, por el que se determinan las especificaciones de gasolinas, gasóleos, fuelóleos y gases licuados del petróleo y se regula el uso de determinados biocarburantes. 2006, pp. 6342-6357.

[82] «ASAE D497.7 MAR2011 Agricultural Machinery Management Data», en ASAE Standards, Michigan: St. Josep, 2011, pp. 372-380.

[83] «ANSI/ASAE S296.4 DEC95 Agricultural Machinery Management Data», en ASAE Standards, Michigan: St. Josep, 1995, pp. 118-120.

[84] «ASAE S313.3 FEB04 Soil Cone Penetrometer», en ASAE Standards, Michigan: St. Josep, 2004, pp. 903-904.

[85] «ASAE D497.4 FEB2003 Agricultural Machinery Management Data», en ASAE Standards, Josep., Michigan: St. Josep, 2003, pp. 273-280.

[86] «EOSDIS Nasa's Earth Observing System Data Information System», EOSDIS NASA's Earth Observing System. [En línea]. Disponible en: http://reverb.echo.nasa.gov. [Accedido: 18-jul-2013].

[87] «ISO 8178-4:1996 - Reciprocating internal combustion engines -- Exhaust emission measurement -- Part 4: Test cycles for different engine applications», en International Organisation of Standardisation, 1996.

[88] «Photovoltaic Geographical Information System (PVGIS)», JRC's Institute for Energy and Transport - PVGIS - European Commission. [En línea]. Disponible en: http://re.jrc.ec.europa.eu/pvgis/. [Accedido: 04-may-2015].